



Instituto Politécnico Nacional
Secretaría de Investigación y Posgrado

Centro de Investigación en Biotecnología Aplicada
Sección de Estudios de Posgrado e Investigación
Programa de posgrado en Biotecnología Aplicada

**Análisis transcriptómico para la
identificación de miRNAs y genes blanco
en plantas de amaranto (*Amaranthus
hypochondriacus*) bajo estrés hídrico**

Para obtener el título de Doctor en Ciencias en
Biotecnología

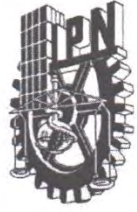
PRESENTA

Marcelino Martínez Núñez

DIRECTORA: Dra. Flor de Fátima Rosas Cárdenas



Tepetítla de Lardizábal, Tlaxcala a 04 de Noviembre de 2019.



INSTITUTO POLITÉCNICO NACIONAL SECRETARIA DE INVESTIGACIÓN Y POSGRADO

ACTA DE REGISTRO DE TEMA DE TESIS Y DESIGNACIÓN DE DIRECTOR DE TESIS

México, D.F. a 02 de Junio del 2017

El Colegio de Profesores de Estudios de Posgrado e Investigación de CIBA-IPN en su sesión ordinaria No. 6 celebrada el día 02 del mes de Junio conoció la solicitud presentada por el(la) alumno(a):

<u>Martínez</u>	<u>Núñez</u>	<u>Marcelino</u>
Apellido paterno	Apellido materno	Nombre (s)

Con registro:

B	1	5	0	6	7	0
---	---	---	---	---	---	---

Aspirante de: DCB

1.- Se designa al aspirante el tema de tesis titulado:

Análisis transcriptómico para la identificación de miRNAs y genes blanco en plantas de amaranto (*Amaranthus hypochondriacus*) bajo estrés hídrico.

De manera general el tema abarcará los siguientes aspectos:

Secuenciación y análisis del transcriptoma no codificante de *Amaranthus hypochondriacus*

Identificación de miRNAs y genes blanco asociados a estrés por sequía

Validación y sobreexpresión de miRNAs

2.- Se designa como Director de Tesis al Profesor:

Dra. Flor de Fátima Rosas Cárdenas

3.- El trabajo de investigación base para el desarrollo de la tesina será elaborado por el alumno en:

Centro de Investigación en Biotecnología Aplicada-IPN

que cuenta con los recursos e infraestructura necesarios.

4.- El interesado deberá asistir a los seminarios desarrollados en el área de adscripción del trabajo desde la fecha en que se suscribe la presente hasta la aceptación de la tesis por la Comisión Revisora correspondiente:

Director(a) de Tesis

Dra. Flor de Fátima Rosas Cárdenas

Aspirante

Marcelino Martínez Núñez

Presidente del Colegio

Dra. María Myrna Solís Oba



INSTITUTO POLITÉCNICO NACIONAL
Centro de Investigación en Biotecnología Aplicada
Unidad Tlaxcala
Dirección



**INSTITUTO POLITÉCNICO NACIONAL
SECRETARÍA DE INVESTIGACIÓN Y POSGRADO**

SIP-14
REP 2017

ACTA DE REVISIÓN DE TESIS

En la Ciudad de Tepetilla de Lardizabal siendo las 12 horas del día 04 del mes de Noviembre del 2019 se reunieron los miembros de la Comisión Revisora de la Tesis,

designada por el Colegio de Profesores de Posgrado de: CIBA-IPN

para examinar la tesis titulada: "Análisis transcriptómico para la identificación de miRNAs y genes blanco en plantas de amaranto (*Amaranthus hypochondriacus*) bajo estrés hídrico"

por el (la) alumno (a):

Apellido Paterno:	Martínez	Apellido Materno:	Núñez	Nombre (s):	Marcelino
-------------------	----------	-------------------	-------	-------------	-----------

Número de registro: B 1 5 0 6 7 0

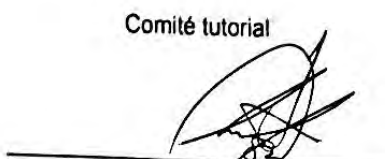
Aspirante del Programa Académico de Posgrado: Doctorado en Ciencias en Biotecnología


Después de la lectura y revisión individual, así como el análisis e intercambio de opiniones, los miembros de la Comisión manifestaron **APROBAR** **NO APROBAR** la tesis, en virtud de los motivos siguientes:


cumple con los requisitos establecidos para poder presentar el examen de grado


Dra. Fabiana Rosas Cárdenas
Profesor colegiado 12884-EB-17

Comité tutorial



Dra. Silvia Luna Suárez
Profesor colegiado 14158-EF-19


Dra. Martha Dolores Bibbins Martínez
Profesor colegiado 14324-EH-19/6


Dr. Mario Alberto Martínez Núñez
Profesor visitante 1205-EA-15


Dr. Stefan de Folter
Profesor CINVESTAV-IPN


Dra. Diana Cortés Espinosa
Presidencia de Colegio


Dr. Fernando López Valdez
14679-EF-19



INSTITUTO POLITÉCNICO NACIONAL
SECRETARÍA DE INVESTIGACIÓN Y POSGRADO

CARTA CESIÓN DE DERECHOS

En la Ciudad de Tepetitla de Lardizábal, Tlaxcala el día 06 del mes Mayo del año 2019, el (la) que suscribe Marcelino Martínez Núñez alumno (a) del Programa de Doctorado en Ciencias en Biotecnología con número de registro B150670, adscrito a Centro de Investigación en Biotecnología Aplicada, manifiesta que es autor (a) intelectual del presente trabajo de Tesis bajo la dirección de Dra. Flor de Fátima Rosas Cárdenas y cede los derechos del trabajo intitulado “Análisis transcriptómico para la identificación de miRNAs y genes blanco en plantas de amaranto (*Amaranthus hypochondriacus*) bajo estrés hídrico”, al Instituto Politécnico Nacional para su difusión, con fines académicos y de investigación.

Los usuarios de la información no deben reproducir el contenido textual, gráficas o datos del trabajo sin el permiso expreso del autor y/o director del trabajo. Este puede ser obtenido escribiendo a la siguiente dirección frosasc@ipn.mx. Si el permiso se otorga, el usuario deberá dar el agradecimiento correspondiente y citar la fuente del mismo.

Marcelino Martínez Núñez
Nombre y firma

Agradecimientos

Agradecemos al Consejo Nacional de Ciencia y Tecnología de México (CONACYT) por el apoyo y financiamiento brindado para el desarrollo de este proyecto. Este trabajo fue financiado por CONACyT CB-2013-221522 y los proyectos SIP 20170477, 20180545 y 20195904.

Productos derivados del presente proyecto de investigación

La productividad del presente proyecto de investigación derivó en la escritura de tres artículos originales que se incluyen en este documento y de los cuales el alumno es el primer autor.

1. **Martínez-Núñez, M.**, P. Vera Hernandez, M. Ruiz, M. López, A. Becerra, S. Suárez and F. d. F. Rosas Cárdenas (2018) Resistencia y tolerancia a estrés abiótico: Mecanismos sofisticados de adaptación de las plantas ante distintas condiciones de estrés. *Frontera Biotecnológica* 5.
2. **Martínez-Núñez, M.**, M. Ruiz-Rivas, P. F. Vera-Hernández, R. Bernal-Muñoz, S. Luna-Suárez and F. F. Rosas-Cárdenas (2019) The phenological growth stages of different amaranth species grown in restricted spaces based in BBCH code. *South African Journal of Botany* 124: 436-443.
3. **Martínez-Núñez, M.**, M. Ruíz-Rivas, R. A. Chávez-Montes, J. G. J. P. F. Vera-Hernández, S. Luna Suárez, S. de Folter, F. F. Rosas-Cárdenas (En proceso de edición) High-throughput sequencing and challenge in sequencing data analysis revealed the genuine miRNAs present in *Amaranthus hypochondriacus* genoma.

Adicionalmente, el autor del presente documento de tesis colaboró en la publicación de un artículo y un capítulo de libro que a continuación se citan.

1. Vera Hernández, P., **Martínez Núñez, M.**, Ruiz Rivas, M., Bibbins Martínez, M., Luna Suárez, S., Rosas Cárdenas, F. (2018) Reference genes for RT-qPCR normalization in different tissues, developmental stages and stress conditions of amaranth. *Plant Biology*.
2. **Martínez-Núñez, M.**, S. de Folter and F. F. Rosas-Cárdenas (2019) Detection of miRNAs by tissue printing and dot blot hybridization. In: de Folter S. (eds) *Plant MicroRNAs. Methods in Molecular Biology*, vol 1932. Humana Press, New York, NY. 151-157.

Finalmente, con el proposito de aplicar el conocimiento teórico que se describe en este documento de tesis y coadyuvar en el mejoramiento genético de amaranto, el autor seleccionó y describió la variedad denominada “Magali” de *Amaranthus cruentus*. Dicha variedad se encuentra en evaluación ante el Servicio Nacional de Inspección y Certificación de Semillas (SNICS), con número de expediente 2790 para el otorgamiento de título de obtentor.

Índice

Abstract:	7
1. Introducción	8
2. Antecedentes.....	11
2.1 MiRNAs: Descubrimiento y biogénesis	11
2.2 Criterios de anotación de miRNAs en plantas	12
2.3 Implicaciones funcionales de los miRNAs	15
2.4 Respuesta de las plantas ante el estrés por sequía	16
2.5 Resistencia y tolerancia a estrés abiótico: Mecanismos sofisticados de adaptación de las plantas ante distintas condiciones de estrés.....	15
2.6 Regulación de la expresión génica en las plantas ante estrés por sequía.....	16
3. Planteamiento del problema	19
4. Justificación.....	20
5. Hipótesis.....	21
6. Objetivo general:.....	22
7. Objetivos particulares:	22
8. Estrategia experimental	23
CAPITULO I: Descripción del ciclo de vida de <i>Amaranthus sp.</i> bajo condiciones de invernadero y determinar la etapa para el tratamiento de sequía.....	24
1. Introducción	25
2. The phenological growth stages of different amaranth species grown in restricted spaces based in BBCH code	26
3. Metodología	27
3.1 Cinética de sequía	27
3.2 Análisis estadístico	28
4. Resultados.....	28
5. Discusión	31
6. Conclusiones	33
CAPITULO II: Predicción bioinformática de miRNAs en <i>Amaranthus hypochondriacus</i> ...	34
1. Introducción	35
2. Metodología	36
2.1. Predicción bioinformática de miRNAs en <i>Amaranthus hypochondriacus</i>	36

2.2. Análisis de la estructura secundaria y plegamiento de pre-miRNAs.....	37
2.3. Predicción de genes blanco	37
2.4. Crecimiento de plantas	38
2.5. Extracción de RNA total.....	38
2.6. Cuantificación y análisis de calidad de RNA	39
2.7. Síntesis de cDNA.....	39
2.8. Validación tejido-específica del perfil de expresión de miRNAs mediante RT-qPCR	40
3. Resultados.....	41
4. Discusión	48
5. Conclusiones	51
CAPITULO III: High-throughput sequencing and challenge in sequencing data analysis revealed the genuine miRNAs present in <i>Amaranthus hypochondriacus</i> genome.....	
1. Abstarct	55
2. Introduction.....	55
3. Material and methods	57
3.1. Plant growth and plant material	57
3.2. Total RNA extraction and quality.....	58
3.3. Construction and sequencing of small RNA libraries.....	58
3.4. sRNA-seq data alalysis.....	59
3.5. Quantitative Real-Time PCR reaction	60
3.6. Prediction of miRNA target and their locations along the <i>A. hypochondriacus</i> genome	61
3.7. Functional classification of orthologs genes and construction of networks	62
4. Results.....	62
4.1. sRNA sequencing, size distribution and chromosomal localization.....	62
4.2. Identification and abundance of genuine-miRNAs in amaranth	63
4.3. Putative miRNA target genes.....	64
4.4. Distributions of miRNAs and their target genes in the amaranth genome.....	65
4.5. Regulatory network target genes-miRNA predicted for amaranth	66
5. Discussion	67
5.1. Conservation, confidence, and abundance of amaranth miRNAs	67
5.2. MiRNAs loci in the amaranth genome.....	68

5.3. Small RNA stress libraries identify stress-related miRNAs.....	70
5.4. miR0005 is an abundant, amaranth-specific miRNA.....	71
6. Conclusions	72
7. Acknowledgments.....	73
8. Author contributions	73
9. Financial support	73
11. References	85
CAPITULO IV Secuenciación del degradoma de <i>Amaranthus hypochondriacus</i> variedad “Gabriela”.....	
1. Introducción:	91
2. Metodología:.....	92
2.1. Construcción de librerías y secuenciación del degradoma de <i>Amaranthus hypochondriacus</i> variedad “Gabriela”	92
2.2. Análisis bioinformático del degradoma de <i>Amaranthus hypochondriacus</i> variedad “Gabriela”	93
3. Resultados:.....	94
4. Discusión:	102
5. Conclusiones:	103
ANEXOS.....	104

Lista de figuras:

Figura 1. Biogénesis y acción de los miRNAs.....	14
Figura 2. Registro fotográfico post-sequía en <i>Amaranthus sp.</i>	30
Figura 3. Plegamiento secundario de secuencias precursoras de miRNAs en <i>A. hypochondriacus</i> ..	43
Figura 4. Red de regulación génica que se predice para <i>Amaranthus hypochondriacus</i>	44
Figura 5. Interacción de miRNAs y genes blanco en <i>Amaranthus hypochondriacus</i>	45
Figura 6. Electroforesis de RNA total	46
Figura 7. Perfil de expresión tejido-específico de miRNAs identificados mediante herramientas computacionales en <i>Amaranthus hypochondriacus</i> v. “Gabriela”	47
Figura 8. Sequencing data analysis of small RNAs of amaranth	74
Figura 9. Abundance of amaranth miRNAs	74
Figura 10. (Figure 3). Location of miRNAs and their targets along chromosomes of <i>A. hypochondriacus</i>	75
Figura 11. Gene ontology classification of conserved miRNAs-target genes.	75
Figura 12. Schematic representation of the significance level of predicted target genes in molecular function and cellular components, based on GO classification	76
Figura 13. Interaction network of target genes and miRNAs obtained with String.	77
Figura 14. Networks of miR397 and miR408 targets genes obtained with the GeneMANIA web server.....	77
Figura 15. Interaction between miRNA targets of miR0005 and localization of target site in PPR target genes.	78
Figura 16. Schematic representation of the significance level of predicted target genes in biological process, based on GO classification	81
Figura 17. Procesos regulados por genes blanco de miRNAs en <i>Amaranthus hypochondriacus</i> v. Gabriela.....	96
Figura 18. Ontología génica en <i>Amaranthus hypochondriacus</i> variedad “Gabriela”.....	97
Figura 19. Clasificación de los procesos regulados por genes blanco de miRNAs de <i>Amaranthus hypochondriacus</i> variedad “Gabriela”.....	99
Figura 20. Expresión diferencial de genes blanco entre plantas control y plantas expuestas a estrés por sequía.	100
Figura 21. Ideograma de circos en donde se muestra el atlas de interacción entre miRNAs y los genes blanco identificados mediante la secuenciación del degradoma en <i>Amaranthus hypochondriacus</i> variedad “Gabriela”.....	101

Lista de tablas:

Tabla 1. Criterios de anotación de miRNAs para plantas.....	15
Tabla 2. Predicción y anotación de genes sensibles a estrés por sequía ubicados en <i>Arabidopsis thaliana</i> a partir de un degradoma publicado para <i>Paulownia australis</i>	18
Tabla 3. Oligonucleotidos y sondas diseñadas para la cuantificación de miRNAs mediante RT-qPCR.....	40
Tabla 4. Predicción bioinformática de miRNAs en <i>Amaranthus hypochondriacus</i>	42
Tabla 5. Genuine miRNAs sequences identified in amaranth.....	79
Tabla 6 Summary of predicted targets genes of miRNAs identified in amaranth.....	80
Tabla 7. Sixteen criteria considered by ShortStack for miRNA identification in amaranth.....	82
Tabla 8. Oligonucleotides for RT-qPCR in Amaranth.....	83
Tabla 9. Composition of libraries raw and clean reads.	84
Tabla 10. DICER-called sequences identified by ShortStack.	84
Tabla 11. Putative target genes of amaranth miRNAs	84
Tabla 12. Classification of target genes based on their functions using the agriGO platform.	84
Tabla 13. Número de genes blanco que se identifican para cada miRNA en el degradoma de <i>Amaranthus hypochondriacus</i> variedad "Gabriela"	95

Resumen:

La sequía es uno de los factores de estrés abiótico más común que afectan el crecimiento, desarrollo y rendimiento de las plantas. Durante su evolución, las plantas han desarrollado diferentes estrategias de defensa que les permite escapar o tolerar a la sequía. En términos moleculares, uno de los mecanismos de defensa contra la sequía es la reprogramación de la expresión génica regulada mediante miRNAs. Muchos genes con diversas funciones han sido implicados en esta tarea, sin embargo, la red de miRNAs que median la respuesta a estrés hídrico sigue siendo desconocida en varias especies de interés agronómico como el amaranto (*Amaranthus hypochondriacus*). El amaranto es un pseudocereal con un alto valor nutritivo debido al contenido de proteínas, aminoácidos y minerales. Dada la importancia alimenticia de este cultivo y su tolerancia a diversas situaciones de estrés medio ambiental, el presente proyecto de investigación se enfocó en el análisis del transcriptoma no codificante de amaranto para identificar los miRNAs que están regulados por déficit de agua, con la finalidad de elucidar las redes de regulación génica que se activa en este cultivo ante el estrés por sequía, para futuras aplicaciones biotecnológicas.

Abstract:

Drought is one of the most common factors of abiotic stress affecting growth, development and yield of plants. During their evolution, plants have developed different defense strategies that allows them to escape or tolerate drought. In molecular terms, one of the defense mechanisms against drought is the reprogramming of gene expression regulated by miRNAs. Many genes with diverse functions have been implicated in this function, however, the miRNAs regulatory network that mediate the response to water stress remains unknown in several species of agronomic interest such as amaranth (*Amaranthus hypochondriacus*). Amaranth is a pseudocereal with a high nutritional value due to protein, amino acids and minerals. Given the nutritional importance of this crop and various situations of environmental stress, the present research project will focus on the analysis of non-coding transcriptome of amaranth to identify miRNAs that are regulated by water deficit in order to elucidate gene regulatory networks that are activated in this crop to drought stress, for future biotechnological applications.

1. Introducción

Los amarantos son dicotiledóneas con hábitos herbáceos y un ciclo de vida anual (Das 2016). Pertenecen al orden *Caryophyllales*, familia *Amaranthaceae*, subfamilia *Amaranthoideae*, genero *Amaranthus* (de Rzedowski and Rzedowski 2001) y de acuerdo con reportes de Waselkov et al. 2018, el género *Amaranthus* incluye aproximadamente 74 especies monoicas o dioicas (Waselkov, Boleda et al. 2018), de las cuales 55 son nativas del continente Americano y el resto de Australia, África, Asia y Europa (Costea, Sanders et al. 2001, Mlakar, Turinek et al. 2010, Janovska, Cepkova et al. 2012, Bayón 2015, Castrillón-Arbeláez and Frier 2016). El amaranto es un pseudocereal con un alto valor nutricional (Cornejo, Novillo et al. 2019) y propiedades nutraceuticas notables (Chakraborty, Chakraborty et al. 2000, Silva-Sánchez, de La Rosa et al. 2008, Huerta-Ocampo and Barba de la Rosa 2011, Caselato-Sousa and Amaya-Farfan 2012, Venskutonis and Kraujalis 2013), se valora además por ser una planta con tolerancia inherente a diferentes factores de estrés (Huerta-Ocampo, Briones-Cerecero et al. 2009, Orona-Tamayo and Paredes-López 2017, Joshi, Sood et al. 2018, Jamalluddin, Massawe et al. 2019), pues es poco susceptible a enfermedades o plagas de insectos (Othim, Ramasamy et al. 2018), además de que es capaz de crecer en suelos pobres y salinos (Omamt, Hammes et al. 2006, Huerta-Ocampo, Barrera-Pacheco et al. 2014, Sarker and Oba 2019), bajo condiciones de altas temperaturas (Wang and Ebert 2012), lluvias irregulares y sequía (Huerta-Ocampo, Briones-Cerecero et al. 2009, Wang and Ebert 2012, Espitia-Rangel 2018, Jamalluddin, Massawe et al. 2019); esto último gracias a su eficiencia del uso del agua, lo que deriva de su capacidad para crecer raíces primarias largas y desarrollar un extenso sistema de raíces laterales, lo que

lo convierte en un cultivo alternativo para la producción sustentable de alimentos en condiciones semiáridas (Stallknecht and Schulz-Schaeffer 1993, Omamt, Hammes et al. 2006, Huerta-Ocampo, Barrera-Pacheco et al. 2014, Castrillón-Arbeláez and Frier 2016, Joshi, Sood et al. 2018). Pese a décadas de investigación, la sequía sigue representando uno de los principales desafíos para la agricultura (Huerta-Ocampo, Briones-Cerecero et al. 2009, Steiner, Briske et al. 2018, Tigkas, Vangelis et al. 2019), pues al ser un evento climático normal y recurrente, cuya aparición, gravedad y tiempo de duración es imposible predecir, limita severamente la productividad de los cultivos (Xoconostle-Cazares, Ramirez-Ortega et al. 2010, Tigkas, Vangelis et al. 2019). La situación se agrava al establecerse interacciones con otros factores de estrés (Chatterjee and Solankey 2015, Cohen, Rapaport et al. 2019), en particular con salinidad, temperaturas extremas, variaciones en la disponibilidad de nutrientes; y el ataque de plagas y enfermedades en las plantas (Ceccarelli and Grando 1996, Suzuki, Rivero et al. 2014, Todaka, Shinozaki et al. 2015, Jain, Ashraf et al. 2019). Sin embargo, las plantas han desarrollado estrategias sofisticadas para enfrentar condiciones climáticas adversas (Xoconostle-Cazares, Ramirez-Ortega et al. 2010, Chatterjee and Solankey 2015, Jain, Ashraf et al. 2019). Entre sus mecanismos de defensa se encuentra la reprogramación de la expresión génica mediada por microRNAs (miRNAs) (Jeong, Park et al. 2011, Ferdous, Hussain et al. 2015, Sharma, Upadhyay et al. 2019). Los miRNAs son una clase de RNAs pequeños no codificantes de aproximadamente 22 nucleótidos de longitud, los cuales se han identificado como importantes reguladores de la expresión génica por la interacción específica con mRNAs blanco en múltiples organismos (Ferreira, Gentile et al. 2012, Liu, Yu et al. 2018). Algunos

miRNAs están funcionalmente conservados a través de diferentes especies de plantas y animales y están regulados por diferentes tipos de estrés (Zhang, Wang et al. 2007, Evers, Huttner et al. 2015, Sharma, Upadhyay et al. 2019). En el presente proyecto de investigación se identificaron mediante secuenciación masiva los miRNAs y genes blanco que están regulados por déficit hídrico en la variedad “Gabriela” de *Amaranthus hypochondriacus L.*, ello con la finalidad de elucidar las redes de regulación génica que se activan en esta planta, así como sus potenciales aplicaciones biotecnológicas para el desarrollo de cultivos con mayor rendimiento ante condiciones de estrés por sequía.

2. Antecedentes

2.1 MiRNAs: Descubrimiento y biogénesis

Investigando el desarrollo larvario de *Caenorhabditis elegans*, Victor Ambros y sus colegas Rosalind Lee y Rhonda Feinbaum descubren en 1993 que *lin-4*, un gen conocido por controlar diferentes fases del desarrollo larvario de este nematodo, codifica para un par de RNAs pequeños (uno de 22 nucleótidos y otro de 61, este último capaz de formar una estructura de tallo-asa y ser el precursor de un RNA más corto), en vez de codificar para una proteína (Lee, Feinbaum et al. 1993, Bartel 2004, Almeida, Reis et al. 2011). En aquel momento, los autores los denominaron RNAs temporales (stRNAs) y no es hasta 2001 cuando son reconocidos como una clase distinta de RNA con funciones de regulación específicas y son nombrados formalmente microRNAs (miRNAs) (Lagos-Quintana, Rauhut et al. 2001, Lee and Ambros 2001). A partir de entonces, el conocimiento sobre miRNAs ha crecido de manera exponencial (Kozomara and Griffiths-Jones 2014, Kozomara, Birgaoanu et al. 2019). En plantas, su biogénesis y las funciones de los miRNAs identificados han sido bien caracterizados en *Arabidopsis thaliana* (Xu, Hu et al. 2018, Wang, Chen et al. 2019). De esta manera sabemos que los miRNAs son una clase de RNAs pequeños de aproximadamente 20-22 nt de longitud, con funciones reguladoras, los cuales están codificados por genes endógenos MIR (Pegler, Grof et al. 2019, Szakonyi, Confraria et al. 2019). Como se muestra en la figura 1, cada miRNA primario es transcrito por una RNA polimerasa II formando estructuras apareadas en doble cadena con forma de tallo-asa de aproximadamente 70 nucleótidos de longitud denominadas pri-miRNAs. El procesamiento de estos pri-miRNAs a pre-

miRNAs es catalizado por una RNasa nuclear de tipo III conocida como *Dicer-like 1* o *DCL1* y asistido por las proteínas de unión a RNA *HYPONASTIC LEAVES1* (*HYL1*) y *SERRATE* (SE) (Yang, Liu et al. 2006, Liu, Yan et al. 2013). Dicho complejo proteico es el encargado de escindir las regiones de RNA no apareadas en doble cadena, dando origen a un dúplex de RNA miRNA/miRNA* (donde miRNA es la hebra guía y miRNA* será la hebra que se degradará) de 20 a 22-nucleotidos de longitud denominado pre-miRNA. Cada hebra del duplex es metilada en su extremo 3' terminal por *HUA ENHANCER 1* (HEN1), lo que las protege de degradación por exonucleasas SDN (*Small RNA Degrading Nuclease*) al ser exportados hacia el citoplasma por *HASTY* (un homólogo de exportina 5) mediante un mecanismo dependiente de *Ran-GTP* (Bohnsack, Czapinski et al. 2004, Chen 2005, Voinnet 2009). Ya en el citoplasma los miRNAs maduros son reclutados por el complejo RISC (*RNA-Induced Silencing Complex*), el cual disocia a estos oligonucleótidos bicatenarios dando como resultado dos cadenas sencillas de RNA, una de estas cadenas es degradada y la otra es transportada por RISC hacia un mRNA blanco con el que es complementario, el grado de complementariedad entre microRNA/mRNA determinará la degradación del mRNA o la represión de su traducción (Figura 1) (Ferreira, Gentile et al. 2012, Khraiwesh, Zhu et al. 2012).

2.2 Criterios de anotación de miRNAs en plantas

Los avances tecnológicos de los últimos años han permitido el desarrollo y el progreso de la secuenciación de alto rendimiento (*High-throughput sequencing HTS*), o también conocida como secuenciación masiva paralela (*massive parallel sequencing [MPS]*)(Morin, Zhao et al. 2010, Wu 2018). Dicha tecnología ha

revolucionado el estudio de sRNAs (small RNAs) o RNAs pequeños por sus siglas en inglés (Dard-Dascot, Naquin et al. 2018), brindándonos la oportunidad de investigar a detalle su perfil de expresión en distintos organismos (Hu, Lan et al. 2017). En plantas, los diferentes métodos de HTS han permitido la identificación de una gran variedad de sRNAs, incluyendo a los miRNAs (Hui, S. et al. 2018, Miao, Ye et al. 2018, Sun, Sun et al. 2018, Xia, Zhao et al. 2018).

En respuesta a la gran cantidad de datos generados mediante técnicas de HTS y al número y variedad de siRNAs endógenos presentes en plantas, se han desarrollado poderosas herramientas bioinformáticas para el análisis de los datos de miRNA-seq (Wang, Lin et al. 2009, Hackenberg, Rodriguez-Ezpeleta et al. 2011, Yang and Li 2011, Axtell 2013, Lei and Sun 2014, Shahid and Axtell 2014). Sin embargo, sigue siendo necesario actualizar y describir puntualmente criterios de identificación para miRNAs de plantas, lo que en el futuro podrá evitar anotaciones erróneas o cuestionables (Meyers, Axtell et al. 2008, Axtell and Meyers 2018). Atendiendo a estas necesidades, Axtell y Meyers en el año 2018 proporcionan criterios actualizados para la anotación segura de miRNAs de plantas. Los criterios actualizados enfatizan la necesidad de identificar mediante HTS los miRNAs descritos en distintas plantas. Dicha identificación debe generarse con suficientes replicas biológicas para evitar duplicaciones y minimizar la anotación de falsos positivos. Los autores argumentan también, que es necesario el desarrollo y la mejora de sistemas de anotación para miRNAs y todas las demás clases de RNAs pequeños de plantas, así como la actualización de las bases de datos (miRBase) en los que estos se reportan (Axtell and Meyers 2018). Los 7 criterios establecidos

por Axtell y Meyers 2018 para la anotación confiable de miRNAs de plantas se describen en la tabla 1.

Biogénesis y función de los miRNAs

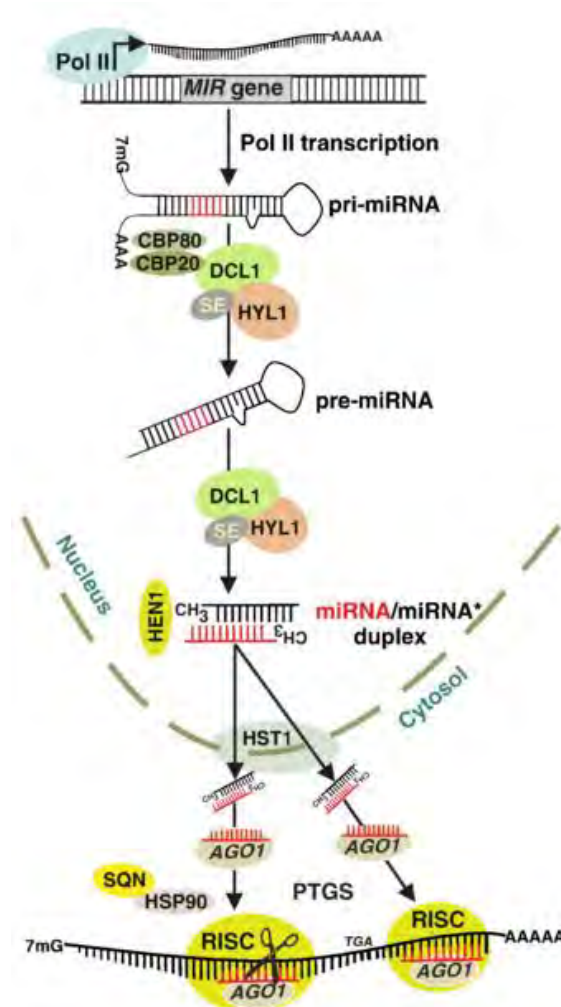


Figura 1. Biogénesis y acción de los miRNAs. Tomada de *Khraiweh et al.*, 2012. Los genes MIR se transcriben inicialmente por una Pol II en RNAs monocatenarios que adoptan una estructura de horquilla llamada *pri-miRNA*. Su posterior procesamiento a *pre-miRNAs* depende de la interacción del complejo formado por DCL1, HYL1 y SE con proteínas CBP (Cap-Binding Proteins) CBP20 y CBP80. Cada hebra del duplex de los pre-miRNAs (miRNA/miRNA*) es metilada en su extremo 3' terminal por HEN1 y posteriormente transportada al citoplasma por HST1. Se selecciona la hebra guía miRNA mediante el complejo RISC y se dirige con ayuda de AGO1 hacia un mRNA blanco, propiciando de esta manera el silenciamiento génico, ya sea por la degradación del mRNA o por la inhibición de su traducción.

Criterios de anotación de miRNAs en plantas	
1	La secuencia precursora de un miRNA no deberá ser mayor a 300 nt y se deberán excluir secuencias que formen plegamientos secundarios grandes (bucles) que impacten en la estructura típica de tallo asa o que interrumpan el dúplex miRNA / miRNA*
2	Descartar la confirmación de un miRNA por hibridación. Solo serán considerados como miRNAs verdaderos aquellos identificados mediante RNA-Seq.
3	Hasta 5 <i>mismatches</i> o bases no coincidentes, de las cuales solo tres pueden ser nucleótidos en protuberancias asimétricas
4	Se puede incluir una variante de posición de nucleótido en el duplex miRNA y miRNA * al calcular la precisión
5	Los miRNAs identificados deberán cumplir con todos los criterios de anotación que se describen en al menos dos librerías independientes de sRNA-seq (réplicas biológicas)
6	Las anotaciones de miRNAs basadas en homología deberán ser consideradas provisionales y a reserva de su identificación mediante sRNA-seq y al cumplimiento de todos los criterios que se describen
7	Secuencias < a 20 nucleótidos y > a 24 nucleótidos no deberán anotarse como miRNAs. Las anotaciones de miRNAs de 23 o 24 nucleótidos requieren evidencia extremadamente robusta.

Tabla 1. Criterios de anotación de miRNAs para plantas. Tabla tomada y modificada de Axtell and Meyers 2018.

2.3 Implicaciones funcionales de los miRNAs

Funcionalmente, los miRNAs de plantas están implicados en la ejecución de múltiples procesos biológicos (Li, Castillo-Gonzalez et al. 2017, Brant and Budak 2018, Manavella, Yang et al. 2019), tales como su biogénesis (Bhat, Bielewicz et al. 2019, Wang, Chen et al. 2019, Wang, Mei et al. 2019), metabolismo, transducción de señales, degradación de proteínas, apoptosis, desarrollo de raíces, tallos, hojas, órganos florales, tiempo de floración y respuesta de auxinas (Vaucheret, Vazquez et al. 2004, Chen 2005, Sunkar, Girke et al. 2005, Kantar, Lucas et al. 2011). Además de estar involucrados en una serie de procesos celulares que permite a las plantas adaptarse a diferentes factores de estrés ambiental (Li, Castillo-Gonzalez et al. 2017, Manavella, Yang et al. 2019); tales como la sequía, salinidad, temperaturas

extremas y déficit de nutrientes en el suelo (Jeong, Park et al. 2011). Para detectar, responder y adaptarse a estos ambientes estresantes, las plantas han desarrollado redes moleculares de regulación, en donde una gran variedad de genes con diversas funciones son inducidos o reprimidos para brindar tolerancia celular y fisiológica (Manavella, Yang et al. 2019). Tradicionalmente, la regulación de la expresión génica ha sido estudiada en gran medida a nivel transcripcional, sin embargo, el descubrimiento de pequeños RNAs (entre ellos los miRNAs) ha hecho evidente la importancia de analizar su regulación postranscripcional, pues ello ha permitido mejorar nuestra comprensión de los mecanismos moleculares que regulan la respuesta de las plantas ante condiciones adversas (Manavella, Yang et al. 2019).

2.4 Respuesta de las plantas ante el estrés por sequía

Las plantas están continuamente expuestas a estímulos ambientales que influyen en su desarrollo, rendimiento y productividad (Khalid, Hussain et al. 2019). Entre las variaciones climáticas de mayor relevancia para los cultivos agrícolas se encuentran las temperaturas extremas (Frío y calor), salinidad y sequía (Johnson and Smith 2003, Chatterjee and Solankey 2015, Ferdous, Hussain et al. 2015, Hackenberg, Gustafson et al. 2015, Khalid, Hussain et al. 2019). La sequía está considerada como una deficiencia constante de la precipitación que afecta amplias zonas de una región determinada; y se traduce en un periodo de clima anormalmente seco y prolongado, en donde la escasez de agua da lugar a un agudo desequilibrio hídrico que impide el crecimiento y el desarrollo de las plantas para completar su ciclo de vida (Farooq, Hussain et al. 2012, Fahad, Hakeem et al. 2019).

Las plantas han desarrollado estrategias fisiológicas y bioquímicas para hacer frente a la sequía (Shinozaki and Yamaguchi-Shinozaki 2007, Xoconostle-Cazares, Ramirez-Ortega et al. 2010, Gamez, Soba et al. 2019), ello se manifiesta mediante: 1) el ajuste estacional de crecimiento para evitar condiciones de estrés; 2) adaptaciones morfológicas, tales como el desarrollo de sistemas radiculares anchos y profundos, reducción de la superficie foliar, y la acumulación de cera en la superficie de la hoja; 3) adaptaciones fisiológicas como el cierre de estomas y abscisión foliar; y 4) cambios metabólicos entre los que se encuentra un ajuste del potencial osmótico, acumulación de solutos, como aminoácidos, azúcares o dehidrinas (Close 1996), inhibición de la fotosíntesis y la represión del crecimiento celular (Chavarria and dos Santos 2012, Ferdous, Hussain et al. 2015). Para una revisión más profunda de los mecanismos de defensa que implementan las plantas ante condiciones de estrés abiótico, consultar el artículo titulado “Resistencia y tolerancia a estrés abiótico: Mecanismos sofisticados de adaptación de las plantas ante distintas condiciones de estrés” ISSN: 2448-8461.

A nivel celular y molecular, las plantas responden y se adaptan a la sequía mediante la modificación de su expresión génica a través de la actividad de miRNAs (Zhou, Liu et al. 2010, Khraiwesh, Zhu et al. 2012, Ferdous, Hussain et al. 2015, Ferdous, Sanchez-Ferrero et al. 2017, Yu, Ni et al. 2019). En las últimas dos décadas, el surgimiento de innovadores métodos computacionales y experimentales ha permitido identificar y predecir un número importante de genes y miRNAs sensibles a déficit hídrico en muchas especies de plantas (Tabla 2) (Seki, Narusaka et al. 2002, Wan, Wu et al. 2011, Ferdous, Hussain et al. 2015, Palmeros-Suárez, Massange-Sánchez et al. 2015, Ferdous, Sanchez-Ferrero et al. 2017),

entre ellas *Arabidopsis thaliana* (Sunkar and Zhu 2004, Liu, Tian et al. 2008, Panda and Sunkar 2015, Xu, Hu et al. 2018), *Oryza sativa* (Zhao, Liang et al. 2007, Zhou, Liu et al. 2010, Pandita and Wani 2019), *Triticum dicoccoides* (Kantar, Lucas et al. 2011), *Zea mays* (Li, Fu et al. 2013), *Phaseolus vulgaris* (Arenas-Huertero, Pérez et al. 2009), *Vigna unguiculata* (Barrera-Figueroa, Gao et al. 2011), *Nicotiana tabacum* (Frazier, Sun et al. 2011), *Glycine max* (Kulcheski, de Oliveira et al. 2011, Ramesh, Govindasamy et al. 2019), *Solanum tuberosum* L. (Zhang, Yang et al. 2014) y *Solanum lycopersicum* (Lopez-Galiano, Sentandreu et al. 2019) entre otros cultivos.

Dada la importancia de la respuesta de las plantas ante adversas condiciones climáticas, así como a la exposición continua a posibles patógenos. Se han establecidos los términos de resistencia y tolerancia, los cuales se han tenido opiniones controversiales, lo que se discute más a detalle en el artículo que se incluye a continuación publicado en la revista de Divulgación Frontera Biotecnológica.



RESISTENCIA Y TOLERANCIA A ESTRÉS ABIÓTICO: MECANISMOS SOFISTICADOS DE ADAPTACIÓN DE LAS PLANTAS ANTE DISTINTAS CONDICIONES DE ESTRÉS.

Martínez Núñez Marcelino¹, Vera Hernández Pedro Fernando¹, Ruiz Rivas Magali¹, Villalobos López Miguel Ángel¹, Arroyo Becerra Analilia¹, Luna Suárez Silvia¹, Rosas Cárdenas Flor de Fátima^{1*}

¹Centro de Investigación en Biotecnología Aplicada del Instituto Politécnico Nacional, Ex-Hacienda San Juan Molino Carretera Estatal Santa Ines Tecuexcomac-Tepetitla Km 1.5, Tlaxcala C.P. 90700, México
Tel. +52 248-48707-65.

*Autor para correspondencia: Dra. Flor de Fátima Rosas Cárdenas, frosasc@ipn.mx

1. Resumen

Las plantas están expuestas continuamente a estímulos ambientales que influyen en su desarrollo, su rendimiento y su productividad. Las plantas han desarrollado diferentes estrategias morfológicas, fisiológicas y bioquímicas para hacer frente a diferentes situaciones de estrés, a lo largo de su historia evolutiva. Entre ellas, la resistencia y la tolerancia a menudo son utilizadas por las plantas para responder a tales situaciones estresantes. Esta pequeña revisión presenta un breve panorama de ambos conceptos en relación a una impresionante diversidad de respuestas de adaptación empleadas por las plantas ante diferentes factores de estrés.

Palabras clave: resistencia, tolerancia, estrés, plantas

2. Abstract

Plants are continuously exposed to environmental stimuli that affect their development, yield and productivity. Along its evolutionary history, plants have developed different morphological, physiological and biochemical strategies to cope at different stress conditions. Among them, resistance and tolerance are often used by plants in response to such stressing situations. This mini review shows a brief view for

both concepts, in their relation to an impressive diversity of adaptive responses used by plants against to different stress factors.

Keywords: resistance, tolerance, stress, plants

3. Introducción

Las plantas han evolucionado desde su aparición para adaptarse a los ambientes diversos a los que a menudo están expuestas. Las respuestas que las plantas muestran ante distintas tensiones les permiten detectar cambios ambientales sutiles y responder inmediatamente a condiciones complejas de estrés, minimizando los daños y conservando recursos valiosos para el crecimiento y la reproducción. Esta gran capacidad de respuesta a los cambios en el ambiente tiene mucho sentido si tomamos en cuenta que las plantas son organismos sésiles. Éstas respuestas implican cambios a nivel transcriptómico, celular y fisiológico (Atkinson y Urwin, 2012) que se traducen en la activación organizada de una red compleja de mecanismos que procuran la adaptación de la planta ante un ambiente hostil (Shabala y Pottosin, 2014).

Evidencia reciente sugiere que la respuesta que ejercen las plantas ante distintos factores de estrés como la sequía, la salinidad, las temperaturas extremas y el déficit de nutrientes, entre otros; es de naturaleza multigénica. Lo anterior, indica que las respuestas celulares a menudo están interconectadas, ejerciendo así la activación sincronizada de múltiples genes que responden al estrés y que se comunican mediante vías de transducción de las señales con otros componentes metabólicos y hormonales (Tuteja, 2007; Udawat et al., 2016). La respuesta de las plantas contra cualquier tipo de estrés, puede involucrar características o mecanismos que evitan la exposición al estrés (resistencia) y/o mecanismos que permiten a la planta contender con el estrés, limitando y reparando el impacto negativo del daño que ha ocurrido a consecuencia de alguna situación de estrés (tolerancia) (Levitt, 1980; Bray et al., 2000). Ambas estrategias se han propuesto como alternativas redundantes propias de la evolución de las plantas (Agrawal et al., 2004). En éste escrito, se presenta una revisión de la aplicación y el empleo de los conceptos de resistencia y tolerancia; además se destacan características que describen a ambos conceptos haciendo alusión a los mecanismos de adaptación sofisticados que presentan las plantas ante condiciones de estrés abiótico como la sequía, la salinidad, el frío y el calor.

Factores de estrés que limitan el desarrollo óptimo de las plantas

Las plantas, al ser organismos sésiles, han desarrollado una capacidad notable para hacer frente a una gama amplia de tensiones ambientales, que de forma individual o en múltiples combinaciones (Atkinson y Urwin, 2012), pueden alterar su metabolismo y dar lugar a efectos negativos sobre su crecimiento, su desarrollo y su productividad (Levitt, 1980; Rao et al., 2006; Rejeb et al., 2014). Entre los factores de estrés pueden incluirse los factores abióticos como la sequía, los cambios drásticos de temperatura, la deficiencia o el exceso de luz, la acumulación de contaminantes, los herbicidas, los cambios en la concentración de sales y de los nutrientes en el suelo; y dentro de los factores bióticos se puede incluir, el ataque de insectos herbívoros y de patógenos (Levitt, 1980; Strauss y Agrawal, 1999; Nicot et al., 2005; Rao et al., 2006; Gill y Tuteja, 2010; Lata y Prasad, 2011; Mitchell et al., 2016). El término “resistencia” se ha acuñado a las respuestas de defensa contra patógenos en donde las plantas resistentes responden mediante mecanismos

que evitan el desarrollo de la enfermedad (inmunes), y las no resistentes (susceptibles) desarrollan la enfermedad. Sin embargo, los términos de resistencia al estrés y tolerancia al estrés, se han usado de forma intercambiable tanto para el estrés biótico como para el estrés abiótico, aunque se reconoce que el término más adecuado para referirse al estrés abiótico es el término tolerancia (antónimo-sensibilidad) (Bray et al., 2000; Rashid, 2009). Las plantas suelen responder hacia cada uno de estos factores de estrés o a la combinación de los mismos, mediante fenómenos complejos que han sido investigados intensamente (Levitt, 1980; Núñez-Farfán et al., 2007). La forma en la que las plantas responden a un entorno medioambiental cambiante suele ser distinto y depende de la etapa de desarrollo en el que se encuentren (Wahid et al., 2007; Nemeskéri et al., 2012), ello les permite adaptarse al conjunto específico de condiciones y las limitaciones presentes en un momento determinado (Lata y Prasad, 2011).

La resistencia y la tolerancia como estrategias de defensa

De forma general, algunos autores reconocen dos estrategias que a menudo utilizan las plantas para su defensa: la resistencia y la tolerancia (Mauricio et al., 1997; Núñez-Farfán et al., 2007; Stout, 2013; Mitchell et al., 2016). La resistencia la definen como “aquellas características intrínsecas de las plantas que les permiten minimizar o limitar el daño causado bajo un estado particular de estrés en un momento determinado y sin que su fenotipo se vea modificado de manera significativa” (Agrawal et al., 2004; Puijalón et al., 2011). Mientras que la tolerancia o compensación hace referencia a “la habilidad que tienen las plantas de soportar cierto nivel de daño sin reducir su rendimiento a causa de un entorno ambiental estresante”, lo que en términos de producción agrícola significa que, pese a las condiciones de estrés, los niveles de rendimiento en un cultivo tolerante se mantendrán por encima del umbral económico (Mauricio et al., 1997; Agrawal et al., 2004; Wahid et al., 2007; Puijalón et al., 2011; Stout, 2013). Ciertas consideraciones teóricas sugieren que bajo condiciones naturales todas las plantas asignan recursos simultáneamente a ambas estrategias, por lo que exhiben un patrón mixto de defensa (Núñez-Farfán et al., 2007).

Resistencia y tolerancia ¿Conceptos mutuamente excluyentes?

Algunos autores han sugerido que la resistencia y la tolerancia representan estrategias redundantes (Van der Meijden et al., 1988; Simms y Triplett, 1994; Fineblum y Rausher, 1995); sin embargo, hoy en día se plantea que ambas estrategias de defensa coexisten de forma estable, y lejos de considerarse conceptos mutuamente excluyentes, se consideran estrategias alternativas (Squeo et al., 1996; Mauricio et al., 1997; Agrawal et al., 2004). Por tal motivo, pese a que las características que hacen tolerante a una planta no impiden el daño ocasionado por los distintos factores de estrés, éstas características sí son capaces de compensar los daños que los enemigos naturales ya han ocasionado sobre ellas; protegiendo de esta manera de los efectos perjudiciales mediante mecanismos sofisticados de adaptación (Levitt, 1980; Mauricio et al., 1997). Conceptualmente los términos de resistencia y tolerancia tienen definiciones distintas; sin embargo, en la práctica es común su uso como sinónimos (Sivasankar et al., 2012), aunque el uso indistinto no ayuda en la tarea de la correcta aplicación de los términos.

Características de resistencia y tolerancia de plantas ante diferentes factores de estrés

Tanto en las estrategias de resistencia como en las de tolerancia es posible distinguir diferentes mecanismos empleados por las plantas para sobrevivir ante una gran cantidad de desafíos ambientales (Figura 1). Ambas estrategias inician inmediatamente después de la exposición a algún entorno estresante, desarrollando mecanismos complejos para percibir las señales externas y para mostrar las respuestas de adaptación que implican cambios morfológicos, fisiológicos y bioquímicos propios de cada especie (Tabla 1) (Bohnert et al., 1995; Shinozaki y Yamaguchi-Shinozaki, 2007). Estos cambios pueden manifestarse como resistencia mediante: 1) el ajuste estacional del crecimiento para evitar las condiciones de estrés; 2) las adaptaciones morfológicas y las adaptaciones fisiológicas, tales como el desarrollo de sistemas radiculares anchos y profundos, el engrosamiento del xilema, el incremento en la densidad de tricomas, el cierre de estomas y la acumulación de cera en la superficie de la hoja, entre otros. O bien como tolerancia, mediante 3) cambios metabólicos entre los que se encuentra un ajuste del potencial osmótico, la biosíntesis de

osmoprotectores y solutos compatibles, la activación de enzimas y los compuestos antioxidantes, la síntesis de poliaminas, la producción de Óxido Nítrico (NO), la modulación fitohormonal, la represión del crecimiento celular, la inducción de vías de señalización mediadas por enzimas y la reprogramación de la expresión génica mediante mecanismos dependientes o independientes de pequeñas moléculas de ácidos nucleicos conocidas como miRNAs, entre otras (Chavarría y dos Santos, 2012).

4. Conclusiones

Recientemente, muchos de los mecanismos por los que las plantas hacen frente a entornos adversos han empezado a comprenderse a profundidad. Con ello, se ha dado lugar al surgimiento de estrategias nuevas de mejoramiento que tienen como finalidad conferir ventajas adaptativas ante diferentes condiciones de estrés, y por ende propiciar el incremento en la productividad de distintos cultivos

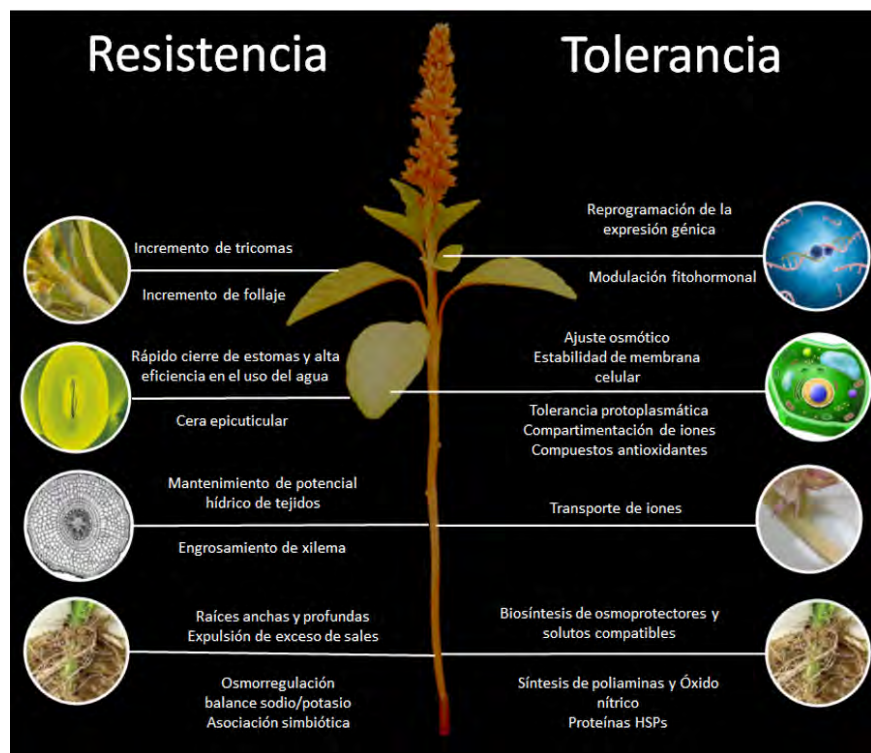


Figura 1: *Amaranthus hybridus*. Ejemplo de una planta que muestra características de resistencia y tolerancia a diferentes factores de estrés abiótico, entre ellos: Salinidad, sequía, y temperaturas extremas. Las respuestas celulares que ejercen las plantas del género *Amaranthus* ante distintos factores de estrés a menudo están interconectadas, lo que sugiere una acción sincronizada de diferentes estrategias que se comunican mediante vías de transducción de la señales con diversos componentes metabólicos y hormonales.

Tabla I. Mecanismos implicados en estrategias de resistencia y tolerancia para el manejo de diferentes factores de estrés abiótico en las plantas.

Estrategias de resistencia y tolerancia ante diferentes factores de estrés abiótico en plantas				
Estrés	Estrategias de resistencia	Referencia	Estrategias de Tolerancia	Referencia
Sequía	<ul style="list-style-type: none"> Mantenimiento del potencial hídrico de los tejidos Floración para completar el ciclo de vida antes de la sequía Desarrollo de raíces profundas Rápido cierre de estomas Alta eficiencia en la captación y uso del agua Presencia de una gruesa capa de cera epicuticular en las hojas Resistencia a fotoinhibición Biosíntesis de ácido abscísico 	(Aiken y Smucker, 1996; Price, et. al, 2002)	<ul style="list-style-type: none"> Biosíntesis de ácido abscísico Mantenimiento de turgencia y volumen celular mediante el ajuste osmótico. Estabilidad de la membrana celular. Se conserva el metabolismo celular pese a un bajo potencial hídrico Síntesis de osmoprotectores y solutos compatibles Expresión de sistemas de protección, detoxificación y reparación celular Síntesis de óxido nítrico Recambio de metabolitos, mensajeros y proteínas Reprogramación de la expresión génica mediada por miRNAs 	(Ferdous, et. al, 2015; Shukla, et. al, 2008; Tripathy, et. al, 2000)
Salinidad	<ul style="list-style-type: none"> Expulsión de exceso de sales Acumulación del exceso de sodio en las vacuolas Aumento en la captación de potasio Balance en la concentración sodio/potasio Incremento de foliaje Acidificación apoplástica Asociación simbiótica de raíces con hongos micorrízicos arbusculares Asociación de raíces con rizobacterias promotoras crecimiento vegetal 	(Farooq, et. al, 2015)	<ul style="list-style-type: none"> Homeostasis y compartimentación de iones Transporte y absorción de iones Ajuste osmótico Biosíntesis de osmoprotectores y solutos compatibles Activación de enzimas y compuestos antioxidantes Síntesis de poliaminas Producción de Óxido Nítrico (NO) Modulación fitohormonal Reprogramación de la expresión génica mediante miRNAs 	(Carillo, et. al, 2011; Deivanai, et. al, 2011; Gupta y Huang, 2014; Hoque, et. al, 2008; Shukla et. al, 2008)
Frío	<ul style="list-style-type: none"> Presencia de una mayor proporción de ácidos grasos insaturados en membrana celular, lo que deriva en una inferior temperatura de transición y por ende en la función celular óptima ante bajas temperaturas Aclimatación celular a frío. Se impide la lisis inducida por la expansión celular y la formación de lípidos hexagonales de fase II 	(Jan y Andrabi, 2009; Steponkus, 1984; Wu, et. al, 1997)	<ul style="list-style-type: none"> Ajuste osmótico. Ajuste del metabolismo celular para tolerar cambios drásticos de temperatura Cambio de estructura y propiedades catalíticas de enzimas que confieren termo-estabilidad celular Estabilidad de la membrana celular. Activación de mecanismos de regulación para restaurar niveles normales de metabolitos Activación de enzimas y compuestos antioxidantes Acumulación de osmolitos para evitar deshidratación celular Síntesis de azúcares solubles, aminoácidos, ácidos orgánicos, poliaminas y lípidos Reprogramación de la expresión génica mediante miRNAs 	(Guy, 1990; Kubiem, et. al, 2003; Nayyar, et. al, 2005; Shukla et. al, 2008; Yadav, 2010)
Calor	<ul style="list-style-type: none"> Reducción del tamaño de las células Movimiento circadiano de las hojas para ocultarlas del exceso de irradiación solar Cierre de los estomas para evitar la pérdida de agua Incremento en la densidad de tricomas para el mantenimiento de un microclima que proporcione sombra y conserve la humedad en la superficie de la epidermis Engrosamiento del xilema 	(Bañon, et. al, 2004; Wahid, et. al, 2007)	<ul style="list-style-type: none"> Ajuste osmótico. Homeostasis hormonal Estabilidad de la membrana celular. Detoxificación de ROS mediante biosíntesis de osmoprotectores Activación de enzimas y compuestos antioxidantes Biosíntesis y acumulación de solutos compatibles Inducción de vías de señalización MAPK y G2PK Activación de vías de señalización moduladas por chaperonas. Expresión de proteínas de choque térmico (HSPs) que permiten la mejora de procesos fisiológicos como fotosíntesis, asimilación de nutrientes y una mejor eficiencia en el uso de agua Reprogramación de la expresión génica mediante miRNAs 	(Fokar, et. al, 1998; Shanahan, et. al, 1990; Shukla, et. al, 2008; Tripathy, et. al, 2000; Wahid, et. al, 2007)

bajo ambientes diferentes. Tanto el término de “resistencia” como el de “tolerancia” son conceptos utilizados para referirse a la capacidad que tienen las plantas de manejar el estrés, y ambos representan estrategias complejas y temas de investigación estudiados ampliamente y vigentes. Por tal motivo, es esencial el conocimiento profundo de las estrategias moleculares que han desarrollado los grupos de plantas diferentes para poder manipular y mejorar la capacidad de las plantas, pues cada una de las estrategias que utilizan, ya sea individualmente o en conjunto, juegan un papel importante en la adaptación a condiciones ambientales adversas.

5. Agradecimientos

Agradecemos al Consejo Nacional de Ciencia y Tecnología (CONACyT) por el proyecto financiado CB2013-221522 y al Instituto Politécnico Nacional por el proyecto financiado SIP-20160215. También agradecemos al CONACyT por las becas otorgadas a MMN, PFVH y MRR.

6. Referencias bibliográficas

• Agrawal, A.A., Conner, J.K., and Stinchcombe, J.R. 2004. Evolution of plant resistance and tolerance to frost damage. *Ecology Letters*. (7): 1199-1208.

• Aiken, R., and Smucker, A. 1996. Root system regulation of whole plant growth. *Annu. Rev. Phytopathol.* 34: (1) 325-346.

• Atkinson, N.J., and Urwin, P.E. 2012. The interaction of plant biotic and abiotic stresses: from genes to the field. *J Exp Bot.* (63): 3523-3543.

• Bañon, S., Fernandez, J., Franco, J., Torrecillas, A., Alarcón, J., and Sánchez-Blanco, M.J. 2004. Effects of water stress and night temperature preconditioning on water relations and morphological and anatomical changes of *Lotus creticus* plants. *Sci. Hortic.* 101(3): 333-342.

• Bohnert, H.J., Nelson, D.E., and Jensen, R.G. 1995. Adaptations to environmental stresses. *Plant Cell.* (7):1099-1111.

• Bray, E., Bailey, S.J., and Weretilnyk, E. 2000. Responses to abiotic stresses. Cap.22 en *Biochemistry and Molecular Biology of Plants*. Buchanan B, Gruissem W, Jones R. Eds. American Society of Plant Physiologists.

• Carillo, P., Annunziata, M.G., Pontecorvo, G., Fuggi, A., and Woodrow, P. 2011. Salinity stress and salt tolerance. *Abiotic Stress Plants-Mech. Adapt.* pp. 21-38

• Chavarria, G., and dos Santos, H.P. 2012. Plant water relations: absorption, transport and control mechanisms: INTECH Open Access Publisher. pp.106-132.

• Deivanai, S., Xavier, R., Vinod, V., Timalata, K., and Lim, O. 2011. Role of exogenous proline in ameliorating salt stress at early stage in two rice cultivars. *J Stress Physiol Biochem.*, 7(4) 157-174.

• Farooq, M., Hussain, M., Wakeel, A., and Siddique, K. H. 2015. Salt stress in maize: effects, resistance mechanisms, and management. *Agron Sustain Dev.* 35(2): 461-481.

- Ferdous, J., Hussain, S.S., and Shi, B.J. 2015. Role of microRNAs in plant drought tolerance. *Plant Biotechnol J*. 13(3): 293-305.
- Fineblum, W.L., and Rausher, M.D. 1995. Tradeoff between resistance and tolerance to herbivore damage in a morning glory. *Nature*. (377): 517-520.
- Fokar, M., Nguyen, H.T., and Blum, A. 1998. Heat tolerance in spring wheat. Estimating cellular thermotolerance and its heritability. *Euphytica*, 104(1): 1-8.
- Gill, S.S., and Tuteja, N. 2010. Reactive oxygen species and antioxidant machinery in abiotic stress tolerance in crop plants. *Plant Physiol Biochem*. (48): 909-930.
- Gupta, B., and Huang, B. 2014. Mechanism of salinity tolerance in plants: physiological, biochemical, and molecular characterization. *Int J Genomics*. 2014. 1-18
- Guy, C.L. 1990. Cold acclimation and freezing stress tolerance: role of protein metabolism. *Annu Rev Plant Biol*. 41(1): 187-223.
- Hoque, M.A., Banu, M.N.A., Nakamura, Y., Shimoishi, Y., and Murata, Y. 2008. Proline and glycinebetaine enhance antioxidant defense and methylglyoxal detoxification systems and reduce NaCl-induced damage in cultured tobacco cells. *J plant physiol*. 165(8): 813-824.
- Jan, N., and Andrabi, K.I. 2009. Cold resistance in plants: A mystery unresolved. *Electron J Biotechnol*. 12(3): 14-15.
- Kubien, D.S., von Caemmerer, S., Furbank, R.T., and Sage, R.F. 2003. C4 photosynthesis at low temperature. A study using transgenic plants with reduced amounts of Rubisco. *Plant Physiol*. 132(3): 1577-1585.
- Lata, C., and Prasad, M. 2011. Role of DREBs in regulation of abiotic stress responses in plants. *J Exp Bot*. (62): 4731-4748.
- Levitt, J. 1980. Responses of plants to environmental stresses. Volume II. Water, radiation, salt, and other stresses: Academic Press.
- Mauricio, R., Rausher, M.D., and Burdick, D.S. 1997. Variation in the defense strategies of plants: are resistance and tolerance mutually exclusive? *Ecology*. (78): 1301-1311.
- Mitchell, C., Brennan, R.M., Graham, J., and Karley, A.J. 2016. Plant Defense against Herbivorous Pests: Exploiting Resistance and Tolerance Traits for Sustainable Crop Protection. *Front Plant Sci*. (7): 1132. 1-8.
- Nayyar, H., Chander, K., Kumar, S., and Bains, T. 2005. Glycine betaine mitigates cold stress damage in chickpea. *Agron Sustain Dev*. 25(3): 381-388.
- Nemeskéri, E., Molnár, k., Víg, R., Dobos, A., and Nagy, J. 2012. Defence Strategies of Annual Plants Against Drought: INTECH Open Access Publisher. pp.133-158.
- Nicot, N., Hausman, J.F., Hoffmann, L. and Evers, D. 2005 Housekeeping gene selection for real-time RT-PCR normalization in potato during biotic and abiotic stress. *J Exp Bot*. (56): 2907-2914.
- Núñez-Farfán, J., Fornoni, J., Valverde, P.L. 2007. The evolution of resistance and tolerance to herbivores. *Annu Rev Ecol Evol Syst*. 541-566.
- Price, A. H., Cairns, J. E., Horton, P., Jones, H. G., and Griffiths, H. 2002. Linking drought resistance mechanisms to drought avoidance in upland rice using a QTL approach: progress and new opportunities to integrate stomatal and mesophyll responses. *J Exp Bot*. 53(371): 989-1004.
- Puijalon, S., Bouma, T.J., Douady, C.J., Groenendael, J.V., Anten, N.P.R., Martel, E., and Bornette, G. 2011. Plant resistance to mechanical stress: evidence of an avoidance-tolerance tradeoff. *New Phytologist*. (191): 1141-1149.
- Rao, K.V., Raghavendra, A.S., and Reddy, K. 2006. Physiology and molecular biology of stress tolerance in plants: Springer. pp.1-345.
- Rashid A. 2009. Stress: Perception and Tolerance. Cap. 6 en *Molecular Physiology and Biotechnology of flowering plants*. Eds. Alpha Science International Ltd. Oxford, U.K.Rejeb, I.B., Pastor, V., and Mauch-Mani, B. 2014. Plant Responses to Simultaneous Biotic and Abiotic Stress: Molecular Mechanisms. *Plants (Basel)*. (3) :458-475.
- Shabala, S., Pottosin, I. 2014. Regulation of potassium transport in plants under hostile conditions: implications for abiotic and biotic stress tolerance. *Physiol Plant*. (151): 257-279.
- Shanahan, J., Edwards, I., Quick, J., and Fenwick, J. 1990. Membrane thermostability and heat tolerance of spring wheat. *Crop Sci*. 30(2): 247-251.
- Shinozaki, K., and Yamaguchi-Shinozaki K. 2007. Gene networks involved in drought stress response and tolerance. *J Exp Bot*. (58): 221-227.
- Shukla, L.I., Chinnusamy, V., and Sunkar, R. 2008. The role of microRNAs and other endogenous small RNAs in plant stress responses. *Biochim Biophys Acta*. 1779(11): 743-748.
 - Simms, E.L., Triplett, J. 1994. Costs and benefits of plant responses to disease: resistance and tolerance. *Evolution*. 1973-1985.
 - Sivasankar, S., Williams, R.W., and Greene, T.W. 2012. Abiotic stress tolerance in plants: an industry perspective. *Improving Crop Resistance to Abiotic Stress, Volume I & Volume 2*:27-47.
 - Squeo, F.A., Rada, F., García, C., Ponce, M., Rojas, A., Azócar, A. 1996. Cold resistance mechanisms in high desert Andean plants. *Oecol*. (105): 552-555.
 - Steponkus, P. L. 1984. Role of the plasma membrane in freezing injury and cold acclimation. *Annu Rev Plant Physiol*. 35(1): 543-584.
- Stout, M.J. 2013. Reevaluating the conceptual framework for applied research on host-plant resistance. *Insect Sci*. (20): 263-272.
- Strauss, S.Y., and Agrawal, A.A. 1999. The ecology and evolution of plant tolerance to herbivory. *Trends Ecol Evol*. (14): 179-185.
- Tripathy, J., Zhang, J., Robin, S., Nguyen, T.T., and Nguyen, H. 2000. QTLs for cell-membrane stability mapped in rice (*Oryza sativa* L.) under drought stress. *Theor Appl Genet*. 100(8): 1197-1202.
- Tuteja, N. 2007. Mechanisms of high salinity tolerance in plants. *Methods Enzymol*. (428): 419-438.
- Udawat, P., Jha, R.K., Sinha, D., Mishra, A., and Jha, B. 2016. Overexpression of a Cytosolic Abiotic Stress Responsive Universal Stress Protein (SbUSP) Mitigates Salt and Osmotic Stress in Transgenic Tobacco Plants. *Front Plant Sci*. 7:518.
- Van der Meijden, E., Wijn, M., Verkaar, H.J. 1988. Defence and regrowth, alternative plant strategies in the struggle against herbivores. *Oikos*: 355-363.
- Wahid, A., Gelani, S., Ashraf, M., Foolad, M.R. 2007. Heat tolerance in plants: an overview. *Environ Exp Bot*. 61:199-223.
- Wu, J., Lightner, J., and Warwick, N. 1997. Low-temperature damage and subsequent recovery of fabI mutant *Arabidopsis* exposed to 2 [deg] C. *Plant Physiol*. 113(2): 347-356.
- Yadav, S.K. 2010. Cold stress tolerance mechanisms in plants. A review. *Agron Sustain Dev*. 30(3): 515-527.



2.6 Regulación de la expresión génica en las plantas ante estrés por sequía

Las respuestas que las plantas manifiestan ante distintas tensiones les permiten detectar cambios ambientales precisos y responder a complejas condiciones de estrés, minimizando los daños y conservando recursos valiosos para el crecimiento y la reproducción (Atkinson and Urwin 2012, Takahashi, Kuromori et al. 2018). Para detectar, responder y adaptarse a estos ambientes estresantes, las plantas han desarrollado redes moleculares de regulación, en donde una gran variedad de genes con diversas funciones son inducidos o reprimidos para brindar tolerancia celular y fisiológica (Shinozaki and Yamaguchi-Shinozaki 2007, Takahashi, Kuromori et al. 2018, Bashir, Matsui et al. 2019, Nemali and van Iersel 2019). Varias herramientas de genómica funcional han permitido avanzar en la comprensión de la percepción y transducción de señales, así como en la elucidación de las redes moleculares de regulación asociadas a estrés (Takahashi, Kuromori et al. 2018). Estas herramientas han revelado varios genes y factores de transcripción inducibles ante estrés por sequía (Tabla 2); (Valliyodan and Nguyen 2006, Takahashi, Kuromori et al. 2018), los cuales se han clasificado en dos grupos principales; el primer grupo está implicado en cascadas de señalización y en control transcripcional, mientras que los miembros del segundo grupo han sido vinculados a la protección de las membranas celulares; es el caso de osmoprotectores, antioxidantes y catalizadores de especies reactivas de oxígeno (ROS).

Predicción de genes sensibles a sequía en <i>Arabidopsis thaliana</i>			
miRNA	GenID	Nombre	Anotación
	834345	SPL2	squamosa promoter binding protein-like 2 [Arabidopsis thaliana]
miR156a/b/c	835126	SPL13A	Squamosa promoter-binding protein-like (SBP domain) transcription factor family protein [Arabidopsis thaliana]
	841749	SPL4	squamosa promoter binding protein-like 4 [Arabidopsis thaliana (thale cress)]
	834345	SPL2	squamosa promoter binding protein-like 2 [Arabidopsis thaliana (thale cress)]
miR156d	835126	SPL13A	Squamosa promoter-binding protein-like (SBP domain) transcription factor family protein [Arabidopsis thaliana (thale cress)]
	841749	SPL4	squamosa promoter binding protein-like 4 [Arabidopsis thaliana (thale cress)]
	834345	SPL2	squamosa promoter binding protein-like 2 [Arabidopsis thaliana]
miR157	835126	SPL13A	Squamosa promoter-binding protein-like (SBP domain) transcription factor family protein [Arabidopsis thaliana]
	830497	MYB33	myb domain protein 33 [Arabidopsis thaliana (thale cress)]
miR159	820317	MYB65	myb domain protein 65 [Arabidopsis thaliana (thale cress)]
	820318	MYB66	myb domain protein 65 [Arabidopsis thaliana (thale cress)]
	829131	ARF16	auxin response factor 16 [Arabidopsis thaliana (thale cress)]
miR160	829132	ARF17	auxin response factor 16 [Arabidopsis thaliana (thale cress)]
	817382	ARF10	auxin response factor 10 [Arabidopsis thaliana (thale cress)]
	829131	ARF16	auxin response factor 16 [Arabidopsis thaliana (thale cress)]
	829132	ARF17	auxin response factor 16 [Arabidopsis thaliana (thale cress)]
	829131	ARF16	auxin response factor 16 [Arabidopsis thaliana (thale cress)]
miR166a/b	829131	ARF16	auxin response factor 16 [Arabidopsis thaliana (thale cress)]
	832295	ELM1	fission ELM1-like protein (DUF1022) [Arabidopsis thaliana (thale cress)]
	833672	ARF8	auxin response factor 8 [Arabidopsis thaliana (thale cress)]
miR167a/b/c/d/e	833672	ARF8	auxin response factor 8 [Arabidopsis thaliana (thale cress)]
	833672	ARF8	auxin response factor 8 [Arabidopsis thaliana (thale cress)]
	833672	ARF8	auxin response factor 8 [Arabidopsis thaliana (thale cress)]
	833672	ARF8	auxin response factor 8 [Arabidopsis thaliana (thale cress)]
	839913	ARF6	auxin response factor 6 [Arabidopsis thaliana (thale cress)]
	833672	ARF8	auxin response factor 8 [Arabidopsis thaliana (thale cress)]
	833672	ARF8	auxin response factor 8 [Arabidopsis thaliana (thale cress)]
miR171a/b	833672	ARF8	auxin response factor 8 [Arabidopsis thaliana (thale cress)]
	819124	HAM1	GRAS family transcription factor [Arabidopsis thaliana (thale cress)]
miR2118	823826	AT3G46730	NB-ARC domain-containing disease resistance protein [Arabidopsis thaliana (thale cress)]
	823827	AT3G46731	NB-ARC domain-containing disease resistance protein [Arabidopsis thaliana (thale cress)]
	841440	AT1G50180	NB-ARC domain-containing disease resistance protein [Arabidopsis thaliana (thale cress)]
	833508	AT5G35450	Disease resistance protein (CC-NBS-LRR class) family [Arabidopsis thaliana (thale cress)]
miR396	836395	HIR1	SPFH/Band 7/PHB domain-containing membrane-associated protein family [Arabidopsis thaliana(thale cress)]
	844079	AT1G77420	alpha/beta-Hydrolases superfamily protein [Arabidopsis thaliana (thale cress)]
	837250	AT1G07380	Neutral/alkaline non-lysosomal ceramidase [Arabidopsis thaliana (thale cress)]
	844079	AT1G77420	alpha/beta-Hydrolases superfamily protein [Arabidopsis thaliana (thale cress)]
	836395	HIR1	SPFH/Band 7/PHB domain-containing membrane-associated protein family [Arabidopsis thaliana(thale cress)]
miR403a/b	836395	HIR1	SPFH/Band 7/PHB domain-containing membrane-associated protein family [Arabidopsis thaliana(thale cress)]
	840016	AGO2	Argonaute family protein [Arabidopsis thaliana (thale cress)]
	840016	AGO2	Argonaute family protein [Arabidopsis thaliana (thale cress)]
miR482	840016	AGO2	Argonaute family protein [Arabidopsis thaliana (thale cress)]
	823826	AT3G46730	NB-ARC domain-containing disease resistance protein [Arabidopsis thaliana (thale cress)]
	820669	AT3G14460	LRR and NB-ARC domains-containing disease resistance protein [Arabidopsis thaliana(thale cress)]
	823826	AT3G46730	NB-ARC domain-containing disease resistance protein [Arabidopsis thaliana (thale cress)]
	831581	ENH1	rubredoxin family protein [Arabidopsis thaliana (thale cress)]
miR5239	841440	AT1G50180	NB-ARC domain-containing disease resistance protein [Arabidopsis thaliana (thale cress)]
	833508	AT5G35450	Disease resistance protein (CC-NBS-LRR class) family [Arabidopsis thaliana (thale cress)]
	821204	AT3G03620	MATE efflux family protein [Arabidopsis thaliana (thale cress)]
pas-mir59 (unico)	820669	AT3G14460	LRR and NB-ARC domains-containing disease resistance protein [Arabidopsis thaliana(thale cress)]
	831293	RGLG2	RING domain ligase2 [Arabidopsis thaliana (thale cress)]
	831294	RGLG3	RING domain ligase2 [Arabidopsis thaliana (thale cress)]
	836689	GTE7	global transcription factor group E7 [Arabidopsis thaliana (thale cress)]
	836689	GTE7	global transcription factor group E7 [Arabidopsis thaliana (thale cress)]
	821083	BET10	bromodomain and extraterminal domain protein 10 [Arabidopsis thaliana (thale cress)]
	843352	AT1G70160	zinc finger MYND domain protein [Arabidopsis thaliana (thale cress)]
	836689	GTE7	global transcription factor group E7 [Arabidopsis thaliana (thale cress)]
	821083	BET10	bromodomain and extraterminal domain protein 10 [Arabidopsis thaliana (thale cress)]
	836689	GTE7	global transcription factor group E7 [Arabidopsis thaliana (thale cress)]
pas-mir64	838357	AT1G17790	DNA-binding bromodomain-containing protein [Arabidopsis thaliana (thale cress)]
	838358	AT1G17791	DNA-binding bromodomain-containing protein [Arabidopsis thaliana (thale cress)]
	843352	AT1G70160	zinc finger MYND domain protein [Arabidopsis thaliana (thale cress)]
	844288	AtkdsA1	Aldolase-type TIM barrel family protein [Arabidopsis thaliana (thale cress)]
	821640	NF-YA9	nuclear factor Y, subunit A9 [Arabidopsis thaliana (thale cress)]
pas-mir41 (unico)	831124	NF-YA1	nuclear factor Y, subunit A1 [Arabidopsis thaliana (thale cress)]
	831124	NF-YA1	nuclear factor Y, subunit A1 [Arabidopsis thaliana (thale cress)]
pas-mir19	816913	TET8	tetraspanin8 [Arabidopsis thaliana (thale cress)]
	820496	ABCC3	multidrug resistance-associated protein 3 [Arabidopsis thaliana (thale cress)]
	820497	ABCC3	multidrug resistance-associated protein 3 [Arabidopsis thaliana (thale cress)]
pas-mir22a/b (unico)	820498	ABCC3	multidrug resistance-associated protein 3 [Arabidopsis thaliana (thale cress)]
	825294	SDR1	NAD(P)-binding Rossmann-fold superfamily protein [Arabidopsis thaliana (thale cress)]
	820498	ABCC3	multidrug resistance-associated protein 3 [Arabidopsis thaliana (thale cress)]
pas-mir61 (unico)	825151	LETM1	LETM1-like protein [Arabidopsis thaliana (thale cress)]
pas-mir79 (unico)	829324	CYP82C4	cytochrome P450, family 82, subfamily C, polypeptide 4 [Arabidopsis thaliana (thale cress)]
	843361	AT1G70250	receptor serine/threonine kinase [Arabidopsis thaliana (thale cress)]
	838860	AT1G22540	Major facilitator superfamily protein [Arabidopsis thaliana (thale cress)]
	843137	ANN5	annexin 5 [Arabidopsis thaliana (thale cress)]
	839666	STZ	salt tolerance zinc finger [Arabidopsis thaliana (thale cress)]
Unicos	820019	S6K2	serine/threonine protein kinase 2 [Arabidopsis thaliana (thale cress)]
	829324	CYP82C4	cytochrome P450, family 82, subfamily C, polypeptide 4 [Arabidopsis thaliana (thale cress)]
	6240759	AT1G29950	basic helix-loop-helix (bHLH) DNA-binding superfamily protein [Arabidopsis thaliana]
	831124	NF-YA1	nuclear factor Y, subunit A1 [Arabidopsis thaliana (thale cress)]
	831563	AT5G17000	Zinc-binding dehydrogenase family protein [Arabidopsis thaliana (thale cress)]

	830401	AT5G05190	hypothetical protein (DUF3133) [Arabidopsis thaliana (thale cress)]
	818736	AT2G41380	S-adenosyl-L-methionine-dependent methyltransferases superfamily protein [Arabidopsis thaliana (thale cress)]
	AAG10601	AAG10601.1	Unknown protein [Arabidopsis thaliana]
	824234	IDD2	indeterminate(ID)-domain 2 [Arabidopsis thaliana (thale cress)]
	839404	AT1G04830	Ypt/Rab-GAP domain of gyp1p superfamily protein [Arabidopsis thaliana (thale cress)]
	832513	PGL5	6-phosphogluconolactonase 5 [Arabidopsis thaliana (thale cress)]
	836806	IDD1	C2H2-like zinc finger protein [Arabidopsis thaliana (thale cress)]
	818499	AT2G39130	Transmembrane amino acid transporter family protein [Arabidopsis thaliana (thale cress)]
	831257	AT5G14080	Tetratricopeptide repeat (TPR)-like superfamily protein [Arabidopsis thaliana (thale cress)]
	824041	AT3G48800	Sterile alpha motif (SAM) domain-containing protein [Arabidopsis thaliana (thale cress)]
	843361	AT1G70250	receptor serine/threonine kinase [Arabidopsis thaliana (thale cress)]
	830015	FP6	farnesylated protein 6 [Arabidopsis thaliana (thale cress)]
	829672	LOG5	Putative lysine decarboxylase family protein [Arabidopsis thaliana (thale cress)]
	831605	AT5G17390	Adenine nucleotide alpha hydrolases-like superfamily protein [Arabidopsis thaliana]
	838187	AT1G16180	Serinc-domain containing serine and sphingolipid biosynthesis protein [Arabidopsis thaliana (thale cress)]
	816815	GRF1	growth-regulating factor 1 [Arabidopsis thaliana (thale cress)]
	836806	IDD1	C2H2-like zinc finger protein [Arabidopsis thaliana (thale cress)]
	820712	AT3G14830	epstein-barr nuclear antigen [Arabidopsis thaliana (thale cress)]
	842297	NAT7	nucleobase-ascorbate transporter 7 [Arabidopsis thaliana (thale cress)]
	828154	STP7	sugar transporter protein 7 [Arabidopsis thaliana (thale cress)]
	AAF13073.1	AAF13073.1	putative retroelement pol polyprotein [Arabidopsis thaliana]
	820931	AT3G16780	Ribosomal protein L19e family protein [Arabidopsis thaliana (thale cress)]
pas-mir36 (único)	824891	BG3	beta-1,3-glucanase 3 [Arabidopsis thaliana (thale cress)]
	828525	WRKY7	WRKY DNA-binding protein 7 [Arabidopsis thaliana (thale cress)]
	829282	WRKY11	WRKY DNA-binding protein 11 [Arabidopsis thaliana (thale cress)]
	816864	WRKY15	WRKY DNA-binding protein 15 [Arabidopsis thaliana (thale cress)]
pas-mir32 (único)	834344	AT5G43260	chaperone protein dnaJ-like protein [Arabidopsis thaliana (thale cress)]
	834602	AT5G45620	Proteasome component (PCI) domain protein [Arabidopsis thaliana (thale cress)]
	828525	WRKY7	WRKY DNA-binding protein 7 [Arabidopsis thaliana (thale cress)]
	829282	WRKY11	WRKY DNA-binding protein 11 [Arabidopsis thaliana (thale cress)]
	816864	WRKY15	WRKY DNA-binding protein 15 [Arabidopsis thaliana (thale cress)]
	831124	NF-YA1	nuclear factor Y, subunit A1 [Arabidopsis thaliana (thale cress)]
pas-mir66 (único)	843614	NF-YA3	nuclear factor Y, subunit A3 [Arabidopsis thaliana (thale cress)]
	831124	NF-YA1	nuclear factor Y, subunit A1 [Arabidopsis thaliana (thale cress)]
	831124	NF-YA1	nuclear factor Y, subunit A1 [Arabidopsis thaliana (thale cress)]

Tabla 1. Predicción y anotación de genes sensibles a estrés por sequía ubicados en *Arabidopsis thaliana* a partir de un degradoma publicado para *Paulownia australis* (Niu, Wang et al. 2016). La tabla describe una gran variedad de genes que interactúan entre si conformando una red de regulación ante estrés por sequía. Muchos de estos genes están regulados por diferentes miRNAs, algunos de ellos se ubicaron en *A. thaliana* y otros son específicos de *Paulownia australis*.

3. Planteamiento del problema

Los patrones climáticos variables afectan e impactan severamente la producción agrícola mundial. Entre otros factores, la sequía es una de las tensiones ambientales más comunes que afectan el crecimiento, desarrollo y rendimiento de las plantas. Los actuales escenarios de cambio climático predicen períodos prolongados de sequía, lo que ha enfatizado la necesidad de explorar cultivos emergentes que sean capaces de enfrentar condiciones adversas de crecimiento.

Para desarrollar plantas de cultivo con mayor tolerancia al estrés por sequía, es esencial comprender a detalle las redes fisiológicas, bioquímicas y reguladoras de genes que les brindan dichas características; esto permitirá generar estrategias de adaptación en la agricultura basadas en el análisis de características fisiológicas y agronómicas deseables. En este sentido, el cultivo de amaranto ha sido catalogado como tolerante ante distintas situaciones de estrés, por lo que ofrece una alternativa para zonas áridas donde otros cultivos producen granos de baja calidad o no son capaces de establecerse.

Atendiendo a estas necesidades, surge el interés de comprender la reprogramación de la expresión génica regulada mediante miRNAs en amaranto (*Amaranthus hypochondriacus* variedad "Gabriela") como una estrategia desarrollada por las plantas para tolerar el estrés por sequía.

4. Justificación.

La comprensión de las bases moleculares que permiten el desarrollo de estrategias de tolerancia ante estrés abiótico en las plantas, es de fundamental importancia para mejorar la productividad de cultivos. Recientemente, la susceptibilidad en los niveles de expresión de varios miRNAs ante estrés por sequía demuestra su importancia; sin embargo, no se cuenta con ningún análisis de la expresión diferencial de los genes MIRNA en respuesta al estrés por sequía en amaranto. Dada la importancia nutrimental de este cultivo y sus características de resistencia y/o tolerancia, es importante analizar la regulación de miRNAs por déficit de agua, lo que permitirá vislumbrar sus futuras aplicaciones biotecnológicas con la finalidad de generar plantas tolerantes ante estrés por sequía.

5. Hipótesis

El análisis del transcriptoma no codificante de amaranto (*Amaranthus hypochondriacus* variedad “Gabriela”) permitirá identificar los miRNAs que están regulados por déficit de agua y contribuirá a la elucidación de la red o redes de regulación génica que se activa ante el estrés por sequía en este cultivo.

6. Objetivo general:

Analizar el miRNoma de *Amaranthus hypochondriacus* variedad “Gabriela” y la expresión de sus genes blanco bajo condiciones de estrés por sequía haciendo uso de herramientas moleculares que permitan la identificación de miRNAs con posible aplicación biotecnológica

7. Objetivos particulares:

1. Describir el ciclo de vida de *Amaranthus sp* bajo condiciones de invernadero y determinar la etapa para el tratamiento de sequía
2. Explorar el genoma de amaranto utilizando herramientas bioinformáticas para la identificación y selección de miRNAs y la predicción de sus genes blanco.
3. Identificar por secuenciación masiva, miRNAs de plantas de amaranto sometidas a estrés por sequía.
4. Realizar análisis *in-vitro* para la validación de los miRNAs seleccionados y sus respectivos genes blanco.
5. Realizar la caracterización funcional de alguno de los miRNAs previamente validados en amaranto.

8. Estrategia experimental

El presente trabajo de investigación plantea la identificación y el análisis de expresión de miRNAs en plantas de amaranto (*Amaranthus hypochondriacus* V. *Gabriela*) bajo condiciones normales de cultivo y sometidas a estrés por sequía, así como la predicción de sus genes blanco. La estrategia experimental para el cumplimiento de los objetivos que se establecen se dividió en cinco fases experimentales: Fase I: Descripción del ciclo de vida de *Amaranthus sp.* bajo condiciones de invernadero y selección de la etapa considerada para los análisis posteriores, Fase II Predicción bioinformática de miRNAs en *Amaranthus hypochondriacus*, Fase III: Secuenciación masiva de miRNAs en *Amaranthus hypochondriacus* variedad “Gabriela”, Fase IV: Validación de miRNAs y genes blanco identificados y Fase V: Análisis funcional de alguno de los miRNAs previamente validados. Cada una de estas fases se subdivide en etapas que coadyuvan al cumplimiento de cada uno de los objetivos que se plantean en el presente proyecto de investigación. Los resultados de cada fase se incluyen en el capítulo correspondiente a cada objetivo organizando la información en formato de artículos.

CAPITULO I:

Descripción del ciclo de vida de *Amaranthus sp.* bajo condiciones de invernadero y determinar la etapa para el tratamiento de sequía

1. Introducción

La fenología vegetal es el estudio de patrones periódicamente recurrentes de crecimiento y desarrollo de las plantas durante su ciclo de vida (Piao, Liu et al. 2019). En un contexto agronómico, la descripción de la fenología durante el desarrollo vegetativo y reproductivo de las plantas es fundamental para desarrollar estrategias que apoyen el trabajo de investigadores y fitomejoradores en programas de mejoramiento genético. En este sentido, y desde una perspectiva internacional, la escala decimal *Biologische Bundesanstalt Bundessortenamt und Chemische Industrie* (BBCH) nos permite definir los eventos fenológicos de plantas de importancia agrícola (Salazar, Melgarejo et al. 2006, Meier, Bleiholder et al. 2008, Meier, Bleiholder et al. 2009, Archontoulis, Struik et al. 2010, Martinelli and Galasso 2011) y satisfacer así la necesidad de conocimientos básicos sobre la biología y los puntos críticos durante su ciclo de vida (Hack, Bleiholder et al. 1992). Pese a varios intentos de descripción, antes de este trabajo no existía un consenso internacional que diera seguimiento a las distintas etapas de desarrollo del amaranto. Por tal motivo, en la primera parte del presente trabajo de investigación nos dimos a la tarea de establecer una escala estándar como un criterio único para cuantificar la fenología de tres especies distintas del género *Amaranthus*: *Amaranthus hypochondriacus*, *Amaranthus cruentus* y *Amaranthus hybridus*. Para una revisión más detallada de las fases fenológicas que comprenden el ciclo de vida del género *Amaranthus* consultar el artículo titulado “*The phenological growth stages of different amaranth species grown in restricted spaces based in BBCH code*” <https://doi.org/10.1016/j.sajb.2019.05.035>.



The phenological growth stages of different amaranth species grown in restricted spaces based in BBCH code

M. Martínez-Núñez^a, M. Ruiz-Rivas^a, P.F. Vera-Hernández^a, R. Bernal-Muñoz^b,
S. Luna-Suárez^a, F.F. Rosas-Cárdenas^{a,*}

^a Instituto Politécnico Nacional, Centro de Investigación en Biotecnología Aplicada, Ex-Hacienda San Juan Molino Carretera Estatal Tecuexcomac-Tepetitla Km 1.5, Tlaxcala C.P. 90700, México

^b Tecnológico Nacional de México, Instituto Tecnológico del Altiplano de Tlaxcala, Km. 7.5 Carretera Federal San Martín-Tlaxcala, San Diego Xocoyucan, Tlaxcala C.P. 90122, México

ARTICLE INFO

Article history:

Received 6 March 2019

Received in revised form 2 May 2019

Accepted 26 May 2019

Available online xxxx

Edited by MG Kulkarni

Keywords:

BBCH coding system

Phenological stages

Growth

Amaranth development

Panicle

ABSTRACT

Amaranth is a pseudocereal with potential health benefits. Amaranth has recently gained importance due to its high capacity to grow in adverse conditions. Details about the growth and development of amaranth is fundamental to its cultivation, but reports on the phenological growth stages, development, and the life cycle of amaranth are limited. Under normal conditions, amaranth plants are as high as 2.2 m, making their handling difficult. Thus, this study determined the phenological growth stages and life cycle of amaranth in restricted spaces. *Amaranthus cruentus*, *Amaranthus hybridus*, and *Amaranthus hypochondriacus* plants were cultivated in restricted spaces. The physiological and qualitative features as number of leaves, length of plants and leaves, panicle color, were used to determine the different phenological growth stages and life cycle of amaranth plants. The phenological growth stages were described via Biologische Bundesanstalt Bundessortenamt and Chemische Industrie (BBCH) decimal code. Plants between 15 and 22 cm were generated, and each phenological growth stage was easily managed in restricted spaces. The time for each phenological growth stage was examined in different amaranth species and this offered a general representation of the phenological growth stages and life cycle of amaranth. This work established the phenological growth stages of amaranth based on the BBCH coding system managed in restricted spaces. These observations allow us to envision amaranth as a model plant in which each phenological growth stage describing its life cycle is managed easily under limited spaces, which could be an advantage for better manipulation and future studies.

© 2019 SAAB. Published by Elsevier B.V. All rights reserved.

1. Introduction

Amaranth is a crop with high potential for economic exploitation similar to maize, wheat, sorghum, barley, rice, and soybean (Innovation, 1984; Rastogi and Shukla, 2013; Akin-Idowu, 2017). Amaranth has an excellent nutritional value and high genetic and phenotypic diversity (Lee et al., 2008; Brenner et al., 2010; Rastogi and Shukla, 2013; Venkatesh et al., 2014; Akin-Idowu et al., 2016; Stetter et al., 2016). Amaranth is an annual, dicotyledonous and herbaceous plant (Brenner et al., 2010; Akin-Idowu et al., 2016; Das, 2016). Some studies have described amaranth productivity (Das, 2016; Kirillova et al., 2016; Kuluev et al., 2017), cultivation conditions (Das, 2016; Stetter et al., 2016), morphological diversity (Lee et al., 2008; Ray and

Roy, 2009; Akin-Idowu et al., 2016; Das, 2016), adaptability (Lee et al., 2008; Huerta-Ocampo et al., 2014; Massange-Sanchez et al., 2015; Palmeros-Suarez et al., 2015; Vargas-Ortiz et al., 2015; Das, 2016), and new varieties (Akin-Idowu et al., 2016; Das, 2016). Amaranth can also easily adapt to adverse growth conditions (Delano-Frier et al., 2011; Caselato-Sousa and Amaya-Farfan, 2012; Huerta-Ocampo et al., 2014; Das, 2016). Amaranth has a high degree of phenotypic plasticity (Shukla et al., 2010; Khanam and Oba, 2014), defined as the ability of an organism to change its phenotype in response to changes in the environment (Price et al., 2003; Fazlioglu and Bonser, 2016).

Information about the phenological growth stages of crops is fundamental and useful to agriculture. Some studies of the phenological growth stages from maize (Bussel et al., 2015), wheat (Bussel et al., 2015; Ihsan et al., 2016), sorghum (Kumar et al., 2009), barley (Hossain et al., 2012), rice (Zhang et al., 2013; Zhang et al., 2016), and soybean (Choi et al., 2016; Salmeron and Purcell, 2016) have been described; however, information on amaranth's life cycle is limited. In amaranth, as in other crops, it is still necessary to establish a standard scale as a unique criterion to quantify phenology and to analyze the plant structure that enable the formulation of rational plant breeding

Abbreviations: BBCH, Biologische Bundesanstalt Bundessortenamt und Chemische Industrie; E, Episperm; P, Perisperm; SAS/STAT, State-of-the-art Statistical Analysis Software; GGD, Growing degree days; ANOVA, Analysis of variance; LSD, Least Significant Difference.

* Corresponding author.

E-mail address: frosasc@ipn.mx (F.F. Rosas-Cárdenas).

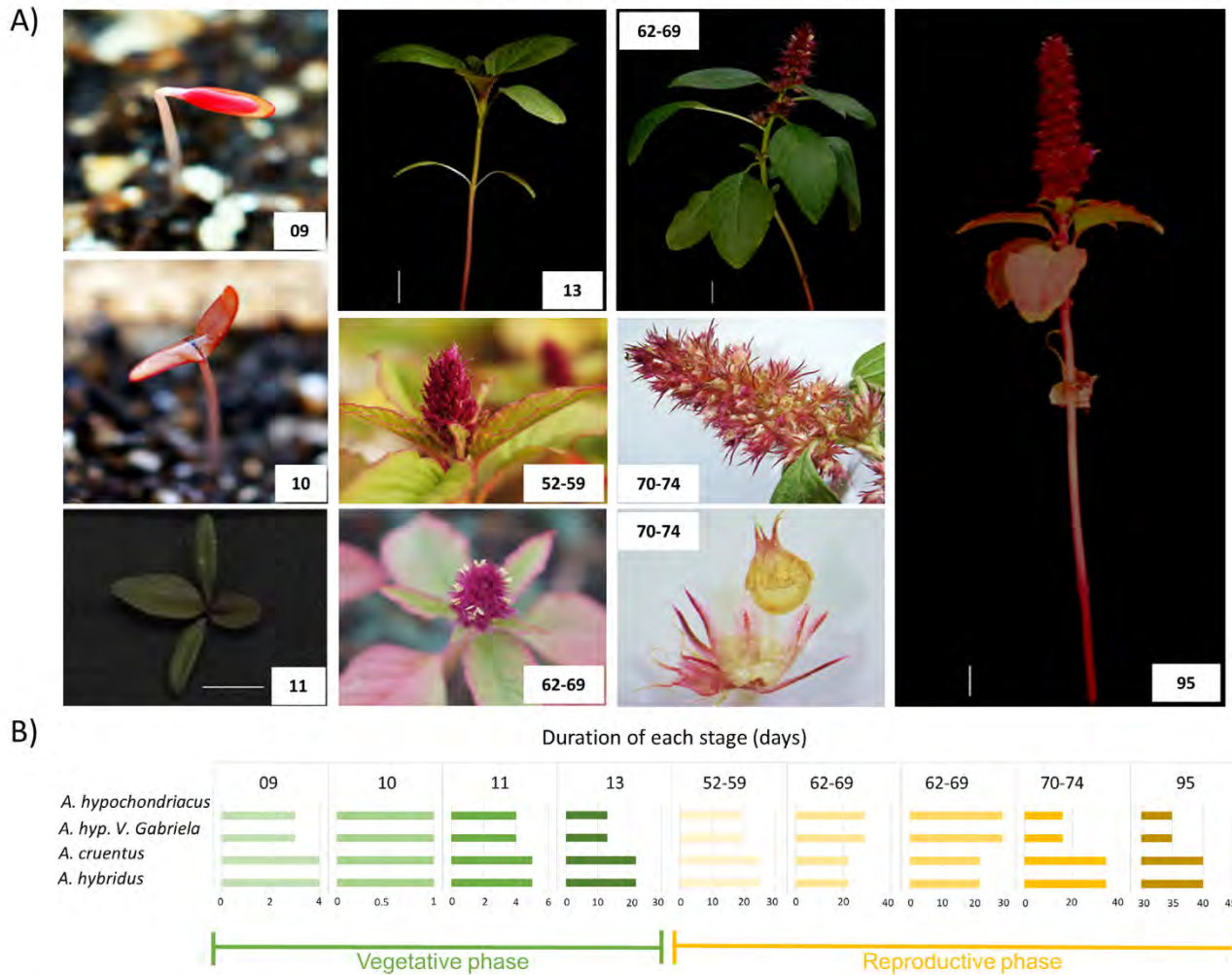


Fig. 1. The phenological growth stages of amaranth in restricted spaces. Representation of growth stages from *A. hypochondriacus* “Gabriela” variety in restricted spaces. The number is the BBCH code. Scale bar, 1 cm.

approach. The BBCH scale is a system for a uniform coding of phenologically similar growth stages of all mono- and dicotyledonous plants using a decimal coding system (Meier et al., 2009). These data were used to compare amaranth's growth in limited spaces. In this research three species and one variety of amaranth were studied in terms of their phenological growth stages and life cycle in restricted spaces. Phenological features were studied for the establishment of the life cycle using the BBCH scale (Hack et al., 1992).

2. Materials and methods

2.1. Plant material

The three *Amaranthus* species were *A. hypochondriacus*, *A. hybridus*, and *A. cruentus* (provided by Dr. Cesar A. Reyes López of Escuela Nacional de Medicina y Homeopatía del Instituto Politécnico Nacional of Mexico), as well as the “Gabriela” variety of *A. hypochondriacus* (generated in the Instituto Tecnológico del Altiplano de Tlaxcala also from Mexico). Seeds were sterilized with 10% sodium hypochlorite commercial solution and 50% ethanol, for 5 and 1 min, respectively. The seeds were rinsed three times for 3 min with sterile water after each immersion.

2.2. Plant growth and monitoring

Polystyrene trays with wells of 2.54 cm × 2.54 cm × 6.5 cm depth were used as restricted spaces to cultivate amaranth. The sterile

substrate was composed of peat moss, perlite, and vermiculite (3:1:1 v/v ratio). The seeds of each species were germinated under semi-controlled greenhouse conditions in polystyrene trays, in February 2016. Plants were grown in the Centro de Investigación en Biotecnología Aplicada del Instituto Politécnico Nacional (CIBA-IPN), Tlaxcala, México (19°16'53.2" N and 98°21'57.3" W; 2260 m above sea level). Plants were grown in short days. The temperature in the greenhouse vary from 21 to 39 °C, and the relative humidity fluctuate between 15.6 and 49%. Irrigation was performed every third day obtaining an average of 85% humidity in the substrate. The humidity was recorded with an MB45 thermobalance (Ohaus Corporation, New Jersey, USA). Twenty plants randomly selected were used to determine the different phenological growth stages in yield. To calculate the daily thermal units, the equation of Gilmore & Rogers (1958) was used ($GGD = [(T_{max} + T_{min})/2] - T_b$), where T_{max} - T_{min} are daily maximum and minimum air temperatures, respectively. T_b is the base temperature, evaluated at 10 °C. The maximum and minimum daily temperatures were obtained from the INIFAP station: 998416, Muñoz de Domingo Arenas, Tlaxcala monitored from February–June 2016.

2.3. Photographic record and microscopy analysis

A photographic record of amaranth species used an SLT-A37K camera (Sony, California, USA) coupled to a macro lens DT 2.8/30. The morphology of complex structures such as flowers and seeds was analyzed in a Zeiss Stemi 508 stereomicroscope, with a Zeiss Axiocam ERC 5s Rev. 2.0 camera; this was visualized with the ZEN lite software (Zeiss, Jena,

Phenological growth stages of Amaranth									
Principal Stage (BBCH code)	0	1			5	6		7	8-9
Stage	(00-09)	(10)	(11)	(12-13)	(50-59)	(60-69)	(60-69)	(70-77)	(80-99)
Phenological growth stages	Germination	Opening of cotyledons	True leaves 2 leaves	5-6 leaves	Apical inflorescence	Anthesis	Axillary inflorescence	Seed development	Ripening and senescence
Days post-seeding	3-4	4-5	8-10	21-32	40-57	69-79		85-113	120-153
GDD °C	13-16	16-20	26-24	63-115	130-218	299-377		410-644	709-731
	Vegetative phase				Development of vegetative structures				
					Reproductive phase				
	Planting				Panicle exertion				

Fig. 2. General schematic representation of the phenological growth stages of amaranth, in restricted spaces. The vegetative and reproductive phase are indicated, as are the life cycle stages of amaranth including duration and days post-seeding for each principal phenotype. GGD, growing degree-days, estimated using the data of the INIFAP Station: 998416, Muñoz de Domingo Arenas, Tlaxcala (February–June 2016), using degree Celsius (°C). Days post seeding: the ranges showed between the different species used in this work.

Table 1

Description of the phenological growth stages of Amaranth sp. according to the BBCH scale.

Principal growth stage BBCH	BBCH Code	Description	
0: Germination	00	Dry seed	
	01	Beginning of seed imbibition	
	03	Seed imbibition completed	
	05	Radicle emerged from seed	
	06	Radicle elongated, root hairs and/or side roots visible	
	08	Emergence of hypocotyl	
	09	Emergence of cotyledons through soil	
	1: Leaf development	10	Cotyledons fully emerged/Opening of cotyledons
		11	First pair of leaves visible
12		Second pair of leaves visible	
13		Five or six leaves visible	
1...		Stages continuous till...	
3: Stem elongation		The longitudinal growth of the main stem occurs in parallel with the leaf development. That is why the coding of the main stadium 3 is omitted	
5: Inflorescence emergence	50	Beginning of panicle emergence (panicle still enclosed by leaves)	
	51	Leaves surrounding inflorescence separated, inflorescence is visible from above	
	52	Panicle visible from the sides (panicle's indeterminate growth habit)	
	59	Inflorescence visible, but all flowers are still closed	
6: Anthesis and axillary inflorescence	60	Beginning of anthesis: main inflorescence flowers with first extruded anthers (acropete flowering)	
	63	Staminate and pistillate flowers visible	
	65	Full flowering: anthers visible on most panicle	
	69	End of flowering: The panicle have completed flowering, but some senesced anthers may remain	
7: Fruit and seed development)	70	Ovary thickening (development of the fertilized ovule)	
	71	Watery ripe: The first visible grains have reached half their final size	
	73	Early milk: Immature grains (the grains show a milky consistency)	
	75	Medium milk: Grains with a white coloration of opaque tone and a pasty consistency	
	77	Late milk: the grain's texture is slightly rough, and their coloration becomes opaque ivory	
8: Ripening Seed ripening	80	Milky grain, grain content soft but dry, easily crushed with fingernails	
	85	Hard dough: Grain content solid, easily crushed with fingernails	
9: Senescence	89	Ripe grain: difficult to crush with fingernails, dry content, the grain has an opaque ivory color on its outside. Ready to harvest.	
	95	Panicle changes color	
	97	Plant dead and collapsing	
	99	Harvested product	

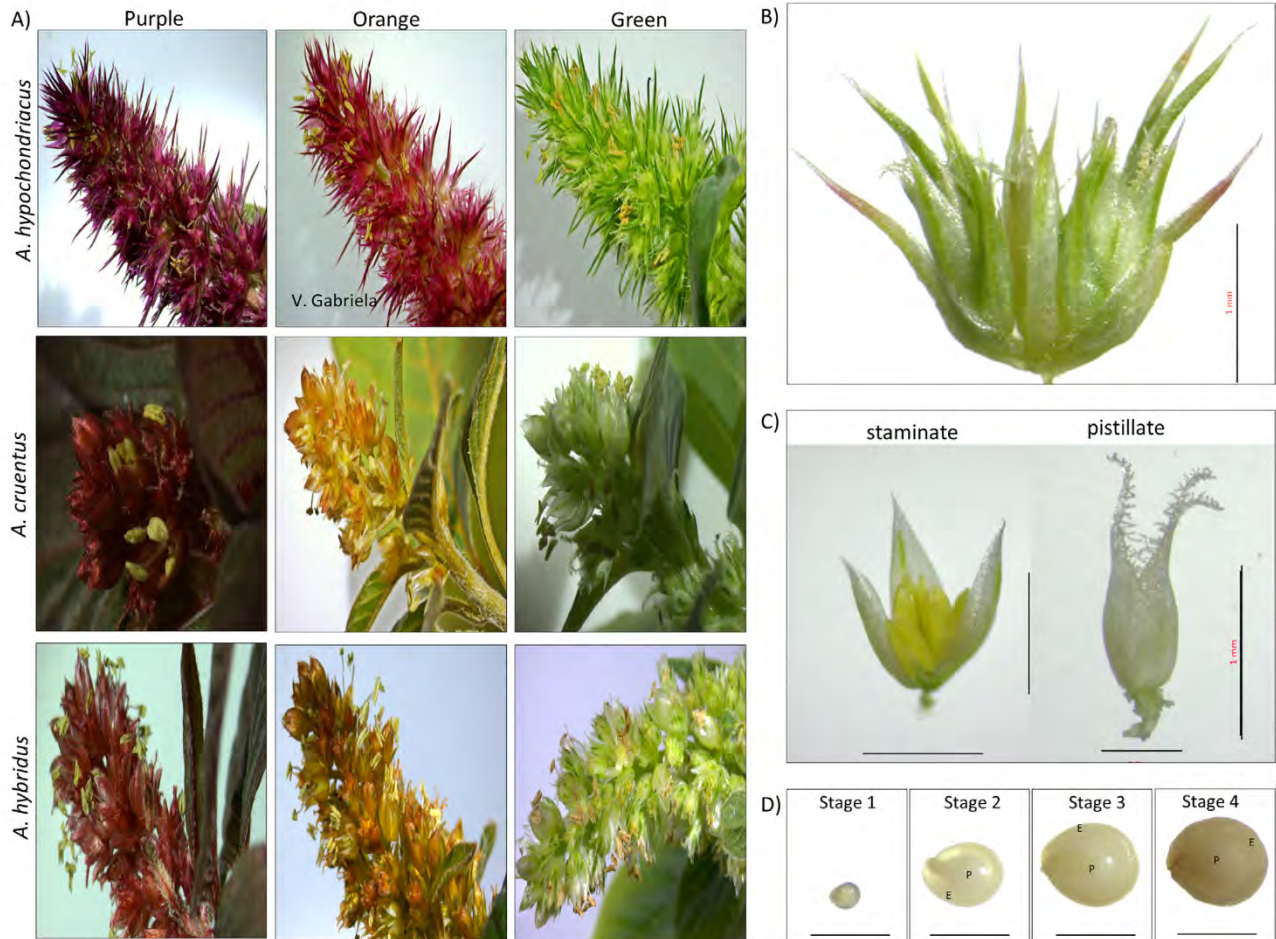


Fig. 3. Development of panicle, flowers, and seeds in amaranth. (A) Panicle of *A. hypochondriacus*, *A. cruentus*, and *A. hybridus* plants, grown in the greenhouse 10 weeks post-seeding; the plants were classified by panicle color. (B) Glomerulus of *A. hypochondriacus*. (C) Male and female flowers in *A. hypochondriacus*. (D) Different stages of seed development. The peripheric embryo or episperm, and perisperm structures are represented by E and P, respectively. Scale bar, 1 mm.

Germany). Twenty pistillate flowers and twenty staminate flowers and fifty seeds per specimen were randomly selected for analysis under microscope.

2.4. Statistical analysis

At least 20 plants randomly selected were used for each species and variety analyzed. For each plant, the length and number of leaves was measured. For the length of leaves, the first true leaf of each plant was measured. The number of leaves was counted at the beginning of the reproductive stage (stage 13). Data from plants in the greenhouse were analyzed using SAS/STAT® software and included variables such as plant height, number, and length of the leaves. Analysis of variance (ANOVA) using Fisher's Least Significant Difference (LSD) test with a significance level of $p < .05$ were performed.

3. Results

3.1. Phenological growth stages of amaranth in restricted spaces

The phenological growth stages of amaranth were studied using specimens grown in limited spaces (Fig. 1A). Plants between 15 and 22 cm were obtained in restricted spaces (Fig. 1A). The period for each phenological stage was analyzed across all species, to prepare a general representation of the phenological growth stages of amaranth. Similar

to other crops, the amaranth life cycle was divided into vegetative and reproductive phases. The BBCH scale was used to establish the amaranth's phenological growth stages. Some principal stages were omitted including the formation of side shoots (stage 2) and stem elongation (stage 3), which coincides with leaf development (stage 1). The growth of harvestable vegetative plant parts (stage 4) was omitted because only the seeds are harvested for these amaranth species. The time needed for each stage varied between species (Fig. 1B). In restricted spaces, the life cycle of amaranth required 120 days for *A. hypochondriacus* and *A. hypochondriacus* variety "Gabriela"; *A. cruentus* and *A. hybridus* needed 153 days (Fig. 2). The vegetative phase showed a rapid increase in size and foliage including the principal stages 0 and 1 on the BBCH code (Figs. 1, 2). The transition from vegetative to reproductive phase started at 40 days post-seeding in *A. hypochondriacus* and "Gabriela" variety; *A. hybridus* and *A. cruentus* started at 57 days post-seeding (Fig. 1B, 2). The principal growth stages 5–9 were included in the reproductive phase (Fig. 2).

3.2. Germination

Stage 0 comprised the germination and included root (stage 05), hypocotyl (stage 08), and cotyledon emergence (stage 09) (Table 1). Stage 09 occurred three days post-seeding in *A. hypochondriacus* and four days post-seeding in *A. cruentus* and *A. hybridus* (Fig. 1B).

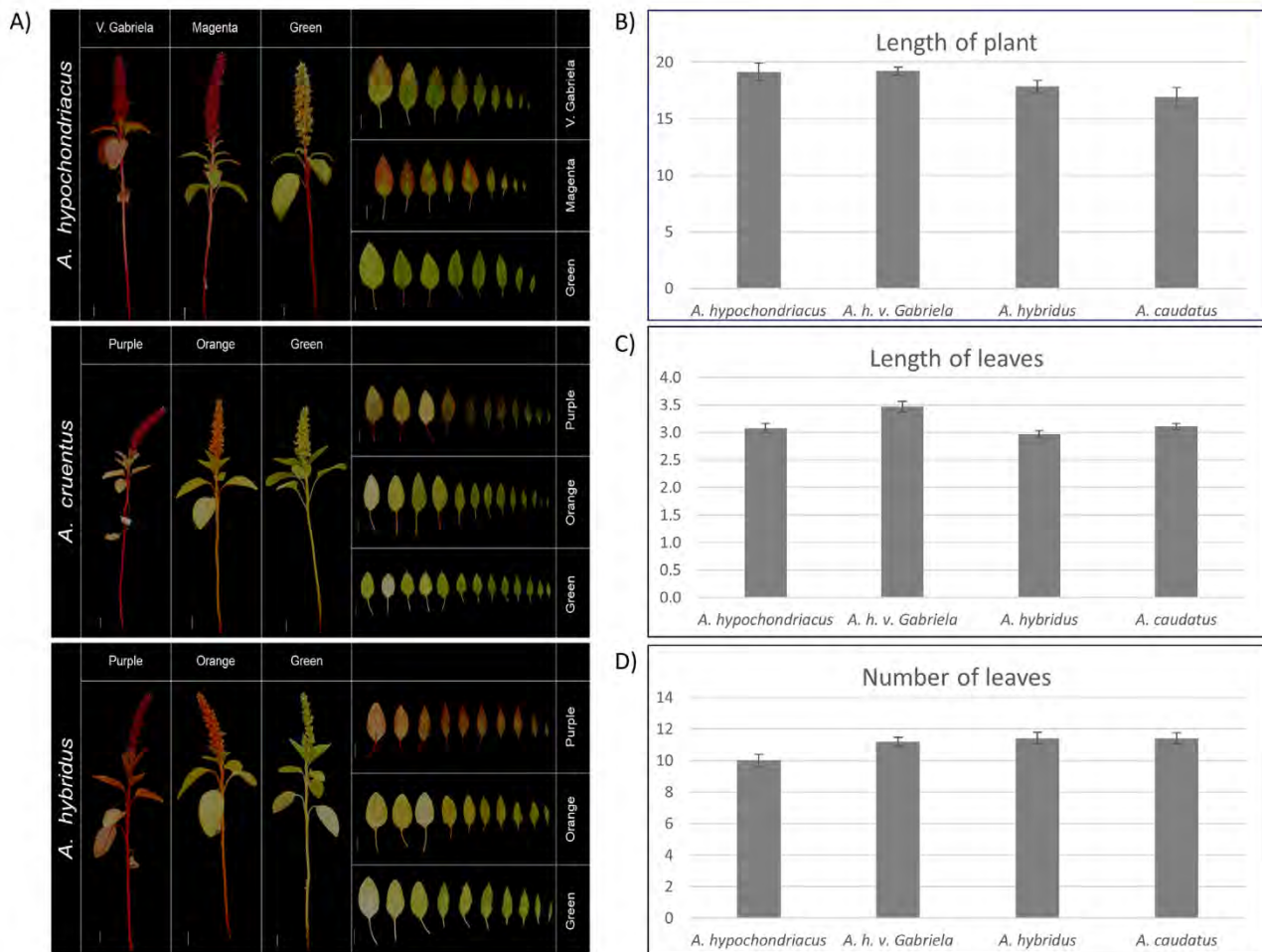


Fig. 4. Phenotype differences of panicle, plant, and leaves between species of amaranth. (A) Comparison of plant whole parts and leaves of different species of amaranth (Stage 8–9). Plants in stage 13 were classified. (B) Plant height, (C) Leaf length, and (D) Number of leaves were analyzed. Analysis of variance using Fisher's Least Significant Difference (LSD) test with significance $P < .05$ was performed.

3.3. Leaf development

The principal growth stage 1 denominated leaf development, included the opening of cotyledons (stage 10) to leaf development (Fig. 1, Table 1). Stage 10 occurred four or five days post-seeding and required just one day. The emergence of true leaves (stage 11) was observed eight to ten days post-seeding and needed four or five days (Figs. 1, 2). Stage 13 was the extended vegetative phase and included plants with five or six leaves (Fig. 1A) this happened 21 days post-seeding in *A. hypochondriacus* and 32 days post-seeding in *A. cruentus* and *A. hybridus* and lasted for 20 days (Figs. 1B, 2).

3.4. Apical inflorescence emergence

The panicle exertion denominated "Principal growth stage 5" and known as inflorescence emergence occurred at various times across species. In *A. hypochondriacus*, and *A. hypochondriacus* variety "Gabriela", the panicles were observed after 40 days post-seeding. This happened at 57 days in *A. hybridus* and *A. cruentus*. (Fig. 1B).

3.5. Anthesis and axillary inflorescence

The principal growth stage 6 includes the anthesis and the outbreak of axillary inflorescences; these processes overlap in the amaranth life cycle (Table 1). *A. hypochondriacus* and *A. hypochondriacus* variety "Gabriela" initiated principal stage 6 around 69 days post-seeding: *A.*

cruentus and *A. hybridus* started ~79 days post-seeding (Fig. 2). There were differences in compaction, density, posture, size of bracts, and color among the panicles of each species (Fig. 3A). Anthesis occurred after panicle emergence (22–29 days).

Unisexual flowers characterized monoecious amaranth i.e., glomerulus (Fig. 3B), staminate, or pistillate (Fig. 3C) (Mlakar et al., 2009; Rastogi and Shukla, 2013). The highest amount of pollen was released in the first three or four days post-anthesis. The pollination usually started with flowers of glomerulus located in the upper half of the panicle. Male flowers (staminate) matured before female flowers (pistillate), i.e., the release of pollen began 1–2 days earlier offering successful fertilization of the female flowers contained in the panicle. Amaranth has indeterminate growth (Pandey and Singh, 2009), and the presence of the vegetative structures continued during the reproductive phase. There was simultaneous appearance of leaves, branches, axillary flowers and flowers on the panicle.

3.6. Fruit and seed development

The principal stage 7 included the fruit and seed development. Seeds of the panicle base were used for monitoring. Fertilization started from the base to the panicle apex, and seeds reached maturity at a different time in each plant. The first stage of seed development included stages 70 and 71 on the BBCH code (Table 1). The first stage of seed development occurred around 85 days post-seeding (five days after fertilization (Fig. 3C)) and lasted approximately one week. This began with the

Life cycle of Amaranth

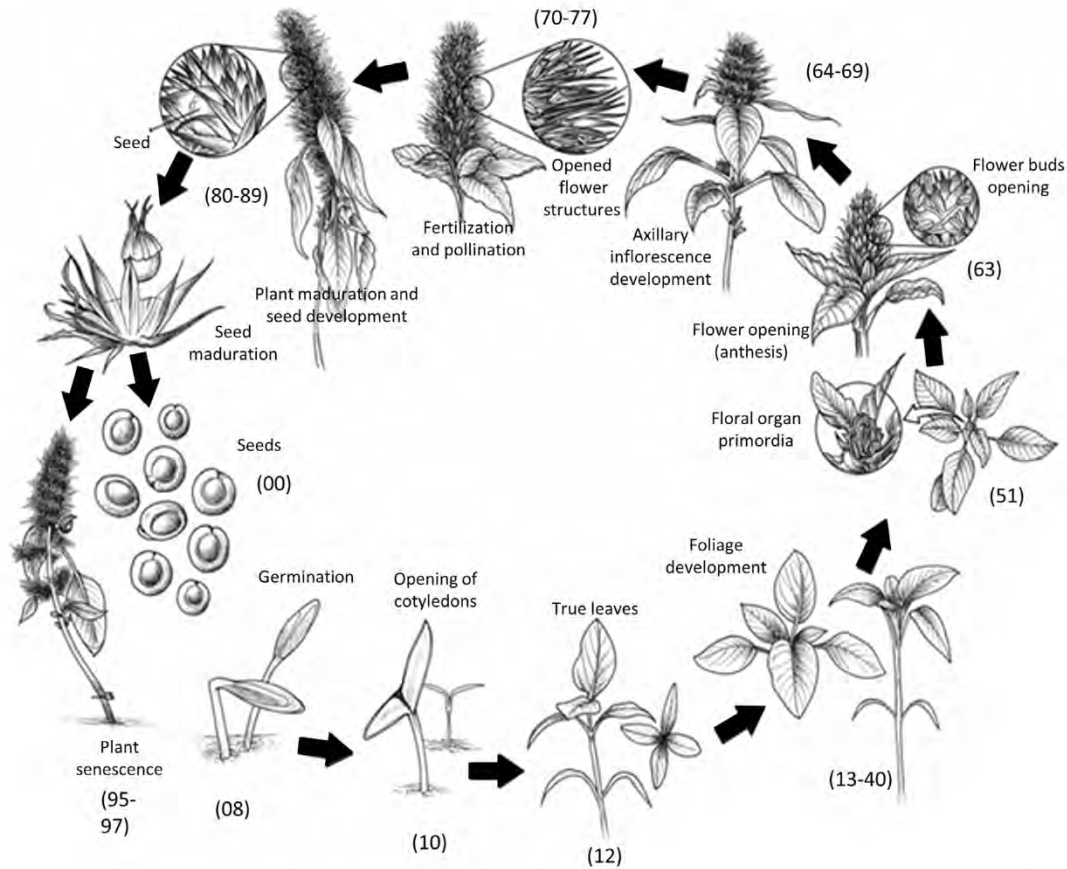


Fig. 5. The life cycle of amaranth. Principal characteristics of amaranth in greenhouse conditions were considered to represent the life cycle of amaranth including germination until seed maturation and plant senescence. The term in parentheses is the BBCH code.

development of the fertilized ovule forming an irregular structure of translucent grayish coloration and mucoid consistency measuring between 0.3 and 0.5 mm long (Fig. 3D).

The second stage of seed development (stage 73) occurred between 100 and 110 days post-seeding for *A. hypochondriacus* and *A. hypochondriacus* variety “Gabriela,” and *A. cruentus* and *A. hybridus*, respectively. The second stage of seed development was characterized by immature grains with a rounded elliptic shape with translucent white color and a soft texture approximately 1 mm long (Fig. 3D). In the second stage, the grains showed a milky consistency that produced viscous white liquid when pressed with fingers. The third stage of seed development (stage 75) occurred at 110 and 120 days post-seeding in *A. hypochondriacus* and *A. hypochondriacus* variety “Gabriela,” and *A. cruentus* and *A. hybridus*, respectively. Here, the rounded elliptical structure of the seeds was preserved, but now with an approximate length of 1.3 mm in diameter (Fig. 3D). These presented a white coloration of dark tone and firmer consistency. The seeds still needed to ripen because they burst and had a pasty consistency with a whitish color when pressed between the fingers. The last stage of seed development (stage 89) included seed ripening began 120 days post-seeding in *A. hypochondriacus* and *A. hypochondriacus* variety “Gabriela” and 153 days post-seeding in *A. cruentus* and *A. hybridus* and ended when the seed was ~1.5 mm in diameter (Fig. 3D). At this time, the seeds retained their rounded elliptical appearance. However, their texture was slightly rough with an opaque ivory coloration (Fig. 3D). The peripheric embryo or episperm (E) formed by the cotyledons and the radicle tip was obvious upon maturity; these surrounded the perisperm (P) or reserve tissue of the seed (Fig. 3D). The complete maturation of

seeds followed the highest degree of physiological maturity; thus, we noted easy detachment of seeds filled with panicles when shaking the plant.

3.7. Ripening and senescence

The maximum degree of physiological maturity in the different amaranth species coincided with the maturation of all seeds. The seeds became hard with an opaque ivory coloration and detached easily from the panicle (stage 89) (Table 1). The overlap between ripening and senescence in amaranth plants (principal growth stages 8 and 9 in the BBCH code, respectively) was observed and occurred 120 or 153 days post-seeding (Fig. 2, Table 1). There was obvious deterioration of the plant including decaying, wilting and change of coloration in leaves, stems, and panicle (Fig. 4). The panicles exhibited the most visible phenotypic changes (Fig. 4).

We studied the diversity of plant coloration in greenhouses (Figs. 3A, 4). The panicle color is the most commonly used criteria to determine physiological maturity (Manikandan and Srimathi, 2015). The bright green panicle was dark green, the lime changed to pale green. The red became a red-brown, and the orange became golden corresponding to stage 95 (Fig. 4, Table 1). The analysis of variance (ANOVA) of plant height did not show a significant difference ($P > .05$) between *A. hypochondriacus* and the “Gabriela” variety of *A. hypochondriacus*, but there was a significant difference ($P > .05$) observed in respect to *A. cruentus* plant height (Fig. 4B). Plants of *A. hypochondriacus* were 6 and 11% taller than *A. hybridus* and *A. cruentus*, respectively. The “Gabriela” variety of *A. hypochondriacus* had the largest leaves (Fig.

4C), and *A. hypochondriacus* had the smallest (Fig. 4D). The analysis of variance between species, showed a significant difference ($P > .05$) in leaves length of the Gabriela" variety of *A. hypochondriacus* (Fig. 4C) and the number of leaves in *A. hypochondriacus*.

4. Discussion

4.1. Relevance of amaranth growth in restricted spaces

Amaranth is a crop with high potential for economic exploitation, due to its excellent nutritional value, and likewise for its high plasticity and easy adaptation to adverse growth conditions (Delano-Frier et al., 2011; Huerta-Ocampo et al., 2014; Khanam and Oba, 2014). Amaranth plants under field conditions range between 2.0 and 2.2 m. The plasticity of amaranth enabled its monitoring in restricted spaces. Plants between 15 and 22 cm were obtained in restricted spaces. These observations highlight the extensive phenotypic plasticity of amaranth. In summary, amaranth growth in restricted spaces presents an interesting and practical tool to establish crops not only for research purposes but also to improve this ancient crop, which could be an advantage for better manipulation such as the selection and development of varieties in small areas.

4.2. The phenological growth stages of amaranth based in BBCH code

The BBCH scale help to define the phenological events of all species of mono- and dicotyledonous plants. The utility of the BBCH scale has been validated in the description of several traits of agronomic interest at specific developmental stages of different plants (i.e. Munger et al., 1997; Erten et al., 2014; Herraiz et al., 2015; Sosa Zuniga et al., 2017). Principal growth stages in different amaranth species included germination, leaf development, inflorescence emergence and flower development, anthesis, development of seeds, ripening of seeds, and senescence were identified. Although differences in the panicle structure and size, and leaf number were observed between species, the main stages that describe the life cycle of amaranth were observed (Fig. 2). Based on the existing BBCH scale eight principal growth stages (stage 0–2, 5–9) were identified in the growth cycle of three amaranth species. The period for each phenological stage of different amaranth species was determined, and the principal stages were monitored allowing to obtain a schematic representation of the phenological growth stages of amaranth (Figs. 1B, 2). As in other plants (Martinelli and Galasso, 2011; Herraiz et al., 2015; Acosta-Quezada et al., 2016), BBCH-scale stage 3 and stage 4 (Stem elongation and development of harvestable vegetative parts respectively) are not applicable to amaranth due to the longitudinal growth of the main stem which occurs in parallel with the leaf development and because in amaranth usually only seeds are harvested. Each principal stage was subdivided into secondary stages to allow a detailed description of the amaranth development (Table 1). The principal characteristics of amaranth grown in restricted spaces based in BBCH code were used to represent the life cycle of amaranth since germination until plant senescence (Fig. 5). The phenological characterization in this crop in restricted spaces is relevant for future studies which would be of great utility for agronomic and botanical research of amaranth.

5. Conclusions

In conclusion, these data allow us to envision amaranth as a model plant in which each phenological growth stage is easily managed under restricted spaces, which could be an advantage for better manipulation and can be considered for future studies, such as the selection and development of varieties in small areas. This could be an advantage for a better manipulation to generate new genetic variation and for laboratory studies. To our knowledge, this is the first study that determines the developmental stages using the BBCH scale, and proposes the life cycle of Amaranth growth under confined spaces conditions. We hope

the BBCH scale established and the life cycle of amaranth will be used to characterize development and facilitate comparison between studies.

Author contributions

MMN did the major experimental work. MRR contributed to the experimental analysis. RBM generated the variety "Gabriela." MMN and FFRC conceived the project. MMN, SLS, and FFRC designed the experiments. MMN, PFVH, and FFRC drafted the manuscript. All authors read and approved the final manuscript.

Conflicts of interest

The authors declare no conflict of interest.

Financial support

MMN, MRR, PFVH, were supported by the Mexican National Council of Science and Technology (CONACyT) fellowship (MMN: 270563, MRR: 251176, PFVH: 287820). This work was financed by the CONACyT grant CB-2013-221522, and SIP grants 20180545 and 20195904.

Acknowledgments

We thank Dr. Cesar Augusto Sandino Reyes López of the National School of Medicine and Homeopathy of the National Polytechnic Institute of Mexico for the donation of amaranth seeds. Thanks to CONACyT and SIP for financial support.

References

- Acosta-Quezada, P.G., Riofrio-Cuenca, T., Rojas, J., Vilanova, S., Plazas, M., Prohens, J., 2016. Phenological growth stages of tree tomato (*Solanum betaceum* Cav.), an emerging fruit crop, according to the basic and extended BBCH scales. *Sci. Hortic.* 199, 216–223. <https://doi.org/10.1016/j.scienta.2015.12.045>.
- Akin-Idowu, P., 2017. Nutritional evaluation of five species of grain amaranth – an underutilized crop. *Int. J. Sci.*, 18–27 <https://doi.org/10.18483/ijSci.1131>.
- Akin-Idowu, P., Gbadegehin, M., Orkpeh, U., Ibitoye, D., Oduola, O., 2016. Characterization of grain amaranth (*Amaranthus* spp.) germplasm in South West Nigeria using morphological, nutritional, and random amplified polymorphic DNA (RAPD) analysis. *Resources* 5, 6. <https://doi.org/10.3390/resources5010006>.
- Brenner, D., Baltensperger, D., Kulakow, P., Lehmann, J., Myers, R., Slabbert, M., Sleugh, B., 2010. Genetic resources and breeding of amaranthus. *Plant Breed. Rev.* 19, 227–285. <https://doi.org/10.1002/9780470650172.ch7>.
- Bussel, L., Stehfest, E., Siebert, S., Müller, C., Ewert, F., 2015. Simulation of the phenological development of wheat and maize at the global scale. *Glob. Ecol. Biogeogr.* 24, 1018–1029. <https://doi.org/10.1111/geb.12351>.
- Caselato-Sousa, V., Amaya-Farfan, J., 2012. State of knowledge on amaranth grain: a comprehensive review. *J. Food Sci.* 77, R93–104. <https://doi.org/10.1111/j.1750-3841.2012.02645.x>.
- Choi, D., Ban, H., Seo, B., Lee, K., Lee, B., 2016. Phenology and seed yield performance of determinate soybean cultivars grown at elevated temperatures in a temperate region. *PLoS One*. 11, e0165977. <https://doi.org/10.1371/journal.pone.0165977>.
- Das, S., 2016. Amaranthus: A Promising Crop of Future. Springer, Singapore <https://doi.org/10.1007/978-981-10-1469-7>.
- Delano-Frier, J., Aviles-Arnaut, H., Casarubias-Castillo, K., Casique-Arroyo, G., Castrillon-Arbelaiz, P., Herrera-Estrella, L., Massange-Sanchez, J., Martinez-Gallardo, N., Parra-Cota, F., Vargas-Ortiz, E., 2011. Transcriptomic analysis of grain amaranth (*Amaranthus hypochondriacus*) using 454 pyrosequencing: comparison with *A. tuberculatus*, expression profiling in stems and in response to biotic and abiotic stress. *BMC Genomics* 12, 363. <https://doi.org/10.1186/1471-2164-12-363>.
- Erten, E., Rossi, C., Yuzugullu, O., Hajnsek, I., 2014. Phenological growth stages of paddy rice according to the BBCH scale and Sar images. *IEEE Int. Geosci. Remote Sens. Symp. (Igarss)*, 1017–1020 <https://doi.org/10.1109/Igarss.2014.6946600>.
- Fazlioglu, F., Bonser, S., 2016. Phenotypic plasticity and specialization in clonal versus non-clonal plants: a data synthesis. *Acta Oecol.* 77, 193–200. <https://doi.org/10.1016/j.actao.2016.10.012>.
- Gilmore, E.C., Rogers, J., 1958. Heat units as a method of measuring maturity in corn. *Agron. J.* 50, 611–615.
- Hack, H., Bleiholder, H., Buhr, L., Meier, U., Schnock-Fricke, U., Weber, E., Witzemberger, A., 1992. Einheitliche codierung der phänologischen entwicklungsstadien mono- und dikotylter pflanzen—erweiterte BBCH-Skala, *Allgemein. Nachrichtenbl. Deut. Pflanzenschutzd.* 44, 265–270.
- Herraiz, F., Vilanova, J.S., Plazas, M., Gramazio, P., Andujar, I., Rodriguez-Burruezo, A., Fita, A., Anderson, G.J., Prohens, J., 2015. Phenological growth stages of pepino (*Solanum muricatum*) according to the BBCH scale. *Sci. Hortic.* 183, 1–7. <https://doi.org/10.1016/j.scienta.2014.12.008>.

- Hossain, A., da Silva, J., Lozovskaya, M., Zvolinsky, V., 2012. High temperature combined with drought affect rainfed spring wheat and barley in South-Eastern Russia: I. Phenology and growth. *Saudi J. Biol. Sci.* 19, 473–487. <https://doi.org/10.1016/j.sjbs.2012.07.005>.
- Huerta-Ocampo, J., Barrera-Pacheco, A., Mendoza-Hernandez, C., Espitia-Rangel, E., Mock, H., Barba de la Rosa, A.P., 2014. Salt stress-induced alterations in the root proteome of *Amaranthus cruentus* L. *J. Proteome Res.* 13, 3607–3627. <https://doi.org/10.1021/pr500153m>.
- Ihsan, M., El-Nakhlawy, F., Ismail, S., Fahad, S., Daur, I., 2016. Wheat phenological development and growth studies as affected by drought and late season high temperature stress under arid environment. *Front. Plant Sci.* 7, 795. <https://doi.org/10.3389/fpls.2016.00795>.
- Innovation NRCAC, 1984. *Amaranth: Modern Prospects for an Ancient Crop*. National Academy Press.
- Khanam, U., Oba, S., 2014. Phenotypic plasticity of vegetable amaranth, *Amaranthus tricolor* L. under a natural climate. *Plant Prod. Sci.* 17, 166–172. <https://doi.org/10.1626/pp.17.166>.
- Kirillova, L., Nazarova, G., Ivanova, E., 2016. Para-aminobenzoic acid stimulates seed germination plant growth, development, photosynthesis and nitrogen assimilation in the amaranth (*Amaranthus L.*). *Agric. Biol. Plant Biol. Sect.* 688.
- Kuluev, B., Mikhaylova, E., Taipova, R., Chemeris, A., 2017. Changes in phenotype of transgenic amaranth *Amaranthus retroflexus* L., overexpressing ARGOS-LIKE gene. *Russ. J. Genet.* 53, 67–75. <https://doi.org/10.1134/S1022795416120061>.
- Kumar, S., Hammer, G., Broad, L., Harland, P., McLean, G., 2009. Modeling environmental effects on phenology and canopy development of diverse sorghum genotypes. *Field Crop Res* 111, 157–165. <https://doi.org/10.1016/j.fcr.2008.11.010>.
- Lee, J., Hong, G., Dixit, A., Chung, J., Ma, K., Lee, J., Kang, H., Cho, Y., Gwag, J., Park, Y., 2008. Characterization of microsatellite loci developed for *Amaranthus hypochondriacus* and their cross-amplifications in wild species. *Conserv. Genet.* 9, 243–246. <https://doi.org/10.1007/s10592-007-9323-1>.
- Manikandan, S., Srimathi, P., 2015. Colour of spike as an index of harvestable maturity of grain amaranth (*Amaranthus hypochondriacus* L.) cv. Suvarna. *Curr. Biot.* 9, 173–177.
- Martinelli, T., Galasso, I., 2011. Phenological growth stages of *Camelina sativa* according to the extended BBCH scale. *Ann. Appl. Biol.* 158, 87–94. <https://doi.org/10.1111/j.1744-7348.2010.00444.x>.
- Massange-Sanchez, J., Palmeros-Suarez, P., Martinez-Gallardo, N., Castrillon-Arbelaez, P., Aviles-Arnaut, H., Alatorre-Cobos, F., Tiessen, A., Delano-Frier, J., 2015. The novel and taxonomically restricted Ah24 gene from grain amaranth (*Amaranthus hypochondriacus*) has a dual role in development and defense. *Front. Plant Sci.* 6, 602. <https://doi.org/10.3389/fpls.2015.00602>.
- Meier, U., Bleiholder, H., Buhr, L., Feller, C., Hack, H., Heß, M., Lancashire, P., Schnock, U., Stauß, R., Van Den Boom, T., 2009. The BBCH system to coding the phenological growth stages of plants—history and publications. *J. für Kulturpflanzen.* 61, 41–52.
- Mlakar, S., Turinek, M., Jakop, M., Bavec, M., Bavec, F., 2009. Nutrition value and use of grain amaranth: potential future application in bread making. *Agricultura* 6.
- Munger, P., Bleiholder, H., Hack, H., Hess, M., Stauss, R., van den Boom, T., Weber, E., 1997. *J. Agron. Crop Sci.* 179, 209–217. <https://doi.org/10.1111/j.1439-037X.1997.tb00519.x>
- Phenological growth stages of the soybean plant (*Glycine max* L. MERR.): codification and description according to the BBCH scale.
- Palmeros-Suarez, P., Massange-Sanchez, J., Martinez-Gallardo, N., Montero-Vargas, J., Gomez-Leyva, J., Delano-Frier, J., 2015. The overexpression of an *Amaranthus hypochondriacus* NF-YC gene modifies growth and confers water deficit stress resistance in *Arabidopsis*. *Plant Sci.* 240, 25–40. <https://doi.org/10.1016/j.plantsci.2015.08.010>.
- Pandey, R., Singh, R., 2009. Genetic improvement of grain amaranths: a review. *Curr. Adv. Agric. Sci.* 1, 61–64.
- Price, T., Qvarnström, A., Irwin, D., 2003. The role of phenotypic plasticity in driving genetic evolution. *Proc. R. Soc. Lond. B: Biol. Sci.* 270, 1433–1440. <https://doi.org/10.1098/rspb.2003.2372>.
- Rastogi, A., Shukla, S., 2013. Amaranth: a new millennium crop of nutraceutical values. *Critic. Rev. Food Sci. Nutr.* 53, 109–125. <https://doi.org/10.1080/10408398.2010.517876>.
- Ray, T., Roy, S., 2009. Genetic diversity of *Amaranthus* species from the Indo-Gangetic plains revealed by RAPD analysis leading to the development of ecotype-specific SCAR marker. *J. Hered.* 100, 338–347. <https://doi.org/10.1093/jhered/esn102>.
- Salmeron, M., Purcell, L., 2016. Simplifying the prediction of phenology with the DSSAT-CROPGRO-soybean model based on relative maturity group and determinacy. *Agr. Syst.* 148, 178–187. <https://doi.org/10.1016/j.agry.2016.07.016>.
- Shukla, S., Bhargava, A., Chatterjee, A., Pandey, A., Mishra, B.K., 2010. Diversity in phenotypic and nutritional traits in vegetable amaranth (*Amaranthus tricolor*), a nutritionally underutilised crop. *J. Sci. Food Agric.* 90, 139–144. <https://doi.org/10.1002/jsfa.3797>.
- Sosa-Zuniga, V., Brito, V., Fuentes, F., Steinfurt, U., 2017. Phenological growth stages of quinoa (*Chenopodium quinoa*) based on the BBCH scale. *Ann. Appl. Biol.* 171, 117–124. <https://doi.org/10.1111/aab.12358>.
- Stetter, M., Zeitler, L., Steinhaus, A., Kroener, K., Biljecki, M., Schmid, K., 2016. Crossing methods and cultivation conditions for rapid production of segregating populations in three grain amaranth species. *Front. Plant Sci.* 7, 816. <https://doi.org/10.3389/fpls.2016.00816>.
- Vargas-Ortiz, E., Delano-Frier, J., Tiessen, A., 2015. The tolerance of grain amaranth (*Amaranthus cruentus* L.) to defoliation during vegetative growth is compromised during flowering. *Plant Physiol. Biochem.* 91, 36–40. <https://doi.org/10.1016/j.plaphy.2015.03.007>.
- Venkatesh, L., Murthy, N., Nehru, S., 2014. Analysis of genetic diversity in grain amaranth (*Amaranthus* spp.). *Ind. J. Genet. Plant Breed.* 74, 522–525. <https://doi.org/10.5958/0975-6906.2014.00882.7>.
- Zhang, D., Yuan, Z., An, G., Dreni, L., Hu, J., Kater, M., 2013. Panicle development. In: Zhang, Q., Wing, A.R. (Eds.), *Genetics and Genomics of Rice*. Springer New York, New York, NY, pp. 279–295.
- Zhang, T., Li, T., Yang, X., Simelton, E., 2016. Model biases in rice phenology under warmer climates. *Sci. Rep.* 6, 27355. <https://doi.org/10.1038/srep27355>.

3. Metodología

3.1 Cinética de sequía

En referencia a la clasificación de las diferentes etapas fenológicas del ciclo de vida de *Amaranthus sp.* que se describen anteriormente (Martínez-Núñez, Ruiz-Rivas et al. 2019), se realizó una cinética de sequía para establecer cual es estado fenológico más susceptible en amaranto ante esta condición de estrés. Para ello se establecieron monitoreos en plantas de 4, 15, 20, 30, 40, 50, 60 y 90 días de edad, lo que equivale a los estados 5, 8, 12, 20, 50, 59, 69, y 80 de la escala BBCH descrita para amaranto (Martínez-Núñez, Ruiz-Rivas et al. 2019). Las especies monitoreadas fueron: *A. hypochondriacus*, *A. hybridus*, *A. caudatus* y la variedad Gabriela de *A. hypochondriacus*. Para cada uno de los tiempos referidos se utilizaron 12 plantas control y 12 plantas tratamiento. Ambas se cultivaron bajo condiciones semi-controladas de invernadero (Martínez-Núñez, Ruiz-Rivas et al. 2019), pero al llegar a la edad que se establecen para cada tiempo, se suspendió el suministro de agua en los tratamientos, mientras que en las plantas control continuó el riego normal sin interrupciones durante todo su ciclo de vida. Con la finalidad de evidenciar el déficit hídrico en el sustrato que crecen las plantas, se cuantificó la Humedad Relativa (HR) en un gramo de sustrato mediante una termobalanza Probacssa MB45 (Ohaus Corporation, New Jersey, USA). El cuadro de estrés en las plantas de amaranto se valoró visualmente con el marchitamiento de las plantas y se correlacionó a un promedio del ~ 8 % de HR en el sustrato. Tras determinar con ambos parámetros el cuadro de estrés en las plantas de amaranto, se reanudó

el riego y se realizó un registro fotográfico de las plantas reanimadas con una cámara SLT-A37K (Sony, California, USA) acoplada a un lente macro *DT 2.8/30 MACRO SAM*.

Las observaciones de las plantas recuperadas tras el tratamiento de sequía fueron tomadas como referencia para determinar el estado fenológico más susceptible a este tipo de estrés, e Identificar parámetros cuantitativos para apreciar las consecuencias de un periodo de sequía en las plantas que lograran reanimarse y concluir su ciclo de vida. El parámetro registrado y comparado entre tratamientos y plantas control fue la longitud total de la planta.

3.2 Análisis estadístico

El análisis estadístico con el que se evaluó la longitud total de la planta entre tratamientos se realizó mediante análisis de varianza (ANOVA) para un diseño de bloques al azar y comparación de medias por la prueba de *Tukey* utilizando el paquete estadístico SAS versión 9.0. El análisis se realizó con un nivel de significancia $P < 0.05$. Los datos analizados se graficaron en el *software Microsoft Excel* versión 2013.

4. Resultados

Tanto el registro fotográfico como el Análisis de Varianza (ANOVA) permitieron apreciar el efecto que tiene un proceso de sequía sobre las plantas de *Amarantus sp.* Visualmente fue posible corroborar que durante el ciclo de vida de *A. hypochondriacus*, *A. hybridus*, *A. caudatus* y la variedad “Gabriela” de *A.*

hypochondriacus, el estrés por sequía tiene consecuencias que pueden manifestarse en un impedimento del crecimiento general en las plantas, menor longitud de las hojas, impedimento de transición de la fase vegetativa a la fase reproductiva (plantas de 15, 20, 50 y 60 días de edad) y en los casos más severos la muerte del organismo (plantas 4, 30 y 40 días de edad, Figura 2 y 3).

Por otra parte, el análisis estadístico de la longitud total de las plantas como una variable de daño ante condiciones de estrés por sequía, nos indica que hay diferencias significativas ($P < 0.05$) en el crecimiento y desarrollo de las plantas de *A. hypochondriacus* v. Gabriela y *A. hybridus* con respecto a sus plantas control en los tratamientos de 15, 20, 50 y 60 días de edad. Esta diferencia se manifiesta con plantas control de entre 19.21 en *A. hypochondriacus* v. Gabriela y plantas de 17.9 cm en *A. hybridus*, mientras que en los tratamientos podemos observar plantas de entre 13.52-17.28 cm y 10.7 y 15.7 cm en *A. hypochondriacus* v. Gabriela y *A. hybridus* respectivamente. La reducción del crecimiento en plantas de *A. hypochondriacus* y *A. cruentus* con respecto a sus plantas control es evidente solo en los tratamientos de 15, 50 y 60 días de edad, pues en ambas especies (*A. hypochondriacus* y *A. cruentus*), las plantas de 20 días de edad que crecieron bajo condiciones de estrés por sequía tienen un crecimiento mayor en comparación con sus plantas control; 21.41 cm y 19.14 cm en *A. hypochondriacus* y 19.6 y 16.9 en *A. cruentus* respectivamente.

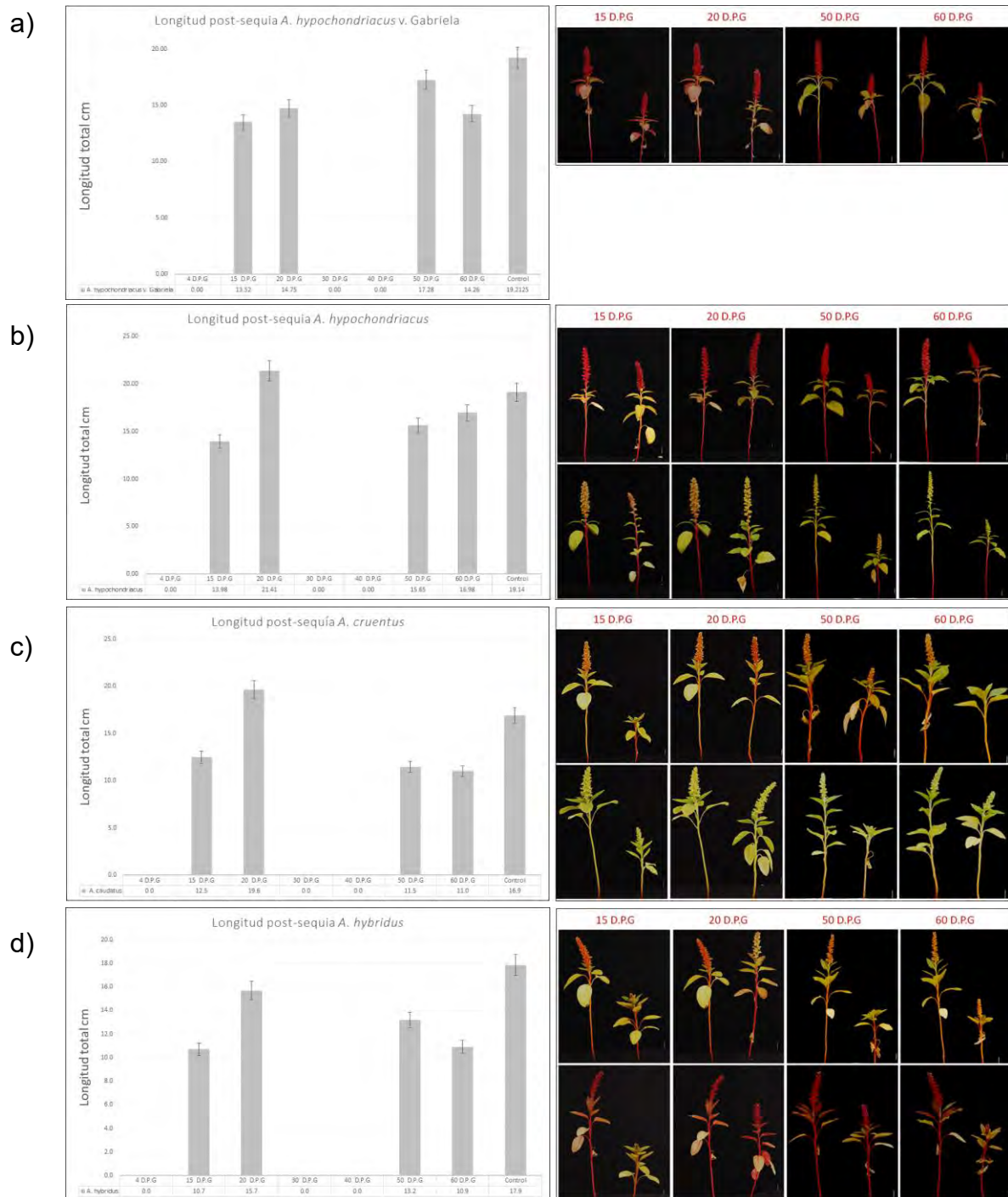


Figura 1. Registro fotográfico post-sequia en *Amaranthus* sp. Longitud y registro fotográfico post-sequia de plantas de amaranto a) *A. hypochondriacus* v. Gabriela, b) *A. hypochondriacus*, c) *A. cruentus* y d) *A. hybridus*. Las plantas se sometieron a estrés por sequía a los 4, 15, 20, 30, 40, 50, 60 y 90 días de edad. Las plantas de 4, 30 y 40 días de edad murieron (datos no mostrados). A los 15, 20, 50 y 60 Días de edad las consecuencias de sequía se manifiestan en un impedimento en el desarrollo de las plantas. El Análisis de Varianza (ANOVA)

y la comparación de medias por test de Tukey demuestran diferencias significativas ($P < 0.05$) entre las plantas control y cada uno de los tratamientos. Medias con la misma letra no son significativamente diferentes.

5. Discusión

Las observaciones realizadas durante la cinética de sequía sugieren que el estado fenológico más susceptible ante esta condición de estrés en amaranto se ubica al inicio de las primeras etapas post-germinación (plántulas de 4 días de edad, estado BBCH 5) y durante el inicio de la fase reproductiva (plantas de 30-40 días de edad; estado BBCH 20-50). Estos resultados son coherentes con lo reportado en otros cultivos de importancia agrícola tales como *Avena sativa* L. (Mut, Akay et al. 2010) y *Medicago sativa* L (Wang, Kim et al. 2009) y *Oryza sativa* (Boonjung and Fukai 1996), pues al igual que en amaranto, las primeras etapas como plántulas y el inicio de la fase reproductiva representan las etapas más críticas ante una situación de estrés por sequía (Boonjung and Fukai 1996, Harris, Tripathi et al. 2002, Ahmad, Ahmad et al. 2009, Sukiran, Ma et al. 2019).

En cultivos como *Oryza sativa* (Blackwell, Meyer et al. 1985, Novero, O'Toole et al. 1985, Turner, O'Toole et al. 1986), *Triticum durum* (Boutraa, Akhkha et al. 2010) y *Zea mays* L (Çakir 2004) se ha observado que la producción de biomasa en las plantas disminuye al disminuir la disponibilidad de agua. En amaranto ocurre exactamente lo mismo, pues aquellas plantas que logran sobrevivir al estrés generado (plantas de 15, 20, 50 y 60 días de edad) presentan alteraciones considerables en su desarrollo, impedimento en el crecimiento, y retraso o pérdida de la capacidad de generar panojas (Figura 2). Desde un punto de vista fisiológico y bioquímico es conocido que el estrés por sequía disminuye progresivamente las tasas de asimilación de CO_2 debido a la reducción de la conductancia estomática;

lo que a su vez impacta en el tamaño de las hojas, la extensión de los tallos y la proliferación de las raíces; perturba las relaciones hídricas de las plantas y reduce la eficiencia del uso del agua. Altera los pigmentos fotosintéticos y reduce el intercambio de gases, lo que lleva a una reducción en el crecimiento y la productividad de las plantas (Anjum, Xie et al. 2011). El crecimiento celular se considera uno de los procesos fisiológicos más sensibles al estrés por sequía ya que propicia la reducción de la presión de turgencia; además, bajo déficit hídrico, el alargamiento celular de las plantas superiores se inhibe mediante la interrupción del flujo de agua desde el xilema a las células alargadoras circundantes (Nonami 1998). En consecuencia, un déficit en el alargamiento y la expansión celular dan como resultado un crecimiento reducido y rasgos inferiores de rendimiento (Hussain, Malik et al. 2008), tal y como pudimos observar en las distintas especies de amaranto sometidas a estrés por sequía.

6. Conclusiones

- El amaranto es un cultivo de ciclo corto que alcanza la madurez fisiológica aproximadamente a los cuatro meses de edad.
- Bajo condiciones de invernadero, la plasticidad fenotípica del amaranto nos permite obtener plantas completamente desarrolladas de aproximadamente 20 cm de altura.
- La escala decimal *Biologische Bundesanstalt Bundessortenamt und Chemische Industrie* (BBCH), nos permite distinguir (bajo un consenso internacional) las distintas etapas de desarrollo del amaranto durante su ciclo de vida.
- El ciclo de vida del amaranto, desde la germinación hasta la senescencia, puede dividirse en 9 etapas, 4 describen la fase vegetativa (00-13) y 5 la fase reproductiva (60-99).
- El desarrollo de las plantas de amaranto bajo condiciones de estrés por sequía se ve impactado con severas consecuencias que impiden la transición de la fase vegetativa a la fase reproductiva y limitan el crecimiento y desarrollo de estructuras foliares en plantas de 15, 20, 50 y 60 días de edad.
- Durante el ciclo de vida del amaranto, los estados fenológicos especialmente susceptibles ante condiciones de estrés por sequía se ubican al inicio de las primeras etapas post-germinación (plántulas de 4 días de edad, estado BBCH 5) y durante el inicio de la fase reproductiva (plantas de 30-40 días de edad, estado BBCH 20-50).

CAPITULO II:

Predicción bioinformática de miRNAs en *Amaranthus hypochondriacus*

1. Introducción

Por lo menos 36 familias de miRNAs en plantas están clasificadas como “conservadas” (Chavez Montes, de Fatima Rosas-Cardenas et al. 2014, Axtell and Meyers 2018). Aunado a ello, la disponibilidad de potentes herramientas bioinformáticas (Lei and Sun 2014, Shahid and Axtell 2014) y de bases de datos que almacenan una gran cantidad de secuencias EST (*Expressed Sequence Tag*) y secuencias GSS (*Genome Survey Sequences*), ha facilitado enormemente la predicción computacional de miRNAs por homología de secuencias (Sunkar and Jagadeeswaran 2008, Ye, Chen et al. 2013, Huang, Zou et al. 2014). En los últimos años, se ha demostrado en *Arabidopsis thaliana* (Sunkar and Zhu 2004, Wang, Reyes et al. 2004), *Oryza sativa* (Archak and Nagaraju 2007), *Zea mays* (Zhang, Chia et al. 2009), *Hordeum vulgare* (Colaiacovo, Subacchi et al. 2010), *Glycine max* (Kulcheski, de Oliveira et al. 2011), *Gossypium hirsutum* (Kwak, Wang et al. 2009), *Sorghum bicolor* (Du, Wu et al. 2010), y *Musa spp* (Chai, Feng et al. 2015) entre otras plantas; que la detección computacional de miRNAs es exitosa y efectiva, sobre todo para el descubrimiento de nuevos miRNAs que generalmente no pueden ser detectados debido a su bajo nivel de expresión y / o expresión espacio-temporal (Jones-Rhoades and Bartel 2004, Adai, Johnson et al. 2005, Huang, Zou et al. 2014). Sin embargo, la homología como único criterio de identificación no es suficiente, y en complemento debe predecirse la estructura secundaria del pre-miRNA junto con el cálculo de la energía libre de plegamiento. De igual manera, la predicción bioinformática de miRNAs debe validarse experimentalmente para reducir el número de falsos positivos identificados (Adai, Johnson et al. 2005, Zhang, Pan et al. 2005, Yin, Li et al. 2008).

En el capítulo II del presente proyecto de investigación, los avances en la obtención del genoma de *Amaranthus hypochondriacus* (Clouse, Adhikary et al. 2016) y el uso de herramientas bioinformáticas nos permitió la identificación de 534 secuencias precursoras pertenecientes a 26 familias distintas de miRNAs. La anotación de sus genes blanco indica que los miRNAs identificados están involucrados en la regulación del crecimiento y desarrollo de las plantas, la respuesta al estrés ambiental, la transducción de señales y la invasión de patógenos. Adicionalmente, la validación de 14 miRNAs mediante RT-qPCR sugiere que existe una expresión diferencial tejido específica entre hojas, tallos, panojas y raíces en plantas de *Amaranthus hypochondriacus* variedad “Gabriela”.

2. Metodología

2.1. Predicción bioinformática de miRNAs en *Amaranthus hypochondriacus*

El genoma de referencia y los transcriptomas empleados para la predicción bioinformática de miRNAs se encuentran disponibles en el portal *Phytozome v.12.1* (<https://phytozome.jgi.doe.gov/pz/portal.html>) y corresponde a la variedad “*Revancha*” de *Amaranthus hypochondriacus*. Para mayor información respecto al ensamble y anotación del genoma y los transcriptomas de *Amaranthus hypochondriacus* consultar: https://phytozome.jgi.doe.gov/pz/portal.html#!info?alias=Org_Ahypochondriacus_er, (Clouse, Adhikary et al. 2016).

Para iniciar el análisis, se obtuvieron todas las secuencias de los miARNs maduros conocidos de *Viridiplantae* reportadas en la base de datos miRBase (<http://www.mirbase.org/>, Release 21, enero de 2018). Mediante la herramienta

BLAST de Phytozome v12.1, las secuencias obtenidas (miRNAs maduros) se mapearon contra las EST (Expressed Sequence Tag) y GSS (Genome Survey Sequences) de *Amaranthus hypochondriacus*. 150 nt rio arriba y 150 nt rio abajo de las regiones apareadas (miRNAs maduros) se tomaron como posibles precursores de miRNAs.

2.2. Análisis de la estructura secundaria y plegamiento de pre-miRNAs

El análisis de la estructura secundaria y el cálculo de la energía libre de plegamiento de los posibles precursores de miRNAs se realizó utilizando RNAfold web server (<http://rna.tbi.univie.ac.at/cgi-bin/RNAWebSuite/RNAfold.cgi>). Los criterios para identificar los potenciales miRNAs en *Amaranthus hypochondriacus* fueron los siguientes: (1) los miRNA maduros que se predicen no pueden tener más de 3 *mismatches* con respecto al miRNA conocido, (2) la secuencia del pre-miRNA debe plegarse y adaptar una estructura secundaria en forma de horquilla. En uno de los brazos de esta horquilla debe ubicarse el miRNA maduro, (3) no hay formación de bucles en el dúplex miRNA/miRNA*, (4) el contenido de A + U en el pre-miRNA puede varía entre el 30% y 70% y, (5) la estructura secundaria predicha debe tener una energía libre de plegamiento menor o igual a -20 kcal/mol ($MFE \leq -20$ kcal / mol).

2.3. Predicción de genes blanco

Una vez identificados los posibles miRNAs en el genoma y los transcriptomas de *Amaranthus hypochondriacus*, se realizó la predicción de genes blanco mediante el software en línea psRNATarget (Dai, Zhuang et al. 2018)

(<http://plantgrn.noble.org/psRNATarget/>). Los parámetros que se siguieron fueron los siguientes: (1) expectativa máxima de 3.0, (2) longitud de puntuación complementaria (hspsize) de 20 pb, (3) máxima energía de accesibilidad permitida para que el blanco pueda despegarse del sitio destino 25.0, (4) considerar 17 pb rio arriba y 13 pb rio abajo alrededor del sitio de reconocimiento (gen blanco) y, (5) el sitio de corte del miRNA maduro debe situarse entre el nt 9 y el nt 11 de su secuencia.

2.4. Crecimiento de plantas

Semillas de *Amaranthus hypochondriacus* variedad Gabriela fueron sembradas bajo condiciones de invernadero tal y como se menciona anteriormente (Martínez-Núñez, Ruiz-Rivas et al. 2019). Durante la fase reproductiva se colectaron hojas, tallos, inflorescencias y raíces de 10 plantas. El tejido colectado se pulverizó en N₂ líquido y se almacenó de forma independiente a -80 °C hasta su uso.

2.5. Extracción de RNA total

La extracción de RNA total de cada uno de los tejidos colectados se realizó mediante *ZR Plant RNA MiniPrep kit* siguiendo las especificaciones del fabricante (Zymo Research, Irvine, CA, EE. UU.), brevemente: Se colocó 20 mg el tejido pulverizado en un tubo de lisis ZR BashingBead™, se agregaron 800 µl de buffer de lisis. La muestra se agitó en vórtex y se centrifugó a 13000 rpm durante 1 minuto. El sobrenadante se transfirió a una columna Zymo-Spin™ IIC, se centrifugó durante 30 segundos a 13000 rpm y se recuperó el fluido. Se añadió un volumen de etanol y la mezcla se colocó en una columna IIC Zymo-Spin™ y se centrifugó durante 30

s a 13000 rpm. Posteriormente, se añadieron 400 μ l de *RNA Prep Buffer* a la columna y se centrifugó durante 30 s a 13000 rpm. A continuación, se añadieron 700 μ l de Buffer de lavado y se centrifugó la columna durante 30 s a 13000 rpm. Se añadió 400 μ l de buffer de lavado a la columna y se centrifugó durante 2 minutos, se añadieron 35 μ l de agua libre de DNasa/RNasa directamente a la matriz de la columna y se centrifugó durante 30 s. Finalmente, se transfirió el RNA recuperado a la columna Zymo-Spin™ IV-HRC y se centrifugó a 13000 rpm durante 1 minuto.

2.6. Cuantificación y análisis de calidad de RNA

El RNA total se cuantificó utilizando un espectrofotómetro NuDrop NAS-99 (ATCGene, Piscataway, NJ, EE. UU.) buscando satisfacer los siguientes parámetros: $A_{260}/A_{280} = 1.8 - 2.2$; $A_{260}/A_{230} \geq 2.0$. Adicionalmente, la calidad e integridad del RNA se verificó mediante electroforesis en un gel de agarosa al 1.5 %.

2.7. Síntesis de cDNA

El cDNA se sintetizó a partir de 500 ng de RNA total utilizando un oligo dT y la retro-transcriptasa M-MLV (Sigma, Saint Louis, Missouri, USA) de acuerdo con las instrucciones del fabricante. Brevemente: En un tubo de 200 μ l se agregó 1 μ l dNTPs 10 mM, 1 μ l oligo dT a una concentración de 3 μ M, 500 ng de RNA y agua grado biología molecular hasta un volumen final de 10 μ l. se mezcló de forma homogénea y se incubó la muestra a 70 °C por 10 minutos. Posteriormente se colocaron los tubos en hielo y se agregaron los siguientes componentes: 2 μ l de buffer M-MLV *Reverse Transcriptase* 10X, 1 μ l de retro-transcriptasa M-MLV, 0.5 μ l

de inhibidor de RNAsas (40 units/ μ l), y 6.5 μ l de agua grado biología molecular para un volumen final de 20 μ l. La reacción se incubó a 37 °C durante 60 minutos. Finalmente, la retro-transcriptasa M-MLV se desactivo a 90 °C durante 10 min.

2.8. Validación tejido-específica del perfil de expresión de miRNAs mediante RT-qPCR

Las reacciones de RT-qPCR para cada miRNA se realizaron con un *primer* FW específico y un *primer* RV universal (Tabla 3). Los productos de PCR se detectaron mediante una sonda universal TaqMan en un equipo de PCR en tiempo real StepOne™ (Applied Biosystems, Foster City, CA, EE. UU.).

Oligonucleotidos y sondas diseñadas para la cuantificación de miRNAs mediante RT-qPCR

Nombre	miRNA	Descripción	nt	Secuencia
FRC-0219	QmiR156	Specific F-primer	21	CTGACAGAAGAGAGTGAGCAC
FRC-0220	QmiR159	Specific F-primer	21	CTTTGGATTGAAGGGAGCTCT
FRC-0221	QmiR160	Specific F-primer	18	TGCCTGGCTCCCTGTATG
FRC-0222	QmiR164	Specific F-primer	18	ATGGAGAAGCAGGGCACG
FRC-0223	QmiR167	Specific F-primer	20	CTGAAGCTGCCAGCATGATC
FRC-0224	QmiR169	Specific F-primer	19	CCAGCCAAGGATGACTTGC
FRC-0225	QmiR171	Specific F-primer	17	CGTGATTGAGCCGTGCC
FRC-0226	QAhyimiR319	Specific F-primer	19	CGATTGGACTGAAGGGAGC
FRC-0228	QmiR393	Specific F-primer	21	TCCAAAGGGATCGCATTGATC
FRC-0229	QmiR394	Specific F-primer	20	TTGGCATTCTGTCCACCTCC
FRC-0230	QmiR396	Specific F-primer	22	GTTCCACAGCTTTCTGAACTG
FRC-0231	QmiR397	Specific F-primer	21	TCATTGAGTGCAGCGTTGATG
FRC-0232	QmiR408	Specific F-primer	18	GCACTGCCTCTCCCTGG
FRC-0233	QAhyimiR444	Specific F-primer	17	TGTGCAGTTGCTGCCGC
FRC-0234	QmiR166	Specific F-primer	19	TCGGACCAGGCTTCATTCC
FRC-0245		Universal R-primer	18	CAGTGCAGGGTCCGAGGT
FRC-0246		S-Poly (T) primer	49	GTGCAGGGTCCGAGGTCAGAGCCACCTGGCAATTTTTTTTTTTTTTTT
FRC-0247		Universal S-Poly (T) probe	32	CAGAGCCACCTGGCAATTT FAM / TAMRA

Tabla 1. Oligonucleotidos y sondas diseñadas para la cuantificación de miRNAs mediante RT-qPCR

La mezcla de reacción para RT-qPCR se preparó con 5 µl de TaqProbe 2x qPCR MasterMix-ROX (Applied Biological Materials, Canadá), 0.3 µl de primer RV universal 400 nM, 0.3 µl de primer FW 300 nM (específico para cada miRNA), 0.4 µl de la sonda universal TaqMan 10 µM y 4 µl de cDNA diluido que corresponde a 5 ng del RNA poliadenilado. El volumen final de la reacción fue de 10 µl y se preparó en placas de 96 pocillos (Applied Biosystems, Foster City, CA, EE. UU.). Las condiciones de la reacción fueron las siguientes: 95 °C durante 10 min, 95 °C durante 15 s (40 ciclos), y 60 °C durante 40 s. Se utilizaron dos réplicas técnicas y tres réplicas biológicas de cada muestra para el análisis de RT-qPCR. El nivel de expresión de cada miRNA maduro se registró mediante el ciclo umbral (Ct) y se normalizó contra los genes *housekeeping* *Ahy_U3* y *Ahy_snor71* de amaranto.

3. Resultados

Se obtuvieron 10,404 secuencias maduras reportadas para todos los miembros de la *Viridiplantae* miRBase. El mapeo de las secuencias obtenidas sobre los transcriptomas permitió la identificación de solo 5 miRNAs (miR166, miR171, miR172, miR396 y miR5141), mientras que en el genoma se logró la identificación de 534 secuencias precursoras pertenecientes a 26 familias distintas de miRNAs (Figura 4). Dentro de los miRNAs identificados encontramos 17 catalogados como de alta confianza y 9 reportados con anterioridad en plantas, aunque no bajo la categoría de alta confianza (Figura 4).

Predicción bioinformática de miRNAs en *Amaranthus hypochondriacus*

	Qseqid	sseqid	pident	length	qstart	qend	sstart	send	evaluate	bitscore
1	zma-MIR156c	Scaffold_1	92.683	82	24	101	33359912	33359831	1.04E-24	115
2	cca-MIR160b	Scaffold_8	93.478	46	6	51	7373070	7373025	5.22E-11	69.4
3	gma-MIR162a	Scaffold_15	100	31	4	34	2776621	2776591	7.39E-08	58.4
4	aly-MIR164b	Scaffold_10	95.455	44	21	64	16167686	16167644	5.72E-11	69.4
5	aly-MIR166a	Scaffold_7	94.595	37	67	102	5884255	5884219	3.01E-07	56.5
6	ghr-MIR167a	Scaffold_4	100	28	113	140	16148769	16148796	6.47E-06	52.8
7	lus-MIR168a	Scaffold_7	84.746	59	197	251	11575957	11575899	8.80E-07	56.5
8	aly-MIR169h	Scaffold_10	80	135	9	141	16167704	16167584	6.23E-16	86.1
9	ath-MIR171c	Scaffold_5	100	29	129	157	23104012	23103984	1.98E-06	54.7
10	aly-MIR172d	Scaffold_8	97.143	35	1	35	860257	860223	4.08E-08	60.2
11	ath-MIR319b	Scaffold_12	94.595	37	123	157	2009884	2009920	5.51E-07	56.5
12	aly-MIR390a	Scaffold_15	97.143	35	1	35	606107	606073	4.08E-08	60.2
13	aly-MIR394b	Scaffold_5	100	30	14	43	23104061	23104032	5.51E-07	56.5
14	nta-MIR395a	Contig584 q uiver	82.54	189	17	198	2585	2400	1.79E-37	158
15	aaU-MIR396	Scaffold_10	85.075	67	106	172	8250350	8250415	2.64E-10	67.6
16	ghr-MIR398	Scaffold_9	92.683	41	104	144	1639253	1639293	3.66E-08	60.2
17	csi-MIR408	Contig177 q uiver	76.074	163	3	160	443126	442973	5.20E-12	73.1
18	atr-MIR828	Scaffold_16	95.833	48	110	157	2587478	2587524	4.11E-13	76.8
19	tae-MIR1122c	Scaffold_10	97.531	162	1	162	6233030	6233191	1.04E-73	278
20	tae-MIR1134	Scaffold_7	96.875	64	37	100	13007768	13007707	4.40E-22	106
21	peu-MIR2916	Scaffold_7	96.875	32	11	42	18739040	18739009	1.48E-06	54.7
22	ptc-MIR481b	Scaffold_10	100	28	67	94	22154071	22154044	3.59E-06	52.8
23	rgl-MIR5141	Scaffold_6	87.692	65	1	65	4159421	4159484	2.09E-12	75
24	gma-MIR6300	Scaffold_15	95.455	44	6	49	606117	606075	5.87E-11	69.4
25	stu-MIR8005c	Contig116 q uiver	91.209	91	1	91	710	620	7.08E-28	124
26	ath-MIR8175	Scaffold_7	100	28	52	79	19891115	19891088	9.05E-06	52.8

Tabla 2. Predicción bioinformática de miRNAs en *Amaranthus hypochondriacus*.

Respetando los criterios establecidos para la identificación de miRNAs, solo se consideraron válidas aquellas secuencias de miRNAs maduros que presentaron menos de tres *mismatches*. La mayoría de los miRNAs identificados (53.8 % =14/26) presentaron una longitud de 21 nt. Sin embargo, también fue posible observar miRNAs de 18 nt (3.8 % =1/26), 19 nt (3.8 % =1/26), 20 nt (15.3 % =4/26), 22 nt (3.8

% =1/26), 23 nt (3.8 % =1/26) y 24 nt (15.3 % =4/26) de longitud. Las longitudes de las secuencias mapeadas variaron de 28 nt a 189 nt con un porcentaje de identidad de entre 76 y 100 %, mientras que el contenido de A + U en los precursores fue en promedio de 49.32%. El análisis del plegamiento secundario realizado mediante RNAFold corroboró que las secuencias identificadas como posibles precursores muestran un plegamiento estable en forma de horquilla y con un valor promedio de MFE de -45.3 kcal/mol (Fig 2). De igual manera, el plegamiento secundario de las secuencias precursoras demuestra que no se forman bucles que interrumpan la estabilidad del duplex miRNA/miRNA*. Adicionalmente, la identidad de las secuencias identificadas como pre-miRNAs fue corroborada mediante BLAST en la base de datos NCBI *National Center for Biotechnology Information* (<https://www.ncbi.nlm.nih.gov/>), dando como resultado que cada una de las secuencias obtenidas corresponden a precursores de miRNAs identificados con anterioridad en otras plantas.

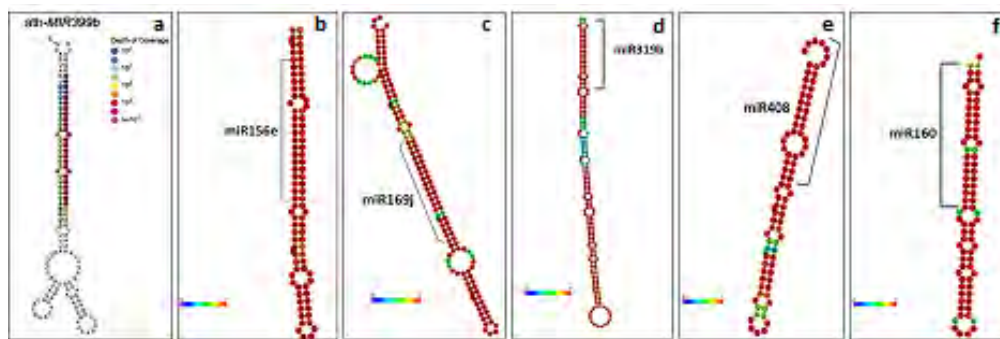


Figura 2. Plegamiento secundario de secuencias precursoras de miRNAs en *A. hypochondriacus*. El análisis de las secuencias precursoras de miRNAs se realizó mediante el software RNAfold, ello permitió corroborar que el plegamiento secundario corresponde a la estructura típica en forma de tallo-asa de los miRNAs. De izquierda a derecha: 12a ejemplo de la secuencia del ath-MIR399b que cumple con los criterios establecidos por Axtell y Meyers, 2018. 12b-12f: Secuencias precursoras de miRNAs de *A. hypochondriacus* que cumplen con los criterios establecidos por Axtell y Meyers, 2018.

Por otro lado, la predicción de genes blanco que se realizó mediante *psRNA Target* facilitó la identificación de por lo menos 22 genes que se encuentran regulados a nivel post-transcripcional mediante miRNAs en *Amaranthus hypochondriacus* (Figura 1). Entre los genes identificados se encuentran BRH1: *Brassinosteroid-responsive*, RING-H2 Finger Protein RHF2A, SPL9: *SPL9 squamosa promoter binding protein-like 9*, MYB: *myb-like HTH transcriptional regulator family protein*, TCP4: *TCP family transcription factor 4*, CSD1: *Copper/zinc superoxide dismutase 1*, COX: *Cytochrome C oxidase*, RCN1: *ARM repeat superfamily protein*, BR11: ATBRI1, BIN1, BRI1, CBB2, DWF2 *Leucine-rich receptor-like protein kinase family protein*, NF-YA1: *NF-YA1 nuclear factor Y, subunit A1* (Figura 1).

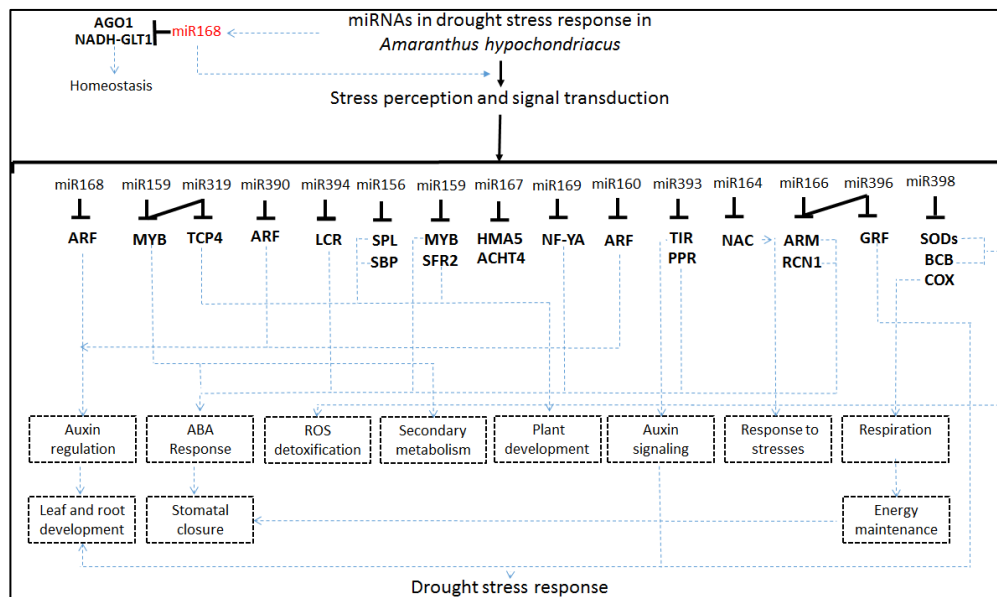


Figura 3. Red de regulación génica que se predice para *Amaranthus hypochondriacus*. Modificado de (Ding et al., 2013). Red de regulación génica en la que se muestran 15 miRNAs y sus respectivos genes blanco que se predicen en *A. hypochondriacus*. La predicción de genes blanco permite identificar factores de transcripción, genes que codifican para proteínas de metabolismo secundario y genes sensibles a estrés por sequía. Su función es variada y va desde la regulación por fitohormonas, detoxificación de ROS, desarrollo de la planta y respuesta a estrés.

La anotación funcional de los genes blanco de los miRNAs identificados, sugiere su participación en la regulación de por lo menos 11 procesos fisiológicos distintos, tales como regulación del desarrollo, biosíntesis de auxinas, respuesta a Ácido abscísico (ABA), detoxificación de Especies Reactivas de Oxígeno (ROS), metabolismo secundario, señalización por auxinas, respuestas ante distintas situaciones de estrés, respiración celular, fijación de CO₂, cierre de estomas y mantenimiento de energía en las plantas de amaranto (Figuras 1 y 2).

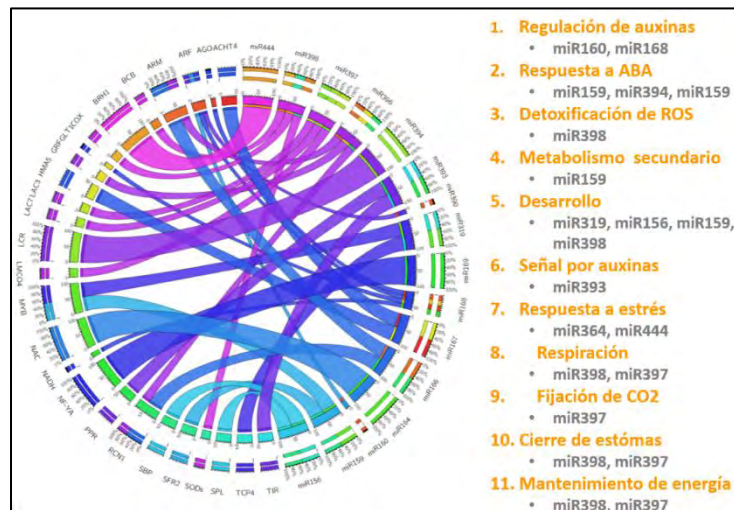


Figura 4. Interacción de miRNAs y genes blanco en *Amaranthus hypochondriacus*. Ideograma de circos en donde se representa la red de regulación génica entre miRNAs y sus respectivos genes blanco en *A. hypochondriacus*.

Para examinar el nivel de expresión de los miRNAs que se predicen, se utilizó RNA total aislado de flores, hojas, raíces y tallos de plantas de *Amaranthus hypochondriacus* variedad “Gabriela” durante la fase reproductiva (Fig). La concentración del RNA obtenido osciló entre 13.3 y 36.7 ng/μ; mientras que la absorbancia 260/280 y 260/230 se reportó entre 1.15-1.89 y 1.17-1.8 respectivamente.

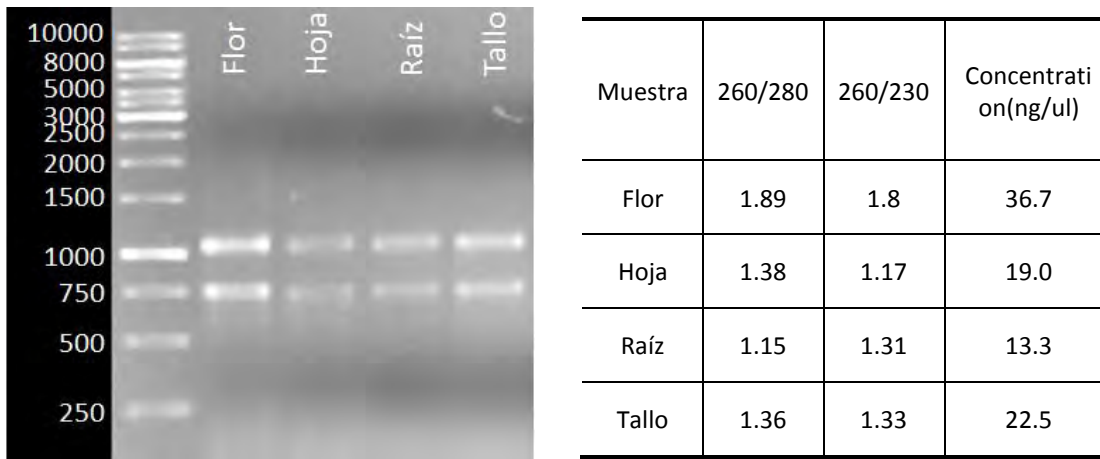


Figura 5. Electroforesis de RNA total. Electroforesis en gel de agarosa al 1.5% en donde se puede observar la integridad del RNA total de flores, hojas, tallos y raíces de *Amaranthus hypochondriacus* v. "Gabriela". Adicionalmente se muestra la concentración de cada muestra, así como su absorbancia 260/280 y 260/230.

Mediante el equipo StepOne™ (Applied Biosystems, Foster City, CA, EE. UU.) fue posible detectar señales positivas que permitieron confirmar la presencia de estos miRNAs en los distintos tejidos seleccionados; lo cual demuestra una alta tasa de precisión para la identificación computacional de miRNAs. Los niveles de expresión de cada miRNA cuantificado fue variable en los distintos tejidos analizados, es decir, es posible reconocer un patrón de expresión tejido-específico para cada miRNA (Fig. 3). Los mayores niveles de expresión lo presentaron el miR169 y el miR171 en los cuatro tejidos analizados. Mientras que los miR160, miR393, miR397 y miR408 se expresan en niveles basales tanto en flores, hojas, raíces y tallos. En un nivel intermedio de expresión, fue posible detectar al miR156, miR164, miR166, miR167, miR319, miR394, miR396, y miR444.

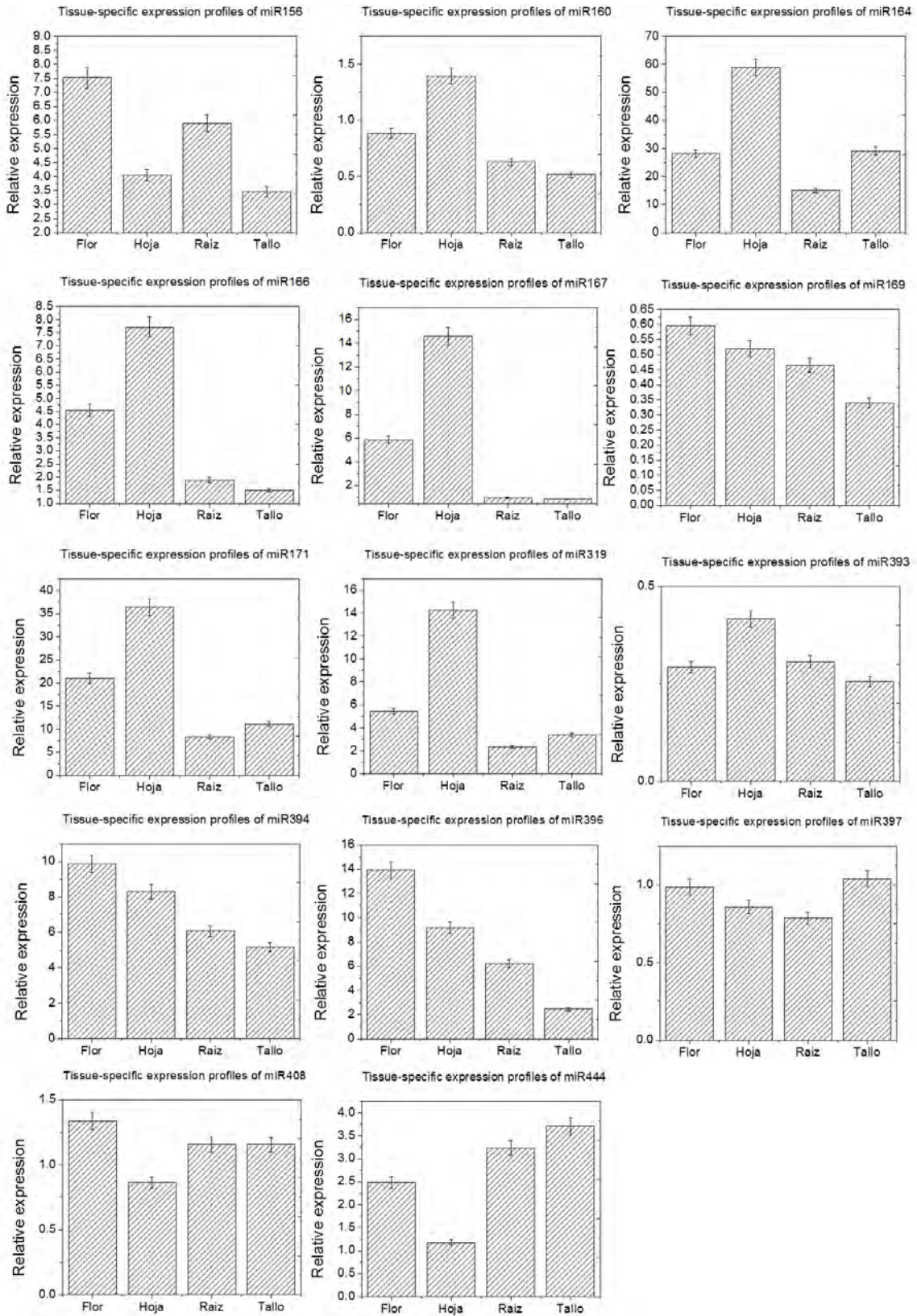


Figura 6. Perfil de expresión tejido-específico de miRNAs identificados mediante herramientas computacionales en *Amaranthus hypochondriacus* v. "Gabriela".

4. Discusión

Desde el descubrimiento de los primeros miRNAs en los años 90's (Lee, Feinbaum et al. 1993), los métodos computacionales han sido una herramienta valiosa para comprender la biología de dichas moléculas (Yoon and De Micheli 2006).

En comparación con otros métodos como clonación y secuenciación masiva, el uso de herramientas bioinformáticas para la predicción de miRNAs es una de las estrategias más efectivas, rápidas y accesibles (Jones-Rhoades and Bartel 2004, Huang, Zou et al. 2014).

Se tiene evidencia de que al menos ~36 familias de miRNAs están conservadas en plantas superiores (Axtell and Meyers 2018). Por tal motivo, la búsqueda de secuencias homólogas en el genoma de varios grupos taxonómicos de plantas ha permitido la identificación de miRNAs previamente descritos. En 2008 *Sunkar y Jagadeeswaran* realizaron la predicción bioinformática de 682 miRNAs en 155 especies distintas de plantas (Sunkar and Jagadeeswaran 2008); los autores reportan que entre las especies de plantas con mayor número de miRNAs conservados se encuentran *Zea mays* (23 miRNAs), *Sorghum bicolor* (19 miRNAs), *Triticum spp* (15 miRNAs), *Citrus sps* (14 miRNAs), *Vitis vinífera* (12 miRNAs), *Solanum lycopersicum* (11 miRNAs), *Saccharum officinarum* (10 miRNAs) y *Solanum tuberosum* (7 miRNAs). Adicionalmente, reportan cinco familias de miRNAs conservadas en gimnospermas (miR159, miR160, miR164, miR166 y miR168) y dos (miR396 y miR408) en *Selaginella*. De igual manera, Du et al. 2010 y Chai et al. 2015 encuentra 89 y 32 secuencias que potencialmente pueden clasificarse dentro de 17 y 13 familias distintas de miRNAs para *Sorghum bicolor* y

Musa spp respectivamente (Du, Wu et al. 2010, Chai, Feng et al. 2015). Los resultados que los autores reportan son congruentes con lo que nosotros encontramos en el genoma de *Amaranthus hypochondriacus*, pues las 534 secuencias precursoras que identificamos corresponden a 26 familias distintas de miRNAs en plantas; 17 clasificadas como conservadas y 9 reportadas como únicas, es decir solo han sido registrados con anterioridad en un grupo taxonómico de Plantas.

Los miRNAs identificados *in silico* presentan un tamaño de entre 20-24 nt como resultado de la actividad de las proteínas DICER-LIKE (DCL) (Gascioli, Mallory et al. 2005, Henderson, Zhang et al. 2006), siendo los de 21 nt los de mayor abundancia. Estos resultados son consistentes con la distribución de tamaño típica de angiospermas, como *Oryza sativa* (Morin, Aksay et al. 2008), *Medicago truncatula* (Szittyá, Moxon et al. 2008) y *Cucumis sativus* (Martínez, Forment et al. 2011)

Por otro lado, 16 de las 17 familias de miRNAs que identificamos mediante homología, corresponden a miRNAs previamente reportados en *Amaranthus tricolor* por secuenciación masiva (Liu, Peng et al. 2018), lo que en gran medida avala la eficiencia de la predicción bioinformática de miRNAs en *Amaranthus hypochondriacus*. Además del miR169 (clasificado como de alta confianza en miRBase), los miR828, miR1122, miR1134, miR2916, miR481, miR5141, miR6300, miR8005, y miR8175 que se predicen para *Amaranthus hypochondriacus*, no aparecen en la secuenciación masiva de miRNAs para *Amaranthus tricolor* (Liu, Peng et al. 2018), lo cual es coherente al tratarse de miRNAs específicos (Kozomara and Griffiths-Jones 2014, Axtell and Meyers 2018), cuya expresión es particular de

ciertas especies y tejidos o etapas de desarrollo (Jones-Rhoades and Bartel 2004, Adai, Johnson et al. 2005, Huang, Zou et al. 2014, Qin, Li et al. 2014). A pesar de esto, algunos miRNAs no conservados se expresan abundantemente en tejidos específicos o se inducen ante condiciones particulares, lo que sugiere que podrían estar cumpliendo un papel fisiológico importante en *Amaranthus hypochondriacus* ante adaptaciones ambientales especiales (Qin, Li et al. 2014).

Como sucede en otras plantas de interés agronómico como *Zapallito italiano* (Mao, Li et al. 2012), *Vitis vinifera* (Mica, Piccolo et al. 2009), *Triticum aestivum* (Pandey, Joshi et al. 2014) y *Medicago sativa L* (Pokoo, Ren et al. 2018), la validación experimental de 14 miRNAs mediante RT-qPCR en *Amaranthus hypochondriacus* nos permitió identificar que durante la fase reproductiva existe un patrón de expresión tejido-específico entre inflorescencias, hojas, raíces y tallos de *Amaranthus hypochondriacus* variedad “Gabriela”. La expresión y acumulación diferencial de miRNAs en etapas y tejidos específicos juegan un papel muy importante en la identidad, diferenciación y funciones fisiológicas de las plantas (Sunkar, Girke et al. 2005). Ejemplo de ello es la expresión diferencial del miR159, miR397, miR156 y miR408 en hojas y de los miR164, miR166, miR171 y miR390 en raíces de *Papaver somniferum*, *Solanum tuberosum* y *Hordeum vulgare* (Kantar, Unver et al. 2010, Unver, Parmaksız et al. 2010, Yang, Liu et al. 2010), donde se considera que estos miRNAs tienen una función crucial durante el desarrollo de hojas y raíces respectivamente.

Finalmente, tal y como sucede en otras plantas (Zhang, Pan et al. 2006, Yang, Xue et al. 2007, Rubio-Somoza and Weigel 2011), la anotación funcional de los genes blanco que se identificaron para los miRNAs de *Amaranthus*

hypochondriacus , sugiere su participación en distintos procesos fisiológicos tales como regulación de la transcripción, diferenciación celular, desarrollo, transición de la fase vegetativa a la fase reproductiva, fotosíntesis, defensa contra distintos factores de estrés, vías de señalización y estímulo hormonal.

5. Conclusiones

- La disponibilidad de herramientas computacionales y el acceso a bases de datos públicas para la obtención de secuencias genómicas, ha facilitado la identificación *in silico* de miRNAs de plantas.
- La predicción bioinformática sobre el genoma y los transcriptomas de *Amaranthus hypochondriacus* permitió la identificación de 26 familias de miRNAs reportadas con anterioridad para distintos grupos taxonómicos de plantas.
- 17 de los miRNAs identificados están clasificados como de alta confianza en la base de datos miRBase, mientras que los 9 restantes corresponden a miRNAs únicos.
- La predicción bioinformática de genes blanco permitió la identificación de al menos 22 genes distintos que se encuentran regulados a nivel post-transcripcional mediante miRNAs en *Amaranthus hypochondriacus*.
- La anotación funcional de los genes blanco identificados sugiere su participación en la regulación de procesos biológicos esenciales para el

crecimiento, desarrollo y respuesta ante distintas situaciones de estrés en *Amaranthus hypochondriacus*.

- La detección de miRNAs mediante RT-qPCR demuestra una alta tasa de precisión para la identificación computacional de miRNAs en *Amaranthus hypochondriacus*.
- La cuantificación mediante RT-qPCR permitió reconocer un patrón de expresión tejido-específico para 14 miRNAs en inflorescencias, hojas, tallos, y raíces de *Amaranthus hypochondriacus*.

CAPITULO III:

High-throughput sequencing and challenge in sequencing data analysis revealed the genuine miRNAs present in *Amaranthus hypochondriacus* genome

1 **High-throughput sequencing and challenge in sequencing data analysis**
2 **revealed the genuine miRNAs present in *Amaranthus hypochondriacus***
3 **genome**

4 Marcelino Martínez Núñez¹⁺, Magali Ruíz Rivas¹⁺, Josefát Gregorio Jorge², Pedro
5 Fernando Vera Hernández¹, Silvia Luna Suárez¹, Stefan de Folter³, Ricardo Aarón
6 Chávez Montes³, Flor de Fátima Rosas Cárdenas¹.

7

8 ¹Instituto Politécnico Nacional, Centro de Investigación en Biotecnología Aplicada.
9 Ex-Hacienda San Juan Molino Carretera Estatal Tecuexcomac-Tepetitla Km 1.5,
10 C.P. 90700, Tlaxcala México.

11 ²Consejo Nacional de Ciencia y Tecnología - Centro de Investigación en
12 Biotecnología Aplicada del Instituto Politécnico Nacional (CIBA-IPN), Av.
13 Insurgentes Sur 1582, Col. Crédito Constructor, Del. Benito Juárez, Ciudad de
14 México, México.

15 ³Unidad de Genómica Avanzada (LANGEBIO), Centro de Investigación y de
16 Estudios Avanzados del Instituto Politécnico Nacional (CINVESTAV-IPN), Km. 9.6
17 Libramiento Norte, Carretera Irapuato-León, CP 36824 Irapuato, Guanajuato,
18 México.

19 +These authors contributed equally to this work

20 **Key words:** amaranth, sRNAs sequencing, miRNA, ShortStack, MIRNA loci.

21 **1. Abstract**

22 Amaranth has been proposed as an exceptional alternative for food security and
23 climate change mitigation. Since this crop can adapt to extreme and adverse growth
24 conditions, an understanding of its stress response mechanisms represents an
25 opportunity for crop improvement. One of these stress-responsive mechanisms
26 involves the activity of microRNAs (miRNAs), which are key molecules for the
27 regulation and fine-tuning of gene expression. Information about the distribution,
28 abundance, or specificity of these molecules in amaranth species is scarce. Here,
29 small RNAs of the *Amaranthus hypocondriacus* variety “Gabriela” were sequenced
30 using Illumina technology, followed by miRNAs loci identification in the amaranth
31 genome using the ShortStack software. Likewise a target genes in the version 2.1
32 of the amaranth genome were identified using psRNATarget and phytozome. Fifty-
33 three genuine miRNAs sequences were identified, of which thirty-three belong to
34 conserved families, and fourteen are novel miRNA sequences. We identified 539
35 putative miRNA target genes in amaranth were identified that, together with the
36 functional categorization of the corresponding *Arabidopsis thaliana* homologs,
37 suggest that they are involved in growth, development, and stress responses.
38 Among the identified miRNAs, we identified a representative group of miRNAs
39 involved in oxidoreductase activity in amaranth, and a novel miRNA which could play
40 an important role regulating PPR proteins. Our results provide evidence of genuine
41 miRNA sequences in the amaranth and provide the basis for future research on
42 miRNA and target genes in this important species to understand the environmental
43 response and genetic improvement.

44 **2. Introduction**

45 The genus *Amaranthus* L., collectively known as amaranth, is a pseudocereal
46 classified into approximately 74 species (Costea and DeMason 2001; Castrillón-
47 Arbeláez and Frier 2016; Das 2016; Waselkov et al. 2018). Its a promising plant
48 genus due to its remarkable nutraceutical and functional properties and its benefits
49 for human health (Silva-Sánchez et al. 2008; Huerta-Ocampo and Barba de la Rosa
50 2011). Amaranth is a plant with high plasticity which is associated to the modulation

51 of development in response to environmental changes, which can adapt to extreme
52 and adverse growth conditions (Rastogi and Shukla 2013; Khanam and Oba 2014;
53 Joshi et al. 2018; Jamalluddin et al. 2019). It exhibits a remarkable capacity to grow
54 under semiarid conditions, which makes it in an excellent crop alternative in regions
55 where other grains cannot be cultivated (Aguilar-Hernandez et al. 2011; Delano-Frier
56 et al. 2011; Massange-Sanchez et al. 2016), which turn to amaranth as an interesting
57 model for known the mechanisms implied in these ambiental advantages. All plants,
58 including amaranth, have encoded capability for stress perception, signaling, and
59 response (Delano-Frier et al. 2011; Atkinson and Urwin 2012; Casique-Arroyo et al.
60 2014; Castrillón-Arbeláez and Frier 2016; Hakim et al. 2018). One of these response
61 mechanisms to environmental conditions is mediated by the activity of small RNAs
62 (sRNAs) included the microRNAs (miRNAs) (Ferdous et al. 2015; Ferdous et al.
63 2017; Liu et al. 2018). MiRNAs represent less than 10% of the total number of sRNAs
64 (Jones-Rhoades et al. 2006; Chavez et al. 2014); however, their conservation and
65 abundance are essential to underlie many of the phenotypic differences between
66 species and determinate their function in specific conditions (Chen and Rajewsky
67 2007; Rosas-Cárdenas and de Folter 2017). Most of the conserved miRNAs across
68 the plant kingdom target transcription factors (TFs), which are key regulators of
69 nearly all essential biological processes, from modulating development, plant
70 metabolic processes, to stress responses (Axtell 2008; Qin et al. 2014; Shi et al.
71 2016; Djami-Tchatchou et al. 2017; Samad et al. 2017). Which suggest that the study
72 of this molecules in plants that can adapt to extreme and adverse growth conditions
73 could help to understand the mechanisms involved. The progress in genomic
74 research of different plant species, coupled with the next-generation sequencing
75 methods, has resulted in extensive data sets of sRNAs, from which many miRNAs
76 have been annotated (Kozomara and Griffiths-Jones 2014; Lei and Sun 2014; Axtell
77 and Meyers 2018; Kozomara et al. 2019). Nevertheless, the majority of miRNAs
78 annotations obtained by sequence homology alone and/or predicted from stem-loop
79 structures are questionable (Kozomara and Griffiths-Jones 2014; Budak and Akpinar
80 2015; Johnson et al. 2016; Axtell and Meyers 2018; Gramzow and Theissen 2019).
81 Therefore, additional criteria are needed in order to consider a miRNA as genuine

82 instead (Axtell and Meyers 2018; Kozomara et al. 2019). Attending to these needs,
83 and given the complexity of plant sRNA populations, packages have emerged such
84 as ShortStack, which was developed to comprehensively analyze reference-aligned
85 sRNA-seq data (Axtell 2013; Shahid and Axtell 2014; Johnson et al. 2016; Axtell and
86 Meyers 2018). Currently, miRNA sequences annotated in miRBase (in release 22)
87 classified as high confidence miRNAs are few. For example, seven high confidence
88 miRNAs for Maize (*Zea mays*), 19 high confidence miRNAs for wheat (*Triticum*
89 *aestivum*), 20 high confidence miRNAs for rice (*Oryza sativa*), and nine high
90 confidence miRNAs for grape vine (*Vitis vinifera*) have been annotated. In this work,
91 we used small RNA sequencing and the ShortStack software (Johnson et al. 2016)
92 to identify miRNA loci present in the Amaranth genome. Likewise, we predicted
93 miRNA target genes, their location and possible function in amaranth, providing the
94 first evidence of genuine miRNA sequences in amaranth and the basis for future
95 research on miRNA and target genes in amaranth.

96

97 **3. Material and methods**

98 **3.1. Plant growth and plant material**

99

100 Seeds of the “Gabriela” variety of *Amaranthus hypochondriacus* L. were sterilized
101 with 10% sodium hypochlorite for 5 min, followed by a treatment with 50% ethanol
102 for 1 min. After each immersion, seeds were washed three times for 3 min with sterile
103 water. Seedlings were grown in restricted spaces as reported previously (Martínez-
104 Núñez et al. 2019). Briefly, seeds were sown in 1" x 1" x 2.5" polystyrene trays
105 containing sterile Sunshine Mix 3 germination mixture (SunGro Horticulture,
106 Bellevue, WA). Plants were grown in a greenhouse under natural daylight conditions
107 (photoperiod of 14 h light/10 h dark at 21-39 °C). Thirty days-old seedlings were
108 submitted to four different environmental conditions included control, cold, heat, and
109 drought. The cold and heat treatments were carried out at XX°C by XX h and XX°C
110 by X h, respectively. The drought treatment lasted three days until we observed

111 obvious damage in the aerial part. After treatments, the aerial part of twenty plants
112 was collected in each biological replicate and frozen immediately in liquid N₂, ground
113 to a fine powder, and stored at -80°C until use. Also, panicle, leaves, root, and stems
114 tissues were collected. Three biological replicates for each condition and tissue were
115 obtained.

116 **3.2. Total RNA extraction and quality**

117

118 Total RNA was extracted using the ZR plant RNA MiniPrep™ kit (Zymo Research,
119 Irvine, CA, USA) according to the manufacturer's instructions. Briefly, 20 mg of tissue
120 previously pulverized was placed into a ZR BashingBead™ Lysis tube, 800 µl of
121 RNA Lysis Buffer was added. The sample was vortex and centrifuged at 13000 rpm
122 for 1 min. The supernatant was transferred into a Zymo-Spin™ IIC Column,
123 centrifuged for 30 s, and the flow-through was recovered. One volume ethanol was
124 added, and the mixture was placed in a Zymo-Spin™ IIC Column and centrifuged
125 for 30 s. Subsequently, 400 µl of RNA Prep Buffer was added to the column, which
126 was centrifuged for 30 s. Next, 700 µl of RNA Wash Buffer was added to the column,
127 and it was centrifuged for 30 s. 400 µl of RNA Wash Buffer was added to the column,
128 and it was centrifuged for 2 min, 35 µl of DNase/RNase-Free water were added
129 directly to the column matrix, and it was centrifuged for 30 s. Finally, it was
130 transferred the eluted RNA into a prepared Zymo-Spin™ IV-HRC Spin Filter Tube in
131 an RNase-free tube, and it was centrifuged at 13000 rpm for 1 min. Total RNA was
132 quantified using a NAS-99 *NuDrop* spectrophotometer (ATCGene, Piscataway, NJ,
133 USA). The RNA quality and integrity was verified in agarose gel electrophoresis.
134 RNA Integrity Number (RIN) values were obtained using an Agilent 2100 Bioanalyzer
135 system (Agilent Technologies, Santa Clara, CA, USA). Subsequent analyses were
136 conducted with RNA samples that satisfied the following criteria: $A_{260/280} = 1.8 - 2.2$;
137 $A_{260/230} \geq 2.0$; 28S/18S RNA ratio > 1.5; and RIN value ≥ 6.0 .

138 **3.3. Construction and sequencing of small RNA libraries**

139

140 Twelve sRNA libraries were constructed in the Unidad de Secuenciación Masiva
141 de DNA of Instituto de Biotecnología, UNAM, using the NEXTFLEX® Small RNA-

142 Seq Kit v3 (Illumina® Compatible) (Bioo Scientific), according to the manufacturer's
143 protocol. Briefly, one µg of total RNA in 10.5 µL of Nuclease-free Water was used
144 for each library. Samples were heated at 70 °C for 2 min and then immediately
145 placed on ice for 5 min. After, 1 µL of NEXTFLEX® 3' 4N Adenylated Adapter, 7 µL
146 of NEXTFLEX® 3' Ligation Buffer and 1.5 µL of NEXTFLEX® 3' Ligation Enzyme
147 Mix was added and incubated at 25 °C during 2 h. Subsequently, excess of 3'
148 adapter was removed and inactivated following the instructions of manufacturer. 14
149 µL of Purified NEXTFLEX® 3' 4N Adenylated Adapter Ligated RNA from previous
150 steps, 1.5 uL of NEXTFLEX® 5' 4N adapter previously heated to 70 °C during 2 min,
151 7.5 µL of NEXTFLEX® 5' Ligation Buffer and 2 µL of NEXTFLEX® 5' Ligation
152 Enzyme Mix was added and incubated for 1 h at 20 °C in a thermocycler with heated
153 lid turned off. After ligation of 3' and 5' adapters, for reverse transcription first-strand
154 synthesis, 13 µL of NEXTFLEX® RT Buffer and 2 uL of M-MuLV Reverse
155 Transcriptase, incubated at 42 °C during 30 minutes and then 10 minutes at 90 °C
156 to denature enzyme. After purification of cDNA reaction with magnetic beads, the
157 construction was amplified by PCR reaction according to the manufacturer's
158 recommendation. Libraries were purified by PAGE following instructions in the
159 protocol. Final library was analyzed in a Bioanalyzer 2100 device and quantified by
160 a fluorometer (Qubit) using the Qubit High Sensitivity Assay Kit. Libraries were
161 sequenced using the NextSeq device by 1x75 cycles (Illumina, San Diego, CA,
162 USA).

163 **3.4. sRNA-seq data analysis**

164 Raw reads in FASTQ format were prepared for analysis using Atropos (Didion et al.
165 2017). First, the adapter sequence was discarded with the options -e 0.12 -q 20 -a
166 TGG AATTCTCGGGTGCCAAGG (error rate of 12%, minimum base quality of 20, 3'
167 adapter removal). The sequence length histogram of the resulting libraries presented
168 two peaks at 29 and 32 nucleotides, an indication of the presence of an extra eight
169 bases, four at the 5' end and four at the 3' end. These bases were removed with a
170 second round of Atropos with the options -u 4 -u -4. -m 12 -M 30 (remove four bases
171 from the 5' end, four bases from the 3' end, minimum sequences length of 12

172 nucleotides, the maximum length of 30 nucleotides). Processed reads were used as
173 input for ShortStack version 3.8.5 (Johnson et al. 2016) with the parameters --mincov
174 3 --dicermin 20 --dicermax 30 --foldsize 1000, using the 16 Scaffolds of the
175 *Amaranthus hypochondriacus* genome v2.1 available at Phytozome 12
176 (<https://phytozome.jgi.doe.gov/>) (Clouse et al. 2016) as reference. The resulting
177 trimmed fasta file was then mapped against the *A. hypochondriacus* genome using
178 bowtie version 0.12.8 (McCormick et al. 2011). The bowtie output was piped through
179 the “Prep_bam.pl” script (part of the ShortStack package; [http://axtell-lab-
180 psu.weebly.com/shortstack.html](http://axtell-lab-
180 psu.weebly.com/shortstack.html)) version 0.1.1 to produce a properly formatted and
181 sorted BAM alignment file. The read counts reported by ShortStack were normalized
182 to reads per million (RPM). Fifteen criteria considered by ShortStack (Table S1) were
183 taken into account, including alignment in the locus, size, abundance, RNA fold of
184 locus, and miRNA*. The data generated by ShortStack analysis of miRNAs
185 sequences were used to locate each miRNA along the scaffolds of *A.*
186 *hypochondriacus* (v2.1) deposited in the Phytozome 12 database
187 (<https://phytozome.jgi.doe.gov/>).

188 3.5. Quantitative Real-Time PCR reaction

189

190 sRNAs were extracted from 20 mg of frozen aerial tissue using the LiCl method
191 (Rosas-Cardenas et al. 2011). RNA concentration and purity were determined as
192 described above. Quantification of plant miRNAs can be made using S-Poly(T)
193 method (Kang et al. 2012), 500 ng of enriched sRNA were poly(A) tailed using *E.*
194 *coli* Poly(A) Polymerase (New England Biolabs, Massachusetts) with some
195 adjustments (Kang et al. 2012; Vera-Hernández et al. 2019). Briefly, to 500 ng of
196 sRNA was added 1 µl of 10x Poly(A) polymerase reaction buffer, 1 µl of 10 mM ATP,
197 0.1 µl of Ribonuclease Inhibitor (Sigma Aldrich, USA), and 0.8 units of Poly(A)
198 polymerase, with a total volume of 10 µl. The reaction mixture was incubated at 37°C
199 for 40 min, and inactivated at 65°C for 5 min. The tailed sRNA from the last reaction
200 was mixed in 8 µl reaction that contained 2 µl of the polyadenylation reaction product,
201 1 µl of 0.1 µM RT primer (Table S2), and 0.5 µl of 10 mM dNTP. The mix was heated

202 to 65°C for 5 min, and ice cooled for 2 min. After, 1 µl of MMLV 10 x reaction buffer,
203 0.1 µl of Ribonuclease Inhibitor, and 100 units of MMLV Reverse Transcriptase
204 (Sigma Aldrich, USA) were added to the reaction. The cDNA synthesis reactions
205 were performed at 25°C for 20 min, 37°C for 60 min, followed by 70°C for 10 min.
206 qRT-PCR reactions for each miRNA were performed with a specific forward primer
207 and a universal reverse primer (Table S2). PCR products were detected by a
208 universal TaqMan probe on the StepOne™ Real-Time PCR System (Applied
209 Biosystems, Foster City, CA, USA). The qRT-PCR mixture contained 5 µl of
210 TaqProbe 2x qPCR MasterMix with ROX (Applied Biological Materials, Canada), 0.3
211 µl of 400 nM of universal RV primer, 0.3 µl of 300 nM of miRNA-specific primer, and
212 0.4 µl of 10 µM universal TaqMan probe, 4 µl of diluted cDNA that corresponded at
213 5 ng of enriched sRNA polyadenylated, in a final volume of 10 µl. qRT-PCR with no
214 template was also performed for each primer pair as a control. The reaction cycle
215 was 95°C for 10 min; 40 cycles of 95°C for 15 s, and 60°C for 40 s, in 96-well optical
216 reaction plates (Applied Biosystems, Foster City, CA, USA). Two technical and three
217 biological replicates of each sample were used for the qRT-PCR analysis. The
218 expression level of each mature miRNA was recorded by the threshold cycle (Ct)
219 and normalized against housekeeping genes *Ahy_U3* and *Ahy_snor71* from
220 amaranth (Table S2).

221 **3.6. Prediction of miRNA target and their locations along the *A.*** 222 ***hypochondriacus* genome**

223
224 Target identification of miRNA candidates was conducted based on the online tool
225 psRNATarget (<http://plantgrn.noble.org/psRNATarget/>) (Dai et al. 2018). Parameters
226 such as 2 mismatches, minimal free energy lower than -28.2 kcal/mol, and an
227 expectation value of ≤ 3 were used. Accordingly, coding sequences (CDS) of miRNA
228 targets predicted by psRNATarget were aligned against the version 2.1 of the
229 genome to obtain gene description and location. In addition, CDS were also aligned
230 against the NCBI nucleotide database for obtaining the best match. Finally, putative
231 orthologs of miRNA targets corresponding to *Arabidopsis thaliana* were extracted
232 among the protein homologs found in Phytozome.

233 **3.7. Functional classification of orthologs genes and construction of** 234 **networks** 235

236 Enriched Gene Ontology categories was carried out with the putative *Arabidopsis*
237 *thaliana* orthologs, corresponding to the miRNA targets of *Amaranthus*
238 *hypochondriacus* predicted by psRNATarget. In that sense, putative orthologs of
239 miRNA targets were submitted to AgriGO v2.0 (<http://bioinfo.cau.edu.cn/agriGO/>)
240 (Tian et al. 2017) selecting the singular enrichment analysis (SEA) for this purpose.
241 On the other hand, gene network associations among miRNA targets were obtained
242 with the STRING software (Szklarczyk et al. 2017), and the GENEMANIA webserver
243 (<http://genemania.org/>) (Warde-Farley et al. 2010).

244 **4. Results**

245 **4.1. sRNA sequencing, size distribution and chromosomal localization** 246

247 The main objective of this study was to identify miRNA sequences present in the
248 *Amaranthus hypochondriacus* L. genome. For this, we used high-throughput
249 sequencing, for the aerial part of 30 days-old amaranth seedlings control or treated
250 were used as the source of sRNAs, which has been proven to be an efficient tissue
251 for the early detection of drought (Huerta-Ocampo et al. 2009), cold and heat stress
252 response in amaranth (data no shown). Twelve libraries were sequenced using
253 Illumina high-throughput technology. The number of reads for each library is
254 presented in Table S3. An average of 3.8 millions of clean reads for each library was
255 obtained, except one low library with low number of read (library 7 In Table S3) that
256 was discarded. Between 15000 to 35000 ShortStack identified clusters were present
257 in each Amaranth genome scaffold. The majority of these clusters had abundances
258 of 10 reads or lower (Figure 1a), similar to previous reports in wheat (*Triticum*
259 *aestivum* L.) (Zhou et al. 2015), blueberry (*Vaccinium ashei*) (Li et al. 2018), winter
260 turnip rape (*Brassica rapa* L.) (Zeng et al. 2018), and banana (*Musa paradisiaca*)
261 (Zhu et al. 2019). A total of 360,380 DICER-called sequences were identified by
262 ShortStack, ranging from 18 to 30-nt in length (Table S4). The abundance
263 distribution histogram of sRNAs indicates that 24-nt sRNA class is the most

264 abundant, followed by the 23-nt sequences (Figure 1b). This distribution is consistent
265 with the known plant sRNA distribution (Chavez et al. 2014). Additionally, 30-nt
266 sRNAs sequences were also abundant (Figure 1b), which has been observed in
267 hexaploid wheat (*T. aestivum* L.) cultivar Neimai8 (Zhou et al. 2015), and Grapevine
268 (Jiu et al. 2019).

269 **4.2. Identification and abundance of genuine-miRNAs in amaranth**

270

271 According to the ShortStack criteria, more than 99 % (99.98%) of sRNA clusters
272 identified were not classified as miRNAs, the N6 and N11 criteria (Table S1) were
273 the most common causes (Figure 1c). ShortStack identified 53 miRNA clusters and
274 42 unique miRNA sequences, which were named using the first four letters of the
275 species (Ahyp) and up to four digits as identifiers. For conserved miRNAs, the digits
276 correspond to the miRBase family to which the miRNA belongs (Table 1). According
277 to the criteria of Axtell and Meyers (2018), 39 sequences that belonged to 21 miRNA
278 families were classified as conserved miRNAs, and 14 cluster, corresponding to 14
279 miRNA families, were classified as novel miRNA of amaranth (Table 1). We divided
280 the conserved miRNAs into “high confidence” and “low conserved miRNAs”. The first
281 set included 18 sequences classified as members of miR156, miR159, miR160,
282 miR164, miR166, miR167, miR168, miR171, miR172, miR319, miR390, miR393,
283 miR395 and miR396 families, which are highly conserved across all the phylogeny
284 of terrestrial plant species (Chavez et al. 2014; Qin et al. 2014; Axtell and Meyers
285 2018) (Table 1). The low conserved miRNAs, which are miRNAs that are missing in
286 some species (Chavez et al. 2014) included 12 sequences that correspond to
287 miR162, miR397, miR398, miR399, miR408, miR535, and miR2111 families (Table
288 1).

289 Novel miRNAs were divided in two categories, the “similar to other miRNAs” and the
290 “amaranth-specific miRNAs”. On one hand, the “similar to other miRNAs” group
291 included the following miRNAs: miR0008 (similar to pab-miR3627a/mtr-miR5225a),
292 miR0010 (similar to mtr-miR5225a), miR0011 (similar to lja-miR11161-5p), miR0012
293 (similar to mtr-miR2630a), miR0013 (similar to ppe-miR482c), miR0014 (similar to

294 bmo-miR-3301), and miR0015 (two mismatches respect to gra-miR482d). On the
295 other hand, the “amaranth-specific miRNAs” group, which are sequences that do not
296 resemble to any sequence present in miRBase, included the following miRNAs:
297 miR0001-miR0006, and miR0009 (Table 1).

298 Abundance of amaranth miRNAs varies drastically founding sequences ranging from
299 0.28 to 96,113 RPM (Figure 2). MiRNAs were divided by abundance in four groups
300 (Figure 2a). In Group I, sequences with >1000 RPM were clustered, including
301 miRNAs such as miR159 (with 36, 843 RPM), miR396, miR167, miR319, and
302 miR166. The Group II included sequences between 100-1000 RPM that
303 corresponded to miR535, miR172, miR164, miR0013, and miR398, miR162a,
304 miR156, miR0015, miR168, miR160, and miR408 (Figure 2a). In the Group III were
305 included sequences (between 10-100 RPM) included to miR0005, miR0008,
306 miR171, miR397 miR0010, miR0012, miR390, miR393, miR2111, miR399, and
307 miR0002. Finally, in the group IV with expression levels <10 RPM were clustered
308 the following miRNAs: miR0001, miR395, miR0009, miR0014, miR0011, miR0006,
309 miR0003, and miR0004 (Figure 2a). Importantly, sequencing data were validated by
310 qRT-PCR analysis using six conserved miRNAs (miR159, miR171, miR319,
311 miR397, miR408, miR535) and two novel miRNAs (miR0002, and miR0005) (Figure
312 2b). In general, a correlation between conservation and abundance was observed
313 among miRNAs sequenced and the miRNAs evaluated by qRT-PCR (Figure 2),
314 which showed that the abundance identified by sequencing is appropriate.

315 **4.3. Putative miRNA target genes**

316

317 We next used the major RNA sequence of our ShortStack identified miRNA clusters
318 to identify their putative targets using the psRNATarget web server
319 ([http://plantgrn.noble.org/psRNATarget/.](http://plantgrn.noble.org/psRNATarget/)) with default parameters, except for an
320 expectation value, for which ≤ 3 was established (Dai et al. 2018). According, we
321 identified a total of 537 target genes for the 53 miRNAs, and the number of targets
322 per miRNA sequence varied greatly. For instance, we predicted 45 target genes for
323 miR0005, whereas only one target was predicted for miR0008 (Table S5). Among
324 the putative targets for conserved miRNAs, important TF were predicted (Table 2),

325 including *SPL6* (a *miR156/miR157* target), *TOE*, *TCP* (*miR319*), *ABI5* (*miR172*), and
326 *AP2* (*miR172*). The predicted target genes identified for conserved miRNAs included
327 *miR156*, *miR159*, *miR168*, *miR172*, and *miR319* were similar to those that have
328 been reported in other species (Aukerman and Sakai 2003; Xian et al. 2014; Koyama
329 et al. 2017; Zheng et al. 2017), suggesting that these miRNAs play the same role in
330 amaranth. Several laccases genes were predicted as targets of *miR397* and
331 *miR408*, both classified as low conserved miRNAs. Several genes were identified as
332 target for specific amaranth miRNAs. *miR0005* was the novel miRNA with more
333 target genes, among the target genes we identified *BASS2*, and a group of 35
334 Pentatricopeptide repeat-containing (PPR) proteins (Table 2, S5). Suggesting a
335 important role of specific miRNAs in amaranth.

336

337 **4.4. Distributions of miRNAs and their target genes in the amaranth** 338 **genome**

339

340 In plants, miRNAs families vary in size and genomic organization (Li and Mao 2007).
341 Therefore, to elucidate particular features in the miRNA diversification and genome
342 organization miRNAs have been localized in chromosomes (e.g., *Oryza sativa*
343 (Baldrich et al. 2016) and *Zea mays* (Zhang et al. 2009)). In plants, miRNAs families
344 vary in size and genomic organization (Li and Mao 2007). We localize both miRNAs
345 and putative target genes in the different amaranth scaffolds (Figure 3). Throughout
346 the amaranth genome we found five *miR156* loci, four *miR2111* loci, three *miR166*
347 and *miR167* loci, and two *miR160*, *miR171*, *miR172*, *miR319*, *miR396* and *miR535*
348 loci, and only one locus for the rest miRNAs included the novel miRNAs (Figure 3a).
349 Most miRNAs were located at the extreme regions, except in the scaffolds 9 and 12,
350 in which several miRNAs were located in the central region (Figure 3a), in these
351 scaffolds, a major number of miRNAs was detected (Figure 3b). We identified, a
352 polycistronic MIRNA loci for *miRx* y *miRX2* which originated of the same precursor,
353 as in observed in other plants (Wang et al. 2007; Griffiths-Jones et al. 2008; Merchan
354 et al. 2009; Zhang et al. 2009; Guo et al. 2012; Baldrich et al. 2016). On the other

355 hand, we localized 34 and 33 target genes in the scaffold 2 and 4, respectively;
356 whereas the scaffold 14 contained the minor number of targets genes (Figure 3c).

357 **4.5. Regulatory network target genes-miRNA predicted for amaranth**

358

359 For a better interpretation of the possible role of miRNAs in amaranth, an ontology
360 (GO) of target genes in *Arabidopsis thaliana* were constructed using agriGO (Figure
361 4, Table S6). A hierarchical organization was obtained (Figure S1). Of 261 orthologs
362 genes predicted for 53 miRNAs, 254 genes were found with GO annotation (Table
363 S6). The GO-biological process revealed that the putative targets of amaranth
364 miRNAs are significantly involved in a broad range of functions, such as cellular
365 processes (148 targets), metabolic processes (135 targets), biological regulation (86
366 targets), response to stimulus (78 targets), single-organisms process (130 targets),
367 multicellular organismal process (67 targets) and developmental processes (70
368 targets) (Figure S1, Table S6). In general, GO terms enriched suggest that miRNAs
369 targets of 53 amaranth miRNAs are involved in the growth and development
370 process. Conserved miRNAs targets were involved in 101 biological processes, 47
371 molecular functions, and 15 cellular components (Figure 4). Novel miRNAs targets
372 were involved in XX biological processes, XX molecular functions, and XX cellular
373 components (Figure 4, Table S6). Respect to cellular component and molecular
374 function, the most representative processes were intracellular membrane-bounded
375 organelle and oxidoreductase activity, respectively (Figure 5). GO enrichment
376 analysis revealed that the target genes of conserved miRNAs appeared to be
377 enriched in XXX, while the target genes of novel miRNAs were significantly related
378 to response of XXX (Figure4). We visualized the functional protein association
379 network of target genes using the string software (Figure 6). Interestingly, the string
380 analysis showed that miR159, the most abundant miRNA in amaranth, play a key
381 interaction with target genes of conserved (miR162, miR396, miR156, miR390,
382 miR397, miR393, miR395, miR535) and novel miRNAs (miR004, miR0013, and
383 miR0010) (Figure 6). Within the subnetwork formed by miR159 we found a direct
384 association with target genes of miR162, miR396, miR156, miR390, miR397,
385 miR393, miR395, miR535, as well as with target genes for novel miRNAs miR004,

386 miR0013, and miR0010 (Figure 6). We observed another important sub-network for
387 miR162, miR156 and miR168. In the former case, genes encoding proteins with
388 laccase activity were found in a region involving miR397 and miR408 (Figure 6), for
389 which a match with GO enrichment analysis in molecular function was found. The
390 target genes involved in this set are regulated by miR397, miR399, and miR408. The
391 interaction between miRNA targets of miR397 and miR408 was analyzed on
392 GENEMANIA showing these miRNAs regulate different genes of the laccases family
393 (Figure 7a). Importantly, the expression of miR397 and miR408 was analyzed in
394 panicle, leaves, roots, and stems of amaranth plants, showing that these miRNAs
395 are differentially expressed in all tissues (Figure 7b), indicating that the miRNA
396 abundance is tissue-dependent. Likewise, the interaction between miRNA targets of
397 miR0005 was analyzed on GENEMANIA showing this miRNA regulate both TF and
398 PPR and other proteins (Figure 8).

399 **5. Discussion**

400 **5.1. Conservation, confidence, and abundance of amaranth miRNAs**

401

402 In this work we used eleven small RNA libraries and the ShortStack script to identify
403 miRNAs present in the *A. hypochondriacus* genome. By using the most stringent
404 criteria, we have minimized false-positives; thereby, our study provides valuable
405 information for annotation and classification of miRNAs in *A. hypochondriacus* with
406 a higher degree of accuracy. In that sense, we identified 53 miRNAs, of which 27
407 was classified as “high confidence”, 12 as “low conservation”, 7 as “similar to other
408 miRNAs” and 7 as “amaranth-specific” (Table 1). In the case of high confidence
409 miRNAs, they have been classified based on the pattern of mapped reads
410 (Kozomara and Griffiths-Jones 2014). Moreover, the 27 high confidence amaranth
411 miRNAs were also the most abundant, a correlation that has been commonly
412 observed in previous studies (Sunkar et al. 2008; Chavez et al. 2014; Qin et al.
413 2014).

414 For instance, miR156, miR159 and miR166 have been reported as the most
415 abundant miRNAs in several plants (Zhang et al. 2006; Chavez et al. 2014; He et al.
416 2019; Ravichandran et al. 2019). According, miR159, miR396, miR167, miR319 and
417 miR166 were the most abundant miRNAs found in *A. hypochondriacus* (Figure 2a).
418 Particularly, miR159 was the most abundant miRNA family that we identified in this
419 work, similar to what has been reported for *A. tricolor* (Liu et al. 2018). This suggests
420 that miR159 is the most abundant miRNA family in amaranth species. Inversely,
421 plant species-specific miRNAs have low abundances (Zhu et al. 2013; Xia et al.
422 2016), being the same case in amaranth (Figure 2). Of our 7 identified amaranth-
423 specific miRNAs, 6 have low abundances, ranging from 0.18 to 11.2 RPM. A special
424 case was MiR0005, the only amaranth-specific miRNA with high abundance miRNA
425 is discussed below.

426

427 **5.2. MiRNAs loci in the amaranth genome**

428

429 The identified miRNAs and their putative target genes did not show a distribution
430 pattern in the amaranth genome (Figure 3). However, we found a correlation
431 between conserved and novel miRNAs loci number, identifying one loci for novel
432 miRNAs. We identified different loci number in amaranth genome for some
433 conserved miRNAs like miR156, miR166, and miR167. Suggesting that these
434 miRNAs appeared before amaranth genome polyploidization, just as it has
435 happened in other plants (Guddeti et al. 2005; Maher et al. 2006; Katiyar et al. 2012;
436 Ye et al. 2013). For novel or similar to other miRNAs, we found one loci. We
437 observed an interesting case for miR2111, for which we identified three loci in the
438 amaranth genome, which has been identified only in eudicot species, and recently,
439 has been considered as high confidence miRNA (Peláez et al. 2012), suggesting
440 this miRNA could play an important role in eudicot species, included amaranth,
441 which is discussed below.

442

443

444

445 **Conserved and possible novel roles for conserved amaranth miRNAs**

446 Categorization of miRNA target genes according to their function in biological,
447 cellular component and molecular, found that conserved amaranth miRNAs are
448 involved in fundamental biological processes xxx. This in agreement to previous
449 studies in other plant species, which have shown that conserved miRNAs are
450 involved in A B C (Floyd and Bowman 2004; Jasinski et al. 2010; Song et al. 2017;
451 Liu et al. 2018). For example, miR166 represses to *PHB*, *PHV*, and *REV HD-ZIP III*
452 genes in Arabidopsis to avoid adaxialization of the abaxial side (Sakaguchi and
453 Watanabe, 2011). We found at *REV*, *ATHB-8*, and *ATHB-15* as target genes in
454 amaranth, for which we would expect that its function is also conserved, suggesting
455 that such as in *A. thaliana*, miR166 regulate the abaxial side in leaves (Sakaguchi
456 and Watanabe 2012).

457 The regulatory network determined by String, which involves target genes suggests
458 that certain miRNAs are located in important hubs within networks, whereas others
459 could be acting on specific pathways (Figure 6). In fact, an important interaction of a
460 miR159 target genes with other miRNAs target genes both conserved and novel
461 miRNAs was observed (Figure 6). Likewise, we found both sequencing and qRT-
462 PCR that miR159 is the most abundant miRNA, suggesting that miR159 is a key
463 regulator in amaranth. In *A. thaliana*, miR159 functions upstream of miR156 to
464 modulate vegetative to reproductive phase transition. MYB33, a target of miR159,
465 serves as an activator of miR156a,c as well as *SPL9* to regulate vegetative phase
466 change in Arabidopsis (Guo et al. 2017). This principle seems to be fulfilled in
467 amaranth where miR159 was highly expressed versus miR156, suggesting that as
468 in *A. thaliana*, the miR159 -> miR156 regulation could also be associated with the
469 appearance of leaves, and branches during the reproductive phase through the
470 regulation of *MYB* genes (Alonso-Peral et al. 2010). In amaranth we found several
471 genes as targets of miR159 included *MYB21*, and *SPL6*, *SPL7*, *SPL12*, and *SPL17*
472 between the targets of miR156. *TCP3*, *TPC4*, *AOX1*, a protein phosphatase 2C a
473 cyclic nucleotide-binding/kinase domain-containing protein, and uncharacterized N-
474 acetyltransferase *yfc52* (*yfc52*) were also identified as putative target genes of
475 miR159, suggesting that miR159 plays different roles included species-specific

476 roles. In fact, an important interaction of a miR159 target genes with other miRNAs
477 target genes both conserved and novel miRNAs was observed (Figure 6) suggesting
478 that miR159 is a key regulator in amaranth, and that furthermore of conserved
479 functions, miR159 could plays different roles species-specific.

480 **5.3. Small RNA stress libraries identify stress-related miRNAs**

481 Several of the target genes predicted for our identified miRNAs have a role in stress
482 responses. This was expected, since our small RNA libraries were obtained from
483 stress-treated plants. For example, miR0015 and miR0013 classified as “similar to
484 other miRNAs” target pathogen response proteins: disease resistance protein RPS5
485 for miR0015, and a putative late blight resistance protein homolog R1B-14 for
486 miR0013. MiR0015 and miR0013 have three and two mismatches with respect to
487 gra-miR482d and ppe-miR482c, respectively. MiRNA sequences that belong to the
488 miR482 family are not identical and have mismatches between them, suggesting
489 that miR0013 and miR0015 could belong to this family. This is also consistent with
490 the fact that, in *Solanum* species, the miR482 family regulates a class of pathogen-
491 resistance genes, nucleotide-binding site leucine-rich repeat genes (*NBS-LRRs*; de
492 Vries et al. 2018), suggesting similar to miRNAs reported in other species, miR0013
493 and miR0015 could target genes associated to same process.

494 Several miRNAs included miR397, miR398, miR408, and miR2111 involved in
495 oxidoreductase activity were found in amaranth. Oxidoreductase activity was the
496 most significant process observed in relation to molecular function in amaranth
497 (Figure 5). miR2111 is a high confidence miRNA of low abundance (Axtell and
498 Meyers 2018), that has been found in *Brassica napus*, *Brassica rapa*, *Arabidopsis*
499 *thaliana*, *Arabidopsis lyrata*, *Cucumis melo*, and *Glicine max* (miRbase release 22.1)
500 (Kozomara et al. 2019), Three target genes are predicted in amaranth: *FUBP1* (Far
501 upstream element-binding protein 1), *DEK-like*, and F-box/kelch-repeat protein
502 At3g27150. *DEK3* contributes to modulation of *Arabidopsis thaliana* chromatin
503 structure and function and is crucial for stress tolerance (Waidmann et al. 2014). In
504 *Nicotiana tabacum* also matched with F-box/kelch-repeat protein At3g27150 (Huen
505 et al. 2018). F-box proteins are involved in the controlled ubiquitin-dependent
506 degradation of proteins triggered in response to various stimuli during growth and/or

507 diverse stress conditions in amaranth (Delano-Frier et al. 2011). In *Phaseolus*
508 *vulgaris*, miR2111 undergoes shoot-to-root translocation to control rhizobial infection
509 through posttranscriptional regulation of the symbiosis suppressor Too much love
510 (TML) in roots (Tsikou et al. 2018). The miR2111-*TML* regulatory node ensures
511 activation of feedback regulation to balance infection and nodulation events (Tsikou
512 et al. 2018). This suggest that, in amaranth, miR2111 could also have an important
513 role in biotic stress.

514 Different laccases genes were putative target for miR397 and miR408 (Figure 7a).
515 Laccases are known targets of miR397 and miR408 in *Oryza sativa*, *Citrus Cinesis*,
516 and *Arabidopsis thaliana* (Huang et al. 2016; Song et al. 2017; Carrió-Seguí et al.
517 2019). Laccases are encoded by a multigene family, which play roles in the oxidation
518 of flavonoids and the change of the lignin composition of plants under biotic and
519 abiotic stresses conditions (Liu et al. 2017). The overexpression of a putative rice
520 laccase precursor of *OsChl1* in *Arabidopsis thaliana* results in an increased
521 tolerance to drought and salinity stress (Cho et al. 2014). In *Beckmannia syzigachne*
522 plants, miR397 is upregulated in herbicide resistant plants versus sensitive plants
523 versus sensitive plants, whereas laccase expression and activity show the opposite
524 trend (Pan et al. 2017). Since miR397 and miR408 are relatively abundant and
525 conserved miRNAs, it is likely that their function in amaranth is also conserved.
526 Then, we could suggest that, similar that in *Beckmannia syzigachne* a possible
527 relationship between herbicide resistance described in *Palmer amaranth* (Chandi et
528 al. 2013), and ability to tolerate drought stress, could be associated to miR397,
529 miR408 and laccase levels in amaranth species. Likewise, is possible consider that
530 the lignin and biomass could be are affected by miR397, miR408 and laccases
531 relation in amaranth.

532 **5.4. miR0005 is an abundant, amaranth-specific miRNA**

533 Contrary to the other amaranth-specific miRNAs that we identified, miR0005 has an
534 abundance of XYZ RPM (Figure 2). It is not common for a species-specific miRNA
535 to have high abundance, and this would suggest that miR0005 plays an important
536 role in amaranth species. Among the 45 target genes predicted for miR0005 we
537 found a group of 35 PPR proteins (Figure 8a). PPR proteins are RNA binding

538 proteins that facilitate processing, splicing, editing, stability and translation of RNAs
539 (Schmitz-Linneweber and Small 2008; Manna 2015). Several PPRs play important
540 roles in various biotic and abiotic stresses (Tadini et al. 2016; Paieri et al. 2018; Wu
541 et al. 2018; Xing et al. 2018), including heat stress in maize leaves, which a specific
542 miRNA was identified as responsive to heat stress (He et al. 2019). Among the
543 predicted target PPR genes, we found to genomes uncoupled 1 (GUN1). GUN1 is a
544 central integrator of chloroplast retrograde signaling pathways and plays a role in
545 multiple stress-related retrograde signaling pathways (Tadini et al. 2016; Paieri et al.
546 2018; Wu et al. 2018, Zhao et al. 2019), the regulation of *ABI4* expression, and
547 photooxidative stress responses in *Arabidopsis thaliana* (Koussevitzky et al. 2007).

548 Other predicted target of miR0005 is PPR40. Knock-out of PPR40 in *Arabidopsis*
549 *thaliana* resulted in increased accumulation of ROS, and lipid peroxidation and
550 superoxide dismutase activity (Zsigmond et al. 2008). Additional target gene for
551 miR0005 is *BASS2*. The *BASS2* protein is localized at the chloroplast envelope
552 membrane, and is highly abundant in C4 plants that have the sodium-dependent
553 pyruvate transporter (Furumoto et al. 2011). *Arabidopsis thaliana* *BASS2*
554 overexpression lines produced seeds that were larger and heavier and contained
555 10-37% more oil than those of the wild type (Lee et al. 2017). All these data suggest
556 that a link exists between oxidative stress response and seed yield, and the
557 abundance of miR0005 could be a key regulator of stress response and seed yield
558 in amaranth.

559 Likewise, although miR0005 is a specific miRNA their abundance was high
560 compared with other specific miRNAs. Since amaranth is considered as a crop
561 tolerant to high temperatures, it will be necessary to validate the PPR genes, which
562 are putatively targeted by miR0005. The next step will be the functional analysis of
563 specific amaranth miRNAs.

564

565 **6. Conclusions**

566 The comparative genomics approaches by ShortStack allow us to ensure 53 genuine
567 miRNAs of *Amaranthus hypochondriacus*. 539 putative target genes were identified
568 in amaranth. MiRNAs and miRNA-targets genes identified in amaranth genome
569 suggest their participation in different cellular and metabolic processes that regulate
570 the development and its response to different environmental stimulus in this crop,
571 founding an interesting relation of miR159 with novel and conserved miRNAs, and
572 evident interaction between miR397, miR398, and miR408 associated to
573 oxidoreductase activity in amaranth. Likewise, the next step will be the functional
574 analysis of specific amaranth miRNAs, such as miR0005, for which a group of 35
575 PPR proteins were predicted as target genes included GUN1. Summarily, we hope
576 that our results could serve as reference material for researchers interested in
577 Amaranth miRNA biology. Which will be useful in unraveling the molecular
578 mechanisms underlying environmental conditions responses and genetic
579 improvement in Amaranth. Our work is an important step for understanding miRNA-
580 mediated stress-response mechanisms in Amaranth, and therefore understanding
581 the ability of this crop to adapt to non-optimal growth conditions.

582 **7. Acknowledgments**

583 Thanks to Dra. Martha Dolores Bibbins Martínez who have generously provided
584 equipment StepOnePlus Real-Time PCR System.

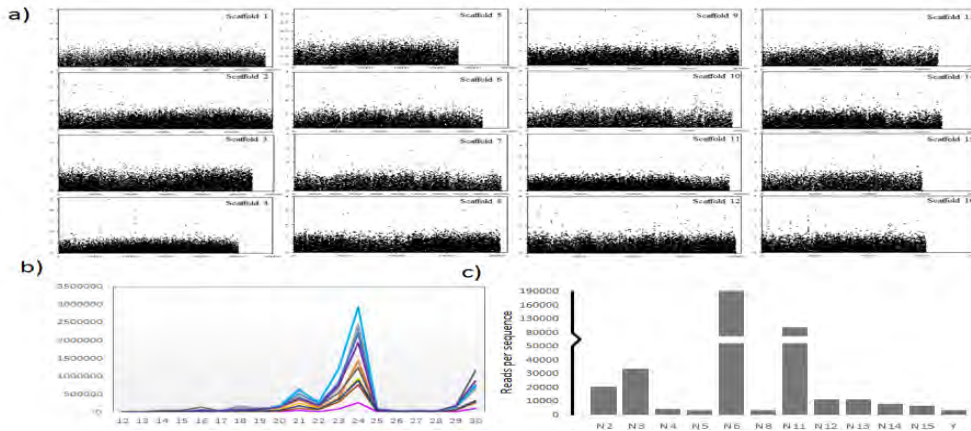
585 **8. Author contributions**

586 MMN, MRR, and FFRC conceived the project. MMN, MRR, and FFRC designed the
587 experiments. MMN and MRR performed most of the experimental work. PFVH and
588 MMN performed the qRT-PCR. RACM, and MRR performed bioinformatics work.
589 JGJ, MMN, MRR, RACM and FFRC participate in data integration. SdF, SLS, RACM,
590 MRR and FFRC participate in result analysis. MMN, and FFRC drafted the
591 manuscript. All authors revised and approved the final manuscript.

592 **9. Financial support**

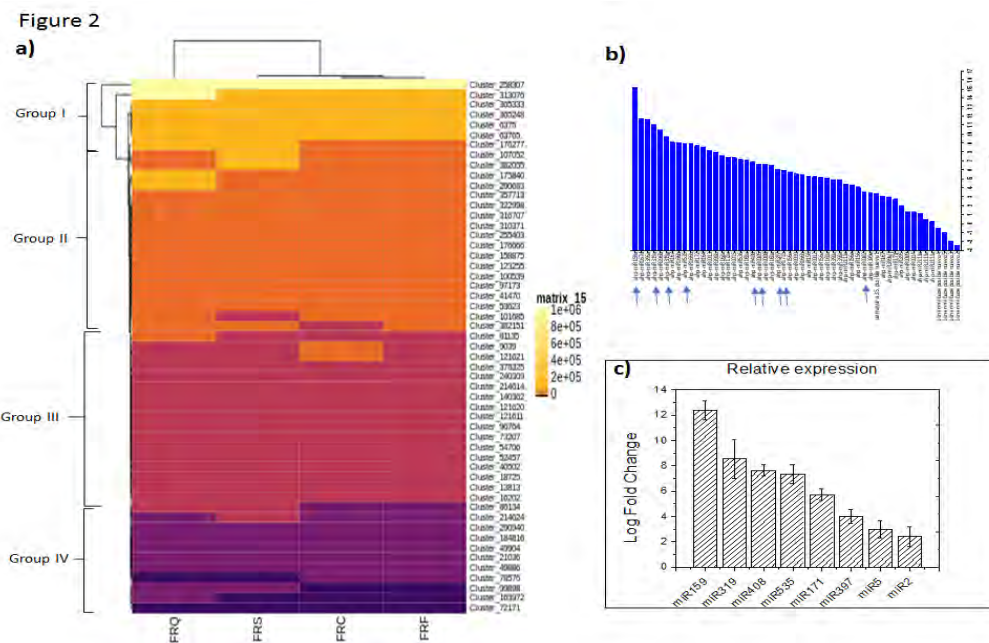
593 MMN, MRR, and PFVH were supported by the Mexican National Council of Science
 594 and Technology (CONACyT) fellowship. This work was financed by CONACyT grant
 595 221522, and SIP grants 20180545 and 20195904.

596 **Figures**



597

598 **Figure 7** (Figure 1). Sequencing data analysis of small RNAs of amaranth. a) Distribution of unique sequences
 599 in the amaranth genome. The sequences were distributed between the sixteen amaranth scaffolds. Sequences
 600 with more of one sequence per million were represented. The X-axis, represented each sequence identified by
 601 sequencing; and Y-axis, represent the abundance expressed as the base 10 logarithms of RPM. b) Length
 602 distribution of sRNAs sequences. c) Classification of unique read sequences discarded in each ShortStack
 603 criteria. Details of ShortStack criteria can be found in Table S1.

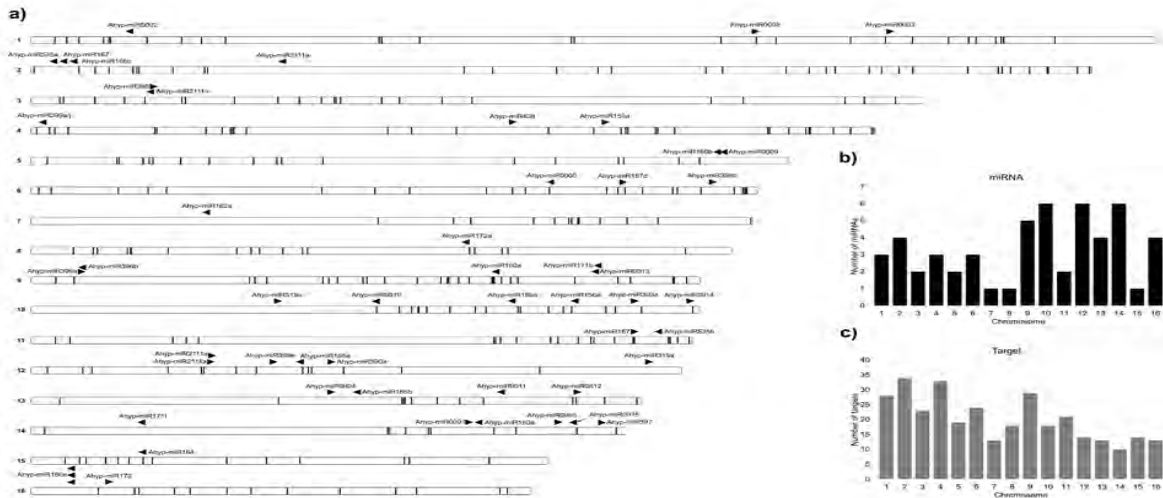


604

605 **Figura 8.** (Figure 2). Abundance of amaranth miRNAs. a) Abundance of miRNAs obtained by sequencing in
 606 drought, cold and heat stress treatment. The abundance was expressed as the base 2 logarithms of RPM. b)
 607 Abundance of miRNAs obtained by sequencing of aerial part of plants control. c) Validation of miRNAs by
 608 quantitative real-time RT-PCR in the aerial part of plants control amaranth.

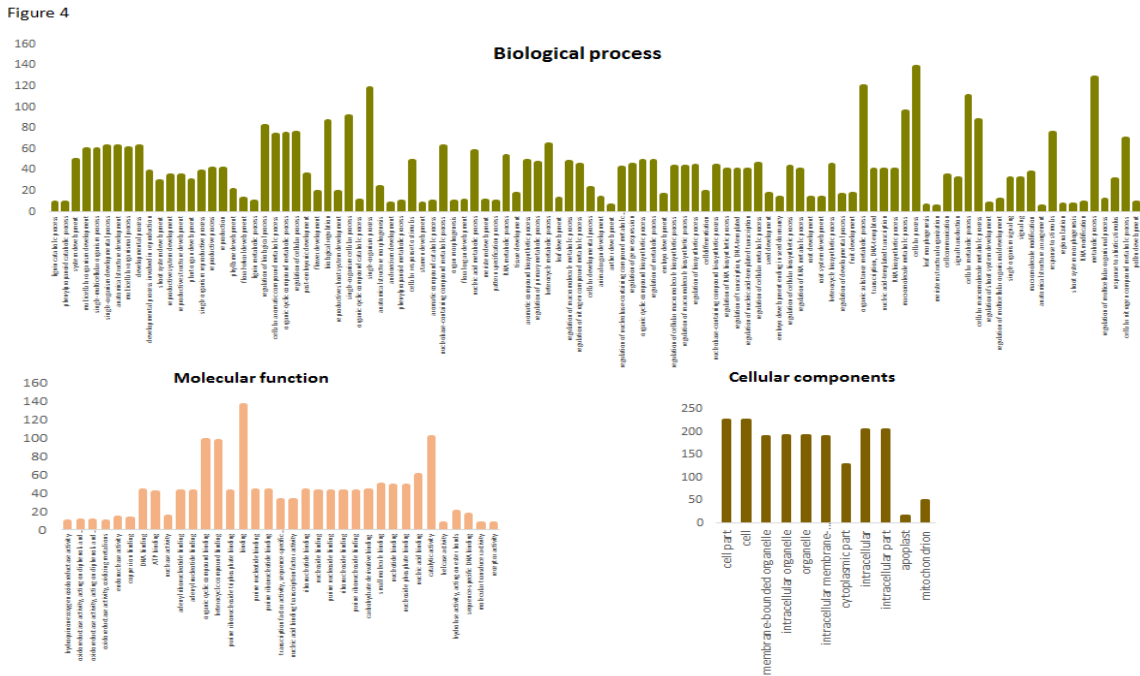
609

Figure 3



610

611 **Figura 9** (Figure 3). Location of miRNAs and their targets along chromosomes of *A. hypochondriacus*. a) Fifty-
 612 three annotated miRNAs by ShortStack are shown as arrows above chromosomes. MiRNA targets are
 613 represented as thin vertical black lines in each chromosome. Unfilled triangles below chromosomes indicate
 614 genes that are targeted by two different miRNAs. b) The number of miRNAs, and c) Number of targets in each
 615 chromosome. MiRNAs that target the same gene as shown in a) (unfilled triangles). Details can be found in Table
 616 S5. Schematic representation of *A. hypochondriacus* chromosomes is based on Lightfoot et al., 2017.

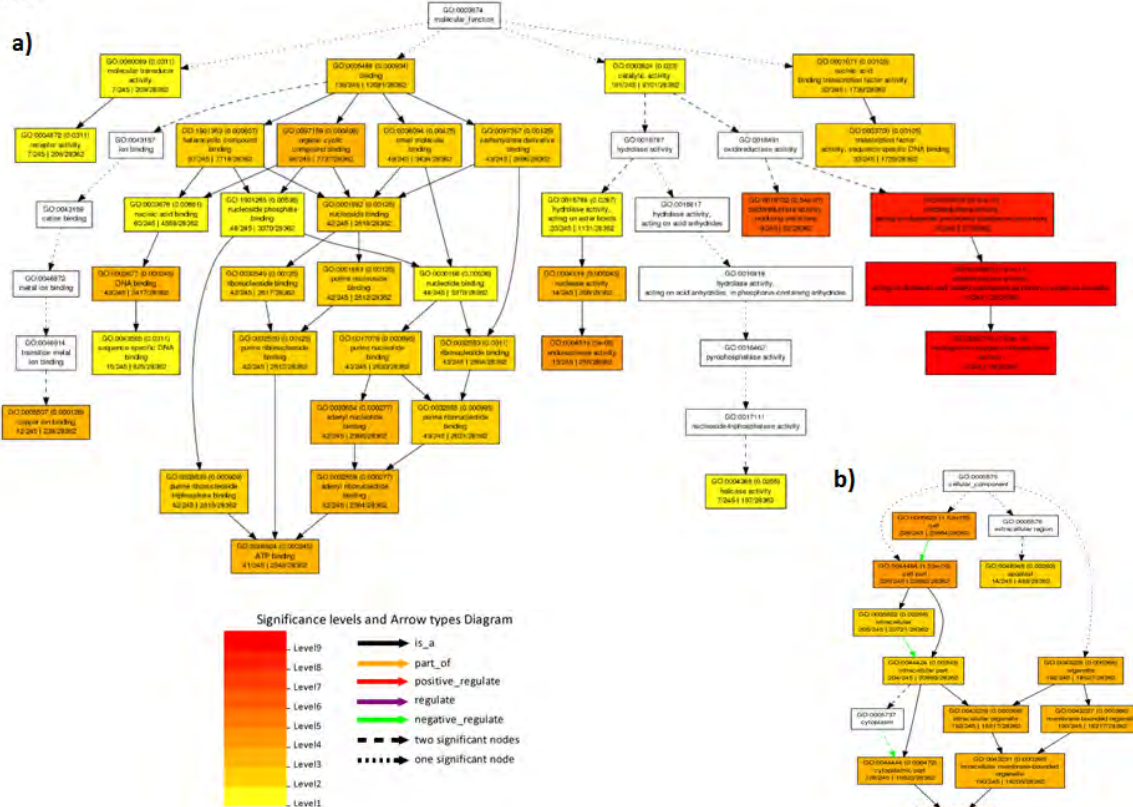


617

618 **Figure 10** (Figure 4). Gene ontology classification of conserved miRNAs-target genes. Orthologs genes of
 619 Arabidopsis corresponding to the miRNA targets of amaranth were used. a) GO-biological processes
 620 classification of target transcripts for expressed miRNAs in amaranth. b) GO-cellular functions classification of
 621 target transcripts for expressed miRNAs in amaranth. c) GO-Cellular processes classification of target transcripts
 622 for expressed miRNAs in amaranth. Details can be found in Table S6.

623

Figure 5



624

625 **Figura 11** (Figure 5). Schematic representation of the significance level of predicted target genes in molecular
 626 function and cellular components, based on GO classification. Orthologs genes of *Arabidopsis* corresponding to
 627 the miRNA targets of amaranth were used. a) Molecular function of miRNA targets, based on GO classification.
 628 b) GO-Cellular components. The processes with statistical significance are denoted in red color. AgriGO was
 629 used to analyze GO categorization of genes. Red color means terms with higher statistical significance. Inside
 630 the box: GO term, adjusted p-value, GO description, item number mapping the GO in the query list and
 631 background, and the total number of query list and background.

632

633

634

635

656 **Tables**

miRNA	miRNA sequence	miRNA location (Scaffold)	strand
Ahyp-miR156a	UGACAGAAGAGAGUGAGCAC	10	(-)
Ahyp-miR156b	UUGACAGAAGAGAGUGAGCAC	10	(-)
Ahyp-miR156e	CUGACAGAAGAUAGAGAGCAC	16,16,16	(-)
Ahyp-miR159a	UUUGGAUUGAAGGGAGCUCUA	4	(+)
Ahyp-miR160a	UGCCUGGCUCUUGUAUGCCA	9,14	(-)
Ahyp-miR164	UGGAGAAGCAGGGCAGUGCA	15	(-)
Ahyp-miR166b	UCGGACCAGGCUUCAUUCDDC	2,5,13	(-)
Ahyp-miR167	UGAAGCUGCCAGCAUGAUCUG	2,6,11	(-)(+)(+)
Ahyp-miR168a	UCGCUUGGUGCAGGUUGGGAA	12	(-)
Ahyp-miR171b	UUGAGCCGUGCCAUAUCCCG	9	(-)
Ahyp-miR171f	UUGAGCCGCGCCAUAUCACU	14	(-)
Ahyp-miR172a	AGAAUCUUGAUGAUCUGCAU	8	(-)
Ahyp-miR172	AGAAUCUUGAUGAUCUGCAG	16	(+)
Ahyp-miR319a	UUGGACUGAAGGGAGCUCUCCU	10,12	(+)
Ahyp-miR390a	AAGCUCAGGAGGGGAUAGCGCC	12	(+)
Ahyp-miR393a	UCCAAGGGGAUCGCAUUGAUC	10	(+)
Ahyp-miR395	CUGAAGUGUUUGGGGAACUC	3	(+)
Ahyp-miR396a	UUCCACAGCUUUCUUGAACUG	9	(+)
Ahyp-miR396b	UUCCACAGCUUUCUUGAACUU	9	(-)
Ahyp-miR2111a	UAAUCUGCAUCCUGAGGCUCA	2,3,12,12	(-)(-)(+)(+)
Ahyp-miR162a	UCGAUAAACCUCUGCAUCCAG	7	(-)
Ahyp-miR397a	UUGAGUGCAGCAUUGAUGAAA	14	(+)
Ahyp-miR398b	UGUGUUCUCAGGUUCGCCCCUG	6	(+)
Ahyp-miR399j	UGCCAAAGGAGAGUUGCCCUA	4	(-)
Ahyp-miR399e	CGCCAAAGGAGAGUUGCCUC	12	(+)
Ahyp-miR408	UGCACUGCCUUCUCCUGGCA	4	(+)
Ahyp-miR535a	UGACGAUGAGAGAGCACGC	2	(-)
Ahyp-miR535a	UGACGAUGAGAGAGCACGC	11	(-)
Ahyp-miR0001	AGAAUCGGGUCUUGUCUCAGUUGG	14	(+)
Ahyp-miR0002	UUUAGGCCAUUGAUGAGGGUUAU	1	(-)
Ahyp-miR0003	CUUUACAACACGGCCGAUGUA	1	(+)
Ahyp-miR0004	UUGCAUAGUUUUUUUUUAC	13	(+)
Ahyp-miR0005	UAUAGGUGACAACAUUAGGUU	6	(-)
Ahyp-miR0006	UCGUCACAUGAUCGCCCAUU	14	(+)
Ahyp-miR0009	UAUACAAGAUUCAUGAAUAA	5	(-)
Ahyp-miR0008	UUUACUGCGCAGGAGGGGAUGA	1	(+)
Ahyp-miR0010	CGCAGGAGAGAUGACAUGAGCU	10	(-)
Ahyp-miR0011	UUCUGUCCUUCAUGAUUUUGG	13	(+)
Ahyp-miR0012	UGGAUUUGGCCUUGGAUUUGU	13	(+)
Ahyp-miR0013	UUCCAAGACCCCAUCCCAA	9	(-)
Ahyp-miR0014	UACUGAUAGUAACAUGUUGCG	10	(+)
Ahyp-miR0015	UUUCCUAGACCCCAUCCCAA	14	(-)

657

658 **Table 3** (Table 1). Genuine miRNAs sequences identified in amaranth. The sequences were classified in
659 conserved miRNAs and novel miRNA. The conserved miRNAs were divided into high confidence and low
660 conserved. The novel miRNAs were divided in similar to other miRNAs and specific. The name assigned,
661 sequence, miRNA location, and strand for each miRNA are presented.

miRNA	Target genes number	Putative amaranth target genes
Ahypo-miR156	26	SPL6 (2), RTNLB2, SPL16 (2), SPL17 (2), SPL12 (2), Wdfy3, TUBA1, NCAPD3 (2), TIC32 (2), GRV2
Ahypo-miR159	11	GAM1 (4), AOX1, Protein phosphatase 2C and cyclic nucleotide-binding/kinase domain-containing protein, TOP3, TCP4, ycf52
Ahypo-miR160	4	ARF17 (2), ARF18 (3)
Ahypo-miR164	8	NAC021, NAC100 (3), PUB4, BETAA-AD, Protein UK (2).
Ahypo-miR166	5	ATHB-8, ATHB-15 (3), REV (2)
Ahypo-miR167	7	Thioredoxin-like 1-1 (2), MED14, ABCG15, BAK1
Ahypo-miR168	4	AGO1A (2), PXMP2/4 family protein 4, Probable inactive receptor kinase At4g23740
Ahypo-miR171	6	SCL15, SCL16, 6-FEH, Ahypo-miR (3)
Ahypo-miR171	8	SCL6, SCL15, CRK15, Ahypo-miR (2)
Ahypo-miR172	12	TOE2, AP2 (3), CNOT10, IMP1, SEU, WAPAL (2), Unc13, HCBT1
Ahypo-miR319	10	GAM1, TOP3, TCP4, GRX515, trap-2, ACBP4, MET1B, PCF5, TOP3, Protein UK
Ahypo-miR390	6	UMK3, Systemin receptor SR160, NIK3, WRKY33, Annexin-like protein RI4, TIF3D1
Ahypo-miR393	9	AFB3, TIR1 (2), ddb2, PTI3, GEM, Probable inactive receptor kinase, Protein UK (2)
Ahypo-miR395	8	ST1, APS1, RGA4, rnf-5, FH13, PFK3, AAP7, Protein UK (1)
Ahypo-miR396	28	ALA4, LECRK18, WNK4, EMB1796, MADS-box protein JOINTLESS, JMU25, TAR2, GRF5, GRF2, GRF4, TEB, GRF10, GRF8, GRF4, GRF2, GRF1, LECRK18, ABIS, PMES4, Neutral ceramidase, Probable protein phosphatase 2C 71, Efl1ad, Phosphatidylinositol 3-kinase, Probable pectinesterase/pectinesterase inhibitor 34, protein UK (3)
Ahypo-miR162	7	Similar to Ferredoxin--NADP reductase, ergic3, DppB, DCL1, MEK1, slmo, efg1
Ahypo-miR397	28	LAC 2(2), LAC3, LAC7, lvsA, IRX12, LAC12, LAC17 (3), LAC22, Pentatricopeptide repeat-containing protein At5g55840, NIC2, protein UK (4), CRS2-associated factor 1, MORCS, Probable bifunctional methylthioribulose-1-phosphate dehydratase/enolase-phosphatase E1 1, PMAA, NET4A, EMB1270, TT10 (2), Rapid alkalization factor
Ahypo-miR398	2	SODCC, Ahypo-miR
Ahypo-miR399	6	UBC24, AVT1, PHT1-4, TOM9-2, CAT2, mdn1
Ahypo-miR399	4	UBC24, AVT1, PHT1-4, ASP1
Ahypo-miR399	5	UBC24, PHT1-4, ASP1, IRX15, nep1
Ahypo-miR408	7	Basic blue protein (2), LAC12 (2), LAC13, BHLH68, protein UK
Ahypo-miR535	6	Ahypo-miR (2), Casparian strip membrane protein 1, BRG1, SKP1B, miRO1
Ahypo-miR2111	3	F-box/kelch-repeat protein At3g27150, FUBP3, DEK
Ahypo-miR0001	15	Mediator-associated protein 2, DEGPB, POB1, FIP1, BHLH130, PUS7, ACOT13, ARAD1, EXPA32, GAOA, FAO4A, Pa2g4, UK (3)
Ahypo-miR0002	7	Ahypo-miR (2), Putative pentatricopeptide repeat-containing protein At1g12700, Auxin-induced protein 10A5, CVB561D, AMPP, CHRS
Ahypo-miR0003	3	Ge-3b, SYM1, TSP11, UK (1)
Ahypo-miR0004	18	ERD4, WBC30, FAO4A, PLR1, AP-1 complex subunit gamma-2, JMU25, Probable LRR receptor-like serine/threonine-protein kinase, Protein HGH1 homolog, lvsC, ERD4, CYPB1EB, PBS1: Serine/threonine-protein kinase PBS1 (Arabidopsis thaliana) CSLE1 (2), SG1, cys5, MSRAS, UK (2)
Ahypo-miR0005	45	AUL1, BASS2, COL5, AMB1025, EMB1444, EMB2745, KAT2, KCS4, POT4, rf1, WLIM1, AKR4CB, Ahypo-miR (3), Pentatricopeptide repeat-containing protein (34 sequences)
Ahypo-miR0006	1	Adenylate kinase 5, chloroplastic.
Ahypo-miR0009	6	ORP1C, PCMP-H40, F-box/FBD/LRR-repeat protein At1g13570, KINESIN-13A, Putative chromatin-remodeling complex ATPase chain, Ahypo-miR
Ahypo-miR0008	1	ATRX2
Ahypo-miR0010	3	ACAB, Aspartic proteinase-like protein 1
Ahypo-miR0011	16	Thioredoxin F-type, chloroplastic, RAD50, Ncl1, PCMP-E2B, PCMP-H2B, Bud13, HTH, RGA4, PCMP-H26, sirB, Pentatricopeptide repeat-containing protein At3g48250, Protein UK (5).
Ahypo-miR0012	3	SYNCRIP, YSL7, Ahypo-miR
Ahypo-miR0013	3	R1B-14, TPP2, ATHB-15
Ahypo-miR0014	3	Eukaryotic translation initiation factor 3 subunit L, Rad9a, protein UK
Ahypo-miR0015	2	RP55, SRD2

662

663 **Tabla 4** (Table 2). Summary of predicted targets genes of miRNAs identified in amaranth. The number of target
664 genes for each miRNA is indicated. The complementary information for miRNAs is presented in table S5.

665

666

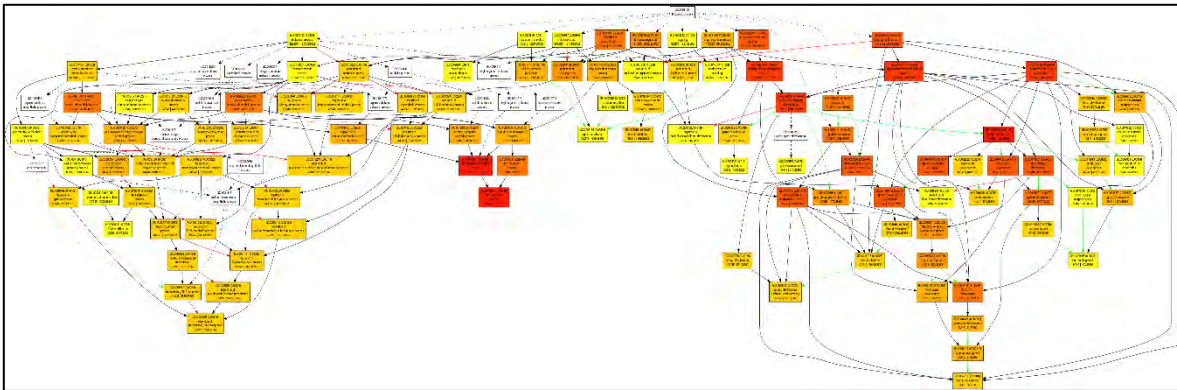
667

668

669

670

671 **Supplementary figures**



672

673 **Figure 15** (Figure S1). Schematic representation of the significance level of predicted target genes in biological
674 process, based on GO classification. Orthologs genes of Arabidopsis corresponding to the miRNA targets of
675 amaranth were used. The processes with statistical significance are denoted in red color. AgriGO was used to
676 analyze GO categorization of genes. Red color means terms with higher statistical significance. Inside the box:
677 GO term, adjusted p-value, GO description, item number mapping the GO in the query list and background, and
678 the total number of query list and background.

679

680

681

682

683

684

685

686

687

688

689

690

691

692 **Supplementary tables**

Criteria	Description
N0	Not analyzed due to run in nohp mode
N1	No reads at all aligned in locus
N2	Dicermin-Dicermax
N3	Major RNA abundance was less than 2 reads
N4	Major RNA length is not in the Dicer size range defined by Dicermin-Dicermax
N5	Locus size is > than maximum allowed for RNA folding per option foldsize (default is 300 nts)
N6	Locus is not stranded (>20% and <80% of reads aligned to top strand)
N7	RNA folding attempt failed at locus (if occurs, possible bug?)
N8	Strand of possible mature miRNA is opposite to that of the locus
N9	Retrieval of possible mature miRNA position failed (if occurs, possible bug?)
N10	General failure to compute miRNA-star position (if occurs, possible bug?)
N11	Possible mature miRNA had > 5 unpaired bases in predicted precursor secondary structure
N12	Possible mature miRNA was not contained in a single predicted hairpin
N13	Possible miRNA/miRNA* duplex had >2 bulges and/or >3 bulged nts
N14	Imprecise processing: Reads for possible miRNA, miRNA-star, and their 3p variants added up to less than 50% of the total reads at the locus
N15	Maybe. Passed all tests EXCEPT that the miRNA-star was not sequenced. INSUFFICIENT evidence to support a de novo annotation of a new miRNA family
Y	Yes. Passed all tests INCLUDING sequencing of the exact miRNA-star. Can support a de novo annotation of a new miRNA family

693

694 **Table 5** (Table S1). Sixteen criteria considered by ShortStack for miRNA identification in amaranth.

695

696

697

698

Gene name	Tm (°C)		Primer sequence
miR0002	58.4	FW	TGTTAAGGCCATTGATGAGGGT
miR0005	59.4	FW	GTATCGGATGATGGTGGGTC
miR535	59.4	FW	TGACGATGAGAGAGAGCACG
miR319	59.8	FW	TATTGGACTGAAGGAGCTCC
miR397	60.3	FW	CGGTTGAGTGCAGCATTGATGA
miR408	61.0	FW	TGCACTGCCTCTCCCTGG
miR159	60.3	FW	GGTTTGGATTGAAGGGAGCTCT
miR171	59.8	FW	ATTGAGCCGTCCAATATCCC
Universal R-primer	60.5	RV	CAGTGCAGGGTCCGAGGT
S-Poly (T) primer	74.6		GTGCAGGGTCCGAGGTCAGAGCCACCTGGGCA ATTTTTTTTTTTTTTT
Universal S-Poly (T) probe	59.4		CAGAGCCACCTGGGCAATTT FAM / TAMRA
Ahy_U3		FW	CGGCTACTGCTTCTGTCTG
Ahy_snor71		FW	ATAAGGACTCACCAGGATCTTG

699

700 **Tabla 6** (Table S2). Oligonucleotides for RT-qPCR in Amaranth. Locus, primer sequences, Tm for eight miRNAs
701 are indicated. Universal R-primer, S-Poly (T) primer, and Universal S-Poly (T) probe information are indicated.
702 Likewise, the oligonucleotides for control genes (Ahy-U3 and Ahy-snor71) are indicated.

703

Sample	Raw reads	Clean reads
Library 1	5934157	5720872
Library 2	5122623	3188905
Library 3	6318324	5161663
Library 4	6755973	2401779
Library 5	6882462	5357672
Library 6	7481309	6574338
Library 7	5383628	646491
Library 8	5688256	1717408
Library 9	5433946	4452029
Library 10	6062762	4922545
Library 11	6289193	2166912

704

705 **Tabla 7** (Table S3). Composition of libraries raw and clean reads.

706

707 **Tabla 8** (Table S4). DICER-called sequences identified by ShortStack. Sequences ranged between 18 to 30-nt
708 in length.709 **Tabla 9** (Table S5). Putative target genes of amaranth miRNAs. The putative target genes were annotated using
710 the psRNATarget web server. The number of target genes was determined with a cut off from expectation ≤ 3 .
711 The homolog of target genes obtained by aligned in NCBI of the transcript and sequences identified in phytozome
712 amaranth are presented.713 **Tabla 10** (Table S6). Classification of target genes based on their functions using the agriGO platform.

714

715

716

717

718 **11. References**

- 719 Aguilar-Hernandez HS, Santos L, Leon-Galvan L, Barrera-Pacheco A, Espitia-Rangel E, De Leon-Rodriguez A, Guevara-
720 Gonzalez RG, Barba de la Rosa AP (2011) Identification of calcium stress induced genes in amaranth leaves through
721 suppression subtractive hybridization. *J Plant Physiol* 168(17): 2102-2109. doi:10.1016/j.jplph.2011.06.006
722
- 723 Alonso-Peral M, Li J, Li Y, Allen R, Schnippenkoetter W, Ohms S, White R, Millar A (2010) The MicroRNA159-Regulated
724 GAMYB-like Genes Inhibit Growth and Promote Programmed Cell Death in Arabidopsis. *Plant physiology* 154: 757-771.
725 doi:10.2307/20779830
726
- 727 Atkinson NJ, Urwin PE (2012) The interaction of plant biotic and abiotic stresses: from genes to the field. *J Exp Bot* 63(10):
728 3523-3543. doi:10.1093/jxb/ers100
729
- 730 Aukerman MJ, Sakai H (2003) Regulation of flowering time and floral organ identity by a MicroRNA and its APETALA2-like
731 target genes. *Plant Cell* 15(11): 2730-2741. doi:10.1105/tpc.016238
732
- 733 Axtell MJ (2008) Evolution of microRNAs and their targets: Are all microRNAs biologically relevant?. *Biochimica Et Biophysica*
734 *Acta-Gene Regulatory Mechanisms* 1779(11): 725-734. doi:10.1016/j.bbagr.2008.02.007
735
- 736 Axtell MJ (2013) ShortStack: comprehensive annotation and quantification of small RNA genes. *RNA* 19(6): 740-751.
737 doi:10.1261/rna.035279.112
738
- 739 Axtell MJ, Meyers BC (2018) Revisiting criteria for plant miRNA annotation in the era of big data. *Plant Cell* 30(2), 272-
740 284. doi:10.1105/tpc.17.00851
741
- 742 Baldrich P, Hsing YI, San Segundo B (2016) Genome-Wide Analysis of Polycistronic MicroRNAs in Cultivated and Wild Rice.
743 *Genome Biol Evol* 8(4): 1104-1114. doi:10.1093/gbe/evw062
744
- 745 Budak H, Akpinar BA (2015) Plant miRNAs: biogenesis, organization and origins. *Funct Integr Genomics* 15(5): 523-531.
746 doi:10.1007/s10142-015-0451-2
747
- 748 Carrió-Seguí A, Ruiz-Rivero O, Villamayor-Belinchón L, Puig S, Perea-García A, Peñarrubia L (2019) The Altered Expression
749 of microRNA408 Influences the Arabidopsis Response to Iron Deficiency. *Frontiers in Plant Science* 10(324).
750 doi:10.3389/fpls.2019.00324
751
- 752 Casique-Arroyo G, Martinez-Gallardo N, de la Vara LG, and Delano-Frier JP (2014) Betacyanin Biosynthetic Genes and
753 Enzymes Are Differentially Induced by (a)biotic Stress in *Amaranthus hypochondriacus*. *PLoS One* 9(6). doi:ARTN
754 e9901210.1371/journal.pone.0099012
755
- 756 Castrillón-Arbeláez PA, Frier JPD (2016) Secondary Metabolism in *Amaranthus* spp. A Genomic Approach to Understand Its
757 Diversity and Responsiveness to Stress in Marginally Studied Crops with High Agronomic Potential. *Abiotic and Biotic Stress*
758 *in Plants-Recent Advances and Future Perspectives*, InTech.
759
- 760 Chandi A, Jordan DL, York AC, Milla-Lewis SR, Burton JD, Culpepper AS, Whitaker JR (2013) Interference and control of
761 glyphosate-resistant and-susceptible Palmer amaranth (*Amaranthus palmeri*) populations under greenhouse conditions. *Weed*
762 *science* 61(2): 259-266. <http://dx.doi.org/10.1614/WS-D-12-00063.1>
763
- 764 Chavez Montes RA, Rosas-Cardenas FF, De Paoli E, Accerbi M, Rymarquis LA, Mahalingam G, Marsch-Martinez N, Meyers
765 BC, Green PJ, de Folter S (2014) Sample sequencing of vascular plants demonstrates widespread conservation and
766 divergence of microRNAs. *Nat Commun* 5: 3722. doi:10.1038/ncomms4722.
767
- 768 Chen K, Rajewsky N (2007) The evolution of gene regulation by transcription factors and microRNAs. *Nature Reviews Genetics*
769 8(2): 93. doi:10.1038/nrg1990
770
- 771 Cho HY, Lee C, Hwang SG, Park YC, Lim HL, Jang CS (2014) Overexpression of the OsChl1 gene, encoding a putative
772 laccase precursor, increases tolerance to drought and salinity stress in transgenic Arabidopsis. *Gene* 552(1): 98-105.
773 doi:10.1016/j.gene.2014.09.018
774
- 775 Clouse JW, Adhikary D, Page JT, Ramaraj T, Deyholos MK, Udall JA, Fairbanks DJ, Jellen EN, Maughan PJ, (2016) The
776 *Amaranth* Genome: Genome, Transcriptome, and Physical Map Assembly. *The Plant Genome* 9(1).
777 doi:10.3835/plantgenome2015.07.0062
778
- 779 Costea M, DeMason DA (2001) Stem morphology and anatomy in *Amaranthus* L. (*Amaranthaceae*) - Taxonomic significance.
780 *Journal of the Torrey Botanical Society* 128(3): 254-281. doi:Doi 10.2307/3088717
781
- 782 Dai X, Zhuang Z, Zhao PX (2018) psRNATarget: a plant small RNA target analysis server (2017 release). *Nucleic Acids Res*
783 46(W1): W49-W54. doi:10.1093/nar/gky316
784
- 785 Das S (2016) *Amaranthus: A Promising Crop of Future*, Springer Singapore
786

- 787 de Vries S, Kukuk A, von Dahlen JK, Schnake A, Kloesges T, Rose LE (2018) Expression profiling across wild and cultivated
788 tomatoes supports the relevance of early miR482/2118 suppression for Phytophthora resistance. Proceedings of the Royal
789 Society B: Biological Sciences 285(1873): 20172560. <https://doi.org/10.1098/rspb.2017.2560>
- 790
791 Delano-Frier JP, Aviles-Arnaut H, Casarrubias-Castillo K, Casique-Arroyo G, Castrillon-Arbelaes PA, Herrera-Estrella L,
792 Massange-Sanchez J, Martinez-Gallardo NA, Parra-Cota FI, Vargas-Ortiz E, Estrada-Hernandez MG (2011) Transcriptomic
793 analysis of grain amaranth (*Amaranthus hypochondriacus*) using 454 pyrosequencing: comparison with *A. tuberculatus*,
794 expression profiling in stems and in response to biotic and abiotic stress. BMC Genomics 12: 363. doi:10.1186/1471-2164-12-
795 363
- 796
797 Didion JP, Martin M, Collins FS (2017) Atropos: specific, sensitive, and speedy trimming of sequencing reads. PeerJ 5: e3720.
798 doi:10.7717/peerj.3720
- 799
800 Djami-Tchatchou AT, Sanan-Mishra N, Ntushelo K, Dubery IA (2017) Functional Roles of microRNAs in Agronomically
801 Important Plants-Potential as Targets for Crop Improvement and Protection. Front Plant Sci 8: 378.
802 doi:10.3389/fpls.2017.00378
- 803
804 Ferdous J, Hussain SS, Shi BJ (2015) Role of microRNAs in plant drought tolerance. Plant Biotechnol J 13(3): 293-305.
805 doi:10.1111/pbi.12318
- 806 Ferdous J, Sanchez-Ferrero JC, Langridge P, Milne L, Chowdhury J, Brien C, Tricker PJ (2017). Differential expression of
807 microRNAs and potential targets under drought stress in barley. Plant Cell Environ 40(1): 11-24. doi:10.1111/pce.12764
- 808
809 Floyd SK, Bowman JL (2004) Gene regulation: ancient microRNA target sequences in plants. Nature 428(6982): 485.
810 doi:10.1038/428485a
- 811
812 Furumoto T, Yamaguchi T, Ohshima-Ichie Y, Nakamura M, Tsuchida-Iwata Y, Shimamura M, Ohnishi J, Hata S, Gowik U,
813 Westhoff P, Bräutigam A, Weber APM, Izui K (2011) A plastidial sodium-dependent pyruvate transporter. Nature 476(7361):
814 472-475. doi:10.1038/nature10250
- 815
816 Gramzow L, Theissen G (2019) Plant miRNA Conservation and Evolution. Methods Mol Biol 1932: 41-50. doi:10.1007/978-1-
817 4939-9042-9_3
- 818
819 Guddeti S, Zhang DC, Li AL, Leseberg CH, Kang H, Li XG, Zhai WX, Johns MA, Mao L (2005) Molecular evolution of the rice
820 miR395 gene family. Cell Res 15(8): 631-638. doi:10.1038/sj.cr.7290333
- 821
822 Guo C, Xu Y, Shi M, Lai Y, Wu X, Wang H, Zhu Z, Poethig RS, Wu G (2017) Repression of miR156 by miR159 Regulates the
823 Timing of the Juvenile-to-Adult Transition in Arabidopsis. Plant Cell 29(6): 1293-1304. doi:10.1105/tpc.16.00975
- 824
825 Hakim, Ullah A, Hussain A, Shaban M, Khan AH, Alariqi M, Gul S, Jun Z, Lin S, Li J, Jin S, Munis MFH (2018) Osmotin: A
826 plant defense tool against biotic and abiotic stresses. Plant Physiol Biochem 123: 149-159. doi:10.1016/j.plaphy.2017.12.012
- 827
828 He J, Jiang Z, Gao L, You C, Ma X, Wang X, Xu X, Mo B, Chen X, Liu L (2019) Genome-wide transcript and small RNA profiling
829 reveals transcriptomic responses to heat stress. Plant Physiology: pp.00403.02019. doi:10.1104/pp.19.00403
- 830
831 Huang JH, Qi YP, Wen SX, Guo P, Chen XM, Chen LS (2016) Illumina microRNA profiles reveal the involvement of miR397a
832 in Citrus adaptation to long-term boron toxicity via modulating secondary cell-wall biosynthesis. Scientific Reports 6(1): 22900.
833 doi:10.1038/srep22900
- 834
835 Huen A, Bally J, Smith P (2018) Identification and characterisation of microRNAs and their target genes in phosphate-starved
836 *Nicotiana benthamiana* by small RNA deep sequencing and 5'RACE analysis. BMC Genomics 19(1):940. doi:10.1186/s12864-
837 018-5258-9
- 838
839 Huerta-Ocampo JA, Barba de la Rosa AP (2011) Amaranth: a pseudo-cereal with nutraceutical properties. Current Nutrition
840 & Food Science 7(1): 1-9. doi: [10.2174/157340111794941076](https://doi.org/10.2174/157340111794941076)
- 841
842 Huerta-Ocampo JA, Briones-Cerecero EP, Mendoza-Hernández G, De Leon-Rodriguez A, Barba de la Rosa AP (2009)
843 Proteomic analysis of amaranth (*Amaranthus hypochondriacus* L.) leaves under drought stress. International journal of plant
844 sciences 170(8): 990-998. <https://doi.org/10.1086/605119>
- 845
846 Jamalluddin N, Massawe FJ, Symonds RC (2019) Transpiration efficiency of Amaranth (*Amaranthus* sp.) in response to
847 drought stress. The Journal of Horticultural Science and Biotechnology 94(4): 448-459. doi:10.1080/14620316.2018.1537725
- 848
849 Jasinski S, Vialette-Guiraud ACM, Scutt CP (2010). The evolutionary-developmental analysis of plant microRNAs.
850 Philosophical transactions of the Royal Society of London. Series B, Biological sciences 365(1539): 469-476.
851 doi:10.1098/rstb.2009.0246
- 852
853 Jiu S, Leng X, Haider MS, Dong T, Guan L, Xie Z, Li X, Shangguan L, Fang J (2019) Identification of copper (Cu) stress-
854 responsive grapevine microRNAs and their target genes by high-throughput sequencing. R Soc Open Sci 6(1): 180735.
855 doi:10.1098/rsos.180735
- 856

- 857 Johnson NR, Yeoh JM, Coruh C, Axtell MJ (2016) Improved Placement of Multi-mapping Small RNAs. *G3 (Bethesda)* 6(7):
858 2103-2111. doi:10.1534/g3.116.030452
859
- 860 Jones-Rhoades MW, Bartel DP, Bartel B (2006) MicroRNAs and their regulatory roles in plants. *Annual Review of Plant Biology*
861 57: 19-53. doi:10.1146/annurev.arplant.57.032905.105218
862
- 863 Joshi DC, Sood S, Hosahatti R, Kant L, Pattanayak A, Kumar A, Yadav D, Stetter MG (2018) From zero to hero: the past,
864 present and future of grain amaranth breeding. *Theoretical and Applied Genetics*. doi:10.1007/s00122-018-3138-y
865
- 866 Kang K, Zhang X, Liu H, Wang Z, Zhong J, Huang Z, Peng X, Zeng Y, Wang Y, Yang Y (2012). A novel real-time PCR assay
867 of microRNAs using S-Poly (T), a specific oligo (dT) reverse transcription primer with excellent sensitivity and specificity. *PLoS*
868 *one* 7(11): e48536. doi:10.1371/journal.pone.0048536.
869
- 870 Katiyar A, Smita S, Chinnusamy V, Pandey DM, Bansal K (2012) Identification of miRNAs in sorghum by using bioinformatics
871 approach. *Plant Signal Behav* 7(2): 246-259. doi:10.4161/psb.18914
872
- 873 Khanam UKS, Oba S (2014) Phenotypic Plasticity of Vegetable Amaranth, *Amaranthus tricolor* L. under a Natural Climate.
874 *Plant Production Science* 17(2): 166-172. doi:10.1626/Pps.17.166
875
- 876 Koussevitzky S, Nott A, Mockler TC, Hong F, Sachetto-Martins G, Surpin M, Lim J, Mittler R, Chory J (2007) Signals from
877 chloroplasts converge to regulate nuclear gene expression. *Science* 316(5825): 715-719. doi: [10.1126/science.1140516](https://doi.org/10.1126/science.1140516)
878
- 879 Koyama T, Sato F, Ohme-Takagi M (2017) Roles of miR319 and TCP Transcription Factors in Leaf Development. *Plant Physiol*
880 175(2): 874-885. doi:10.1104/pp.17.00732
881
- 882 Kozomara A, Birgaoanu M, Griffiths-Jones S (2019) miRBase: from microRNA sequences to function. *Nucleic Acids Res*
883 47(D1): D155-D162. doi:10.1093/nar/gky1141
884
- 885 Kozomara A, Griffiths-Jones S (2013) miRBase: annotating high confidence microRNAs using deep sequencing data. *Nucleic*
886 *Acids Res* 42(D1), D68-D73. doi:10.1093/nar/gkt1181
887
- 888 Lee EJ, Oh M, Hwang JU, Li-Beisson Y, Nishida I, Lee Y (2017) Seed-specific overexpression of the pyruvate transporter
889 BASS2 increases oil content in Arabidopsis seeds. *Frontiers in plant science* 8: 194. doi: 10.3389/fpls.2017.00194
890
- 891 Lei J, Sun Y (2014) miR-PREFeR: an accurate, fast and easy-to-use plant miRNA prediction tool using small RNA-Seq data.
892 *Bioinformatics* 30(19): 2837-2839. doi:10.1093/bioinformatics/btu380
893
- 894 Li A, Mao L (2007) Evolution of plant microRNA gene families. *Cell Res* 17(3): 212-218. doi:10.1038/sj.cr.7310113
895
- 896 Li GP, Wang Y, Lou XM, Li HL, Zhang CQ (2018) Identification of Blueberry miRNAs and Their Targets Based on High-
897 Throughput Sequencing and Degradome Analyses. *International Journal of Molecular Sciences* 19(4). doi:ARTN
898 98310.3390/ijms19040983
899
- 900 Liu H, Yu H, Tang G, Huang T (2018) Small but powerful: function of microRNAs in plant development. *Plant Cell Rep* 37(3):
901 515-528. doi:10.1007/s00299-017-2246-5
902
- 903 Liu Q, Luo L, Wang X, Shen Z, Zheng L (2017) Comprehensive Analysis of Rice Laccase Gene (OsLAC) Family and Ectopic
904 Expression of OsLAC10 Enhances Tolerance to Copper Stress in Arabidopsis. *Int J Mol Sci* 18(2). doi:10.3390/ijms18020209
905
- 906 Liu S, Peng L, Pan J, Wang X, Zhao C, Cheng C, Zhang Z, Lin Y, XuHan X, Lai Z (2018) Identification of microRNAs in the
907 green and red sectors of *Amaranthus tricolor* L. leaves based on Illumina sequencing data, *PeerJ Preprints*
908 6:e26723v1. <https://doi.org/10.7287/peerj.preprints.26723v1>
909
- 910 Maher C, Stein L, Ware D (2006) Evolution of Arabidopsis microRNA families through duplication events. *Genome Research*
911 16(4): 510-519. doi: 10.1101/gr.4680506
912
- 913 Manna S (2015) An overview of pentatricopeptide repeat proteins and their applications. *Biochimie* 113: 93-99.
914 doi:10.1016/j.biochi.2015.04.004
915
- 916 Martínez-Núñez M, Ruiz-Rivas M, Vera-Hernández PF, Bernal-Muñoz R, Luna-Suárez S, Rosas-Cárdenas FF (2019) The
917 phenological growth stages of different amaranth species grown in restricted spaces based in BBCH code. *South African*
918 *Journal of Botany* 124: 436-443. doi:<https://doi.org/10.1016/j.sajb.2019.05.035>
919
- 920 Massange-Sanchez JA, Palmeros-Suarez PA, Espitia-Rangel E, Rodriguez-Arevalo I, Sanchez-Segura L, Martinez-Gallardo
921 NA, Alatorre-Cobos F, Tiessen A, Delano-Frier JP (2016) Overexpression of Grain Amaranth (*Amaranthus hypochondriacus*)
922 AhERF or AhDOF Transcription Factors in Arabidopsis thaliana Increases Water Deficit- and Salt-Stress Tolerance,
923 Respectively, via Contrasting Stress-Amelioration Mechanisms. *PLoS One* 11(10): e0164280.
924 doi:10.1371/journal.pone.0164280
925

- 926 McCormick KP, Willmann MR, Meyers BC (2011) Experimental design, preprocessing, normalization and differential
927 expression analysis of small RNA sequencing experiments. *Silence* 2(1): 2. doi:10.1186/1758-907X-2-2
928
- 929 Paieri F, Tadini L, Manavski N, Kleine T, Ferrari R, Morandini P, Pesaresi P, Meurer J, Leister D (2018) The DEAD-box RNA
930 helicase RH50 is a 23S-4.5 S rRNA maturation factor that functionally overlaps with the plastid signaling factor GUN1. *Plant*
931 *physiology* 176(1): 634-648. <https://doi.org/10.1104/pp.17.01545>
932
- 933 Pan L, Zhao H, Yu Q, Bai L, Dong L (2017) miR397/Laccase Gene Mediated Network Improves Tolerance to Fenoxaprop-P-
934 ethyl in *Beckmannia syzigachne* and *Oryza sativa*. *Frontiers in plant science* 8: 879-879. doi:10.3389/fpls.2017.00879
935
- 936 Peláez P, Trejo MS, Iñiguez LP, Estrada-Navarrete G, Covarrubias AA, Reyes JL, Sanchez F (2012) Identification and
937 characterization of microRNAs in *Phaseolus vulgaris* by high-throughput sequencing. *BMC genomics* 13: 83-83.
938
- 939 Qin Z, Li C, Mao L, Wu L (2014) Novel insights from non-conserved microRNAs in plants *Frontiers in plant science* 5:586
940 doi:10.3389/fpls.2014.00586
941
- 942 Rastogi A, Shukla S (2013) Amaranth: A New Millennium Crop of Nutraceutical Values. *Critical Reviews in Food Science and*
943 *Nutrition* 53(2): 109-125. doi:10.1080/10408398.2010.517876
944
- 945 Ravichandran S, Ragupathy R, Edwards T, Domaratzki M, Cloutier S (2019) MicroRNA-guided regulation of heat stress
946 response in wheat. *BMC genomics* 20(1): 488. doi:10.1186/s12864-019-5799-6
947
- 948 Rosas-Cardenas FF, Duran-Figueroa N, Vielle-Calzada JP, Cruz-Hernandez A, Marsch-Martinez N, de Folter S (2011) A
949 simple and efficient method for isolating small RNAs from different plant species. *Plant Methods* 7: 4. doi:10.1186/1746-4811-
950 7-4
951
- 952 Rosas-Cárdenas FF, de Folter S (2017) Conservation, divergence, and abundance of miRNAs and their effect in plants. In:
953 *Plant Epigenetics*. Springer, pp 1-22
954
- 955 Sakaguchi J, Watanabe Y (2012) miR165/166 and the development of land plants. *Development, growth & differentiation* 54:
956 93-99. doi:10.1111/j.1440-169X.2011.01318.x
957
- 958 Samad AFA, Sajad M, Nazaruiddin N, Fauzi IA, Murad AMA, Zainal Z, Ismail I (2017) MicroRNA and Transcription Factor: Key
959 Players in Plant Regulatory Network. *Front Plant Sci* 8. doi:Artn 56510.3389/Fpls.2017.00565
960
- 961 Schmitz-Linneweber C, Small I (2008) Pentatricopeptide repeat proteins: a socket set for organelle gene expression. *Trends*
962 *in plant science* 13(12): 663-670. doi:10.1016/j.tplants.2008.10.001.
963
- 964 Shahid S, Axtell MJ (2014) Identification and annotation of small RNA genes using ShortStack. *Methods*. 67(1), 20-27.
965 doi:10.1016/j.ymeth.2013.10.004
966
- 967 Shi T, Wang K, Yang P (2016) Ancient microRNA families that regulate transcription factors are preferentially preserved during
968 plant radiation. *Plant Signal Behav* 11(12): e1261233. doi:10.1080/15592324.2016.1261233
969
- 970 Silva-Sánchez C, de La Rosa AB, León-Galván M, De Lumen B, de León-Rodríguez A, de Mejía EG (2008) Bioactive peptides
971 in amaranth (*Amaranthus hypochondriacus*) seed. *J Agric Food Chem* 56(4): 1233-1240. <https://doi.org/10.1021/jf072911z>
972
- 973 Song G, Zhang R, Zhang S, Li Y, Gao J, Han X, Chen M, Wang J, Li W, Li G (2017) Response of microRNAs to cold treatment
974 in the young spikes of common wheat. *BMC Genomics* 18(1): 212. doi:10.1186/s12864-017-3556-2
975
- 976 Song Z, Zhang L, Wang Y, Li H, Li S, Zhao H, Zhang H (2017) Constitutive Expression of miR408 Improves Biomass and
977 Seed Yield in *Arabidopsis*. *Front Plant Sci* 8: 2114. doi:10.3389/fpls.2017.02114
978
- 979 Sunkar R, Zhou X, Zheng Y, Zhang W, Zhu JK (2008) Identification of novel and candidate miRNAs in rice by high throughput
980 sequencing. *BMC Plant Biol* 8: 25. doi:10.1186/1471-2229-8-25
981
- 982 Szklarczyk D, Morris JH, Cook H, Kuhn M, Wyder S, Simonovic M, Santos A, Doncheva NT, Roth A, Bork P, Jensen LJ, von
983 Mering C (2017) The STRING database in 2017: quality-controlled protein-protein association networks, made broadly
984 accessible. *Nucleic Acids Res* 45(D1): D362-D368. doi:10.1093/nar/gkx937
985
- 986 Tadini L, Pesaresi P, Kleine T, Rossi F, Guljamow A, Sommer F, Mühlhaus T, Schroda M, Masiero S, Pribil M (2016) GUN1
987 controls accumulation of the plastid ribosomal protein S1 at the protein level and interacts with proteins involved in plastid
988 protein homeostasis. *Plant physiology* 170(3): 1817-1830. doi: 10.1104/pp.15.02033
989
- 990 Tian T, Liu Y, Yan H, You Q, Yi X, Du Z, Xu W, Su Z (2017) agriGO v2.0: a GO analysis toolkit for the agricultural community,
991 2017 update. *Nucleic Acids Research* 45(W1): W122-W129. doi:10.1093/nar/gkx382
992
- 993 Tsikou D, Yan Z, Holt DB, Abel NB, Reid DE, Madsen LH, Bhasin H, Sexauer M, Stougaard J, Markmann K (2018). Systemic
994 control of legume susceptibility to rhizobial infection by a mobile microRNA. *Science* 362(6411): 233-236. doi:
995 10.1126/science.aat6907

- 996
997 Vera-Hernández PF, de Folter S, Rosas-Cárdenas FF (2019). Isolation and Detection Methods of Plant miRNAs. In: de Folter
998 S (ed) *Plant MicroRNAs: Methods and Protocols*. Springer, New York, pp 109-120.
999
- 1000 Waidmann S, Kusenda B, Mayerhofer J, Mechtler K, Jonak C (2014) A DEK Domain-Containing Protein Modulates Chromatin
1001 Structure and Function in Arabidopsis. *The Plant cell* 26. doi:10.1105/tpc.114.129254
1002
- 1003 Warde-Farley D, Donaldson SL, Comes O, Zuberi K, Badrawi R, Chao P, Franz M, Grouios C, Kazi F, Lopes CT, Maitland A,
1004 Mostafavi S, Montojo J, Shao Q, Wright G, Bader GD, Morris Q (2010) The GeneMANIA prediction server: biological network
1005 integration for gene prioritization and predicting gene function. *Nucleic Acids Res* 38: W214-220. doi:10.1093/nar/gkq537
1006
- 1007 Waselkov KE, Boleda AS, Olsen KM (2018) A Phylogeny of the Genus *Amaranthus* (amaranthaceae) Based on Several Low-
1008 Copy Nuclear Loci and Chloroplast Regions. *Systematic Botany* 43(2): 439-458. doi.org/10.1600/036364418X697193
1009
- 1010 Wu GZ, Chalvin C, Hoelscher M, Meyer EH, Wu XN, Bock R (2018) Control of retrograde signaling by rapid turnover of
1011 GENOMES UNCOUPLED1. *Plant physiology* 176(3): 2472-2495. doi.org/10.1104/pp.18.00009
- 1012 Xia H, Zhang L, Wu G, Fu C, Long Y, Xiang J, Gan J, Zhou Y, Yu L, Li M (2016) Genome-wide identification and
1013 characterization of microRNAs and target genes in *Lonicera japonica*. *PLoS one* 11(10): e0164140.
1014 doi.org/10.1371/journal.pone.0164140
1015
- 1016 Xian Z, Huang W, Yang Y, Tang N, Zhang C, Ren M, Li Z (2014) miR168 influences phase transition, leaf epinasty, and fruit
1017 development via *SIAGO1s* in tomato. *J Exp Bot* 65(22): 6655-6666. doi:10.1093/jxb/eru387
1018
- 1019 Xing H, Fu X, Yang C, Tang X, Guo L, Li C, Xu C, Luo K (2018) Genome-wide investigation of pentatricopeptide repeat gene
1020 family in poplar and their expression analysis in response to biotic and abiotic stresses. *Scientific Reports* 8(1): 2817.
1021 doi:10.1038/s41598-018-21269-1
1022
- 1023 Ye KY, Chen Y, Hu XW, Guo JC (2013) Computational identification of microRNAs and their targets in apple. *Genes &*
1024 *Genomics* 35(3): 377-385. doi:10.1007/s13258-013-0070-z
1025
- 1026 Zeng X, Xu Y, Jiang J, Zhang F, Ma L, Wu D, Wang Y, Sun W (2018) Identification of cold stress responsive microRNAs in
1027 two winter turnip rape (*Brassica rapa* L.) by high throughput sequencing. *BMC Plant Biol* 18(1): 52. doi:10.1186/s12870-018-
1028 1242-4
1029
- 1030 Zhang B, Pan X, Wang Q, Cobb GP, Anderson TA (2006) Computational identification of microRNAs and their targets.
1031 *Computational biology and chemistry* 30(6): 395-407. doi:10.1016/j.compbiolchem.2006.08.006
1032
- 1033 Zhang L, Chia JM, Kumari S, Stein JC, Liu Z, Narechania A, Maher CA, Guill K, McMullen MD, Ware D (2009) A genome-wide
1034 characterization of microRNA genes in maize. *PLoS Genet* 5(11): e1000716. doi:10.1371/journal.pgen.1000716
1035
- 1036 Zhao X, Huang J, Chory J (2019) GUN1 interacts with MORF2 to regulate plastid RNA editing during retrograde signaling.
1037 *Proceedings of the National Academy of Sciences* 116(20): 10162-10167. doi.org/10.1073/pnas.1820426116
1038
- 1039 Zheng ZH, Reichel M, Deveson I, Wong GG, Li JY, Millar AA (2017) Target RNA Secondary Structure Is a Major Determinant
1040 of miR159 Efficacy. *Plant Physiology* 174(3): 1764-1778. doi:10.1104/pp.16.01898
1041
- 1042 Zhou J, Cheng Y, Yin M, Yang E, Gong W, Liu C, Zheng X, Deng K, Ren Z, Zhang Y (2015) Identification of novel miRNAs
1043 and miRNA expression profiling in wheat hybrid necrosis. *PLoS One* 10(2): e0117507. doi:10.1371/journal.pone.0117507
1044
- 1045 Zhu H, Zhang Y, Tang R, Qu H, Duan X, Jiang Y (2019) Banana sRNAome and degradome identify microRNAs functioning in
1046 differential responses to temperature stress. *BMC Genomics* 20(1): 33. doi:10.1186/s12864-018-5395-1
1047
- 1048 Zhu J, Li WF, Yang W, Qi L, Han S (2013) Identification of microRNAs in *Caragana intermedia* by high-throughput sequencing
1049 and expression analysis of 12 microRNAs and their targets under salt stress. *Plant cell reports* 32: 1339-1349.
1050 doi:10.1007/s00299-013-1446-x
1051
- 1052 Zsigmond L, Rigó G, Szarka A, Székely G, Ötvös K, Darula Z, Medzihradsky KF, Koncz C, Koncz Z, Szabados L (2008)
1053 Arabidopsis PPR40 connects abiotic stress responses to mitochondrial electron transport. *Plant Physiology* 146(4): 1721-
1054 1737. doi: 10.1104/pp.107.111260

CAPITULO IV

Secuenciación del degradoma de *Amaranthus hypochondriacus* variedad "Gabriela"

1. Introducción:

Tanto en plantas como en animales, los miRNAs regulan la expresión génica a nivel postranscripcional reprimiendo la traducción o induciendo la degradación de los mRNAs blanco mediante la unión anti-sentido del miRNA con la región 3'-no traducida (3'-UTR region) del mRNA blanco (Carrington and Ambros 2003, Bartel 2004, Rodriguez, Griffiths-Jones et al. 2004, Unver, Namuth-Covert et al. 2009, Budak and Akpinar 2015, Wang, Zhang et al. 2017). Un solo UTR puede tener sitios de unión para distintos miRNA o múltiples sitios para un solo miRNA, lo que sugiere un control postranscripcional complejo de la expresión génica ejercida por estos RNAs reguladores (Shukla, Singh et al. 2011). En plantas, la identificación de genes blanco se ha realizado mediante métodos computacionales apoyados en la complementariedad y conservación de los miRNAs (Wang, Reyes et al. 2004, Schwab, Palatnik et al. 2005, Pandey, Srivastava et al. 2019), Sin embargo, los algoritmos computacionales actualmente disponibles para la predicción de genes blanco tienen diversos grados de sensibilidad y especificidad; por lo que se requiere de confirmación experimental (Addo-Quaye, Miller et al. 2008). Muchas de estas predicciones se validan de forma independiente clonando y secuenciando los productos de degradación (Llave, Franco-Zorrilla et al. 2011, Wang, Ding et al. 2016, Xia, Zhang et al. 2016). Sin embargo, esta metodología está sesgada hacia la validación de solo unos cuantos genes blanco por especie.

Con la finalidad de analizar el patrón de degradación de RNA de todo el transcriptoma de amaranto, en el capítulo IV del presente proyecto de investigación presentamos la secuenciación del degradoma (También conocido como Análisis Paralelo de Extremos de RNA o PARE) de *Amaranthus hypochondriacus* variedad

“Gabriela”. Dicha técnica es una adaptación de RLM-5'RACE (RNA ligase mediated 5' rapid amplification of cDNA ends) acoplado a un método de secuenciación masiva por síntesis (SBS) utilizando tecnología Illumina. La secuenciación del degradoma reveló la identidad de 721 Genes blanco regulados por 105 familias distintas de miRNAs potencialmente presentes en *Amaranthus hypochondriacus* variedad “Gabriela”. La anotación funcional mostró que dichos genes se encuentran asociados a la regulación de funciones cruciales en los procesos biológicos, incluidos el crecimiento, el desarrollo, la maduración, la respuesta ante estrés biótico/abiótico y la defensa ante patógenos.

2. Metodología:

2.1. Construcción de librerías y secuenciación del degradoma de *Amaranthus hypochondriacus* variedad “Gabriela”

La extracción de RNA total de plantas control y plantas sometidas a estrés por sequía se obtuvo por triplicado mediante *ZR Plant RNA MiniPrep kit* (Zymo Research, Irvine, CA, EE. UU.). La extracción de RNA se realizó a partir del mismo tejido de plantas de *Amaranthus hypochondriacus* variedad “Gabriela” que se utilizó para la secuenciación de miRNAs (Capítulo III). La calidad y cantidad de RNA total se analizó mediante el equipo Bioanalyzer 2100 y RNA 6000 Nano Lab Chip Kit (Agilent Technologies, Santa Clara, CA, EE. UU.). Se realizó un *pull* de las tres réplicas de RNA de cada tratamiento (plantas control y plantas sometidas a estrés por sequía respectivamente).

En la preparación de cada librería se utilizaron 20 µg de RNA total con un RIN > 7.0. El procedimiento para la preparación de las librerías constó de los

siguientes pasos: (1) Se utilizaron 150 ng de poly(A) + RNA como elemento de entrada para el reconocimiento de *primers* aleatorios biotinilados (BPRs), (2) La captura de fragmentos de RNA se realizó mediante estreptavidina y *primers* aleatorios biotinilados, (3) Mediante DNA ligasa T4 se ligaron adaptadores a los extremo 5' monofosfato de cada fragmento de RNA, (4) Se realizó la reacción de RT-PCR, y finalmente (5) Las librerías se secuenciaron en una plataforma Illumina HiSeq 2500 (Agilent Technologies, Santa Clara, CA, United States) en la compañía LC Sciences. Los fragmentos secuenciados corresponden a los primeros 36 nucleótidos del adaptador en los extremos 5' más 50 pb de cada secuencia detectada.

2.2. Análisis bioinformático del degradoma de *Amaranthus hypochondriacus* variedad “Gabriela”

El *pipeline* para el análisis de los datos de secuenciación masiva del degradoma constó de tres grupos de datos de entrada en formato FASTA. 1) Secuencias del degradoma, 2) Un grupo de miRNAs de consulta, y 3) Una base de datos de posibles genes blanco (mRNAs).

Se realizó un análisis de calidad mediante *FastQC* para eliminar lecturas de mala calidad, posteriormente se eliminaron las secuencias adaptadoras utilizando *Cutadapt*. Las lecturas del degradoma se alinearon a mRNAs identificados en *Amaranthus hypochondriacus* (*Phytozome v12.1*). Solo aquellas alineaciones de coincidencia perfecta se conservaron para el análisis de degradación. Todas las lecturas resultantes (*t-signature*) se complementaron inversamente y se alinearon con cada uno de los miRNAs identificados en *Amaranthus hypochondriacus* variedad “Gabriela”. Durante el alineamiento se detectó que el sitio de corte del RNA

degradado se ubicara entre la posición 9 y 11 del miRNA. La identificación de genes blanco se realizó mediante *Targetfinder*. Posteriormente, a través de *Gene Ontology (GO) annotations* (<http://www.geneontology.org/>) y *Kyoto Encyclopedia of Genes and Genomes (KEGG) pathways* (<http://www.genome.jp/kegg/>), se describieron los procesos biológicos, componentes celulares y funciones moleculares en los que participan los genes blanco de los miRNAs identificados. Finalmente, se realizó un análisis de expresión diferencial mediante *DESeq* entre los datos de secuenciación masiva del degradoma de plantas control y plantas expuestas a estrés por sequía.

3. Resultados:

Dos librerías (Control y sequía) del degradoma para *Amaranthus hypochondriacus* variedad “Gabriela” fueron obtenidas mediante secuenciación masiva utilizando tecnología Illumina. 38,335,787 y 25,981,060 lecturas crudas fueron obtenidas para el grupo control y el tratamiento de sequía respectivamente. Después del análisis de calidad y la eliminación de los adaptadores, se obtuvieron 51,182 lecturas únicas para el grupo control y 36,936 lecturas únicas para el tratamiento de sequía. Para ambas librerías, las lecturas que hibridaron perfectamente con los transcritos de *Amaranthus hypochondriacus* se sometieron a un análisis posterior mediante el *software Targetfinder* para la identificación de genes blanco; de esta manera se logró la identificación de 721 genes regulados por 115 familias distintas de miRNAs potencialmente presentes en *Amaranthus hypochondriacus* variedad “Gabriela”.

331 genes blanco (45.9%) identificados en el degradoma de *Amaranthus hypochondriacus* variedad “Gabriela” se encuentran regulados por 22 familias conservadas de miRNAs, mientras que los 390 genes blanco restantes (54.1%) son regulados por miRNAs medianamente conservados y por miRNAs únicos (Tabla 13). El análisis de ontología génica realizado mediante la la plataforma agriGO

Número de genes blanco identificados por cada miRNA			
miRNA	No. de genes	miRNA	No. de genes
miR156j	81	miR5656	1
miR157a-3p	41	miR5658	26
miR158a-3p	4	miR5662	2
miR159c	11	miR5663-5p	3
miR160c-5p	12	miR5997	2
miR161	2	miR771	1
miR162a-3p	4	miR773b-5p	6
miR164c-5p	14	miR774b-3p	2
miR165a-3p	12	miR776	1
miR166g	43	miR777	1
miR167c-5p	8	miR779.2	1
miR168a-5p	2	miR780.2	2
miR169a-5p	32	miR782	2
miR170-5p	3	miR8166	1
miR171c-3p	7	miR8169	1
miR172e-5p	36	miR8170-3p	1
miR1886.3	5	miR8171	1
miR1888a	1	miR8172	3
miR2111b-5p	2	miR823	1
miR2934-5p	4	miR824-3p	1
miR2938	1	miR826b	1
miR319c	13	miR829-5p	2
miR3434-5p	2	miR830-5p	4
miR390a-3p	1	miR834	1
miR391-5p	2	miR835-5p	3
miR393b-5p	5	miR837-5p	5
miR394b-5p	2	miR838	6
miR395f	12	miR841a-5p	1
miR396b-5p	34	miR842	2
miR397a	1	miR843	1
miR398c-3p	3	miR845b	1
miR399f	6	miR846-3p	2
miR407	2	miR847	3
miR408-3p	2	miR852	1
miR414	100	miR854e	5
miR415	2	miR857	1
miR420	2	miR858a	2
miR4228-5p	1	miR859	1
miR447c-3p	1	miR860	1
miR472-5p	2	miR863-5p	1
miR5013	1	miR865-3p	4
miR5014a-5p	2	miR866-3p	2
miR5016	3	miR869.1	3
miR5017-3p	1	miR870-3p	1
miR5018	1	miR482c	3
miR5020c	1	miR6020b	3
miR5021	39	miR6025d	2
miR5025	1	miR6144	3
miR5026	1	miR6146b	3
miR5029	1	miR6150	2
miR5628	2	miR6153	1
miR5632-5p	1	miR6154b	2
miR5638a	2	miR6155	1
miR5640	1	miR6158c	3
miR5641	3	miR6159	1
miR5646	1	miR6161d	1
miR5649b	2	miR6162	1
miR5650	1		

Tabla 11. Número de genes blanco que se identifican para cada miRNA en el degradoma de *Amaranthus hypochondriacus* variedad “Gabriela”. Se identificaron 721 genes blanco regulados por miembros de 115 familias distintas de miRNAs. Las celdas sombreadas corresponden a miRNAs conservados.

(<http://systemsbiology.cau.edu.cn/agriGOv2/>) indica que los genes blanco están involucrados en la regulación de distintos procesos y pueden ser clasificados en tres grupos distintos según las funciones que desempeñan: 1) Genes asociados a la regulación de procesos biológicos, 2) Genes asociados a la regulación de componentes celulares y 3) Genes reguladores de procesos moleculares (Figura 17). Según su función biológica, los genes blanco identificados en amaranto se clasificaron en 25 categorías, mientras que los genes asociados a la regulación de componentes celulares y regulación de procesos moleculares se clasifican en 15 y 10 categorías respectivamente (figura 17).

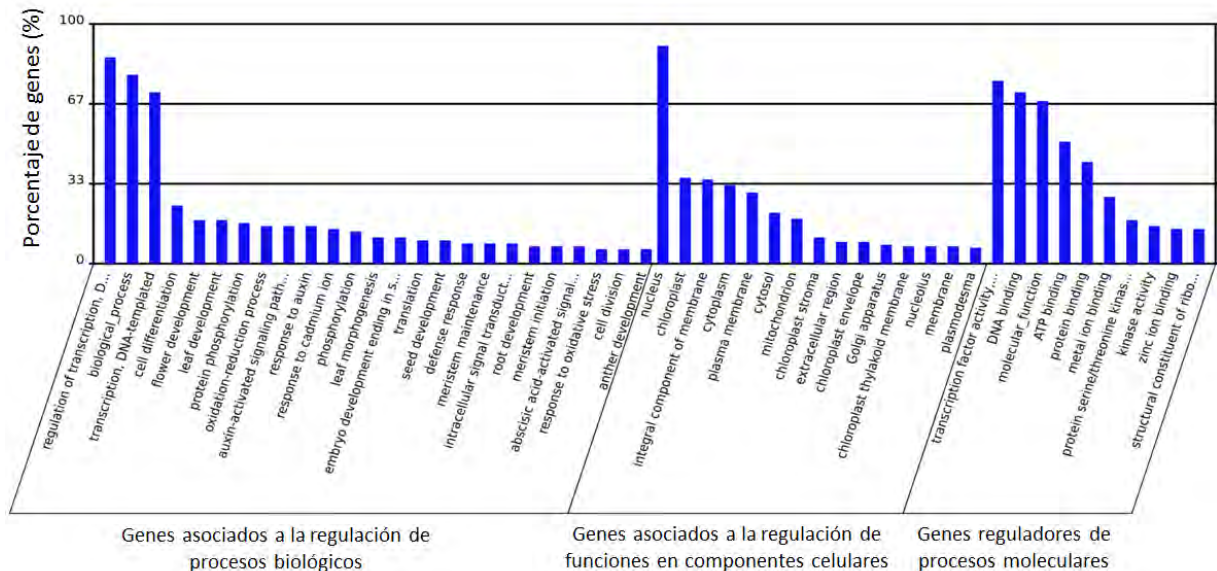


Figura 16. Procesos regulados por genes blanco de miRNAs en *Amaranthus hypochondriacus* v. Gabriela. Según su función, los genes blanco se clasifican en 3 grupos distintos: 1) Genes asociados a la regulación de procesos biológicos, 2) Genes asociados a la regulación de componentes celulares y 3) Genes reguladores de procesos moleculares. Cada grupo está dividido en 25, 15 y 10 categorías respectivamente.

Entre los principales procesos que regulan los genes blanco de miRNAs en *Amaranthus hypochondriacus* variedad “Gabriela” se encuentran: Actividad de factores de transcripción GO:0003700, regulación de la transcripción GO:0006355, GO:0006355, funciones en tilacoides GO:0009579, constitución estructural de ribosomas GO:0003735, respuesta a iones de cadmio GO:0046686, respuesta a

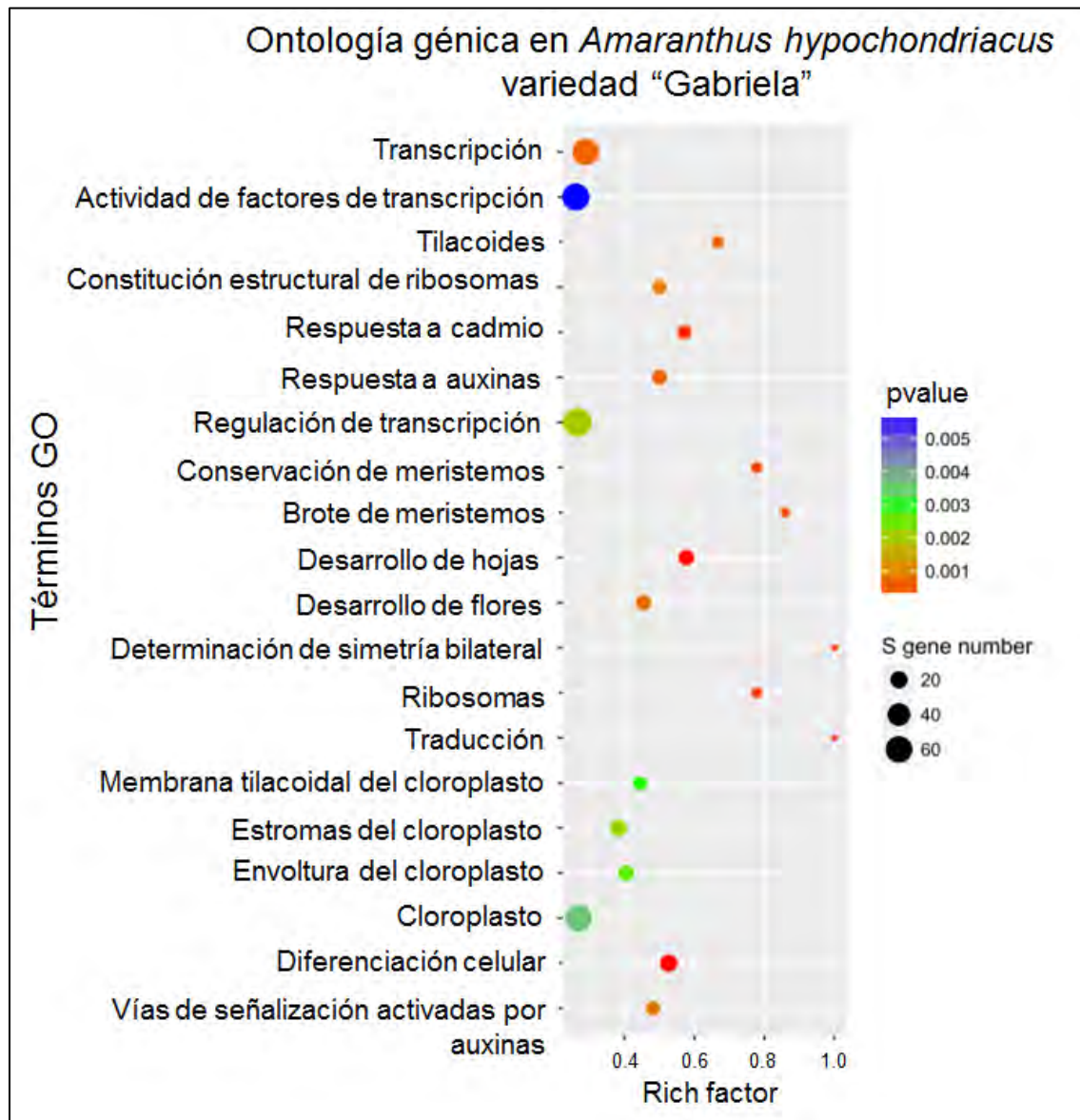


Figura 17. Ontología génica en *Amaranthus hypochondriacus* variedad “Gabriela”. En la imagen es posible apreciar mediante terminos GO, los principales procesos que son regulados mediante los genes blanco identificados en el degradoma de *Amaranthus hypochondriacus* variedad “Gabriela”.

auxinas GO:0009733, brote de meristemos GO:0010014, conservación de meristemos GO:0010073, desarrollo de hojas GO:0048366, desarrollo de flores GO:0009908, determinación de simetría bilateral de la planta GO:0009855, funciones asociadas a ribosomas GO:0022625, traducción GO:0002181, funciones asociadas a la membrana tilacoidal del cloroplasto GO:0009535, procesos realizados en los estromas y envoltura del cloroplastos GO:0009570, GO:0009941,GO:0009507, diferenciación celular GO:0030154, y vías de señalización activadas por auxinas GO:0009734. Los términos GO representados con más frecuencia son aquellos asociados a vías centrales de regulación en donde participan miembros de diferentes familias de factores de transcripción, tales como PCF5 (transcription factor PCF5-like), HOX16 (homeobox-leucine zipper protein HOX16-like), SIGE (sigma factor E), SPL16 (squamosa promoter-binding-like protein 16), SPL2 (squamosa promoter binding protein-like 2), SPL3 (squamosa promoter binding protein-like 3), ATHB-8 (homeobox-leucine zipper protein ATHB-8), AP2 (Integrase-type DNA-binding superfamily protein), NFYA1 (nuclear factor Y, subunit A1), ARF22 (auxin response factor 22), TCP4 (TCP family transcription factor 4), ATHB-15 (Homeobox-leucine zipper family protein / lipid-binding START domain-containing protein), ARF17 (auxin response factor 17), REV (Homeobox-leucine zipper family protein / lipid-binding START domain-containing protein), NAC100 (NAC domain containing protein 100), ARF22 (auxin response factor 22), AUX28 (auxin-induced protein AUX28), NFYA9 (nuclear factor Y, subunit A9), RAP2-4 (related to AP2 4), MYB44 (transcription factor MYB44-like), SPL17 (squamosa promoter-binding-like protein 17), SPL6 (Squamosa promoter-binding protein-like (SBP domain) transcription factor family protein), DOF2.5 (dof zinc finger

protein DOF2.5-like), RLT2 (Homeodomain-like transcriptional regulator), NFYA5 (nuclear factor Y, subunit A5), ARF8 (auxin response factor 8), RAP2-7 (Related to AP2.7) y ERF061 (ethylene-responsive transcription factor ERF061-like) entre otros.

Mediante *KEGG pathways* (<http://www.genome.jp/kegg/>) fue posible determinar que los genes identificados en el degradoma de amaranto desempeñan papeles reguladores importantes en muchos aspectos de la biología vegetal de amaranto, incluido los procesos de adaptación ambiental, metabolismo, el procesamiento de información genética, el procesamiento de información ambiental, y procesos celulares como transporte y catabolismo celular (Figura 19).

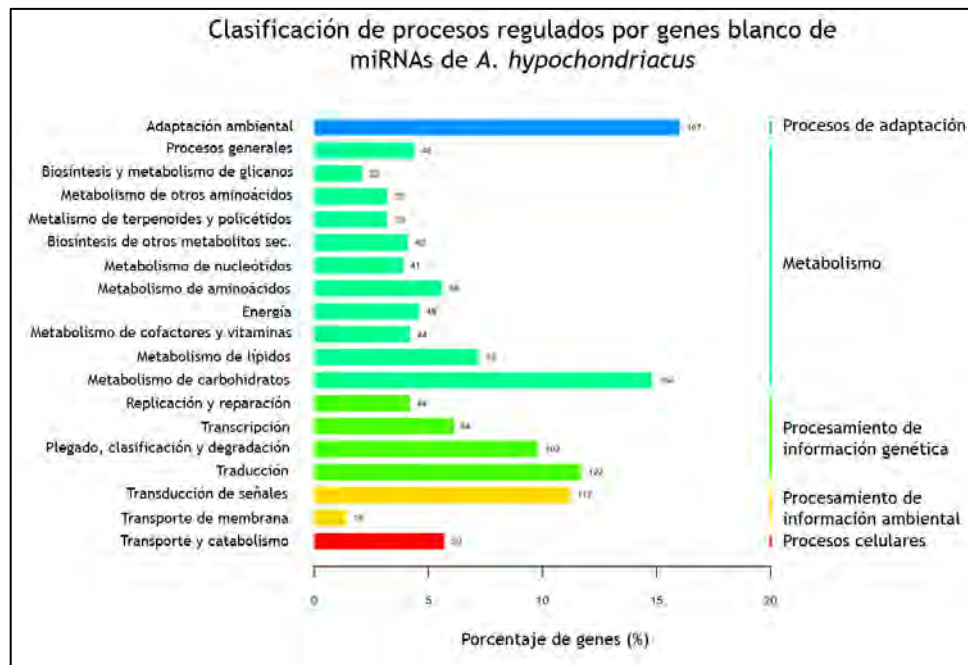


Figura 18. Clasificación de los procesos regulados por genes blanco de miRNAs de *Amaranthus hypochondriacus* variedad "Gabriela". Mediante *Kyoto Encyclopedia of Genes and Genomes (KEGG) pathways* se identificó que los genes blanco anotados en el degradoma de amaranto desempeñan funciones importantes que van desde la regulación de procesos de adaptación ambiental, regulación del metabolismo, el procesamiento de información genética, el procesamiento de información ambiental, y la regulación de distintos procesos celulares en las plantas

Del atlas de genes blanco que se obtuvo con la secuenciación del degradoma de *Amaranthus hypochondriacus* variedad “Gabriela”, se identificaron que aquellos que se encuentran regulados por 19 de las 22 familias de miRNAs clasificadas como conservadas, se expresan diferencialmente entre plantas control y plantas que fueron expuestas a estrés por sequía (figura 20).

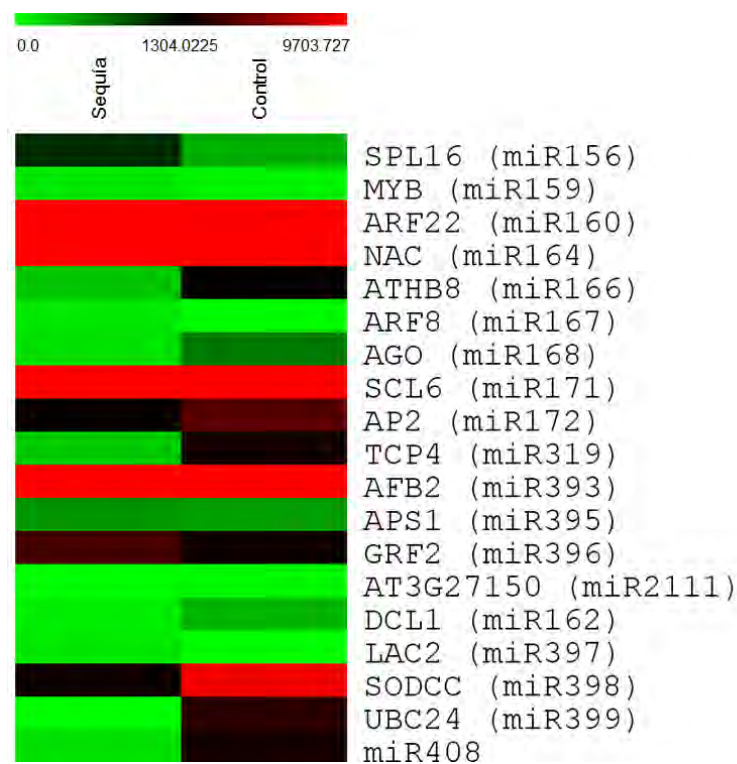


Figura 19. Expresión diferencial de genes blanco entre plantas control y plantas expuestas a estrés por sequía. En el análisis se consideró solo aquellos genes regulados por miRNAs conservados en *Amaranthus hypochondriacus* variedad “Gabriela”

Entre los genes diferencialmente expresados entre plantas control y plantas expuestas a estrés por sequía se encuentran: SPL (squamosa promoter-binding-like protein), MYB44 (transcription factor MYB-like), ARF (auxin response factor),

4. Discusión:

El análisis del Degradoma permitió la identificación de 721 genes regulados por 115 familias distintas de miRNAs potencialmente presentes en la variedad “Gabriela” de *Amaranthus hypochondriacus*. Dado que solo 26 y 42 familias distintas de miRNAs han sido identificadas en amaranto mediante predicción bioinformática y secuenciación masiva respectivamente (Capítulo II y III), las 73 familias restante y la regulación que ejercen sobre sus genes blanco se consideran preeliminares a reserva de su confirmación experimental. Entre los genes identificados como blancos de miRNAs en *Amaranthus hypochondriacus* “variedad “Gabriela”, 331 se encuentran regulados por 22 familias clasificadas como conservadas en la base de datos de miRBase (Kozamara). Muchos de estos genes regulados por miRNAs se expresan de forma diferencial entre plantas control y plantas sometidas a estrés por sequía, lo cual es coherente con reportes anteriores en plantas como *Paulownia australis* (Niu, Wang et al. 2016), *Dactylis glomerata* L. (Ji, Chen et al. 2018), *Hordeum vulgare* (Ferdous, Sanchez-Ferrero et al. 2017) y *Lycopersicon esculentum* (Candar-Cakir, Arican et al. 2016).

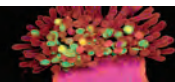
Los resultados mostrados aquí revelaron que el presente estudio está de acuerdo con los informes anteriores en diversas especies de plantas como el trigo (Achakzai, Barozai et al.2018), maíz (Fu, Zhang et al.2017), arroz (Huang, Jiejie et al. 2018), tomate (Liu, Yu et al.2018) y cebada (Kuang, Shen et al.2019), ya que, como en estos cultivos, los genes objetivo de miARN de amaranto están involucrados en una amplia gama de redes reguladoras que es crítica para el crecimiento, desarrollo y sostenibilidad de las plantas en las diferentes condiciones ambientales. Este

hallazgo sugiere la importancia de ciertos miARN como nodos en las redes de regulación génica, mientras que otros podrían estar actuando en vías específicas.

5. Conclusiones:


- La secuenciación del degradoma de *Amaranthus hypochondriacus* variedad “Gabriela” representa un atlas de interacción entre miRNAs y los genes blanco que se regulan en plantas control y plantas expuestas a estrés por sequía.
- El análisis del degradoma de *Amaranthus hypochondriacus* variedad “Gabriela” proporcionó evidencia molecular de la participación de ciertos miRNAs en la respuesta ante condiciones de estrés por sequía en amaranto.
- Los hallazgos que aquí se reportan proporcionan una base para futuras investigaciones de miRNAs que responden a estrés en *Amaranthus hypochondriacus*, lo cual puede ayudar para dilucidar los mecanismos moleculares que subyacen a las adaptaciones ante distintas condiciones de estrés en amaranto.

ANEXOS



RESEARCH PAPER

Reference genes for RT-qPCR normalisation in different tissues, developmental stages and stress conditions of amaranth

F. P. Vera Hernández, M. Martínez Núñez, M. Ruiz Rivas, R. E. Vázquez Portillo, M. D. Bibbins Martínez, S. Luna Suárez & F. de F. Rosas Cárdenas 

Instituto Politécnico Nacional, Centro de Investigación en Biotecnología Aplicada (CIBA-IPN), Ex-Hacienda San Juan Molino Carretera Estatal Tecuexcomac-Tepetitla, Tlaxcala, México

Keywords

Amaranth; gene expression; normalisation; quantitative real-time PCR; reference genes.

Correspondence

F. de F. Rosas Cárdenas, Instituto Politécnico Nacional, Centro de Investigación en Biotecnología Aplicada (CIBA-IPN) Ex-Hacienda San Juan Molino Carretera Estatal Tecuexcomac-Tepetitla Km 1.5, Tlaxcala C.P. 90700, México.
E-mail: frosasc@ipn.mx

Editor

E. Flenmetakis

Received: 16 November 2017; Accepted: 23 March 2018

doi:10.1111/plb.12725

ABSTRACT

- Studies of gene expression are very important for the identification of genes that participate in different biological processes. Currently, reverse transcription quantitative real-time PCR (RT-qPCR) is a high-throughput, sensitive and widely used method for gene expression analysis. Nevertheless, RT-qPCR requires precise normalisation of data to avoid the misinterpretation of experimental data. In this sense, the selection of reference genes is critical for gene expression analysis. At this time, several studies focus on the selection of reference genes in several species. However, the identification and validation of reference genes for the normalisation of RT-qPCR have not been described in amaranth.
- A set of seven housekeeping genes were analysed using RT-qPCR, to determine the most stable reference genes in amaranth for normalisation of gene expression analysis. Transcript stability and gene expression level of candidate reference genes were analysed in different tissues, at different developmental stages and under different types of stress. The data were compared using the geNorm, NormFinder and Bestkeeper statistical methods.
- The reference genes optimum for normalisation of data varied with respect to treatment. The results indicate that *AhyMDH*, *AhyGAPDH*, *AhyEF-1 α* and *AhyACT* would be optimum for accurate normalisation of experimental data, when all treatment are analysed in the same experiment.
- This study presents the most stable reference genes for normalisation of gene expression analysis in amaranth, which will contribute significantly to future gene studies of this species.

INTRODUCTION

Amaranth consumption has many health benefits, among which are its antihypertensive (de la Rosa *et al.* 2010; Lado *et al.* 2015), antimicrobial (Lipkin *et al.* 2005), antitumor (Ieliseieva *et al.* 2006) and cholesterol-lowering (Berger *et al.* 2003; Shin *et al.* 2004; Pasko *et al.* 2011; Chmelik *et al.* 2013) effects. Amaranth has evolved complex mechanisms to tolerate extremely adverse growing conditions; moreover, it resists different types of biotic and abiotic stress (Delano-Frier *et al.* 2011; Huerta-Ocampo *et al.* 2014; Massange-Sanchez *et al.* 2016; Palmeros-Suarez *et al.* 2017), is easy to grow in agriculturally marginal lands and has high potential for economic exploitation (Emokaro *et al.* 2007; Mlakar *et al.* 2010; Janssen *et al.* 2017). *Amaranthus hypocondriacus* has a diploid karyotype ($2n = 32$; Radwan *et al.* 2014). A draft genome of *A. hypocondriacus* var. Plainsman that covers 377 Mb of the estimated genome size of 466 Mb has been assembled (Clouse *et al.* 2016) and has been the focus of various transcriptomic studies (Riggins *et al.* 2010; Delano-Frier *et al.* 2011; Liu *et al.* 2014). Some of the libraries available on NCBI databases on amaranth are derived from experiments conducted on plants exposed to either different types of stress, such as drought, water stress, bacteria, salt stress and insect herbivores (Accession PRJNA65409); different

development stages or experiments conducted on various tissues (accession PRJNA263128). The draft transcriptome of amaranth has been assembled, mapped and functionally annotated, and is available on public databases (Clouse *et al.* 2016).

A large number of genes are involved in processes such as plant development, differentiation or mounting responses that enable tolerance to different types of biotic and abiotic stress. Amaranth has evolved various mechanisms to tolerate some biotic and abiotic stresses, such as the capacity to increase expression of choline monoxygenase (CMO), which catalyses the synthesis of glycine betaine in response to salinity and drought (Russell *et al.* 1998); up-regulation of transcription factors; DNA-binding of One Zinc Finger 1 (*DOF1*) and Mini Zinc Finger 1 (*MIF1*). These involve a coordinated response comprising osmolyte accumulation, expression of proteins that reduce damage by reactive oxygen species and regulation of transcription factors related to plant growth control (Huerta-Ocampo *et al.* 2011). However, the molecular mechanisms behind these processes are not entirely understood. Transcriptional analysis with reverse transcription quantitative real-time PCR (RT-qPCR) is useful for functional interpretation of genes and can improve the quantification of gene expression profiles. RT-qPCR has become the preferred method for gene expression quantification. Currently, some studies focus on the

selection of reference genes in several organisms (e.g. Bevitore *et al.* 2014; Ferdous *et al.* 2015; Singh *et al.* 2015; Li *et al.* 2017); however, the identification of reference genes for the normalisation of RT-qPCR has not been described in amaranth. This study evaluated genes to determine the most stable reference genes and analysed transcript stability of these genes in different tissues, developmental stages and under different types of stress in amaranth.

MATERIAL AND METHODS

Plant growth conditions

Amaranth seeds (*A. hypochondriacus* var. Gabriela) were surface sterilised with 10% sodium hypochlorite solution (NaClO₄) and sown in polystyrene trays with 1" × 1" × 2.5" wells, at the end of winter in February 2016. Each well was filled with a sterile substrate composed of Perlite, vermiculite and peat moss (i3:1:1 v/v). Germination trays were kept under semi-controlled greenhouse conditions at the Center for Research in Applied Biotechnology, National Polytechnic Institute of Mexico in Tlaxcala at 2,260 m a.s.l. (19°16'53.2"N, 98°21'57.3" W).

Plant treatment and tissue collection

The different experimental conditions used in this study are shown in Table 1. Briefly, 60-day-old amaranth plants were dissected to obtain leaf, stem, root and panicle tissues samples for further analysis. To gather tissues from various development stages of the amaranth life cycle, plants were collected at different stages of development, corresponding to the opening of cotyledons, five to six leaves, apical inflorescence and seed development (Martínez-Núñez *et al.* in process). For abiotic stress treatments, 30-day-old seedlings were transferred to environmental chambers. Cold treatment was performed at 4 °C compared to the control temperature of 25 °C, with tissue then collected after 48 h of cold treatment. Heat treatment was performed at 42 °C for 48 h. For drought stress, irrigation was

Table 1. Plant tissue and treatments used for RT-qPCR normalisation. The table present tissues and treatment conditions used in each experimental set for RT-qPCR analysis.

Group	Tissue	Collection time (Days post-germination)	Treatment
Different Tissue	Leaves	60 days	–
	Stem	60 days	–
	Root	60 days	–
	Panicle	60 days	–
Different stages	Aerial tissue	3 days	–
	Aerial tissue	43 days	–
	Aerial tissue	60 days	–
	Aerial tissue	90 days	–
Different types of stress	Aerial tissue	32 days	48 h at 4 °C
	Aerial tissue	32 days	48 h at 42 °C
	Aerial tissue	33 days	Not irrigation for 72 h
	Aerial tissue	32 days	25 °C with normal irrigation
	Aerial tissue	35 days	15 days of exposition at <i>Macrosiphum sp</i>
	Aerial tissue	32 days	Normal conditions

suspended until a relative humidity of 8% (after 72 h) was achieved in the substrate, after which the control was regularly irrigated, and the foliar tissue samples then collected. For biotic stress treatment, aphids identified as *Macrosiphum sp.* were collected in the field, with 20-day-old seedlings then transferred to a contention chamber under greenhouse conditions. The amaranth plants were infested with approximately five aphids per plant; after 15 days, the foliar tissue was collected. Three biological replicates were used for each experiment, while samples were collected and immediately frozen in liquid nitrogen and stored at –80 °C.

Isolation of RNA and quality controls

The samples were ground to a fine powder with a pestle and mortar in liquid nitrogen, and 50 mg used for RNA isolation. Total RNA was extracted using the TRIzol reagent (Invitrogen, Carlsbad, CA, USA) according to the manufacturer's instructions. The integrity of the RNA samples was judged using agarose gel electrophoresis. The concentration of each sample was measured using UVIS Drop UVS-99 (Avans, Taipei, Taiwan). Samples with a 260/280 ratio of between 1.8 and 2.1 and a 260/230 ratio of approximately 2 or slightly above were used for the analysis.

Selection of candidate reference genes and primer design

Arabidopsis thaliana and *Beta vulgaris* genes were downloaded from GenBank (<https://www.ncbi.nlm.nih.gov/genbank>) and used as query sequences to retrieve homologous genes from *A. hypochondriacus*. Seven commonly employed candidate reference genes, actin (*AhyACT*), β -tubulin (*Ahy β -TUB*), glyceraldehyde 3-phosphate dehydrogenase (*AhyGAPDH*), S-adenosylmethionine decarboxylase (*AhySAMDC*), elongation factor 1-alpha (*AhyEF-1 α*), 18S ribosomal RNA (*Ahy18S-rRNA*) and malate dehydrogenase (*AhyMDH*) were selected (Table 2). Based on the gene sequence obtained from the transcriptome assembly database (Clouse *et al.* 2016) available at Phytozome (phytozome.jgi.doe.gov), primers were designed using Primer Express 2.0 software (Applied Biosystems, Foster City, CA, USA) under default parameters (Table 2).

Reverse transcription quantitative real-time PCR conditions

First-strand cDNA was synthesised with 1 μ g total RNA in a final reaction volume of 20 μ l, using M-MLV Reverse Transcriptase (Sigma-Aldrich, St. Louis, MI, USA) and according to the manufacturer's instructions. The RT-qPCR mixture contained 4 μ l diluted cDNA (corresponding to a 1 ng starting amount of RNA), 5 μ l 2 × Power SYBR Green PCR Master Mix (Applied Biosystems) and 400 nM of each gene-specific primer in a final volume of 10 μ l. RT-qPCRs with no template controls were also performed for each primer pair. Real-Time PCR reactions were performed with the StepOnePlus Real-Time PCR System and software (Applied Biosystems). All RT-qPCRs were performed under the following conditions: 10 min at 95 °C, 40 cycles of 15 s at 95 °C and 1 min at 60 °C in 96-well optical reaction plates (Applied Biosystems). The specificity of amplicons was verified *via* melting curve analysis (60 to 95 °C) after 40 cycles and agarose gel electrophoresis. Two technical and three biological replicates of each sample were used for the qPCR analysis.

Table 2. Candidate reference genes for RT-qPCR normalisation in amaranth. Gene information, including amplicon length, primers and Tm for seven candidate reference genes.

Gene name	Symbol	Gene length	Amplicon length (bp)	Tm (°C)	Locus (phytozome)	Primer sequence
Actin	<i>AhyACT</i>	1134	178	79.1	AHYPO_019031	FW CGTGACCTGACTGATTACCTTA RV GCTCGTAGTTCCTCAATGGC
β-Tubulin	<i>Ahyβ-TUB</i>	1069	81	76.8	AHYPO_019789	FW GGAAGGAATGGACGAGATGG RV TCTTGATACTGCTGATACTCTGC
Glyceraldehyde 3-phosphate dehydrogenase	<i>AhyGAPDH</i>	1383	195	80.1	AHYPO_013553	FW TCAAGGAGGAATCCGAGGGC RV AGTCAACAACACGGGAACCTG
S-Adenosylmethionine decarboxylase	<i>AhySAMDC</i>	2591	195	81.0	AHYPO_016008	FW GCTCCGTGCAATCCCACCTA RV CCCATCACAAGCCCTTGCT
Elongation Factor 1-alpha	<i>AhyEF-1A</i>	1377	224	80.4	AHYPO_001308	FW ACTGTGCTATCCTCATTATTG RV GTTGTAAACCACCTTCTTC
18S ribosomal RNA	<i>Ahy18S</i>	1630	109	81.0	AH006866*	FW CCATAAACGATGCCGACCAG RV AGCCTTGCGACCATACTCC
Malate Dehydrogenase	<i>AhyMDH</i>	1539	136	78.5	AHYPO_021284	FW TGCTCCCAACTGCAAGGTTT RV ACCAAGTGCCCTGTTGTGAT

*Genebank accession for *Amaranthus caudatus* 18S ribosomal RNA. Actin oligonucleotides were reported in Massange-Sanchez *et al.* (2016).

Efficiency of PCR

A series of six-five-fold dilutions (1:1, 1:5, 1:25, 1:125, 1:625 and 1:3125) of cDNA from *A. hypochondriacus* were used to generate the standard curves. The PCR efficiency (E) and correlation coefficient (R^2) were determined for each gene using the linear regression model. PCR efficiency of between 90 and 110% and $R^2 > 0.99$ was considered acceptable.

Analysis of gene expression variation

The expression level of genes in each reaction was determined using the cycle threshold (Cq; cycle at which fluorescence from the reaction exceeds a crossing point automatically set by the StepOne software). To analyse expression variation of the candidate reference genes and determine the best reference genes, the Excel-based methods, geNorm (Vandesompele *et al.* 2002), NormFinder (Andersen *et al.* 2004), BestKeeper (Pfaffl *et al.* 2004) and the online tool RefFinder (<http://leonxie.esy.es/RefFinder>) were used. The raw data were directly used with the BestKeeper and RefFinder methods, while for geNorm and NormFinder methods, Cq values were converted into relative quantity values (RQ) via the formula $RQ = E^{-\Delta Cq}$, where E is the validated amplification efficiency of each gene, and ΔCq is the difference between the Cq value and the minimum Cq of each gene among the samples. RefFinder enables assessment of the most stable reference gene by comparing the three Excel methods plus the comparative and Delta CT method (Silver *et al.* 2006). Although RefFinder analyses raw data, assuming 100% efficiency for all genes, the outputs were compared to data obtained by the original software, given that PCR efficiencies are not considered, and they been reported to lead to overestimation of differences between groups (De Spiegelaere *et al.* 2015).

RESULTS

Specificity of primers and efficiency of reference genes

The genes *AhyACT*, *Ahyβ-TUB*, *AhyGAPDH*, *AhySAMDC*, *AhyEF-1α*, *Ahy18S-rRNA* and *AhyMDH* were used for the

RT-qPCR analysis. The primer sequences and transcript information are given in Table 2. Specific primers for the amplification of potential reference genes were designed for SYBR green-based RT-qPCR and synthesised using T4 oligo (Mexico). The amplicon length ranged from 81 to 224 bp (Table 2), with corresponding unique bands observed on agarose electrophoresis gel (Fig. 1A). A single peak of fluorescence was observed on the melting curve (Fig. 1B), indicating that a unique and specific fragment was amplified during RT-qPCR. The R^2 , which shows how the data fit the standard curve, was then calculated. The PCR amplification efficiencies (E) for every gene, which is another parameter that gives information about the reaction and involves experimental factors such as length, secondary structure and GC content of the amplicon, was also calculated. The E of RT-qPCR reactions varied from 1.84 to 2.06 and the R^2 were > 0.9932 (Fig. 2). These results meet the standard ($R^2 > 0.99$, and $1.8 < E < 2.2$) established by Ramakers *et al.* (2003).

Expression profiles of candidate reference genes

Measurement of the expression level of all samples showed some variations among the seven reference genes (Fig. 3). Descriptive statistics were calculated using Minitab 17 Statistical Software (Minitab, State College, USA) for each of the tested genes. The Cq values for the seven genes ranged from 18.52 to 27.85, the majority of these values were between 20 and 25 in all tested samples (Fig. 3). *AhyMDH* had a lower SD, whereas *Ahy18S-rRNA* had the highest SD.

Expression stability of candidate reference genes

The most suitable reference genes were evaluated using RefFinder, geNorm, NormFinder and BestKeeper. The stability ranking of candidate reference genes in 36 individual samples was calculated and identified as 'Total', with the 36 samples divided into three groups denominated as: 'Different types of stress', 'Different tissues' and, 'Different stages of development'. The results obtained with every method are summarised in Table 3.

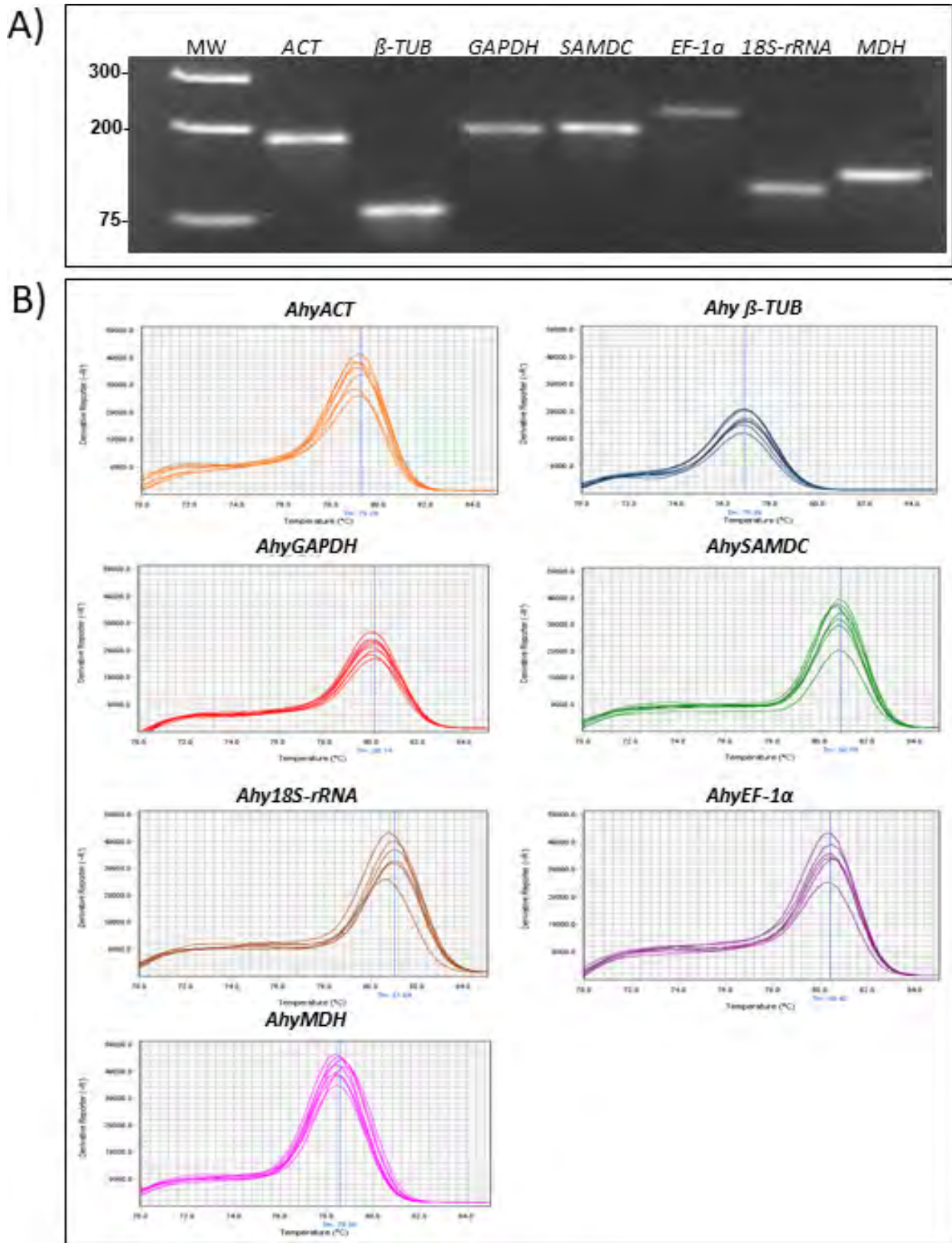


Fig. 1. Specificity of primers and efficiency of reference genes. (A) Electrophoretic analysis of RT-PCR products. Amplicon lengths are indicated in Table 2. Equal amounts of cDNA from all samples were used as template. PCR products were observed with 2.5% agarose gel electrophoresis, 8 cm length, 1X TAE, 7 V/cm, 110 min, and stained with SYBR Gold Nucleic Acid Gel stain. M, GeneRuler 1 kb Plus DNA ladder (ThermoFisher, Waltham, MA, USA). (B) Melting curves of candidate reference genes. Melting curves were generated by heating the amplicon from 70 to 85 °C using the derivative method.

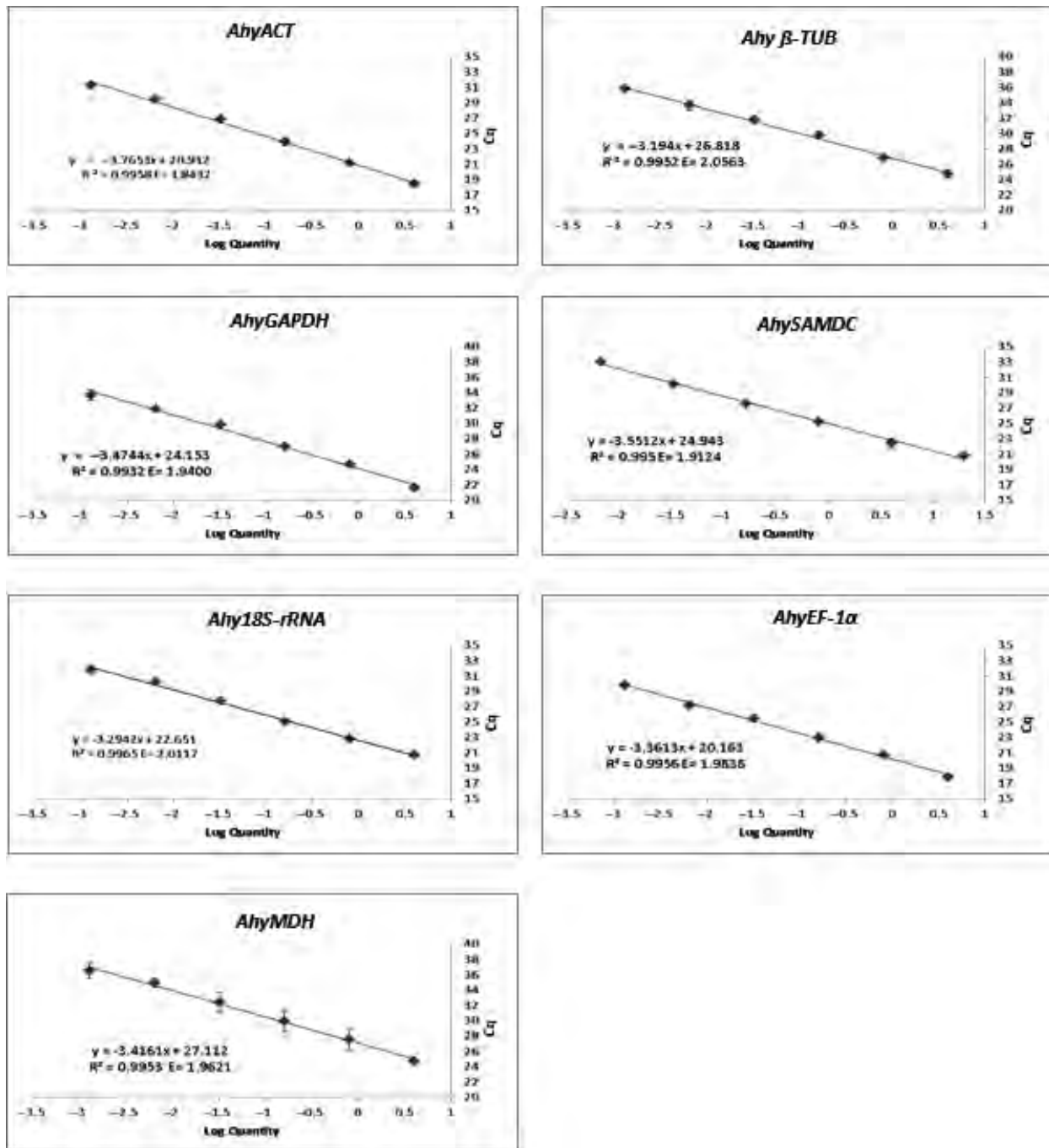


Fig. 2. PCR efficiency and correlation coefficient. The logarithm of each known concentration of starting RNA in the dilution series (x-axis) was plotted against mean of the Cq value for used concentration (y-axis). Slope (efficiency) and correlation coefficient were obtained via linear regression of the standard curve.

As the algorithms used employ different approaches to determine the most stable reference gene, it was found that ranking differed depending on the method employed. Therefore, selection of the most reliable gene for normalisation will depend on the characteristics of every experiment.

Analysis with RefFinder

The RefFinder is a user-friendly tool that integrates four different calculations obtained using gene stability methods. The

online RefFinder tool integrates Bestkeeper, NormFinder and geNorm algorithms and combines them into a 'comprehensive ranking', with outputs from RefFinder and original software obtained from the total samples analysed (Table 4). It has been reported that RefFinder results may be inaccurate because PCR efficiencies are not considered and should only be considered as a guide for deciding which gene to use to normalise PCR data (De Spiegelaere *et al.* 2015). Moreover, results obtained with the original software (NormFinder) are different to those obtained in RefFinder, not only because of the efficiency values

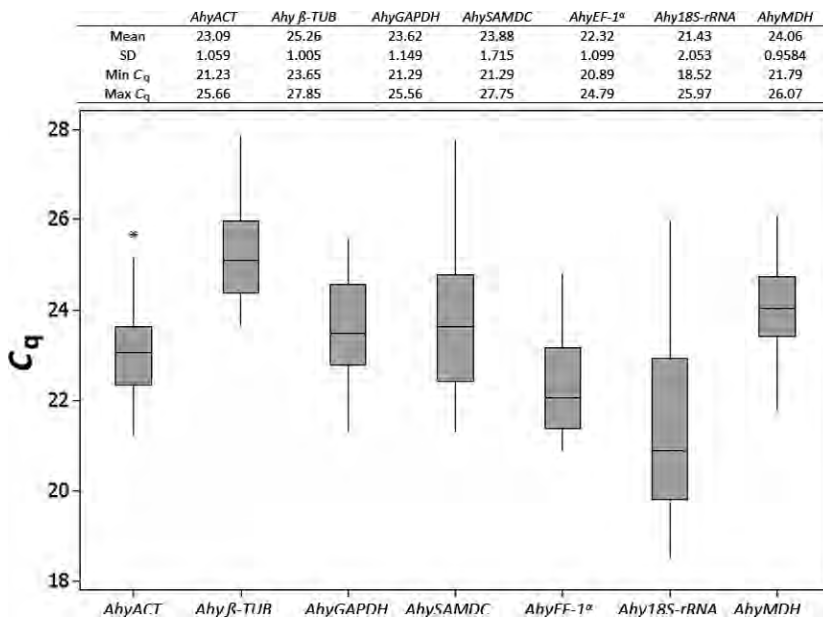


Fig. 3. Descriptive statistics and distribution of C_q-alues of the seven candidate reference genes across all samples in RT-qPCR analysis. (A) Descriptive statistics calculated using Minitab 17. SD, mean and minimum and maximum C_q values for a total of 36 samples. (B) Distribution of C_q values analysed for each gene in all samples. For each gene, distribution of the C_q values is box-plotted from all 72 raw C_q values obtained from the 36 duplicate conditions of amaranth. The borders of the box represent the 25th and the 75th percentiles. The line that divides the box corresponds to the median, while whiskers indicate the highest and lowest C_q values, with the exception of atypical values, which are represented by asterisks.

but also because the original program is able to calculate inter- and intragroup variation, while RefFinder does not allow the user to define groups.

Analysis with GeNorm

The expression stability value (M) for each reference gene was calculated using the geNorm algorithm. A lower M-value

indicates higher stability. For the ‘Total’, ‘Different tissues’ and ‘Different stages of development’ groups, *AhyACT/AhyMDH* was the most stable pair, while *AhyGAPDH/AhyMDH* was the most stable pair in the ‘Different types of stress’ group and *Ahy18S-rRNA* and *AhySAMDC* was the least stable (Fig. 4). Based on calculations of pair-wise variation (V), the geNorm algorithm can determine the optimal number of reference genes for each experimental condition (Fig. 5). It is generally

Table 3. Expression stability and ranking of candidate reference genes using different software for each experimental set. The genes were analysed with BestKeeper, geNorm and NormFinder. Genes were ranked in terms of values obtained from each algorithm used in each group; M, expression stability and SD were used. Normfinder and Genorm used the M, while BestKeeper used SD.

Group	Method	Gene	Ranking of gene expression						
			1	2	3	4	5	6	7
Total	BestKeeper	Gene	<i>AhyMDH</i>	<i>AhyACT</i>	<i>Ahyβ-TUB</i>	<i>AhyEF-1α</i>	<i>AhyGAPDH</i>	<i>AhySAMDC</i>	<i>Ahy18S-rRNA</i>
		SD value	0.729	0.814	0.826	0.902	0.977	1.336	1.707
	Normfinder	Gene	<i>AhyMDH</i>	<i>AhyGAPDH</i>	<i>AhyACT</i>	<i>AhyEF-1α</i>	<i>Ahyβ-TUB</i>	<i>AhySAMDC</i>	<i>Ahy18S-rRNA</i>
		M value	0.086	0.134	0.142	0.172	0.215	0.242	0.339
	Genorm	Gene	<i>AhyACT</i> <i>AhyMDH</i>		<i>AhyGAPDH</i>	<i>AhyEF-1α</i>	<i>Ahyβ-TUB</i>	<i>AhySAMDC</i>	<i>Ahy18S-rRNA</i>
		M value	0.77		0.83	0.87	0.92	1.11	1.32
Different types of stress	BestKeeper	Gene	<i>AhyEF-1α</i>	<i>Ahyβ-TUB</i>	<i>AhyMDH</i>	<i>AhyACT</i>	<i>AhyGAPDH</i>	<i>AhySAMDC</i>	<i>Ahy18S-rRNA</i>
		SD value	0.741	0.751	0.802	0.852	1.071	1.121	1.756
	Normfinder	Gene	<i>AhyMDH</i>	<i>AhyGAPDH</i>	<i>AhyACT</i>	<i>AhyEF-1α</i>	<i>AhySAMDC</i>	<i>Ahyβ-TUB</i>	<i>Ahy18S-rRNA</i>
		M value	0.105	0.151	0.310	0.317	0.348	0.461	0.723
	Genorm	Gene	<i>AhyGAPDH</i> <i>AhyMDH</i>		<i>AhyEF-1α</i>	<i>AhyACT</i>	<i>Ahyβ-TUB</i>	<i>AhySAMDC</i>	<i>Ahy18S-rRNA</i>
		M value	0.597		0.827	0.872	0.997	1.16	1.353
Different tissue	BestKeeper	Gene	<i>AhyMDH</i>	<i>AhyACT</i>	<i>AhySAMDC</i>	<i>Ahyβ-TUB</i>	<i>AhyEF-1α</i>	<i>AhyGAPDH</i>	<i>Ahy18S-rRNA</i>
		SD value	0.66	0.79	0.85	0.87	1.03	1.06	1.39
	Normfinder	Gene	<i>AhyMDH</i>	<i>AhyACT</i>	<i>AhyEF-1α</i>	<i>Ahyβ-TUB</i>	<i>AhySAMDC</i>	<i>AhyGAPDH</i>	<i>Ahy18S-rRNA</i>
		M value	0.137	0.160	0.184	0.262	0.270	0.467	0.664
	Genorm	Gene	<i>AhyACT</i> <i>AhyMDH</i>		<i>AhyEF-1α</i>	<i>Ahyβ-TUB</i>	<i>AhySAMDC</i>	<i>AhyGAPDH</i>	<i>Ahy18S-rRNA</i>
		M value	0.678		0.802	0.841	0.915	1.016	1.297
Different stages of development	BestKeeper	Gene	<i>AhyMDH</i>	<i>AhyGAPDH</i>	<i>AhyACT</i>	<i>Ahyβ-TUB</i>	<i>AhyEF-1α</i>	<i>Ahy18S-rRNA</i>	<i>AhySAMDC</i>
		SD value	0.58	0.65	0.68	0.68	0.84	1.52	1.76
	Normfinder	Gene	<i>AhyACT</i>	<i>AhyMDH</i>	<i>AhyGAPDH</i>	<i>Ahyβ-TUB</i>	<i>AhyEF-1α</i>	<i>Ahy18S-rRNA</i>	<i>AhySAMDC</i>
		M value	0.062	0.072	0.202	0.286	0.351	0.397	0.595
	Genorm	Gene	<i>AhyACT</i> <i>AhyMDH</i>		<i>AhyGAPDH</i>	<i>AhyEF-1α</i>	<i>Ahyβ-TUB</i>	<i>Ahy18S-rRNA</i>	<i>AhySAMDC</i>
		M value	0.375		0.45	0.57	0.625	0.933	1.081

Table 4. Comparison of ranking of candidate reference genes using RefFinder and original software. The genes were analysed with BestKeeper, geNorm and NormFinder using the web-based tool Refinder and original software. M (expression stability value) and SD were used. *and Δ CT method was not compared.

			Ranking of gene expression						
Method			1	2	3	4	5	6	7
Reffinder	Δ CT ^(a)	Gene	<i>AhyMDH</i>	<i>AhyACT</i>	<i>AhyEF-1α</i>	<i>AhyGAPDH</i>	<i>Ahyβ-TUB</i>	<i>AhySAMDC</i>	<i>Ahy18S-rRNA</i>
		Value	1.09	1.2	1.23	1.24	1.36	1.58	1.87
	BestKeeper	Gene	<i>AhyMDH</i>	<i>AhyACT</i>	<i>Ahyβ-TUB</i>	<i>AhyEF-1α</i>	<i>AhyGAPDH</i>	<i>AhySAMDC</i>	<i>Ahy18S-rRNA</i>
		SD value	0.73	0.81	0.83	0.9	0.98	1.34	1.71
	Normfinder	Gene	<i>AhyMDH</i>	<i>AhyACT</i>	<i>AhyGAPDH</i>	<i>AhyEF-1α</i>	<i>Ahyβ-TUB</i>	<i>AhySAMDC</i>	<i>Ahy18S-rRNA</i>
		M value	0.306	0.684	0.761	0.763	1.035	1.259	1.683
	Genorm	Gene	<i>AhyACT</i> <i>AhyMDH</i>		<i>AhyEF-1α</i>	<i>AhyGAPDH</i>	<i>Ahyβ-TUB</i>	<i>AhySAMDC</i>	<i>Ahy18S-rRNA</i>
		M value	0.846		0.871	0.912	0.953	1.164	1.367
	Recommended comprehensive ranking	Gene	<i>AhyMDH</i>	<i>AhyACT</i>	<i>AhyEF-1α</i>	<i>AhyGAPDH</i>	<i>Ahyβ-TUB</i>	<i>AhySAMDC</i>	<i>Ahy18S-rRNA</i>
		Value	1	1.68	3.46	3.94	4.4	6	7
Original software	BestKeeper	Gene	<i>AhyMDH</i>	<i>AhyACT</i>	<i>Ahyβ-TUB</i>	<i>AhyEF-1α</i>	<i>AhyGAPDH</i>	<i>AhySAMDC</i>	<i>Ahy18S-rRNA</i>
		SD value	0.729	0.814	0.826	0.902	0.977	1.336	1.707
	Normfinder	Gene	<i>AhyMDH</i>	<i>AhyGAPDH</i>	<i>AhyACT</i>	<i>AhyEF-1α</i>	<i>Ahyβ-TUB</i>	<i>AhySAMDC</i>	<i>Ahy18S-rRNA</i>
		M value	0.086	0.134	0.142	0.172	0.215	0.242	0.339
	Genorm	Gene	<i>AhyACT</i> <i>AhyMDH</i>		<i>AhyGAPDH</i>	<i>AhyEF-1α</i>	<i>Ahyβ-TUB</i>	<i>AhySAMDC</i>	<i>Ahy18S-rRNA</i>
		M value	0.77		0.83	0.87	0.92	1.11	1.32

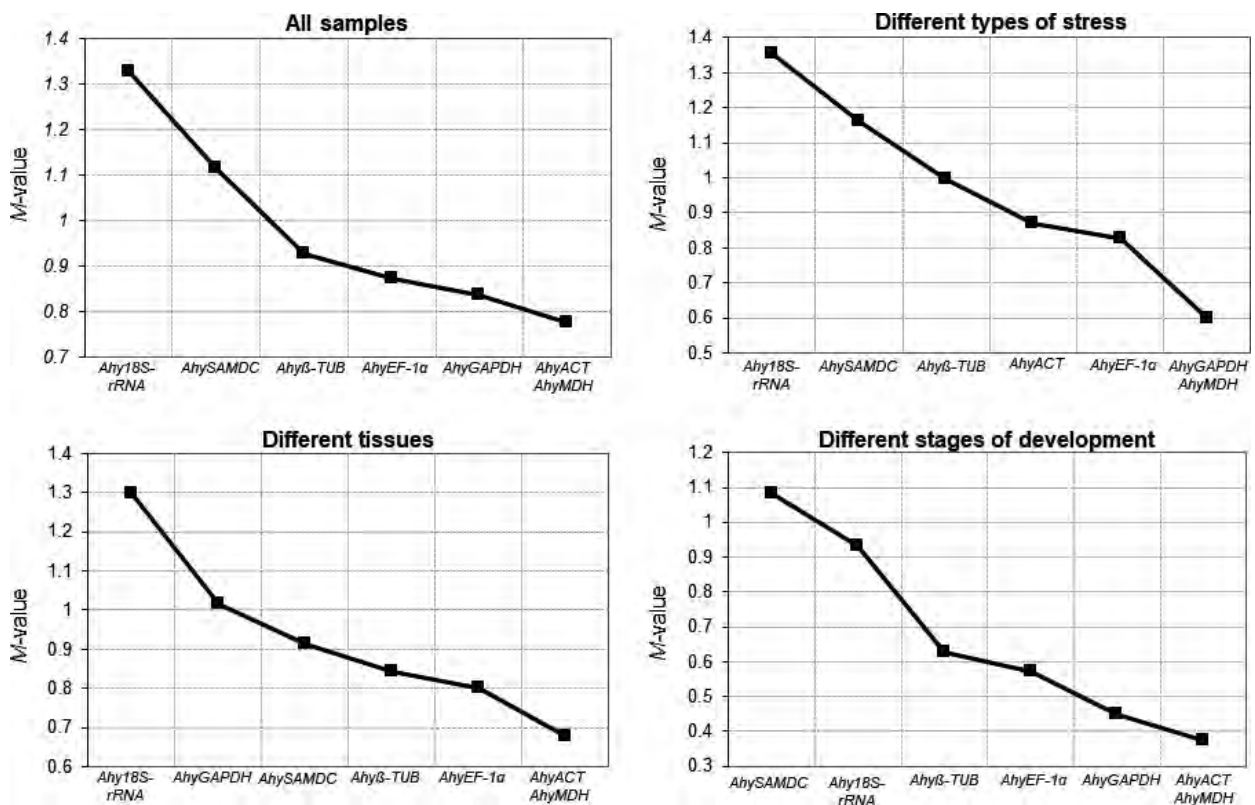


Fig. 4. Gene expression stability and ranking of six reference genes based on geNorm. Expression stability value (M) for each gene was obtained and graphed. The lower the M value, the more stable the gene.

assumed that 0.15 is a cut-off value for determining optimal number of reference genes as Vandesompele *et al.* (2002) decided to take this as a cut-off value, since the inclusion of an additional control gene made no significant contribution to the normalisation factor (NFn + 1) calculated using their data.

However, 0.15 must not be taken as a strict cut-off value but rather as a guide value, depending on the volume of genes and samples tested (Singh *et al.* 2015). The use of only four reference genes in the group ‘Different stages of development’ from the data obtained in this study met this cut-off value (Fig. 5).

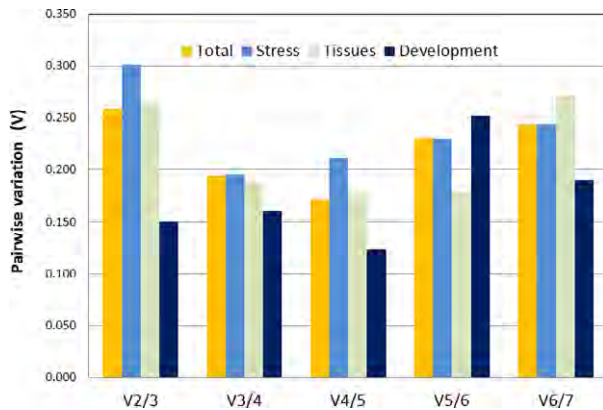


Fig. 5. Analysis of minimum number of reference genes required for RT-qPCR normalisation. Pair-wise variation value (V) was calculated using geNorm to determine the minimum number of reference genes required for normalisation in each experimental set. The graph shows variation in stability with the sequential addition of a subsequent reference gene, starting with the most stably expressed pair of genes (V2/3). From the graph, it can be inferred whether the addition of another gene would have an effect on stability.

However, according to the Primer Design geNorm kit Handbook (Primerdesign 2016), the use of the three best reference genes, which in most conditions include *AhyMDH*, *AhyACT*, *AhyEF-1 α* and *AhyGAPDH*, is a valid normalisation strategy that results in accurate and reliable normalisation of data. These data were not obtained using the RefFinder output.

Analysis with NormFinder

NormFinder calculates gene expression stability by comparing variation between user-defined sample groups (Andersen *et al.* 2004). This study analysed all the samples, identifying results as 'Total' in Table 4. The same three groups were also defined, as in geNorm analysis, with each group subjected to further analysis, and subgroups defined as the three mean Cq values (of two technical replicates each) corresponding to three individual biological replicates for each condition tested. NormFinder calculates intra- and intergroup variations, considering genes with the lowest variation as stable. Analysis of groups of data found similar results to geNorm, with *AhyMDH/AhyACT* the most stable genes in the 'Different types of tissues' and 'Different stages of development' groups, while *AhyGAPDH/AhyMDH* were the most stable pair in 'Different types of stress' group. However, normFinder results differ from geNorm in the 'Total' group, with very different results obtained between the samples, while intergroup variation calculation is a crucial feature in NormFinder analysis. Similar to geNorm, NormFinder found that the least stable genes are, generally, *AhySAMDC* and *Ahy18S-rRNA*.

Analysis with Bestkeeper

The lower of the SD and CV values computed by BestKeeper software ranked *AhyMDH* as the most stable and thus the best reference gene, when all samples were analysed against each other. While these are similar to findings obtained with geNorm and NormFinder, some of the outputs obtained with this method showed discrepancies. For example, some genes ranked as less stable, e.g. *AhySAMDC* and *Ahy β -TUB*, were ranked as

more stable than other genes considered as stable, e.g. *AhyGAPDH* (Table 4).

DISCUSSION

The use of appropriate reference genes can correct inaccuracies in terms of the amount of RNA loaded into the reaction and the efficiency of the reverse transcription, with the intention of obtaining real differential expression of the target genes in experimental treatments. However, the direct transfer of reference genes to non-model plants is limited as not all the genes are expressed in the same manner in different species. While the use of only one housekeeping gene for normalisation of RT-PCR data is a common practice, it has been widely demonstrated that results of this common practice constitute erroneous fold expression calculations (Vandesompele *et al.* 2002; Chan *et al.* 2014).

Chan *et al.* (2014) evaluated methods for identifying reference genes and found that NormFinder and geNorm were consistent with each other in obtaining the highest correlation ($R^2 = 0.987$; Chan *et al.* 2014). Hence it enables suggestions to be made for normalisation of PCR data. For PCR data from amaranth exposed in the same experiment to different stress conditions, with different tissues and different stages of development, it is highly recommended to use the four most stable genes (*AhyMDH*, *AhyGAPDH*, *AhyEF-1 α* and *AhyACT*) to validate normalisation of data.

Data obtained from samples exposed to different types of stress had the highest M values (*i.e.* they are less stable under these conditions). These findings suggest the use of three reference genes, *AhyGAPDH*, *AhyMDH* and either *AhyEF-1 α* or *AhyACT*, when working with samples exposed to biotic or abiotic stress. Furthermore, given that they present similar stability values, the inclusion of a fourth gene would not make a significant contribution to accurate normalisation of PCR data.

Finally, data from samples of different tissues or different stages of development (only one condition per experiment) had low M values (*i.e.* they are more stable under these conditions). This finding suggests use of the pair of genes *AhyACT* and *AhyMDH* as optimal for normalisation of data, while inclusion of a third gene, in terms of development stage, would not make a contribution; however, when working with different tissues, addition of *AhyEF-1 α* would be required for accurate normalisation.

Moreover, the results indicate that *Ahy18S-rRNA* and *AhySAMDC* were, in most cases, inappropriate for use as a control in *A. hypocondriacus* and should be avoided. In summary, this study provides useful information about various reference genes for RT-qPCR studies in amaranth, which will contribute significantly to future gene studies in this valuable species.

ACKNOWLEDGEMENTS

We thank Roberto Bernal Muñoz (Instituto Tecnológico del Altiplano, Tlaxcala, Mexico) for donation of amaranth seeds. PFVH did the major experimental work. MMN, MRR and REVP obtained the plant tissue. PFVH and FFRC conceived the project. PFVH, SLS and FFRC designed the experiments. MDBM helped in technical matters and supplied equipment (StepOnePlus Real-Time PCR System). PFVH and FFRC drafted the manuscript. All authors read and approved the final manuscript. PFVH, MMN, MRR, REVP were supported by a

Mexican National Council of Science and Technology (CONACyT) fellowship. This work was financed by CONACyT (grant 221522) and SIP-IPN (grants 20160215 and 20170477).

REFERENCES

- Andersen C.L., Jensen J.L., Orntoft T.F. (2004) Normalization of real-time quantitative reverse transcription-PCR data: a model-based variance estimation approach to identify genes suited for normalization, applied to bladder and colon cancer data sets. *Cancer Research*, **64**, 5245–5250.
- Berger A., Gremaud G., Baumgartner M., Rein D., Monnard I., Kratky E., Geiger W., Burri J., Dionisi F., Allan M., Lambelet P. (2003) Cholesterol-lowering properties of amaranth grain and oil in hamsters. *International Journal of Vitamin Nutrition Research*, **73**, 39–47.
- Bevitori R., Oliveira M.B., Grossi-de-Sa M.F., Lanna A.C., da Silveira R.D., Petrofeza S. (2014) Selection of optimized candidate reference genes for qRT-PCR normalization in rice (*Oryza sativa* L.) during *Magnaporthe oryzae* infection and drought. *Genetics and Molecular Research*, **13**, 9795–9805.
- Chan O.Y., Keng B.M., Ling M.H. (2014) Correlation and variation-based method for identifying reference genes from large datasets. *Electronic Physician Journal*, **6**, 719–727.
- Chmelik Z., Kotolova H., Piekutowska Z., Horska K., Bartosova L., Suchy P., Kollar P. (2013) A comparison of the impact of amaranth flour and squalene on plasma cholesterol in mice with diet-induced dyslipidemia. *Berliner und Munchener Tierärztliche Wochenschrift*, **126**, 251–255.
- Clouse J.W., Adhikary D., Page J.T., Ramaraj T., Deyholos M.K., Udall J.A., Fairbanks D.J., Jellen E.N., Maughan P.J. (2016) The Amaranth genome: genome, transcriptome, and physical map assembly. *Plant Genome*, **9**, 1–14.
- De Spiegelaere W., Dern-Wieloch J., Weigel R., Schumacher V., Schorle H., Nettersheim D., Bergmann M., Brehm R., Kliesch S., Vandekerckhove L., Fink C. (2015) Reference gene validation for RT-qPCR, a note on different available software packages. *PLoS ONE*, **10**, e0122515.
- Delano-Frier J.P., Aviles-Arnaut H., Casarrubias-Castillo K., Casique-Arroyo G., Castrillon-Arbelaiz P.A., Herrera-Estrella L., Massange-Sanchez J., Martinez-Gallardo N.A., Parra-Cota F.I., Vargas-Ortiz E., Estrada-Hernandez M.G. (2011) Transcriptomic analysis of grain amaranth (*Amaranthus hypochondriacus*) using 454 pyrosequencing: comparison with *A. tuberculatus*, expression profiling in stems and in response to biotic and abiotic stress. *BMC Genomics*, **12**, 363.
- Emokaro C., Ekunwe P., Osifo A. (2007) Profitability and production constraints in dry season amaranth production in Edo South, Nigeria. *Journal of Food, Agriculture & Environment*, **5**, 281.
- Ferdous J., Li Y., Reid N., Langridge P., Shi B.J., Tricker P.J. (2015) Identification of reference genes for quantitative expression analysis of microRNAs and mRNAs in barley under various stress conditions. *PLoS ONE*, **10**, e0118503.
- Huerta-Ocampo J.A., Leon-Galvan M.F., Ortega-Cruz L.B., Barrera-Pacheco A., De Leon-Rodriguez A., Mendoza-Hernandez G., de la Rosa A.P. (2011) Water stress induces up-regulation of DOF1 and MIF1 transcription factors and down-regulation of proteins involved in secondary metabolism in amaranth roots (*Amaranthus hypochondriacus* L.). *Plant Biology*, **13**, 472–482.
- Huerta-Ocampo J.A., Barrera-Pacheco A., Mendoza-Hernandez C.S., Espitia-Rangel E., Mock H.P., Barba de la Rosa A.P. (2014) Salt stress-induced alterations in the root proteome of *Amaranthus cruentus* L. *Journal of Proteome Research*, **13**, 3607–3627.
- Ieliseieva O.P., Kamins'kyi D.V., Cherkas A.P., Ambarova L.I., Vyshemys'ka L.D., Dzhura O.R., Semen Kh O., Makhotina O.O. (2006) Characteristics of amaranth oil effect on the antioxidant system of the liver and blood in mice with malignant lymphoma growth. *Ukrainskii Biokhimičeskii Zhurnal*, **78**, 117–123.
- Janssen F., Pauly A., Rombouts I., Jansens K., Deleu L., Delcour J. (2017) Protein of Amaranth (*Amaranthus* spp.), buckwheat (*Fagopyrum* spp.), and quinoa (*Chenopodium* spp.) proteins: a food science and technology perspective. *Comprehensive reviews in Food Science and Food Safety*, **16**, 39–58.
- Lado M.B., Burini J., Rinaldi G., Anon M.C., Tironi V.A. (2015) Effects of the dietary addition of Amaranth (*Amaranthus mantegazzianus*) protein isolate on antioxidant status, lipid profiles and blood pressure of rats. *Plant Foods for Human Nutrition*, **70**, 371–379.
- Li W., Zhang L., Zhang Y., Wang G., Song D. (2017) Selection and validation of appropriate reference genes for quantitative real-time PCR normalization in staminate and perfect flowers of *Andromonoecious Taihangia rupestris*. *Frontiers in Plant Science*, **8**, 1–13.
- Lipkin A., Anisimova V., Nikonorova A., Babakov A., Krause E., Bienert M., Grishin E., Egorov T. (2005) An antimicrobial peptide Ar-AMP from amaranth (*Amaranthus retroflexus* L.) seeds. *Phytochemistry*, **66**, 2426–2431.
- Liu S., Kuang H., Lai Z. (2014) Transcriptome analysis by Illumina high-throughput paired-end sequencing reveals the complexity of differential gene expression during *in vitro* plantlet growth and flowering in *Amaranthus tricolor* L. *PLoS ONE*, **9**, e100919.
- Massange-Sanchez J.A., Palmeros-Suarez P.A., Espitia-Rangel E., Rodriguez-Arevalo I., Sanchez-Segura L., Martinez-Gallardo N.A., Alatorre-Cobos F., Tiessen A., Delano-Frier J.P. (2016) Overexpression of grain Amaranth (*Amaranthus hypochondriacus*) AhERF or AhDOF transcription factors in *Arabidopsis thaliana* increases water deficit and salt stress tolerance, respectively, via contrasting stress-amelioration mechanisms. *PLoS ONE*, **11**, e0164280.
- Mlakar S.G., Turinek M., Jakop M., Bavec M., Bavec F. (2010) Grain amaranth as an alternative and perspective crop in temperate climate. *Journal for Geography*, **5**, 135–145.
- Palmeros-Suarez P.A., Massange-Sanchez J.A., Sanchez-Segura L., Martinez-Gallardo N.A., Espitia Rangel E., Gomez-Leyva J.F., Delano-Frier J.P. (2017) AhDGR2, an amaranth abiotic stress-induced DUF642 protein gene, modifies cell wall structure and composition and causes salt and ABA hypersensitivity in transgenic *Arabidopsis*. *Planta*, **245**, 623–640.
- Pasko P., Barton H., Zagrodzki P., Gorinstein S. (2011) Effect of amaranth seeds (*Amaranthus cruentus*) in the diet on some biochemical parameters and essential trace elements in blood of high fructose-fed rats. *Natural Products Research*, **25**, 844–849.
- Pfaffl M.W., Tichopad A., Prgomet C., Neuvians T.P. (2004) Determination of stable housekeeping genes, differentially regulated target genes and sample integrity: BestKeeper–Excel-based tool using pairwise correlations. *Biotechnology Letters*, **26**, 509–515.
- Primerdesign. (2016) *geNorm primer only kit Handbook*. Primerdesign, Cambridge, UK.
- Radwan S.A.-A., Badr S., Mira M.M., Helmy R. (2014) Genetic variability and phylogenetic relationships in amaranthus using karyotype. *JBR*, **53**, 53–70.
- Ramakers C., Ruijter J.M., Deprez R.H., Moorman A.F. (2003) Assumption-free analysis of quantitative real-time polymerase chain reaction (PCR) data. *Neuroscience Letters*, **339**, 62–66.
- Riggins C.W., Peng Y., Stewart C.N. Jr, Tranel P.J. (2010) Characterization of *de novo* transcriptome for waterhemp (*Amaranthus tuberculatus*) using GS-FLX 454 pyrosequencing and its application for studies of herbicide target-site genes. *Pest Management Science*, **66**, 1042–1052.
- de la Rosa A.P., Montoya A.B., Martinez-Cuevas P., Hernandez-Ledesma B., Leon-Galvan M.F., De Leon-Rodriguez A., Gonzalez C. (2010) Tryptic amaranth glutelin digests induce endothelial nitric oxide production through inhibition of ACE: antihypertensive role of amaranth peptides. *Nitric Oxide*, **23**, 106–111.
- Russell B.L., Rathinasabapathi B., Hanson A.D. (1998) Osmotic stress induces expression of choline monoxygenase in sugar beet and amaranth. *Plant Physiology*, **116**, 859–865.
- Shin D.H., Heo H.J., Lee Y.J., Kim H.K. (2004) Amaranth squalene reduces serum and liver lipid levels in rats fed a cholesterol diet. *British Journal of Biomedical Science*, **61**, 11–14.
- Silver N., Best S., Jiang J., Thein S.L. (2006) Selection of housekeeping genes for gene expression studies in human reticulocytes using real-time PCR. *BMC Molecular Biology*, **7**, 33.
- Singh V., Kaul S.C., Wadhwa R., Pati P.K. (2015) Evaluation and selection of candidate reference genes for normalization of quantitative RT-PCR in *Withania somnifera* (L.) Dunal. *PLoS ONE*, **10**, e0118860.
- Vandesompele J., De Preter K., Pattyn F., Poppe B., Van Roy N., De Paeppe A., Speleman F. (2002) Accurate normalization of real-time quantitative RT-PCR data by geometric averaging of multiple internal control genes. *Genome Biology*, **3**, 1–12. RESEARCH0034.

CONFLICT OF INTEREST

The authors declare no conflict of interest.



Chapter 11

Detection of miRNAs by Tissue Printing and Dot Blot Hybridization

Marcelino Martínez Núñez, Stefan de Folter,
and Flor de Fátima Rosas-Cárdenas

Abstract

Tissue printing and dot blot are simple techniques to detect miRNA expression and localization, allowing a better understanding of the function of a miRNA. In this work, we describe a tissue printing and a dot blot hybridization protocol for miRNA detection and localization in plant tissues, which opens the possibility of analyzing spatiotemporal expression patterns of miRNAs.

Key words microRNAs, Tissue printing, Dot blot, Nylon membrane, Hybridization, miRNA detection

1 Introduction

There is a great interest in knowing the expression pattern of miRNAs in plants. Different methods are available, and one of them is tissue printing hybridization. The basic principle of tissue printing is that the contents of cells at the surface of a freshly cut tissue section can be transferred to an adhesive or absorptive surface by simple contact [1, 2]. The tissue printing hybridization technique is rapid and efficient, useful for determining the specific tissue-level localization of many molecules that are blotted directly from a surface of a sectioned organ onto a nylon or nitrocellulose membrane [3–9]. The main advantage of tissue printing versus other methods as Northern blot hybridization or in situ hybridization is that no RNA extraction is required for the preparation of thin tissue sections and it allows the simultaneous analysis of many samples. Another advantage is that tissue printing can be used for big tissues that are often difficult to section for in situ hybridizations [3, 10]. It has been shown that techniques to immobilize small RNA molecules of <100 nucleotides in length such as UV cross-linking limit the detection efficiency siRNAs (short-

interfering RNAs) and miRNAs [11]. Therefore, cross-linking with 1-ethyl-3-(3-dimethylaminopropyl) carbodiimide (EDC) should be used, which enhances the detection of small RNAs by up to 50-fold [10–13]. The advance in sRNA fixation to membranes using EDC gives the opportunity to improved expression detection of miRNAs [11–14]. Previously, we demonstrated that tissue printing hybridization provides a simple, rapid, and useful protocol to detect miRNAs from different tissues and organs of plant species [3, 4]. Moreover, we showed the possibility to detect the expression of miRNAs in fruit juice using a dot blot hybridization approach [3].

Here, we provide a simple, rapid, and useful protocol to detect miRNAs from different tissues and organs of plant species by tissue printing and dot blot hybridization (Fig. 1). Tissue printing hybridization allows the detection of miRNAs, maintaining information on their localization in the tissue (Figs. 2a and 3), and the dot blot hybridization method allows the detecting of miRNAs in liquid

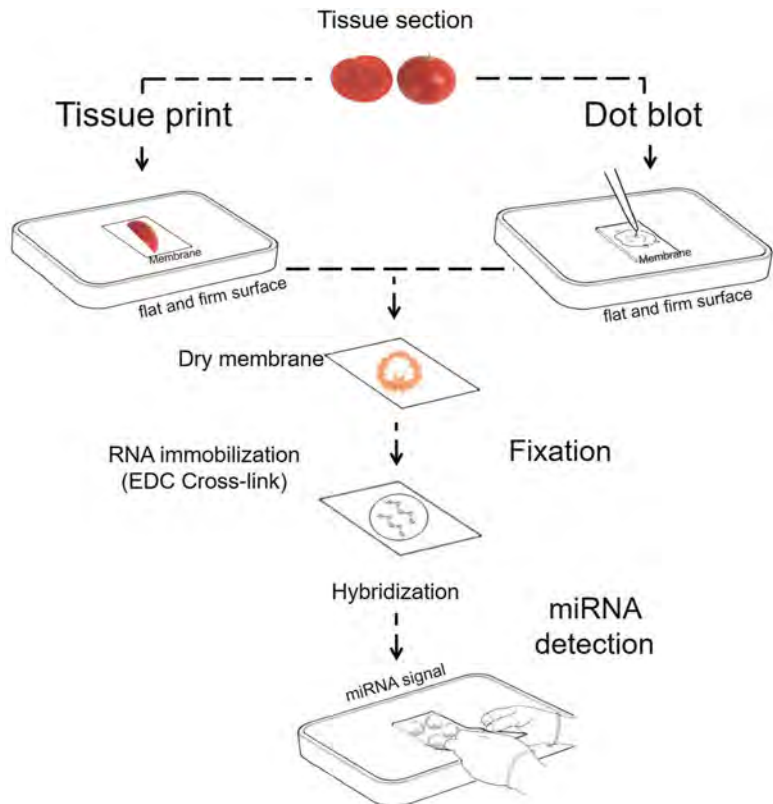


Fig. 1 Schematic representation of the tissue printing and dot blot methods. The diagram illustrates the three main steps for tissue printing and dot blot hybridization: (1) tissue printing and the dot blot step; (2) fixation of sRNAs to the membrane; and (3) the hybridization detection step

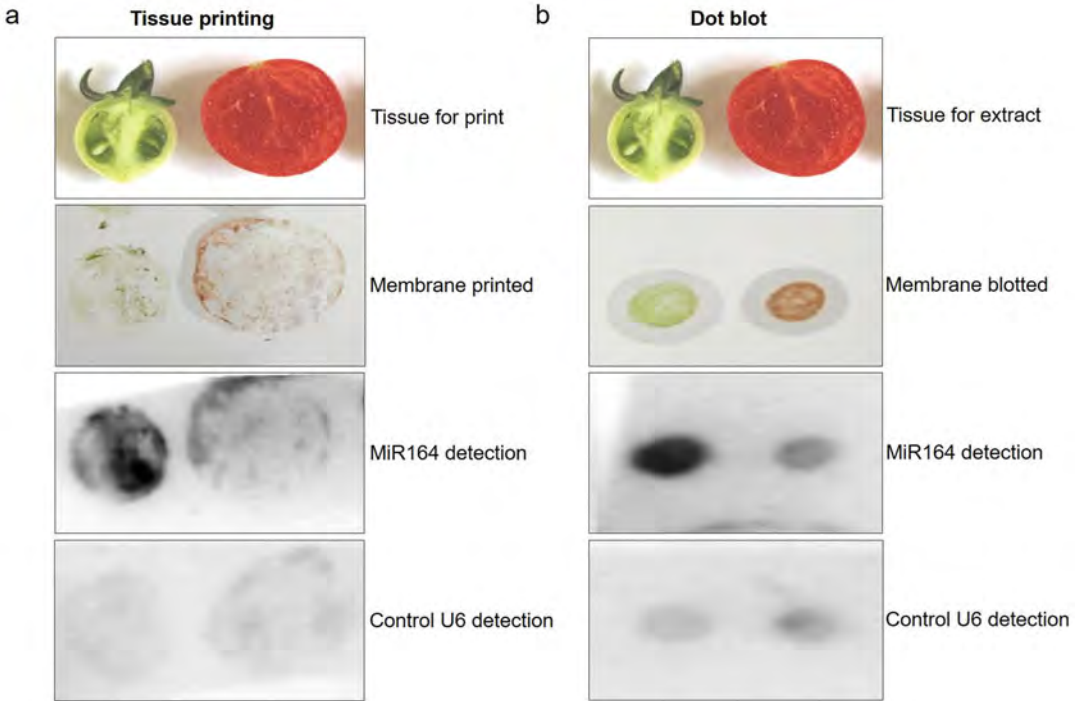


Fig. 2 miRNA detection by tissue printing and dot blot hybridization in different stages of tomato fruit. (a) Tissue printing hybridization. (b) Dot blot hybridization. The juice for the dot blot hybridization was obtained of the tissue used for tissue printing. The membranes were fixed and then hybridized with ³²P-labeled oligonucleotide probe complementary to miR164 or to the nucleolar U6 (positive control)

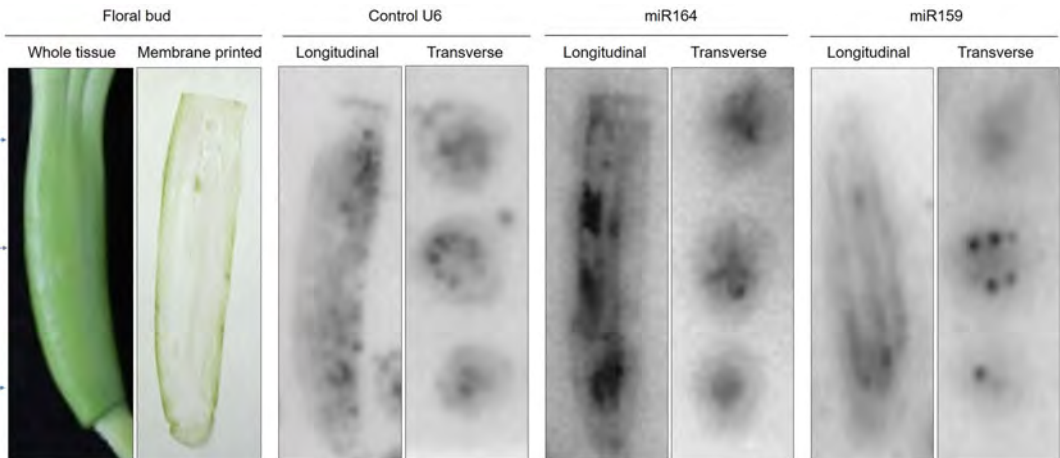


Fig. 3 Localization of different miRNAs by tissue printing hybridization. Transverse and longitudinal sections of agave floral buds were used for the tissue printing hybridization. Arrows indicate the apical, medial, and basal region where the cuts were made

from a plant tissue/organ such as fruit juice (Fig. 2b). Using tissue printing, it allows to know the spatiotemporal expression pattern of miRNAs (Figs. 2a and 3).

2 Materials

Prepare all solutions using sterile deionized water. Prepare and store all reagents at room temperature (unless indicated otherwise). Wash the plant tissue and dry at room temperature.

2.1 Tissue Print

1. Neutral nylon membrane (Amersham Hybond NX, GE Healthcare).
2. Scalpel.

2.2 Dot Blot

1. Neutral nylon membrane (Amersham Hybond NX, GE Healthcare).

2.3 Fixation of the Membrane

1. 1-Methylimidazole (Sigma–Aldrich).
2. 1-Ethyl-3-(3-dimethylaminopropyl) carbodiimide (EDC; Sigma–Aldrich).
3. EDC fixation solution (fresh): For 12.5 mL, dissolve 0.753 g of EDC in 10 mL of water, add 245 μ L of 12.5 M methylimidazole, and add 150 μ L of 1 M HCl.
4. 3MM Whatman[®] chromatography paper.
5. Aluminum foil.

2.4 Hybridization Analysis

1. Probe label: EasyTides[®] adenosine 5'-triphosphate, (γ -³²P)-6000 Ci/mmol, 10 mCi/mL (370 mBq/mL), 50 mM tricine (pH 7.6) (PerkinElmer).
2. Hybridization solution: Rapid-hyb[™] Buffer (GE Healthcare) is a hybridization buffer ready to use (*see Note 1*).
3. 20 \times SSC solution: put 175.3 g of NaCl and 88.2 g of sodium citrate in a beaker, and add 800 mL of deionized water. Dissolve and adjust the pH to 7.2. Add deionized water to reach a final volume of 1 L. Sterilize the solution by autoclaving at 121 $^{\circ}$ C for 20 min (*see Note 2*).
4. 2 \times SSC wash solution: 10 \times times dilution of 20 \times SSC solution; mix 20 mL of 20 \times SSC solution with 180 mL of deionized water.
5. U6 probe: fragment of small RNA U6 (small nucleolar RNA; oligonucleotide 5'-AGGGGCCATGCTAATCTTCTC-3') was used as a positive control.
6. miR164 probe: oligonucleotide complementary to mature miRNA (5'-TGCACGTGCCCTGCTTCTCCA-3') was used for miR164 detection.

7. miR159 probe: oligonucleotide complementary to mature miRNA (5'-TAGAGCTCCCTTCAATCCAAA-3') was used for miR159 detection.
8. Heating block.
9. Hybridization oven.
10. Transparent plastic foil.
11. Storage phosphor screen (or X-ray film).
12. Exposure cassette.
13. Storm 860 Molecular Imager system (Amersham Biosciences) (or other appropriate equipment).

3 Methods

3.1 Tissue Print

1. Cut a membrane of an appropriate size (*see Note 3*).
2. Cut the tissue in longitudinal or transverse sections.
3. Immediately following the tissue cut, place the tissue with the cut surface face down on the nylon membrane, firmly press the tissue for 30 s (*see Note 4*).
4. Carefully remove the tissue from the membrane, and dry the membrane around 5–20 min at room temperature (*see Note 5*).

3.2 Dot Blot

1. Cut a membrane of an appropriate size (*see Note 6*).
2. Obtain the juice of the tissue of interest, and pipette 10 μL on the nylon membrane, and then dry the membrane at room temperature.

3.3 Fixation of the Membrane

1. Cut three 3MM Whatman[®] chromatography paper of the same size as the membrane, place the membrane on a flat surface with the printed side up, and collocate three 3MM Whatman[®] chromatography papers on top of the membrane, and collocate in a box.
2. Add the EDC fixation solution slowly until the 3MM Whatman[®] chromatography papers are completely covered, and incubate the membrane with the fixation solution for 1 h at 65 °C.
3. Rinse the membrane twice with water, and dry the membranes at room temperature, and afterwards store the membrane(s) in aluminum foil at –20 °C until further use (*see Note 7*).

3.4 Hybridization Analysis

1. Prepare the probe: take 4 μL of 100 μM oligonucleotide and radioactive label by adding 1 μL of T4 Kinase (10 U/ μL), 1 μL [γ -32P] ATP (10 mCi/mL), 4 μL of forward buffer, and 10 μL of water. Incubate the reaction mix at 37 °C for 1 h (*see Note 8*).

2. Pre-hybridize the membrane with 15 mL hybridization solution for 1 h at 42 °C with constant agitation (*see Note 9*).
3. Add the 20 µL labeled probe of interest to the membrane(s), and incubate for 3–24 h at 42 °C with constant agitation (*see Note 10*).
4. Discard the hybridization solution, and wash the membrane with wash solution for 4 min at room temperature.
5. Discard the wash solution, and wash the membrane again for 2 min at room temperature.
6. Put the membrane(s) on a flat surface with absorbent paper to remove the excess of wash solution.
7. Pack/seal the membrane(s) with transparent plastic foil.
8. Place the membrane(s) in an exposure cassette, and place a storage phosphor screen, and close the exposure cassette.
9. Expose the membrane(s) to the storage phosphor screen for ~48 h at room temperature (*see Note 11*).
10. Scan the storage phosphor screen with a Storm 860 scanner, and analyze the signal.

4 Notes

1. Rapid-hyb™ Buffer is a hybridization buffer ready to use, but other hybridization buffers may be used as well.
2. If precipitation is present in the 20× SSC solution, warm the bottle to 37 °C, and mix until completely dissolved prior to dilution.
3. Use gloves for all the manipulations to avoid finger prints on the membrane. Mark the membrane with a graphite pencil to indicate the sample identity/order. Never mark with a pen, because after washes the membrane is stained with this.
4. For tissue with high water content, the tissue can be pressed for 10 s, but for tissues with low water content the tissue can be firmly pressed for 1 min.
5. To avoid double images, be careful when blotting and removing the tissue section from the membrane. The same tissue surface can be reprinted several times; however, we recommended only two prints per tissue section.
6. Dry around 5–20 min at room temperature.
7. Membrane(s) can be stored up to at least 1 year at –20 °C.
8. For the handling of the radioactive probe, follow the manufacturer's safety guide (http://www.perkinelmer.com/lab-solutions/resources/docs/TCH_Phosphorus32.pdf).

9. Rapid-hyb™ Buffer (GE Healthcare) is optimized for use in a wide range of hybridization temperatures (42–70 °C).
10. Hybridization time depends on the expression level of each sRNA or miRNA.
11. We use a Storm 860 Molecular Imager system. However, another system may be used.

Acknowledgments

We thank the Mexican National Council of Science and Technology (CONACyT) for a fellowship to MMN. This work was financed by the CONACyT grant CB-2013-221522, and SIP grants 20170477 and 20180545. Work in the SDF laboratory was financed by the CONACyT grants CB-2012-177739 and FC-2015-2/1061.

References

1. Varner JE, Ye Z (1994) Tissue printing. *FASEB J* 8:378–384
2. Pont-Lezica RF (2015) Localizing proteins by tissue printing. *Methods Mol Biol* 1312:93–104
3. Rosas-Cardenas Fde F, Escobar-Guzman R, Cruz-Hernandez A, Marsch-Martinez N, de Folter S (2015) An efficient method for miRNA detection and localization in crop plants. *Front Plant Sci* 6:99
4. Rosas-Cardenas Fde F, Caballero-Perez J, Gutierrez-Ramos X, Marsch-Martinez N, Cruz-Hernandez A, de Folter S (2015) miRNA expression during prickly pear cactus fruit development. *Planta* 241:435–448
5. Pallás V, Sánchez-Navarro JA, Kinard GR, Di Serio F (2017) Chapter 35 - molecular hybridization techniques for detecting and studying viroids A2 - Hadidi, Ahmed. In: Flores R, Randles JW, Palukaitis P (eds) *Viroids and satelites*. Academic Press, Boston, pp 369–379
6. Simon A, Ruiz L, Velasco L, Janssen D (2018) Absolute quantification of tomato leaf curl new delhi virus spain strain, ToLCNDV-ES: virus accumulation in a host-specific manner. *Plant Dis* 102:165–171
7. Liu YH, Offler CE, Ruan YL (2014) A simple, rapid, and reliable protocol to localize hydrogen peroxide in large plant organs by DAB-mediated tissue printing. *Front Plant Sci* 5:745
8. Pluskota W, Bradford K, Nonogaki H (2011) Tissue-printing methods for localization of RNA and proteins that control seed dormancy and germination. *Methods Mol Biol* 773:329–339
9. Esteves F, Teixeira Santos M, Eiras-Dias JE, Fonseca F (2013) Molecular data mining to improve antibody-based detection of grapevine leafroll-associated virus 1 (GLRaV-1). *J Virol Methods* 194:258–270
10. Damm K, Bach S, Müller KM, Klug G, Burenina OY, Kubareva EA, Grünweller A, Hartmann RK (2015) Improved Northern blot detection of small RNAs using EDC crosslinking and DNA/LNA probes. *Methods Mol Biol* 1296:41–51
11. Pall GS, Hamilton AJ (2008) Improved northern blot method for enhanced detection of small RNA. *Nat Protoc* 3:1077–1084
12. Zhang X, Dong H, Tian Y (2015) Conventional miRNA detection strategies. In: *MicroRNA detection and pathological functions*. Springer, Berlin, pp 23–35
13. Beckmann BM, Grünweller A, Weber MHW, Hartmann RK (2010) Northern blot detection of endogenous small RNAs (~14 nt) in bacterial total RNA extracts. *Nucleic Acids Res* 38:e147
14. Kim SW, Li Z, Moore PS, Monaghan AP, Chang Y, Nichols M, John B (2010) A sensitive non-radioactive northern blot method to detect small RNAs. *Nucleic Acids Res* 38:e98



SOLICITUD DE TÍTULO DE OBTENTOR

INSTRUCCIONES: USE LETRA DE MOLDE. NO VÁLIDO SI PRESENTA TACHADURAS O ENMENDADURAS. ESPACIO SOMBREADO RESERVADO PARA OFICINA DE REGISTRO. EN CASO NECESARIO, UTILIZAR HOJAS ADICIONALES PARA INFORMACIÓN COMPLETA. NO DEJAR ESPACIOS EN BLANCO. EN SU CASO, ESCRIBIR "NO APLICA" (EXCEPTO EN CONCEPTOS SEÑALADOS CON *). PRESENTAR ORIGINAL Y COPIA DE TODA LA DOCUMENTACIÓN.

Recepción de la documentación
FECHA: 01 de Junio de 2018
HORA:

Número de referencia

I. DATOS DEL SOLICITANTE

1. * Nombre o Razón social del obtentor (en caso de ser más de uno, indicar participación que le corresponda en el aprovechamiento y explotación de la variedad)

Instituto Politécnico Nacional

2. * Nacionalidad

Mexicana

3. * Domicilio en territorio nacional para oír y recibir notificaciones

Calle Miguel Othón de Mendizabal

Número S/N

Colonia La Escalera

Ciudad Ciudad de México

Estado Ciudad de México

Código Postal 07320

4. Teléfono / Fax

57296000, Ext. 51975

5. Nombre del representante legal (en su caso)

Lic. Claudia Alejandra Blanco Salazar

6. * Nombre (s) del fitomejorador. En caso de ser más de uno, indicar participación que le corresponda en el aprovechamiento y explotación de la variedad.

Nombre

Participación (%)

Marcelino Martínez Núñez

50 %

Flor de Fátima Rosas Cárdenas

50 %

7. Nombre de beneficiario (s) designados por el solicitante. En caso de ser más de uno, indicar participación.

Nombre

Participación (%)

Instituto Politécnico Nacional

II. DATOS DE LA VARIEDAD

8. * Género y especie		8.1 Nombre común		
<i>Amaranthus cruentus</i>		Amaranto o alegría		
9. * Denominación propuesta de la variedad				
Magali				
10. * Se ha comercializado en México o en el extranjero				
SÍ ()		NO (x)		
En caso afirmativo:				
En México ()		En el extranjero ()		
Desde (fecha):		Desde (fecha):		
		País:		
		Denominación:		
11. * Reivindicación derecho de prioridad				
SÍ ()		NO (x)		
• En caso afirmativo:				
País (es):				
Fecha de presentación en el otro país:				
ANEXAR SOLICITUD O TÍTULO, Y COMPROBANTE DE PAGO DE DERECHOS				
12. * Tipo de variedad		12.1 Nivel de endogamia		
a)	Línea	(x) L	S ₀ () 0	
b)	Híbrido de cruce simple (A x B)	() S	S ₁ () 1	
c)	Híbrido tres líneas (A x B) x D	() T	S ₂ () 2	
d)	Híbrido doble (A x B) x (C x D)	() D	S ₃ (x) 3	
e)	Híbrido intervarietal	() HV	S ₄ () 4	
f)	Variedad de polinización libre	() VL	S ₅ () 5	
g)	Variedad sintética	() VS	S ₆ () 6	
h)	Variedad multilineal	() VM	S ₇ () 7	
i)	Mestizo	() M	S ₈ () 8	
j)	Clon	() C	S ₉ () 9	
k)	Otra (indicar fórmula)_____	() O	>S ₉ () 10	
13. * Progenitores (conforme el esquema de fórmulas indicado en el apartado anterior).				
	PARENTAL A	PARENTAL B	PARENTAL C	PARENTAL D
a) Denominación	<i>Amaranthus cruentus.</i>			
b) Genealogía				
c) Obtentor	Cesar A. Reyes L.			
d) Línea registrada	SÍ () NO (x)	SÍ () NO ()	SÍ () NO ()	SÍ () NO ()
e) Forma parte de variedad ya registrada	SÍ () NO (x)	SÍ () NO ()	SÍ () NO ()	SÍ () NO ()
En caso afirmativo indique denominación de variedad				

18.* Indicar si se trata de material transgénico (conforme definición Ley Federal de Sanidad Vegetal)

SÍ () NO (x)
En caso afirmativo, ¿cuenta con certificado fitosanitario correspondiente?

SÍ () NO ()
ANEXAR CERTIFICADO O PERMISO FITOSANITARIO

19. Otros datos relevantes

III. DOCUMENTACIÓN COMPLEMENTARIA

- a) Comprobante del pago de derechos ()
- b) Personalidad del representante (instrumento legal) ()
- c) Informe técnico (descripción varietal) ()
- d) Material de propagación ()
- e) Derecho de prioridad (solicitud o título) ()
- f) Certificado fitosanitario ()
- g) Pagos adicionales ()
Especificar
- h) Otros ()
Especificar

Recibe:

Cargo:

Rúbrica:

Para la revisión de la solicitud invariablemente deberá presentar anexo el informe técnico y el comprobante de pago correspondiente.

DECLARO, BAJO PROTESTA DE DECIR VERDAD, QUE LOS DATOS QUE SE PROPORCIONAN SON CORRECTOS Y CORRESPONDEN A LA VARIEDAD QUE SE INDICA, Y ME COMPROMETO A FACILITAR, A PETICIÓN DE LA SECRETARÍA, LA INFORMACIÓN, MATERIAL VEGETAL O LAS VERIFICACIONES QUE SEAN REQUERIDAS POR LA MISMA.

México, D.F. a 01 de Junio de 2018.

Firma M. C. Marcelino Martínez Núñez

C. Lic. Claudia Alejandra Blanco Salazar
NOMBRE DEL SOLICITANTE O REPRESENTANTE LEGAL

INFORMES
Servicio Nacional de Inspección y Certificación de Semillas (SNICS)

Av. Presidente Juárez Núm. 13
54000 Tlalnepantla, Estado de México
Tels: +52 (55) 3622 0667; 3622-0668; 3622-0669; 3622-0670
Web site: <http://snics.sagarpa.gob.mx>



*Descripción intervarietal de
Amaranthus cruentus
variedad Magali*


M. en C. Marcelino Martínez Núñez
mmartinezn1202@alumno.ipn.mx

Descripción de *Amaranthus cruentus* variedad CIBA


Carácter 1: Especie:

Amaranthus cruentus


Carácter 2. Cotiledones: Coloración antociánica.

	Pigmentación antociánica	Calificación
	1) Ausente	
	2) Presente	X
Figura 2. Pigmentación antociánica		

Carácter 3. Plántula: Coloración antociánica del hipocótilo.

	Pigmentación antociánica del hipocótilo	Calificación
	1) presente	X
	2) Ausente	
Figura 3. coloración antociánica del hipocótilo		

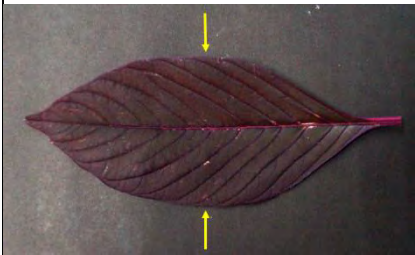
Carácter 4. Plántula: Intensidad de la coloración antociánica del hipocótilo.

	Intensidad de la pigmentación antociánica del hipocótilo	Calificación
	1) Débil	
	2) Media	X
Figura 4. Intensidad de la pigmentación antociánica del hipocótilo	3) Fuerte	


Carácter 5. Hoja joven: Longitud

	Longitud	Valor (cm)	Calificación
	1) Corta	< 7.5	
	2) Mediana	7.5-10.5	
Figura 5. Longitud de hoja joven	3) Larga	> 10.5	X


Carácter 6. Hoja joven: Ancho

	Anchura	Valor (cm)	Calificación
	1) Estrecha	< 5	
	2) Media	5-6	
Figura 6. Anchura de la hoja	3) Ancha	>6	X


Carácter 7. Hoja joven: Proporción largo/ancho

	Proporción largo/ancho	Valor (cm)	Calificación
	1) Chica	> 1.6	
	2) Media	1.6-1.8	
Figura 7. Proporción largo/ancho de la hoja	3) Grande	> 1.8	X


Carácter 8. Hoja joven: Posición del lado más ancho de la hoja

	Posición de la parte más ancha	Calificación
	1) En medio o ligeramente hacia la base	X
	2) Moderadamente hacia la base	
Figura 8. Posición de la parte más ancha de la hoja	3) Fuertemente hacia la base	


Carácter 9. Hoja joven: Prominencia de las nervaduras

	Prominencia de nervaduras	Calificación
	1) Débil	
	2) Media	
Figura 9. Prominencia de nervaduras	3) Fuerte	X


Carácter 10. Hoja joven: Color principal del haz

	Color principal del haz	Calificación
	1) Verde claro	
	2) Verde medio	
	3) Verde oscuro	
	4) Rojo	
Figura 10. Color principal del haz	5) Púrpura	X


Carácter 11. Hoja joven: Distribución de la coloración en el haz al inicio del crecimiento

	Distribución del segundo color en el haz	Calificación
	1) Área basal pigmentada	
	2) Mancha central	
	3) Una franja en forma de "V"	
	4) Dos franjas en forma de "V"	
	5) Margen y venas pigmentadas	X
Figura 11. Distribución del segundo color en el haz	6) En franja	


Carácter 12. Hoja joven: Color en el envés

	Color en el envés	Calificación
	1) Verde	
	2) Rojo	
Figura 12. Color del envés	3) Púrpura	X

Carácter 13. Hoja: Tipo de Margen

	Margen	Calificación
	1) Entero	X
	2) Ondulado	
Figura 13. Margen de la hoja		


Carácter 14. Planta: Ciclo al inicio de emergencia de la inflorescencia

	Época de aparición de inflorescencia	Valor (días)	Calificación
	1) Precoz	< 59	X
	2) Media	59-75	
Figura 14. Aparición de inflorescencia	3) Tardía	>75	


Carácter 15. Inflorescencia: Ciclo a floración

	Época floración	Valor (días)	Calificación
	1) Precoz	60-70	
	2) Media	70-80	X
Figura 15. Época floración	3) Tardía	>80	


Carácter 16. Tallo: Color

	Color	Calificación
	1) Verde	
	2) Amarillo	
	3) Rosa	
	4) Rojo	
	5) Purpura	X
Figura 16. Color del tallo		


Carácter 17. Tallo: Color de las estrías

	Color de las rayas	Calificación
	1) Rojo	
	2) Purpura	X
Figura 17: Color de las estrías		

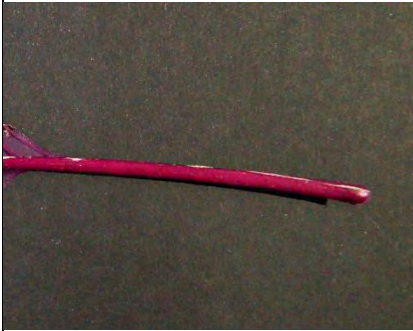
Carácter 18. Lámina de la hoja: color principal

	Color principal de la hoja	Calificación
	1) Verde claro	
	2) Verde medio	
	3) Verde oscuro	
Figura 18: Color principal de la hoja	4) Rojo/Purpura	X

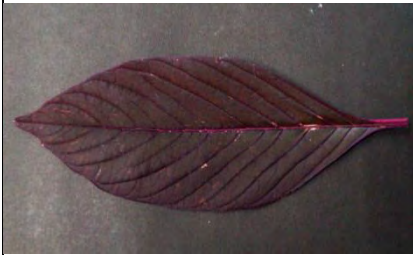
Carácter 19. Pecíolo: Coloración antociánica

	Pigmentación antociánica	Calificación
	1) Ausente	
	2) Presente	X
Figura 19. Pigmentación antociánica del pecíolo		

Carácter 20. Pecíolo: Intensidad de la coloración antociánica

	Intensidad de la pigmentación antociánica	Calificación
	1) Muy débil	
	2) Débil	
	3) Media	
	4) Fuerte	
Figura 20. Intensidad de la pigmentación antociánica del pecíolo	5) Muy fuerte	X

Carácter 21. Lamina de la hoja: presencia de mancha


	Presencia de mancha	Calificación
	1) Ausente	X
	2) Presente	
Figura 21. Presencia de mancha		

Carácter 22. Lamina de la hoja: Tamaño de la mancha con relación al limbo (Omitido)


Carácter 23. Lamina de la hoja: Color de la mancha (Omitido)

Carácter 24. Lamina de la hoja: Forma de la mancha (Omitido)

Carácter 25. Inflorescencia: Color

	Color	Calificación
	1) Amarillo	
	2) Verde	
	3) Rosa	
	4) Rojo	
	5) Púrpura	X
	6) Pardo	
Figura 25. Color de la floración		


Carácter 26. Inflorescencia: Densidad de los glomérulos

	Densidad de los glomérulos	Calificación
	1) Laxa	X
	2) Media	
Figura 26: Floración: Densidad de los glomérulos	3) Densa	


Carácter 27. Inflorescencia: Compactación

	Compactación	Calificación
	1) Compacta	
	2) Intermedia	
Figura 27: Compactación de la inflorescencia	3) Abierta	X


Carácter 28. Inflorescencia: Tipo

	Tipo de inflorescencia	Calificación
	1) Amarantiforme	X
	2) Glomerulada	
Figura 28: Tipo de inflorescencia		


Carácter 29. Inflorescencia: Número de flores femeninas por glomérulo

	Número de flores femeninas por glomérulo	Valor	Calificación
	1) Pocas	< 100	X
	2) Medias	100-150	
Figura 29: Flores femeninas por glomérulo	3) Muchas	> 150	


Carácter 30. Inflorescencia: Tamaño de las brácteas con relación al urtículo

	Longitud de las brácteas con relación al urtículo	Calificación
	1) Más pequeñas	
	2) Igual	X
Figura 30: Longitud de las brácteas con relación al urtículo	3) Mas grandes	


Carácter 31. Inflorescencia: Hábito de crecimiento

	Hábito de crecimiento	Calificación
	1) Determinado	
	2) Indeterminado	X
Figura 31: Hábito de crecimiento		

Carácter 32. Inflorescencia: Postura

	Postura	Grados	Calificación
	1) Erecta o débilmente recurvado	0°-10°	
	2) Moderadamente recurvada	65°-110°	X
Figura 32: Postura de la inflorescencia	3) Fuertemente recurvada	165°-180°	


Carácter 33. Inflorescencia: Longitud

	Longitud	Valor (m)	Calificación
	1) Corta	< 0.6 m	
	2) Media	0.6-1.0 m	X
Figura 33. Longitud de la inflorescencia	3) Larga	> 1.0 m	


Carácter 34. Planta: Ciclo a madurez

	Ciclo a madurez	Días	Calificación
	1) Precoz	< 120	
	2) Intermedio	120-140	X
Figura 34: Ciclo a madurez	3) Tardío	> 140	

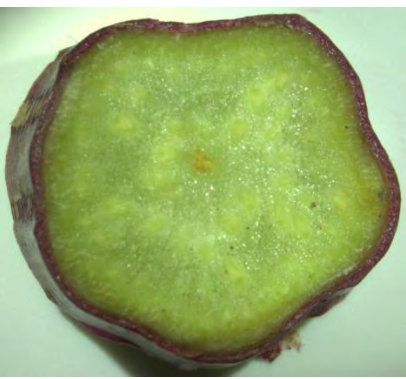
Carácter 35. Planta: altura

	Longitud	Valor (m)	Calificación
	1) Baja	< 1.5	
	2) Media	1.5-2.5	X
Figura 35: Altura de la planta	3) Alta	> 2.5	


Carácter 36. Tallo: Coloración antociánica de la base

	Coloración antociánica de la base	Calificación
	1) Ausente	
	2) Presente	X
Figura 36: Coloración antociánica de la base		


Carácter 37. Tallo: Forma de la sección transversal

	Forma de la sección transversal	Calificación
	1) Circular	
	2) Ondulado	X
Figura 37: Forma de la sección transversal del tallo		

Carácter 38. Semilla: Color

	Color	Calificación
	1) Blanco	X
	2) Amarillo	
	3) Rosa	
	4) Café	
Figura 38: Color de la semilla	5) Negro	

Carácter 39. Semilla: Forma

	Forma	Calificación
	1) Elipsoidal	
	2) Discoide	X
Figura 39. Forma de la semilla		

Carácter 40. Semilla: Tipo

	Tipo	Calificación
	1) Cristalino	
	2) Harinoso	X
Figura 40. Tipo de semilla		

Carácter 41. Semilla: Peso de 1000 semillas

	Peso de 1000 semillas	Peso (gramos)	Calificación
	1) Bajo	< 0.6	
	2) Medio	0.6-1.0	X
Figura 41. Peso de 1000 semillas	3) Alto	> 1.0	

Bibliografía

- Adai, A., C. Johnson, S. Mlotshwa, S. Archer-Evans, V. Manocha, V. Vance and V. Sundaresan (2005). "Computational prediction of miRNAs in *Arabidopsis thaliana*." Genome research **15**(1): 78-91.
- Addo-Quaye, C., W. Miller and M. J. Axtell (2008). "CleaveLand: a pipeline for using degradome data to find cleaved small RNA targets." Bioinformatics **25**(1): 130-131.
- Ahmad, S., R. Ahmad, M. Y. Ashraf, M. Ashraf and E. A. Waraich (2009). "Sunflower (*Helianthus annuus* L.) response to drought stress at germination and seedling growth stages." Pak. J. Bot **41**(2): 647-654.
- Almeida, M. I., R. M. Reis and G. A. Calin (2011). "MicroRNA history: discovery, recent applications, and next frontiers." Mutation Research/Fundamental and Molecular Mechanisms of Mutagenesis **717**(1): 1-8.
- Anjum, S. A., X.-y. Xie, L.-c. Wang, M. F. Saleem, C. Man and W. Lei (2011). "Morphological, physiological and biochemical responses of plants to drought stress." African journal of agricultural research **6**(9): 2026-2032.
- Archak, S. and J. Nagaraju (2007). "Computational prediction of rice (*Oryza sativa*) miRNA targets." Genomics, proteomics & bioinformatics **5**(3-4): 196-206.
- Archontoulis, S. V., P. C. Struik, J. Vos and N. G. Danalatos (2010). "Phenological growth stages of *Cynara cardunculus*: codification and description according to the BBCH scale." Annals of Applied Biology **156**(2): 253-270.
- Arenas-Huertero, C., B. Pérez, F. Rabanal, D. Blanco-Melo, C. De la Rosa, G. Estrada-Navarrete, F. Sanchez, A. A. Covarrubias and J. L. Reyes (2009). "Conserved and novel miRNAs in the legume *Phaseolus vulgaris* in response to stress." Plant molecular biology **70**(4): 385-401.
- Atkinson, N. J. and P. E. Urwin (2012). "The interaction of plant biotic and abiotic stresses: from genes to the field." J Exp Bot **63**(10): 3523-3543.
- Axtell, M. J. (2013). "ShortStack: comprehensive annotation and quantification of small RNA genes." RNA **19**(6): 740-751.
- Axtell, M. J. and B. C. Meyers (2018). "Revisiting criteria for plant miRNA annotation in the era of big data." Plant Cell.
- Barrera-Figueroa, B. E., L. Gao, N. N. Diop, Z. Wu, J. D. Ehlers, P. A. Roberts, T. J. Close, J. K. Zhu and R. Liu (2011). "Identification and comparative analysis of drought-associated microRNAs in two cowpea genotypes." BMC Plant Biol **11**: 127.
- Bartel, D. P. (2004). "MicroRNAs: genomics, biogenesis, mechanism, and function." cell **116**(2): 281-297.
- Bashir, K., A. Matsui, S. Rasheed and M. Seki (2019). "Recent advances in the characterization of plant transcriptomes in response to drought, salinity, heat, and cold stress." F1000Res **8**.
- Bayón, N. D. (2015). "Revisión Taxonómica de las Especies Monoicas de *Amaranthus* (*Amaranthaceae*): *Amaranthus* subg. *Amaranthus* y *Amaranthus* subg. *Albersia*." Annals of the Missouri Botanical Garden **101**(2): 261-383, 123.
- Bhat, S. S., D. Bielewicz, N. Grzelak, T. Gulanicz, Z. Bodi, L. Szewc, M. Bajczyk, J. Dolata, D. J. Smolinski, R. G. Fray, A. Jarmolowski and Z. Szweykowska-Kulinska (2019). "mRNA adenosine methylase (MTA) deposits m⁶A on pri-miRNAs to modulate miRNA biogenesis in *Arabidopsis thaliana*." bioRxiv: 557900.
- Blackwell, J. B., W. Meyer and R. C. G. Smith (1985). "Growth and yield of rice under sprinkler irrigation on a free-draining soil." Australian Journal of Experimental Agriculture - AUST J EXP AGR **25**.
- Bohnsack, M. T., K. Czaplinski and D. GÖRlich (2004). "Exportin 5 is a RanGTP-dependent dsRNA-binding protein that mediates nuclear export of pre-miRNAs." RNA **10**(2): 185-191.

Boonjung, H. and S. Fukai (1996). "Effects of soil water deficit at different growth stages on rice growth and yield under upland conditions. 2. Phenology, biomass production and yield." Field Crops Research **48**(1): 47-55.

Boutraa, T., A. Akhka, A. A. Al-Shoaibi and A. M. Alhejeli (2010). "Effect of water stress on growth and water use efficiency (WUE) of some wheat cultivars (*Triticum durum*) grown in Saudi Arabia." Journal of Taibah University for Science **3**: 39-48.

Brant, E. J. and H. Budak (2018). "Plant Small Non-coding RNAs and Their Roles in Biotic Stresses." Frontiers in Plant Science **9**.

Budak, H. and B. A. Akpinar (2015). "Plant miRNAs: biogenesis, organization and origins." Funct Integr Genomics **15**(5): 523-531.

Çakir, R. (2004). "Effect of water stress at different development stages on vegetative and reproductive growth of corn." Field Crops Research **89**(1): 1-16.

Carrington, J. C. and V. Ambros (2003). "Role of microRNAs in plant and animal development." Science **301**(5631): 336-338.

Caselato-Sousa, V. M. and J. Amaya-Farfan (2012). "State of Knowledge on Amaranth Grain: A Comprehensive Review." Journal of Food Science **77**(4): R93-R104.

Castrillón-Arbeláez, P. A. and J. P. D. Frier (2016). Secondary Metabolism in *Amaranthus* spp.—A Genomic Approach to Understand Its Diversity and Responsiveness to Stress in Marginally Studied Crops with High Agronomic Potential. Abiotic and Biotic Stress in Plants-Recent Advances and Future Perspectives, InTech.

Ceccarelli, S. and S. Grandi (1996). "Drought as a challenge for the plant breeder." Plant Growth Regulation **20**(2): 149-155.

Chai, J., R. Feng, H. Shi, M. Ren, Y. Zhang and J. Wang (2015). "Bioinformatic identification and expression analysis of banana microRNAs and their targets." PLoS One **10**(4): e0123083.

Chakraborty, S., N. Chakraborty and A. Datta (2000). "Increased nutritive value of transgenic potato by expressing a nonallergenic seed albumin gene from *Amaranthus hypochondriacus*." Proc Natl Acad Sci U S A **97**(7): 3724-3729.

Chatterjee, A. and S. Solankey (2015). "Functional physiology in drought tolerance of vegetable crops: an approach to mitigate climate change impact." Climate Dynamics in Horticultural Science **1**: 149-171.

Chavarria, G. and H. P. dos Santos (2012). Plant water relations: absorption, transport and control mechanisms, INTECH Open Access Publisher.

Chavez Montes, R. A., F. de Fatima Rosas-Cardenas, E. De Paoli, M. Accerbi, L. A. Rymarquis, G. Mahalingam, N. Marsch-Martinez, B. C. Meyers, P. J. Green and S. de Folter (2014). "Sample sequencing of vascular plants demonstrates widespread conservation and divergence of microRNAs." Nat Commun **5**: 3722.

Chen, X. (2005). "MicroRNA biogenesis and function in plants." FEBS Lett **579**(26): 5923-5931.

Close, T. J. (1996). "Dehydrins: Emergence of a biochemical role of a family of plant dehydration proteins." Physiologia Plantarum **97**(4): 795-803.

Clouse, J. W., D. Adhikary, J. T. Page, T. Ramaraj, M. K. Deyholos, J. A. Udall, D. J. Fairbanks, E. N. Jellen and P. J. Maughan (2016). "The Amaranth Genome: Genome, Transcriptome, and Physical Map Assembly." The Plant Genome **9**(1).

Cohen, I., T. Rapaport, V. Chalifa-Caspi and S. Rachmilevitch (2019). "Synergistic effects of abiotic stresses in plants: a case study of nitrogen limitation and saturating light intensity in *Arabidopsis thaliana*." Physiol Plant **165**(4): 755-767.

Colaiacovo, M., A. Subacchi, P. Bagnaresi, A. Lamontanara, L. Cattivelli and P. Faccioli (2010). "A computational-based update on microRNAs and their targets in barley (*Hordeum vulgare* L.)." BMC genomics **11**(1): 595.

- Cornejo, F., G. Novillo, E. Villacrés and C. M. Rosell (2019). "Evaluation of the physicochemical and nutritional changes in two amaranth species (*Amaranthus quitensis* and *Amaranthus caudatus*) after germination." Food Research International.
- Costea, M., A. Sanders and G. Waines (2001). "PRELIMINARY RESULTS TOWARD A REVISION OF THE AMARANTHUS HYBRIDUS SPECIES COMPLEX (AMARANTHACEAE)." SIDA, Contributions to Botany **19**(4): 931-974.
- Dai, X., Z. Zhuang and P. X. Zhao (2018). "psRNATarget: a plant small RNA target analysis server (2017 release)." Nucleic Acids Res **46**(W1): W49-W54.
- Dard-Dascot, C., D. Naquin, Y. d'Aubenton-Carafa, K. Alix, C. Thermes and E. van Dijk (2018). "Systematic comparison of small RNA library preparation protocols for next-generation sequencing." BMC Genomics **19**(1): 118.
- Das, S. (2016). Amaranthus: A Promising Crop of Future, Springer Singapore.
- de Rzedowski, G. C. and J. Rzedowski (2001). Flora fanerogámica del Valle de México, Inst. de Ecología.
- Du, J., Y. Wu, X. Fang, J. Cao, L. Zhao and S. Tao (2010). "Prediction of sorghum miRNAs and their targets with computational methods." Chinese Science Bulletin **55**(13): 1263-1270.
- Espitia-Rangel, E. (2018). Breeding of grain amaranth. Amaranth Biology, Chemistry, and Technology: 23-38.
- Evers, M., M. Huttner, A. Dueck, G. Meister and J. C. Engelmann (2015). "miRA: adaptable novel miRNA identification in plants using small RNA sequencing data." BMC Bioinformatics **16**: 370.
- Fahad, S., K. Hakeem and H. Alharby (2019). Drought Tolerance in Plants: Role of Phytohormones and Scavenging System of ROS: 103-113.
- Farooq, M., M. Hussain, A. Wahid and K. Siddique (2012). Drought stress in plants: an overview. Plant responses to drought stress, Springer: 1-33.
- Ferdous, J., S. S. Hussain and B. J. Shi (2015). "Role of microRNAs in plant drought tolerance." Plant Biotechnol J **13**(3): 293-305.
- Ferdous, J., J. C. Sanchez-Ferrero, P. Langridge, L. Milne, J. Chowdhury, C. Brien and P. J. Tricker (2017). "Differential expression of microRNAs and potential targets under drought stress in barley." Plant Cell Environ **40**(1): 11-24.
- Ferreira, T. H., A. Gentile, R. D. Vilela, G. G. Costa, L. I. Dias, L. Endres and M. Menossi (2012). "microRNAs associated with drought response in the bioenergy crop sugarcane (*Saccharum* spp.)." PLoS ONE **7**(10): e46703.
- Frazier, T. P., G. Sun, C. E. Burklew and B. Zhang (2011). "Salt and drought stresses induce the aberrant expression of microRNA genes in tobacco." Mol Biotechnol **49**(2): 159-165.
- Gamez, A. L., D. Soba, A. M. Zamarreno, J. M. Garcia-Mina, I. Aranjuelo and F. Morales (2019). "Effect of Water Stress during Grain Filling on Yield, Quality and Physiological Traits of Illpa and Rainbow Quinoa (*Chenopodium quinoa* Willd.) Cultivars." Plants (Basel) **8**(6).
- Gascioli, V., A. C. Mallory, D. P. Bartel and H. Vaucheret (2005). "Partially redundant functions of Arabidopsis DICER-like enzymes and a role for DCL4 in producing trans-acting siRNAs." Current Biology **15**(16): 1494-1500.
- Hack, H., H. Bleiholder, L. Buhr, U. Meier, U. Schnock-Fricke, E. Weber and A. Witzemberger (1992). "Einheitliche codierung der phänologischen entwicklungsstadien mono-und dikotylar pflanzen—erweiterte BBCH-Skala, Allgemein." Nachrichtenblatt des deutschen Pflanzenschutzdienstes **44**(12): 265-270.
- Hackenberg, M., P. Gustafson, P. Langridge and B. J. Shi (2015). "Differential expression of microRNAs and other small RNAs in barley between water and drought conditions." Plant Biotechnol J **13**(1): 2-13.
- Hackenberg, M., N. Rodriguez-Ezpeleta and A. Aransay (2011). "MiRanalyzer: An update on the detection and analysis of microRNAs in high-throughput sequencing experiments." Nucleic acids research **39**: W132-138.

Harris, D., R. Tripathi and A. Joshi (2002). "On-farm seed priming to improve crop establishment and yield in dry direct-seeded rice." Direct seeding: Research Strategies and Opportunities, International Research Institute, Manila, Philippines: 231-240.

Henderson, I. R., X. Zhang, C. Lu, L. Johnson, B. C. Meyers, P. J. Green and S. E. Jacobsen (2006). "Dissecting Arabidopsis thaliana DICER function in small RNA processing, gene silencing and DNA methylation patterning." Nature genetics **38**(6): 721.

Hu, Y., W. Lan and D. Miller (2017). "Next-Generation Sequencing for MicroRNA Expression Profile." Methods Mol Biol **1617**: 169-177.

Huang, Y., Q. Zou, X. H. Sun and L. P. Zhao (2014). "Computational identification of microRNAs and their targets in perennial Ryegrass (*Lolium perenne*)." Applied biochemistry and biotechnology **173**(4): 1011-1022.

Huerta-Ocampo, J. A. and A. P. Barba de la Rosa (2011). "Amaranth: a pseudo-cereal with nutraceutical properties." Current Nutrition & Food Science **7**(1): 1-9.

Huerta-Ocampo, J. A., A. Barrera-Pacheco, C. S. Mendoza-Hernandez, E. Espitia-Rangel, H. P. Mock and A. P. Barba de la Rosa (2014). "Salt stress-induced alterations in the root proteome of *Amaranthus cruentus* L." J Proteome Res **13**(8): 3607-3627.

Huerta-Ocampo, J. A., A. Barrera-Pacheco, C. S. Mendoza-Hernandez, E. Espitia-Rangel, H. P. Mock and A. P. B. de la Rosa (2014). "Salt Stress-Induced Alterations in the Root Proteome of *Amaranthus cruentus* L." J Proteome Res **13**(8): 3607-3627.

Huerta-Ocampo, J. A., E. P. Briones-Cerecero, G. Mendoza-Hernández, A. De Leon-Rodriguez and A. P. Barba de la Rosa (2009). "Proteomic analysis of amaranth (*Amaranthus hypochondriacus* L.) leaves under drought stress." International journal of plant sciences **170**(8): 990-998.

Hui, Z., H. S. S., H. Michael, B. Natalia, E. Omid, L. Jie, G. Perry and S. Bujun (2018). "Identification and characterisation of a previously unknown drought tolerance-associated microRNA in barley." The Plant Journal **0**(0).

Hussain, M., M. Malik, M. Farooq, M. Ashraf and M. Cheema (2008). "Improving drought tolerance by exogenous application of glycinebetaine and salicylic acid in sunflower." Journal of Agronomy and Crop Science **194**(3): 193-199.

Jain, D., N. Ashraf, J. Khurana and M. S. Kameshwari (2019). The 'Omics' Approach for Crop Improvement Against Drought Stress. Genetic Enhancement of Crops for Tolerance to Abiotic Stress: Mechanisms and Approaches, Vol. I, Springer: 183-204.

Jamalluddin, N., F. J. Massawe and R. C. Symonds (2019). "Transpiration efficiency of Amaranth (*Amaranthus* sp.) in response to drought stress." The Journal of Horticultural Science and Biotechnology **94**(4): 448-459.

Janovska, D., P. H. Cepkova and M. Dzunkova (2012). "Characterisation of the Amaranth Genetic Resources in the Czech Gene Bank." Genetic Diversity in Plants: 457-478.

Jeong, D.-H., S. Park, J. Zhai, S. G. R. Gurazada, E. De Paoli, B. C. Meyers and P. J. Green (2011). "Massive analysis of rice small RNAs: mechanistic implications of regulated microRNAs and variants for differential target RNA cleavage." Plant Cell **23**(12): 4185-4207.

Jeong, D. H., S. Park, J. X. Zhai, S. G. R. Gurazada, E. De Paoli, B. C. Meyers and P. J. Green (2011). "Massive Analysis of Rice Small RNAs: Mechanistic Implications of Regulated MicroRNAs and Variants for Differential Target RNA Cleavage." Plant Cell **23**(12): 4185-4207.

Johnson, J. D. and V. H. Smith (2003). Adverse Impacts Of Drought On Crops And Crop Producers In The West. Western Economics Forum, Western Agricultural Economics Association.

Jones-Rhoades, M. W. and D. P. Bartel (2004). "Computational identification of plant microRNAs and their targets, including a stress-induced miRNA." Molecular cell **14**(6): 787-799.

Joshi, D. C., S. Sood, R. Hosahatti, L. Kant, A. Pattanayak, A. Kumar, D. Yadav and M. G. Stetter (2018). "From zero to hero: the past, present and future of grain amaranth breeding." Theoretical and Applied Genetics.

- Kantar, M., S. J. Lucas and H. Budak (2011). "miRNA expression patterns of *Triticum dicoccoides* in response to shock drought stress." *Planta* **233**(3): 471-484.
- Kantar, M., T. Unver and H. Budak (2010). "Regulation of barley miRNAs upon dehydration stress correlated with target gene expression." *Functional & integrative genomics* **10**(4): 493-507.
- Khalid, M., S. Hussain, S. Ahmad, S. Ejaz, I. Zakir, M. A. Ali, N. Ahmad and M. Anjum (2019). Impacts of Abiotic Stresses on Growth and Development of Plants: 1-8.
- Khraiwesh, B., J. K. Zhu and J. Zhu (2012). "Role of miRNAs and siRNAs in biotic and abiotic stress responses of plants." *Biochim Biophys Acta* **1819**(2): 137-148.
- Kozomara, A., M. Birgaoanu and S. Griffiths-Jones (2019). "miRBase: from microRNA sequences to function." *Nucleic Acids Res* **47**(D1): D155-D162.
- Kozomara, A. and S. Griffiths-Jones (2014). "miRBase: annotating high confidence microRNAs using deep sequencing data." *Nucleic Acids Res* **42**(Database issue): D68-73.
- Kulcheski, F. R., L. F. de Oliveira, L. G. Molina, M. P. Almerão, F. A. Rodrigues, J. Marcolino, J. F. Barbosa, R. Stolf-Moreira, A. L. Nepomuceno and F. C. Marcelino-Guimarães (2011). "Identification of novel soybean microRNAs involved in abiotic and biotic stresses." *BMC genomics* **12**(1): 307.
- Kulcheski, F. R., L. F. de Oliveira, L. G. Molina, M. P. Almerao, F. A. Rodrigues, J. Marcolino, J. F. Barbosa, R. Stolf-Moreira, A. L. Nepomuceno, F. C. Marcelino-Guimaraes, R. V. Abdelnoor, L. C. Nascimento, M. F. Carazzolle, G. A. Pereira and R. Margis (2011). "Identification of novel soybean microRNAs involved in abiotic and biotic stresses." *BMC Genomics* **12**: 307.
- Kwak, P. B., Q. Q. Wang, X. S. Chen, C. X. Qiu and Z. M. Yang (2009). "Enrichment of a set of microRNAs during the cotton fiber development." *BMC genomics* **10**(1): 457.
- Lagos-Quintana, M., R. Rauhut, W. Lendeckel and T. Tuschl (2001). "Identification of novel genes coding for small expressed RNAs." *Science* **294**(5543): 853-858.
- Lee, R. C. and V. Ambros (2001). "An extensive class of small RNAs in *Caenorhabditis elegans*." *Science* **294**(5543): 862-864.
- Lee, R. C., R. L. Feinbaum and V. Ambros (1993). "The *C. elegans* heterochronic gene *lin-4* encodes small RNAs with antisense complementarity to *lin-14*." *Cell* **75**(5): 843-854.
- Lei, J. and Y. Sun (2014). "miR-PREFeR: an accurate, fast and easy-to-use plant miRNA prediction tool using small RNA-Seq data." *Bioinformatics* **30**(19): 2837-2839.
- Li, J.-s., F.-I. Fu, M. An, S.-f. Zhou, Y.-h. She and W.-c. Li (2013). "Differential Expression of MicroRNAs in Response to Drought Stress in Maize." *Journal of Integrative Agriculture* **12**(8): 1414-1422.
- Li, S., C. Castillo-Gonzalez, B. Yu and X. Zhang (2017). "The functions of plant small RNAs in development and in stress responses." *Plant J* **90**(4): 654-670.
- Liu, H., H. Yu, G. Tang and T. Huang (2018). "Small but powerful: function of microRNAs in plant development." *Plant Cell Rep* **37**(3): 515-528.
- Liu, H. H., X. Tian, Y. J. Li, C. A. Wu and C. C. Zheng (2008). "Microarray-based analysis of stress-regulated microRNAs in *Arabidopsis thaliana*." *RNA* **14**(5): 836-843.
- Liu, Q., Q. Yan, Y. Liu, F. Hong, Z. Sun, L. Shi, Y. Huang and Y. Fang (2013). "Complementation of HYPONASTIC LEAVES1 by double-strand RNA-binding domains of DICER-LIKE1 in nuclear dicing bodies." *Plant physiology* **163**(1): 108-117.
- Liu, S., L. Peng, J. Pan, X. Wang, C. Zhao, C. Cheng, Z. Zhang, Y. Lin, X. XuHan and Z. Lai (2018). Identification of microRNAs in the green and red sectors of *Amaranthus tricolor* L. leaves based on Illumina sequencing data, PeerJ Preprints.

- Llave, C., J. M. Franco-Zorrilla, R. Solano and D. Barajas (2011). Target validation of plant microRNAs. MicroRNAs in Development, Springer: 187-208.
- Lopez-Galiano, M. J., V. Sentandreu, A. C. Martinez-Ramirez, C. Rausell, M. D. Real, G. Camanes, O. Ruiz-Rivero, O. Crespo-Salvador and I. Garcia-Robles (2019). "Identification of Stress Associated microRNAs in *Solanum lycopersicum* by High-Throughput Sequencing." Genes (Basel) **10**(6).
- Manavella, P. A., S. W. Yang and J. Palatnik (2019). "Keep calm and carry on: miRNA biogenesis under stress." Plant J **99**(5): 832-843.
- Mao, W., Z. Li, X. Xia, Y. Li and J. Yu (2012). "A combined approach of high-throughput sequencing and degradome analysis reveals tissue specific expression of microRNAs and their targets in cucumber." PLoS one **7**(3): e33040.
- Martinelli, T. and I. Galasso (2011). "Phenological growth stages of *Camelina sativa* according to the extended BBCH scale." Annals of Applied Biology **158**(1): 87-94.
- Martínez-Núñez, M., M. Ruiz-Rivas, P. F. Vera-Hernández, R. Bernal-Muñoz, S. Luna-Suárez and F. F. Rosas-Cárdenas (2019). "The phenological growth stages of different amaranth species grown in restricted spaces based in BBCH code." South African Journal of Botany **124**: 436-443.
- Martínez, G., J. Forment, C. Llave, V. Pallás and G. Gómez (2011). "High-throughput sequencing, characterization and detection of new and conserved cucumber miRNAs." PLoS one **6**(5): e19523.
- Meier, U., H. Bleiholder, H. Brumme, E. Bruns, B. Mehring, T. Proll and J. Wiegand (2008). Phenological growth stages of roses (*Rosa* sp.): Codification and description according to the BBCH scale.
- Meier, U., H. Bleiholder, L. Buhr, C. Feller, H. Hack, M. Heß, P. D. Lancashire, U. Schnock, R. Stauß and T. Van Den Boom (2009). "The BBCH system to coding the phenological growth stages of plants—history and publications." Journal für Kulturpflanzen **61**(2): 41-52.
- Meyers, B. C., M. J. Axtell, B. Bartel, D. P. Bartel, D. Baulcombe, J. L. Bowman, X. Cao, J. C. Carrington, X. Chen, P. J. Green, S. Griffiths-Jones, S. E. Jacobsen, A. C. Mallory, R. A. Martienssen, R. S. Poethig, Y. Qi, H. Vaucheret, O. Voinnet, Y. Watanabe, D. Weigel and J. K. Zhu (2008). "Criteria for annotation of plant MicroRNAs." Plant Cell **20**(12): 3186-3190.
- Miao, Y., C. Ye, L. Shen, Y. Cao, J. Tu and J. Yu (2018). "Unique miRNome in heat tolerant indica rice var. HT54 seedlings." Ecological Genetics and Genomics **7-8**: 13-22.
- Mica, E., V. Piccolo, M. Delledonne, A. Ferrarini, M. Pezzotti, C. Casati, C. Del Fabbro, G. Valle, A. Policriti, M. Morgante, G. Pesole, M. E. Pè and D. S. Horner (2009). "High throughput approaches reveal splicing of primary microRNA transcripts and tissue specific expression of mature microRNAs in *Vitis vinifera*." BMC Genomics **10**(1): 558.
- Mlakar, S. G., M. Turinek, M. Jakop, M. Bavec and F. Bavec (2010). "Grain amaranth as an alternative and perspective crop in temperate climate." J. Geogr **5**(1): 135-145.
- Morin, R. D., G. Aksay, E. Dolgosheina, H. A. Ebhardt, V. Magrini, E. R. Mardis, S. C. Sahinalp and P. J. Unrau (2008). "Comparative analysis of the small RNA transcriptomes of *Pinus contorta* and *Oryza sativa*." Genome research **18**(4): 571-584.
- Morin, R. D., Y. Zhao, A.-L. Prabhu, N. Dhalla, H. McDonald, P. Pandoh, A. Tam, T. Zeng, M. Hirst and M. Marra (2010). Preparation and Analysis of MicroRNA Libraries Using the Illumina Massively Parallel Sequencing Technology. RNAi and microRNA-Mediated Gene Regulation in Stem Cells: Methods, Protocols, and Applications. B. Zhang and E. J. Stellwag. Totowa, NJ, Humana Press: 173-199.
- Mut, Z., H. Akay and N. Aydin (2010). "Effects of seed size and drought stress on germination and seedling growth of some oat genotypes (*Avena sativa* L.)." Afr J Agr Res **5**.
- Nemali, K. and M. W. van Iersel (2019). "Relating Whole-plant Photosynthesis to Physiological Acclimations at Leaf and Cellular Scales under Drought Stress in Bedding Plants." Journal of the American Society for Horticultural Science **144**(3): 201-208.

Niu, S., Y. Wang, Z. Zhao, M. Deng, L. Cao, L. Yang and G. Fan (2016). "Transcriptome and Degradome of microRNAs and Their Targets in Response to Drought Stress in the Plants of a Diploid and Its Autotetraploid *Paulownia australis*." PLoS One **11**(7): e0158750.

Nonami, H. (1998). "Plant water relations and control of cell elongation at low water potentials." Journal of Plant Research **111**(3): 373-382.

Novero, R. P., J. C. O'Toole, R. T. Cruz and D. P. Garrity (1985). "Leaf water potential, crop growth response, and microclimate of dryland rice under line source sprinkler irrigation." Agricultural and Forest Meteorology **35**(1): 71-82.

Omamt, E. N., P. S. Hammes and P. J. Robbertse (2006). "Differences in salinity tolerance for growth and water-use efficiency in some amaranth (*Amaranthus* spp.) genotypes." New Zealand Journal of Crop and Horticultural Science **34**(1): 11-22.

Orona-Tamayo, D. and O. Paredes-López (2017). Chapter 15 - Amaranth Part 1—Sustainable Crop for the 21st Century: Food Properties and Nutraceuticals for Improving Human Health. Sustainable Protein Sources. S. R. Nadathur, J. P. D. Wanasundara and L. Scanlin. San Diego, Academic Press: 239-256.

Othim, S. T. O., S. Ramasamy, R. Kahuthia-Gathu, T. Dubois, S. Ekesi and K. K. M. Fiaboe (2018). "Expression of Resistance in *Amaranthus* spp. (Caryophyllales: Amaranthaceae): Effects of Selected Accessions on the Behaviour and Biology of the Amaranth Leaf-Webber, *Spoladea recurvalis* (Lepidoptera: Crambidae)." Insects **9**(2).

Palmeros-Suárez, P. A., J. A. Massange-Sánchez, N. A. Martínez-Gallardo, J. M. Montero-Vargas, J. F. Gómez-Leyva and J. P. Délano-Frier (2015). "The overexpression of an *Amaranthus hypochondriacus* NF-YC gene modifies growth and confers water deficit stress resistance in *Arabidopsis*." Plant Science **240**: 25-40.

Panda, S. K. and R. Sunkar (2015). "Nutrient- and other stress-responsive microRNAs in plants: Role for thiol-based redox signaling." Plant Signal Behav **10**(4): e1010916.

Pandey, P., P. K. Srivastava and S. P. Pandey (2019). Prediction of Plant miRNA Targets. Plant MicroRNAs, Springer: 99-107.

Pandey, R., G. Joshi, A. R. Bhardwaj, M. Agarwal and S. Katiyar-Agarwal (2014). "A comprehensive genome-wide study on tissue-specific and abiotic stress-specific miRNAs in *Triticum aestivum*." PLoS One **9**(4): e95800.
Pandita, D. and S. H. Wani (2019). MicroRNA as a Tool for Mitigating Abiotic Stress in Rice (*Oryza sativa* L.). Recent Approaches in Omics for Plant Resilience to Climate Change, Springer: 109-133.

Pegler, J. L., C. P. L. Grof and A. L. Eamens (2019). The Plant microRNA Pathway: The Production and Action Stages. Plant MicroRNAs: Methods and Protocols. S. de Folter. New York, NY, Springer New York: 15-39.

Piao, S., Q. Liu, A. Chen, I. A. Janssens, Y. Fu, J. Dai, L. Liu, X. Lian, M. Shen and X. Zhu (2019). "Plant phenology and global climate change: Current progresses and challenges." Glob Chang Biol **25**(6): 1922-1940.
Pokoo, R., S. Ren, Q. Wang, C. M. Motes, T. D. Hernandez, S. Ahmadi, M. J. Monteros, Y. Zheng and R. Sunkar (2018). "Genotype- and tissue-specific miRNA profiles and their targets in three alfalfa (*Medicago sativa* L.) genotypes." BMC Genomics **19**(10): 913.

Qin, Z., C. Li, L. Mao and L. Wu (2014). "Novel insights from non-conserved microRNAs in plants." Front Plant Sci **5**: 586.

Ramesh, S. V., V. Govindasamy, M. K. Rajesh, A. A. Sabana and S. Praveen (2019). "Stress-responsive miRNAome of *Glycine max* (L.) Merrill: molecular insights and way forward." Planta **249**(5): 1267-1284.

Rodriguez, A., S. Griffiths-Jones, J. L. Ashurst and A. Bradley (2004). "Identification of mammalian microRNA host genes and transcription units." Genome Res **14**(10A): 1902-1910.

Rubio-Somoza, I. and D. Weigel (2011). "MicroRNA networks and developmental plasticity in plants." Trends in plant science **16**(5): 258-264.

Salazar, D. M., P. Melgarejo, R. Martínez, J. J. Martínez, F. Hernández and M. Burguera (2006). "Phenological stages of the guava tree (*Psidium guajava* L.)." Scientia Horticulturae **108**(2): 157-161.

- Sarker, U. and S. Oba (2019). "Salinity stress enhances color parameters, bioactive leaf pigments, vitamins, polyphenols, flavonoids and antioxidant activity in selected *Amaranthus* leafy vegetables." J Sci Food Agric **99**(5): 2275-2284.
- Schwab, R., J. F. Palatnik, M. Rieger, C. Schommer, M. Schmid and D. Weigel (2005). "Specific effects of microRNAs on the plant transcriptome." Developmental cell **8**(4): 517-527.
- Seki, M., M. Narusaka, J. Ishida, T. Nanjo, M. Fujita, Y. Oono, A. Kamiya, M. Nakajima, A. Enju and T. Sakurai (2002). "Monitoring the expression profiles of 7000 *Arabidopsis* genes under drought, cold and high-salinity stresses using a full-length cDNA microarray." The Plant Journal **31**(3): 279-292.
- Shahid, S. and M. J. Axtell (2014). "Identification and annotation of small RNA genes using ShortStack." Methods (San Diego, Calif.) **67**(1): 20-27.
- Sharma, R., S. Upadhyay, B. Bhat, G. Singh, S. Bhattacharya and A. Singh (2019). "Abiotic stress induced miRNA-TF-gene regulatory network: A structural perspective." Genomics.
- Shinozaki, K. and K. Yamaguchi-Shinozaki (2007). "Gene networks involved in drought stress response and tolerance." J Exp Bot **58**(2): 221-227.
- Shinozaki, K. and K. Yamaguchi-Shinozaki (2007). "Gene networks involved in drought stress response and tolerance." J Exp Bot **58**(2): 221-227.
- Shukla, G. C., J. Singh and S. Barik (2011). "MicroRNAs: Processing, Maturation, Target Recognition and Regulatory Functions." Mol Cell Pharmacol **3**(3): 83-92.
- Silva-Sánchez, C., A. B. de La Rosa, M. León-Galván, B. De Lumen, A. de León-Rodríguez and E. G. de Mejía (2008). "Bioactive peptides in amaranth (*Amaranthus hypochondriacus*) seed." J Agric Food Chem **56**(4): 1233-1240.
- Stallknecht, G. F. and J. R. Schulz-Schaeffer (1993). "Amaranth rediscovered." p. 211-218. In: J. Janick and J.E. Simon (eds.), New crops. Wiley, New York.
- Steiner, J. L., D. D. Briske, D. P. Brown and C. M. Rottler (2018). "Vulnerability of Southern Plains agriculture to climate change." Climatic Change **146**(1): 201-218.
- Sukiran, N. L., J. C. Ma, H. Ma and Z. Su (2019). "ANAC019 is required for recovery of reproductive development under drought stress in *Arabidopsis*." Plant molecular biology **99**(1-2): 161-174.
- Sun, L., G. Sun, C. Shi and D. Sun (2018). "Transcriptome analysis reveals new microRNAs-mediated pathway involved in anther development in male sterile wheat." BMC Genomics **19**(1): 333.
- Sunkar, R., T. Girke, P. K. Jain and J.-K. Zhu (2005). "Cloning and characterization of microRNAs from rice." The Plant Cell **17**(5): 1397-1411.
- Sunkar, R., T. Girke, P. K. Jain and J.-K. Zhu (2005). "Cloning and characterization of microRNAs from rice." Plant Cell **17**(5): 1397-1411.
- Sunkar, R. and G. Jagadeeswaran (2008). "In silico identification of conserved microRNAs in large number of diverse plant species." BMC plant biology **8**(1): 37.
- Sunkar, R. and J.-K. Zhu (2004). "Novel and stress-regulated microRNAs and other small RNAs from *Arabidopsis*." The Plant Cell **16**(8): 2001-2019.
- Sunkar, R. and J. K. Zhu (2004). "Novel and stress-regulated microRNAs and other small RNAs from *Arabidopsis*." Plant Cell **16**(8): 2001-2019.
- Suzuki, N., R. M. Rivero, V. Shulaev, E. Blumwald and R. Mittler (2014). "Abiotic and biotic stress combinations." New Phytol **203**(1): 32-43.
- Szakonyi, D., A. Confraria, C. Valerio, P. Duque and D. Staiger (2019). "Editorial: Plant RNA Biology." Front Plant Sci **10**: 887.

- Szittyta, G., S. Moxon, D. M. Santos, R. Jing, M. P. Fevereiro, V. Moulton and T. Dalmay (2008). "High-throughput sequencing of *Medicago truncatula* short RNAs identifies eight new miRNA families." BMC Genomics **9**: 593.
- Takahashi, F., T. Kuromori, H. Sato and K. Shinozaki (2018). Regulatory gene networks in drought stress responses and resistance in plants. Survival Strategies in Extreme Cold and Desiccation, Springer: 189-214.
- Tigkas, D., H. Vangelis and G. Tsakiris (2019). "Drought characterisation based on an agriculture-oriented standardised precipitation index." Theoretical and Applied Climatology **135**(3-4): 1435-1447.
- Todaka, D., K. Shinozaki and K. Yamaguchi-Shinozaki (2015). "Recent advances in the dissection of drought-stress regulatory networks and strategies for development of drought-tolerant transgenic rice plants." Front Plant Sci **6**.
- Turner, N. C., J. C. O'Toole, R. T. Cruz, O. S. Namuco and S. Ahmad (1986). "Responses of seven diverse rice cultivars to water deficits I. Stress development, canopy temperature, leaf rolling and growth." Field Crops Research **13**: 257-271.
- Unver, T., D. M. Namuth-Covert and H. Budak (2009). "Review of current methodological approaches for characterizing microRNAs in plants." Int J Plant Genomics **2009**: 262463.
- Unver, T., I. Parmaksız and E. Dündar (2010). "Identification of conserved micro-RNAs and their target transcripts in opium poppy (*Papaver somniferum* L.)." Plant cell reports **29**(7): 757-769.
- Valliyodan, B. and H. T. Nguyen (2006). "Understanding regulatory networks and engineering for enhanced drought tolerance in plants." Curr Opin Plant Biol **9**(2): 189-195.
- Vaucheret, H., F. Vazquez, P. Crété and D. P. Bartel (2004). "The action of ARGONAUTE1 in the miRNA pathway and its regulation by the miRNA pathway are crucial for plant development." Genes & development **18**(10): 1187-1197.
- Venskutonis, P. R. and P. Kraujalis (2013). "Nutritional Components of Amaranth Seeds and Vegetables: A Review on Composition, Properties, and Uses." Comprehensive Reviews in Food Science and Food Safety **12**(4): 381-412.
- Voinnet, O. (2009). "Origin, biogenesis, and activity of plant microRNAs." Cell **136**(4): 669-687.
- Wan, P., J. Wu, Y. Zhou, J. Xiao, J. Feng, W. Zhao, S. Xiang, G. Jiang and J. Y. Chen (2011). "Computational analysis of drought stress-associated miRNAs and miRNA co-regulation network in *Physcomitrella patens*." Genomics, proteomics & bioinformatics **9**(1): 37-44.
- Wang, H., C. Zhang, Y. Dou, B. Yu, Y. Liu, T. M. Heng-Moss, G. Lu, M. Wachholtz, J. D. Bradshaw, P. Twigg, E. Scully, N. Palmer and G. Sarath (2017). "Insect and plant-derived miRNAs in greenbug (*Schizaphis graminum*) and yellow sugarcane aphid (*Sipha flava*) revealed by deep sequencing." Gene **599**: 68-77.
- Wang, J., S. Chen, N. Jiang, N. Li, X. Wang, Z. Li, X. Li, H. Liu, L. Li, Y. Yang, T. Ni, C. Yu, J. Ma, B. Zheng and G. Ren (2019). "Spliceosome disassembly factors ILP1 and NTR1 promote miRNA biogenesis in *Arabidopsis thaliana*." Nucleic Acids Res **47**(15): 7886-7900.
- Wang, J. L., J. Mei and G. D. Ren (2019). "Plant microRNAs: Biogenesis, Homeostasis, and Degradation." Frontiers in Plant Science **10**.
- Wang, S. and A. Ebert (2012). "Breeding of leafy amaranth for adaptation to climate change." High value vegetables in Southeast Asia: Production, supply and demand: 36-43.
- Wang, W.-B., Y.-H. Kim, H.-S. Lee, K.-Y. Kim, X.-P. Deng and S.-S. Kwak (2009). "Analysis of antioxidant enzyme activity during germination of alfalfa under salt and drought stresses." Plant Physiology and Biochemistry **47**(7): 570-577.
- Wang, W. C., F. M. Lin, W. C. Chang, K. Y. Lin, H. D. Huang and N. S. Lin (2009). "miRExpress: analyzing high-throughput sequencing data for profiling microRNA expression." BMC Bioinformatics **10**: 328.

- Wang, X.-J., J. L. Reyes, N.-H. Chua and T. Gaasterland (2004). "Prediction and identification of *Arabidopsis thaliana* microRNAs and their mRNA targets." Genome biology **5**(9): R65.
- Wang, Y., Y. Ding and J.-Y. Liu (2016). "Identification and profiling of microRNAs expressed in elongating cotton fibers using small RNA deep sequencing." Frontiers in plant science **7**: 1722.
- Waselkov, K. E., A. S. Boleda and K. M. Olsen (2018). "A Phylogeny of the Genus *Amaranthus* (Amaranthaceae) Based on Several Low-Copy Nuclear Loci and Chloroplast Regions." Systematic Botany **43**(2): 439-458, 420.
- Wu, W. (2018). "MicroRNA Sequencing Data Analysis Toolkits." Methods Mol Biol **1699**: 211-215.
- Xia, H., L. Zhang, G. Wu, C. Fu, Y. Long, J. Xiang, J. Gan, Y. Zhou, L. Yu and M. Li (2016). "Genome-wide identification and characterization of microRNAs and target genes in *Lonicera japonica*." PLoS one **11**(10): e0164140.
- Xia, Z., Z. Zhao, M. Li, L. Chen, Z. Jiao, Y. Wu, T. Zhou, W. Yu and Z. Fan (2018). "Identification of miRNAs and their targets in maize in response to Sugarcane mosaic virus infection." Plant Physiology and Biochemistry **125**: 143-152.
- Xoconostle-Cazares, B., F. A. Ramirez-Ortega, L. Flores-Elenes and R. Ruiz-Medrano (2010). "Drought tolerance in crop plants." American Journal of Plant Physiology **5**(5): 241-256.
- Xu, L., Y. Hu, Y. Cao, J. Li, L. Ma, Y. Li and Y. Qi (2018). "An expression atlas of miRNAs in *Arabidopsis thaliana*." Sci China Life Sci **61**(2): 178-189.
- Yang, L., Z. Liu, F. Lu, A. Dong and H. Huang (2006). "SERRATE is a novel nuclear regulator in primary microRNA processing in *Arabidopsis*." The Plant Journal **47**(6): 841-850.
- Yang, T., L. Xue and L. An (2007). "Functional diversity of miRNA in plants." Plant Science **172**(3): 423-432.
- Yang, W., X. Liu, J. Zhang, J. Feng, C. Li and J. Chen (2010). "Prediction and validation of conservative microRNAs of *Solanum tuberosum* L." Molecular biology reports **37**(7): 3081-3087.
- Yang, X. and L. Li (2011). "miRDeep-P: a computational tool for analyzing the microRNA transcriptome in plants." Bioinformatics **27**(18): 2614-2615.
- Ye, K. Y., Y. Chen, X. W. Hu and J. C. Guo (2013). "Computational identification of microRNAs and their targets in apple." Genes & Genomics **35**(3): 377-385.
- Yin, Z., C. Li, X. Han and F. Shen (2008). "Identification of conserved microRNAs and their target genes in tomato (*Lycopersicon esculentum*)." Gene **414**(1-2): 60-66.
- Yoon, S. and G. De Micheli (2006). "Computational identification of microRNAs and their targets." Birth Defects Res C Embryo Today **78**(2): 118-128.
- Yu, Y., Z. Ni, Y. Wang, H. Wan, Z. Hu, Q. Jiang, X. Sun and H. Zhang (2019). "Overexpression of soybean miR169c confers increased drought stress sensitivity in transgenic *Arabidopsis thaliana*." Plant Sci **285**: 68-78.
- Zhang, B., X. Pan, G. P. Cobb and T. A. Anderson (2006). "Plant microRNA: a small regulatory molecule with big impact." Dev Biol **289**(1): 3-16.
- Zhang, B., Q. Wang and X. Pan (2007). "MicroRNAs and their regulatory roles in animals and plants." Journal of cellular physiology **210**(2): 279-289.
- Zhang, B. H., X. P. Pan, Q. L. Wang, P. C. George and T. A. Anderson (2005). "Identification and characterization of new plant microRNAs using EST analysis." Cell research **15**(5): 336.
- Zhang, L., J. M. Chia, S. Kumari, J. C. Stein, Z. Liu, A. Narechania, C. A. Maher, K. Guill, M. D. McMullen and D. Ware (2009). "A genome-wide characterization of microRNA genes in maize." PLoS Genet **5**(11): e1000716.
- Zhang, N., J. Yang, Z. Wang, Y. Wen, J. Wang, W. He, B. Liu, H. Si and D. Wang (2014). "Identification of novel and conserved microRNAs related to drought stress in potato by deep sequencing." PLoS ONE **9**(4): e95489.

Zhao, B., R. Liang, L. Ge, W. Li, H. Xiao, H. Lin, K. Ruan and Y. Jin (2007). "Identification of drought-induced microRNAs in rice." Biochem Biophys Res Commun **354**(2): 585-590.

Zhou, L., Y. Liu, Z. Liu, D. Kong, M. Duan and L. Luo (2010). "Genome-wide identification and analysis of drought-responsive microRNAs in *Oryza sativa*." J Exp Bot **61**(15): 4157-4168.



The phenological growth stages of different amaranth species grown in restricted spaces based in BBCH code

M. Martínez-Núñez^a, M. Ruiz-Rivas^a, P.F. Vera-Hernández^a, R. Bernal-Muñoz^b,
S. Luna-Suárez^a, F.F. Rosas-Cárdenas^{a,*}

^a Instituto Politécnico Nacional, Centro de Investigación en Biotecnología Aplicada, Ex-Hacienda San Juan Molino Carretera Estatal Tecuexcomac-Tepetitla Km 1.5, Tlaxcala C.P. 90700, México

^b Tecnológico Nacional de México, Instituto Tecnológico del Altiplano de Tlaxcala, Km. 7.5 Carretera Federal San Martín-Tlaxcala, San Diego Xocoyucan, Tlaxcala C.P. 90122, México

ARTICLE INFO

Article history:

Received 6 March 2019

Received in revised form 2 May 2019

Accepted 26 May 2019

Available online xxxx

Edited by MG Kulkarni

Keywords:

BBCH coding system

Phenological stages

Growth

Amaranth development

Panicle

ABSTRACT

Amaranth is a pseudocereal with potential health benefits. Amaranth has recently gained importance due to its high capacity to grow in adverse conditions. Details about the growth and development of amaranth is fundamental to its cultivation, but reports on the phenological growth stages, development, and the life cycle of amaranth are limited. Under normal conditions, amaranth plants are as high as 2.2 m, making their handling difficult. Thus, this study determined the phenological growth stages and life cycle of amaranth in restricted spaces. *Amaranthus cruentus*, *Amaranthus hybridus*, and *Amaranthus hypochondriacus* plants were cultivated in restricted spaces. The physiological and qualitative features as number of leaves, length of plants and leaves, panicle color, were used to determine the different phenological growth stages and life cycle of amaranth plants. The phenological growth stages were described via Biologische Bundesanstalt Bundessortenamt and Chemische Industrie (BBCH) decimal code. Plants between 15 and 22 cm were generated, and each phenological growth stage was easily managed in restricted spaces. The time for each phenological growth stage was examined in different amaranth species and this offered a general representation of the phenological growth stages and life cycle of amaranth. This work established the phenological growth stages of amaranth based on the BBCH coding system managed in restricted spaces. These observations allow us to envision amaranth as a model plant in which each phenological growth stage describing its life cycle is managed easily under limited spaces, which could be an advantage for better manipulation and future studies.

© 2019 SAAB. Published by Elsevier B.V. All rights reserved.

1. Introduction

Amaranth is a crop with high potential for economic exploitation similar to maize, wheat, sorghum, barley, rice, and soybean (Innovation, 1984; Rastogi and Shukla, 2013; Akin-Idowu, 2017). Amaranth has an excellent nutritional value and high genetic and phenotypic diversity (Lee et al., 2008; Brenner et al., 2010; Rastogi and Shukla, 2013; Venkatesh et al., 2014; Akin-Idowu et al., 2016; Stetter et al., 2016). Amaranth is an annual, dicotyledonous and herbaceous plant (Brenner et al., 2010; Akin-Idowu et al., 2016; Das, 2016). Some studies have described amaranth productivity (Das, 2016; Kirillova et al., 2016; Kuluev et al., 2017), cultivation conditions (Das, 2016; Stetter et al., 2016), morphological diversity (Lee et al., 2008; Ray and

Roy, 2009; Akin-Idowu et al., 2016; Das, 2016), adaptability (Lee et al., 2008; Huerta-Ocampo et al., 2014; Massange-Sanchez et al., 2015; Palmeros-Suarez et al., 2015; Vargas-Ortiz et al., 2015; Das, 2016), and new varieties (Akin-Idowu et al., 2016; Das, 2016). Amaranth can also easily adapt to adverse growth conditions (Delano-Frier et al., 2011; Caselato-Sousa and Amaya-Farfan, 2012; Huerta-Ocampo et al., 2014; Das, 2016). Amaranth has a high degree of phenotypic plasticity (Shukla et al., 2010; Khanam and Oba, 2014), defined as the ability of an organism to change its phenotype in response to changes in the environment (Price et al., 2003; Fazlioglu and Bonser, 2016).

Information about the phenological growth stages of crops is fundamental and useful to agriculture. Some studies of the phenological growth stages from maize (Bussel et al., 2015), wheat (Bussel et al., 2015; Ihsan et al., 2016), sorghum (Kumar et al., 2009), barley (Hossain et al., 2012), rice (Zhang et al., 2013; Zhang et al., 2016), and soybean (Choi et al., 2016; Salmeron and Purcell, 2016) have been described; however, information on amaranth's life cycle is limited. In amaranth, as in other crops, it is still necessary to establish a standard scale as a unique criterion to quantify phenology and to analyze the plant structure that enable the formulation of rational plant breeding

Abbreviations: BBCH, Biologische Bundesanstalt Bundessortenamt und Chemische Industrie; E, Episperm; P, Perisperm; SAS/STAT, State-of-the-art Statistical Analysis Software; GGD, Growing degree days; ANOVA, Analysis of variance; LSD, Least Significant Difference.

* Corresponding author.

E-mail address: frosasc@ipn.mx (F.F. Rosas-Cárdenas).

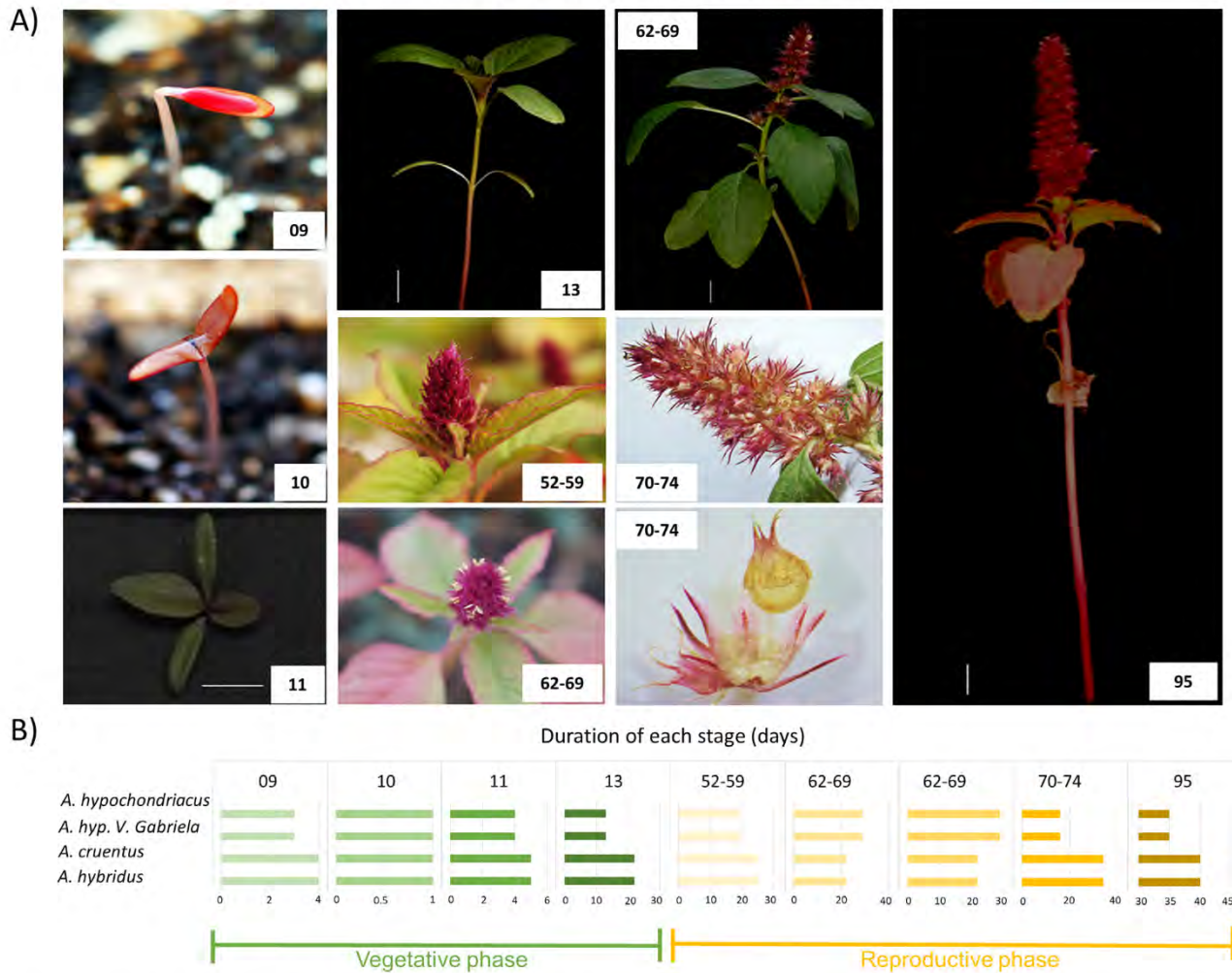


Fig. 1. The phenological growth stages of amaranth in restricted spaces. Representation of growth stages from *A. hypochondriacus* “Gabriela” variety in restricted spaces. The number is the BBCH code. Scale bar, 1 cm.

approach. The BBCH scale is a system for a uniform coding of phenologically similar growth stages of all mono- and dicotyledonous plants using a decimal coding system (Meier et al., 2009). These data were used to compare amaranth's growth in limited spaces. In this research three species and one variety of amaranth were studied in terms of their phenological growth stages and life cycle in restricted spaces. Phenological features were studied for the establishment of the life cycle using the BBCH scale (Hack et al., 1992).

2. Materials and methods

2.1. Plant material

The three *Amaranthus* species were *A. hypochondriacus*, *A. hybridus*, and *A. cruentus* (provided by Dr. Cesar A. Reyes López of Escuela Nacional de Medicina y Homeopatía del Instituto Politécnico Nacional of Mexico), as well as the “Gabriela” variety of *A. hypochondriacus* (generated in the Instituto Tecnológico del Altiplano de Tlaxcala also from Mexico). Seeds were sterilized with 10% sodium hypochlorite commercial solution and 50% ethanol, for 5 and 1 min, respectively. The seeds were rinsed three times for 3 min with sterile water after each immersion.

2.2. Plant growth and monitoring

Polystyrene trays with wells of 2.54 cm × 2.54 cm × 6.5 cm depth were used as restricted spaces to cultivate amaranth. The sterile

substrate was composed of peat moss, perlite, and vermiculite (3:1:1 v/v ratio). The seeds of each species were germinated under semi-controlled greenhouse conditions in polystyrene trays, in February 2016. Plants were grown in the Centro de Investigación en Biotecnología Aplicada del Instituto Politécnico Nacional (CIBA-IPN), Tlaxcala, México (19°16'53.2" N and 98°21'57.3" W; 2260 m above sea level). Plants were grown in short days. The temperature in the greenhouse vary from 21 to 39 °C, and the relative humidity fluctuate between 15.6 and 49%. Irrigation was performed every third day obtaining an average of 85% humidity in the substrate. The humidity was recorded with an MB45 thermobalance (Ohaus Corporation, New Jersey, USA). Twenty plants randomly selected were used to determine the different phenological growth stages in yield. To calculate the daily thermal units, the equation of Gilmore & Rogers (1958) was used ($GGD = [(T_{max} + T_{min})/2] - T_b$), where T_{max} - T_{min} are daily maximum and minimum air temperatures, respectively. T_b is the base temperature, evaluated at 10 °C. The maximum and minimum daily temperatures were obtained from the INIFAP station: 998416, Muñoz de Domingo Arenas, Tlaxcala monitored from February–June 2016.

2.3. Photographic record and microscopy analysis

A photographic record of amaranth species used an SLT-A37K camera (Sony, California, USA) coupled to a macro lens DT 2.8/30. The morphology of complex structures such as flowers and seeds was analyzed in a Zeiss Stemi 508 stereomicroscope, with a Zeiss Axiocam ERC 5s Rev. 2.0 camera; this was visualized with the ZEN lite software (Zeiss, Jena,

Phenological growth stages of Amaranth									
Principal Stage (BBCH code)	0	1			5	6		7	8-9
Stage	(00-09)	(10)	(11)	(12-13)	(50-59)	(60-69)	(60-69)	(70-77)	(80-99)
Phenological growth stages	Germination	Opening of cotyledons	True leaves 2 leaves	5-6 leaves	Apical inflorescence	Anthesis	Axillary inflorescence	Seed development	Ripening and senescence
Days post-seeding	3-4	4-5	8-10	21-32	40-57	69-79		85-113	120-153
GDD °C	13-16	16-20	26-24	63-115	130-218	299-377		410-644	709-731
	Vegetative phase				Development of vegetative structures				
					Reproductive phase				
	Planting				Panicle exertion				

Fig. 2. General schematic representation of the phenological growth stages of amaranth, in restricted spaces. The vegetative and reproductive phase are indicated, as are the life cycle stages of amaranth including duration and days post-seeding for each principal phenotype. GGD, growing degree-days, estimated using the data of the INIFAP Station: 998416, Muñoz de Domingo Arenas, Tlaxcala (February–June 2016), using degree Celsius (°C). Days post seeding: the ranges showed between the different species used in this work.

Table 1

Description of the phenological growth stages of Amaranth sp. according to the BBCH scale.

Principal growth stage BBCH	BBCH Code	Description	
0: Germination	00	Dry seed	
	01	Beginning of seed imbibition	
	03	Seed imbibition completed	
	05	Radicle emerged from seed	
	06	Radicle elongated, root hairs and/or side roots visible	
	08	Emergence of hypocotyl	
	09	Emergence of cotyledons through soil	
	1: Leaf development	10	Cotyledons fully emerged/Opening of cotyledons
		11	First pair of leaves visible
12		Second pair of leaves visible	
13		Five or six leaves visible	
1...		Stages continuous till...	
3: Stem elongation		The longitudinal growth of the main stem occurs in parallel with the leaf development. That is why the coding of the main stadium 3 is omitted	
5: Inflorescence emergence	50	Beginning of panicle emergence (panicle still enclosed by leaves)	
	51	Leaves surrounding inflorescence separated, inflorescence is visible from above	
	52	Panicle visible from the sides (panicle's indeterminate growth habit)	
	59	Inflorescence visible, but all flowers are still closed	
6: Anthesis and axillary inflorescence	60	Beginning of anthesis: main inflorescence flowers with first extruded anthers (acropete flowering)	
	63	Staminate and pistillate flowers visible	
	65	Full flowering: anthers visible on most panicle	
	69	End of flowering: The panicle have completed flowering, but some senesced anthers may remain	
7: Fruit and seed development)	70	Ovary thickening (development of the fertilized ovule)	
	71	Watery ripe: The first visible grains have reached half their final size	
	73	Early milk: Immature grains (the grains show a milky consistency)	
	75	Medium milk: Grains with a white coloration of opaque tone and a pasty consistency	
	77	Late milk: the grain's texture is slightly rough, and their coloration becomes opaque ivory	
8: Ripening Seed ripening	80	Milky grain, grain content soft but dry, easily crushed with fingernails	
	85	Hard dough: Grain content solid, easily crushed with fingernails	
9: Senescence	89	Ripe grain: difficult to crush with fingernails, dry content, the grain has an opaque ivory color on its outside. Ready to harvest.	
	95	Panicle changes color	
	97	Plant dead and collapsing	
	99	Harvested product	

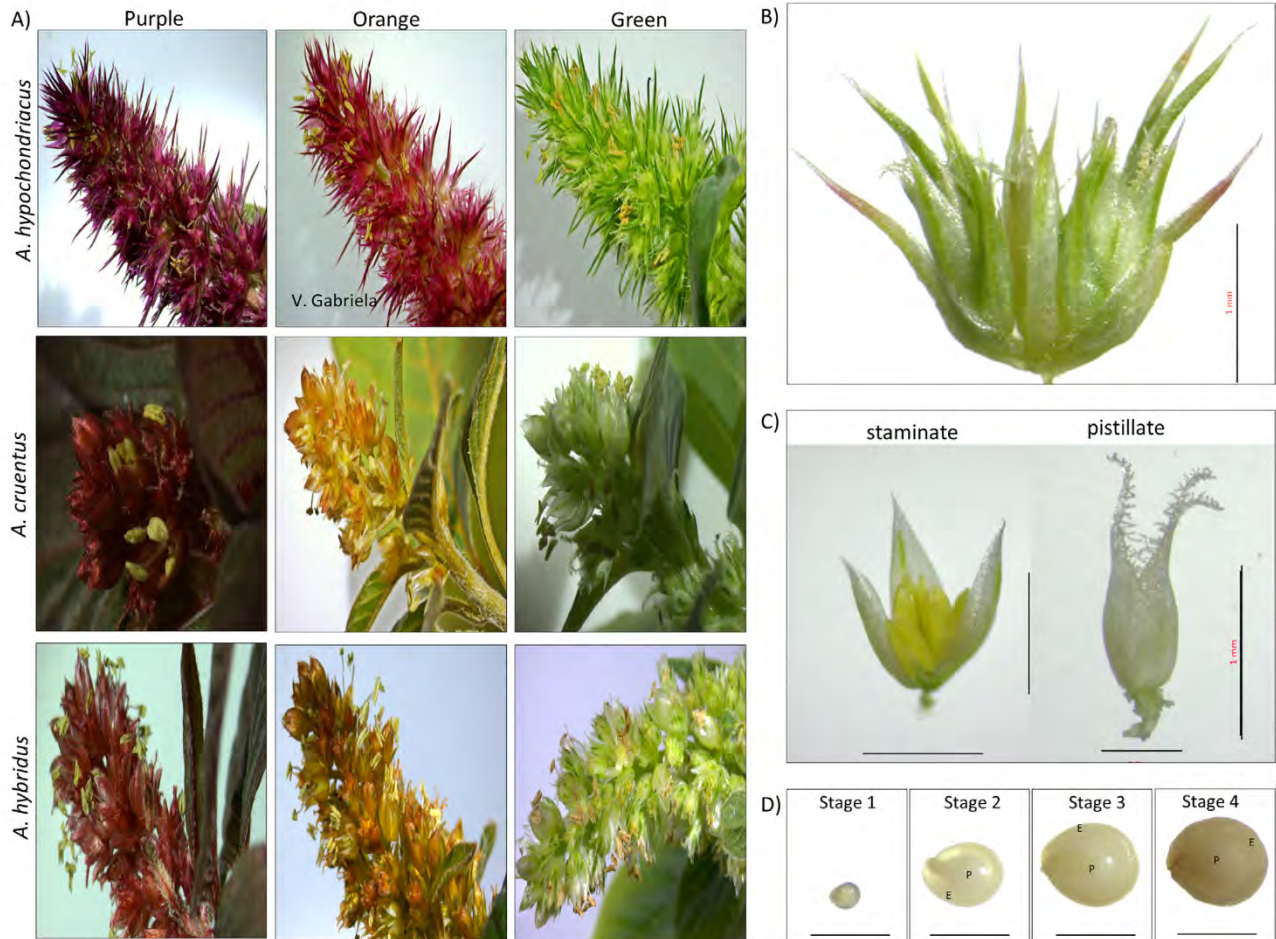


Fig. 3. Development of panicle, flowers, and seeds in amaranth. (A) Panicle of *A. hypochondriacus*, *A. cruentus*, and *A. hybridus* plants, grown in the greenhouse 10 weeks post-seeding; the plants were classified by panicle color. (B) Glomerulus of *A. hypochondriacus*. (C) Male and female flowers in *A. hypochondriacus*. (D) Different stages of seed development. The peripheric embryo or episperm, and perisperm structures are represented by E and P, respectively. Scale bar, 1 mm.

Germany). Twenty pistillate flowers and twenty staminate flowers and fifty seeds per specimen were randomly selected for analysis under microscope.

2.4. Statistical analysis

At least 20 plants randomly selected were used for each species and variety analyzed. For each plant, the length and number of leaves was measured. For the length of leaves, the first true leaf of each plant was measured. The number of leaves was counted at the beginning of the reproductive stage (stage 13). Data from plants in the greenhouse were analyzed using SAS/STAT® software and included variables such as plant height, number, and length of the leaves. Analysis of variance (ANOVA) using Fisher's Least Significant Difference (LSD) test with a significance level of $p < .05$ were performed.

3. Results

3.1. Phenological growth stages of amaranth in restricted spaces

The phenological growth stages of amaranth were studied using specimens grown in limited spaces (Fig. 1A). Plants between 15 and 22 cm were obtained in restricted spaces (Fig. 1A). The period for each phenological stage was analyzed across all species, to prepare a general representation of the phenological growth stages of amaranth. Similar

to other crops, the amaranth life cycle was divided into vegetative and reproductive phases. The BBCH scale was used to establish the amaranth's phenological growth stages. Some principal stages were omitted including the formation of side shoots (stage 2) and stem elongation (stage 3), which coincides with leaf development (stage 1). The growth of harvestable vegetative plant parts (stage 4) was omitted because only the seeds are harvested for these amaranth species. The time needed for each stage varied between species (Fig. 1B). In restricted spaces, the life cycle of amaranth required 120 days for *A. hypochondriacus* and *A. hypochondriacus* variety "Gabriela"; *A. cruentus* and *A. hybridus* needed 153 days (Fig. 2). The vegetative phase showed a rapid increase in size and foliage including the principal stages 0 and 1 on the BBCH code (Figs. 1, 2). The transition from vegetative to reproductive phase started at 40 days post-seeding in *A. hypochondriacus* and "Gabriela" variety; *A. hybridus* and *A. cruentus* started at 57 days post-seeding (Fig. 1B, 2). The principal growth stages 5–9 were included in the reproductive phase (Fig. 2).

3.2. Germination

Stage 0 comprised the germination and included root (stage 05), hypocotyl (stage 08), and cotyledon emergence (stage 09) (Table 1). Stage 09 occurred three days post-seeding in *A. hypochondriacus* and four days post-seeding in *A. cruentus* and *A. hybridus* (Fig. 1B).

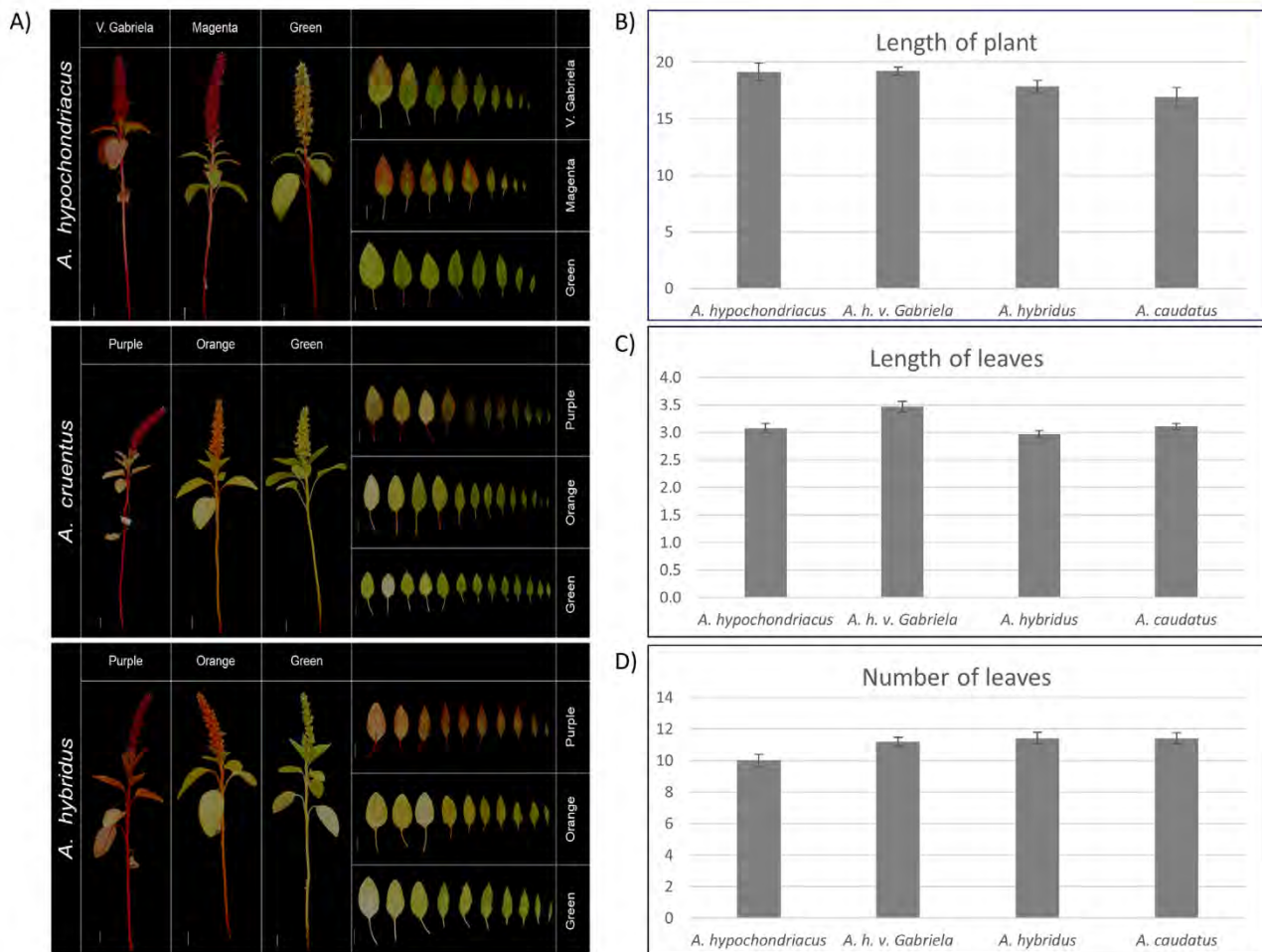


Fig. 4. Phenotype differences of panicle, plant, and leaves between species of amaranth. (A) Comparison of plant whole parts and leaves of different species of amaranth (Stage 8–9). Plants in stage 13 were classified. (B) Plant height, (C) Leaf length, and (D) Number of leaves were analyzed. Analysis of variance using Fisher's Least Significant Difference (LSD) test with significance $P < .05$ was performed.

3.3. Leaf development

The principal growth stage 1 denominated leaf development, included the opening of cotyledons (stage 10) to leaf development (Fig. 1, Table 1). Stage 10 occurred four or five days post-seeding and required just one day. The emergence of true leaves (stage 11) was observed eight to ten days post-seeding and needed four or five days (Figs. 1, 2). Stage 13 was the extended vegetative phase and included plants with five or six leaves (Fig. 1A) this happened 21 days post-seeding in *A. hypochondriacus* and 32 days post-seeding in *A. cruentus* and *A. hybridus* and lasted for 20 days (Figs. 1B, 2).

3.4. Apical inflorescence emergence

The panicle exertion denominated "Principal growth stage 5" and known as inflorescence emergence occurred at various times across species. In *A. hypochondriacus*, and *A. hypochondriacus* variety "Gabriela", the panicles were observed after 40 days post-seeding. This happened at 57 days in *A. hybridus* and *A. cruentus*. (Fig. 1B).

3.5. Anthesis and axillary inflorescence

The principal growth stage 6 includes the anthesis and the outbreak of axillary inflorescences; these processes overlap in the amaranth life cycle (Table 1). *A. hypochondriacus* and *A. hypochondriacus* variety "Gabriela" initiated principal stage 6 around 69 days post-seeding: *A.*

cruentus and *A. hybridus* started ~79 days post-seeding (Fig. 2). There were differences in compaction, density, posture, size of bracts, and color among the panicles of each species (Fig. 3A). Anthesis occurred after panicle emergence (22–29 days).

Unisexual flowers characterized monoecious amaranth i.e., glomerulus (Fig. 3B), staminate, or pistillate (Fig. 3C) (Mlakar et al., 2009; Rastogi and Shukla, 2013). The highest amount of pollen was released in the first three or four days post-anthesis. The pollination usually started with flowers of glomerulus located in the upper half of the panicle. Male flowers (staminate) matured before female flowers (pistillate), i.e., the release of pollen began 1–2 days earlier offering successful fertilization of the female flowers contained in the panicle. Amaranth has indeterminate growth (Pandey and Singh, 2009), and the presence of the vegetative structures continued during the reproductive phase. There was simultaneous appearance of leaves, branches, axillary flowers and flowers on the panicle.

3.6. Fruit and seed development

The principal stage 7 included the fruit and seed development. Seeds of the panicle base were used for monitoring. Fertilization started from the base to the panicle apex, and seeds reached maturity at a different time in each plant. The first stage of seed development included stages 70 and 71 on the BBCH code (Table 1). The first stage of seed development occurred around 85 days post-seeding (five days after fertilization (Fig. 3C)) and lasted approximately one week. This began with the

Life cycle of Amaranth

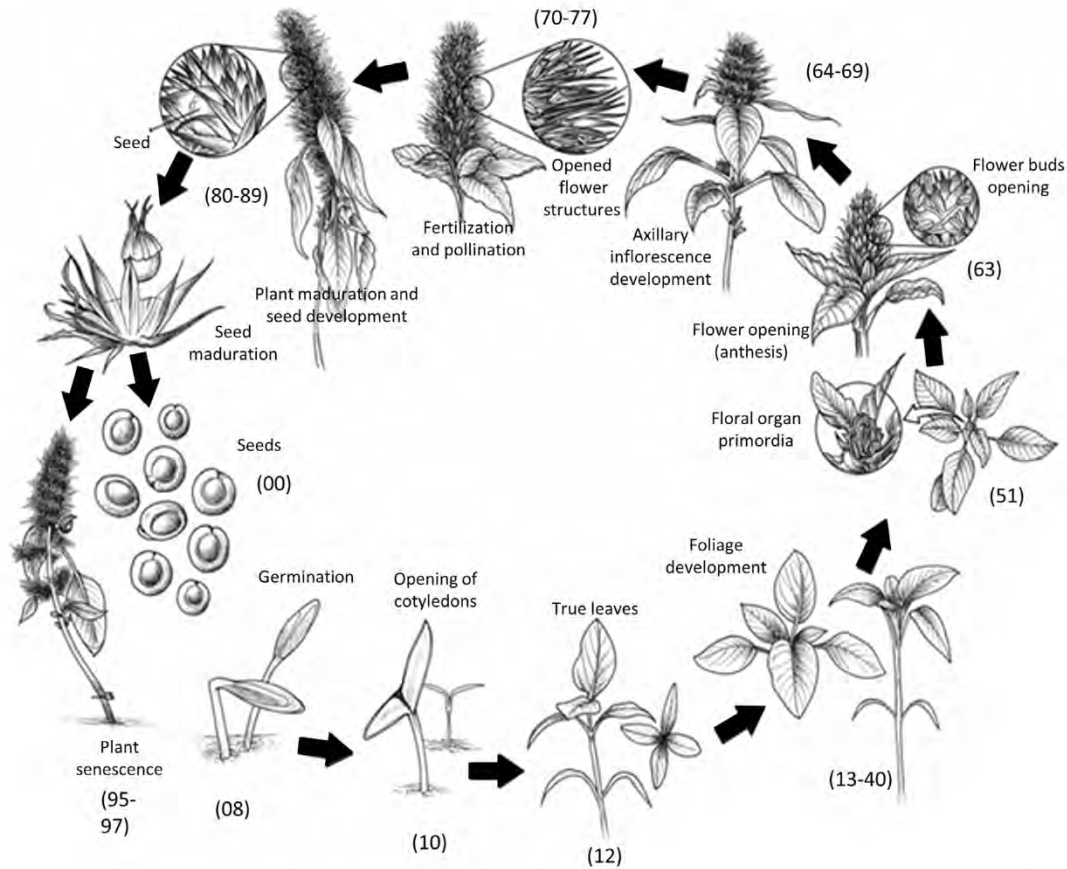


Fig. 5. The life cycle of amaranth. Principal characteristics of amaranth in greenhouse conditions were considered to represent the life cycle of amaranth including germination until seed maturation and plant senescence. The term in parentheses is the BBCH code.

development of the fertilized ovule forming an irregular structure of translucent grayish coloration and mucoid consistency measuring between 0.3 and 0.5 mm long (Fig. 3D).

The second stage of seed development (stage 73) occurred between 100 and 110 days post-seeding for *A. hypochondriacus* and *A. hypochondriacus* variety “Gabriela,” and *A. cruentus* and *A. hybridus*, respectively. The second stage of seed development was characterized by immature grains with a rounded elliptic shape with translucent white color and a soft texture approximately 1 mm long (Fig. 3D). In the second stage, the grains showed a milky consistency that produced viscous white liquid when pressed with fingers. The third stage of seed development (stage 75) occurred at 110 and 120 days post-seeding in *A. hypochondriacus* and *A. hypochondriacus* variety “Gabriela,” and *A. cruentus* and *A. hybridus*, respectively. Here, the rounded elliptical structure of the seeds was preserved, but now with an approximate length of 1.3 mm in diameter (Fig. 3D). These presented a white coloration of dark tone and firmer consistency. The seeds still needed to ripen because they burst and had a pasty consistency with a whitish color when pressed between the fingers. The last stage of seed development (stage 89) included seed ripening began 120 days post-seeding in *A. hypochondriacus* and *A. hypochondriacus* variety “Gabriela” and 153 days post-seeding in *A. cruentus* and *A. hybridus* and ended when the seed was ~1.5 mm in diameter (Fig. 3D). At this time, the seeds retained their rounded elliptical appearance. However, their texture was slightly rough with an opaque ivory coloration (Fig. 3D). The peripheric embryo or episperm (E) formed by the cotyledons and the radicle tip was obvious upon maturity; these surrounded the perisperm (P) or reserve tissue of the seed (Fig. 3D). The complete maturation of

seeds followed the highest degree of physiological maturity; thus, we noted easy detachment of seeds filled with panicles when shaking the plant.

3.7. Ripening and senescence

The maximum degree of physiological maturity in the different amaranth species coincided with the maturation of all seeds. The seeds became hard with an opaque ivory coloration and detached easily from the panicle (stage 89) (Table 1). The overlap between ripening and senescence in amaranth plants (principal growth stages 8 and 9 in the BBCH code, respectively) was observed and occurred 120 or 153 days post-seeding (Fig. 2, Table 1). There was obvious deterioration of the plant including decaying, wilting and change of coloration in leaves, stems, and panicle (Fig. 4). The panicles exhibited the most visible phenotypic changes (Fig. 4).

We studied the diversity of plant coloration in greenhouses (Figs. 3A, 4). The panicle color is the most commonly used criteria to determine physiological maturity (Manikandan and Srimathi, 2015). The bright green panicle was dark green, the lime changed to pale green. The red became a red-brown, and the orange became golden corresponding to stage 95 (Fig. 4, Table 1). The analysis of variance (ANOVA) of plant height did not show a significant difference ($P > .05$) between *A. hypochondriacus* and the “Gabriela” variety of *A. hypochondriacus*, but there was a significant difference ($P > .05$) observed in respect to *A. cruentus* plant height (Fig. 4B). Plants of *A. hypochondriacus* were 6 and 11% taller than *A. hybridus* and *A. cruentus*, respectively. The “Gabriela” variety of *A. hypochondriacus* had the largest leaves (Fig.

4C), and *A. hypochondriacus* had the smallest (Fig. 4D). The analysis of variance between species, showed a significant difference ($P > .05$) in leaves length of the Gabriela" variety of *A. hypochondriacus* (Fig. 4C) and the number of leaves in *A. hypochondriacus*.

4. Discussion

4.1. Relevance of amaranth growth in restricted spaces

Amaranth is a crop with high potential for economic exploitation, due to its excellent nutritional value, and likewise for its high plasticity and easy adaptation to adverse growth conditions (Delano-Frier et al., 2011; Huerta-Ocampo et al., 2014; Khanam and Oba, 2014). Amaranth plants under field conditions range between 2.0 and 2.2 m. The plasticity of amaranth enabled its monitoring in restricted spaces. Plants between 15 and 22 cm were obtained in restricted spaces. These observations highlight the extensive phenotypic plasticity of amaranth. In summary, amaranth growth in restricted spaces presents an interesting and practical tool to establish crops not only for research purposes but also to improve this ancient crop, which could be an advantage for better manipulation such as the selection and development of varieties in small areas.

4.2. The phenological growth stages of amaranth based in BBCH code

The BBCH scale help to define the phenological events of all species of mono- and dicotyledonous plants. The utility of the BBCH scale has been validated in the description of several traits of agronomic interest at specific developmental stages of different plants (i.e. Munger et al., 1997; Erten et al., 2014; Herraiz et al., 2015; Sosa Zuniga et al., 2017). Principal growth stages in different amaranth species included germination, leaf development, inflorescence emergence and flower development, anthesis, development of seeds, ripening of seeds, and senescence were identified. Although differences in the panicle structure and size, and leaf number were observed between species, the main stages that describe the life cycle of amaranth were observed (Fig. 2). Based on the existing BBCH scale eight principal growth stages (stage 0–2, 5–9) were identified in the growth cycle of three amaranth species. The period for each phenological stage of different amaranth species was determined, and the principal stages were monitored allowing to obtain a schematic representation of the phenological growth stages of amaranth (Figs. 1B, 2). As in other plants (Martinelli and Galasso, 2011; Herraiz et al., 2015; Acosta-Quezada et al., 2016), BBCH-scale stage 3 and stage 4 (Stem elongation and development of harvestable vegetative parts respectively) are not applicable to amaranth due to the longitudinal growth of the main stem which occurs in parallel with the leaf development and because in amaranth usually only seeds are harvested. Each principal stage was subdivided into secondary stages to allow a detailed description of the amaranth development (Table 1). The principal characteristics of amaranth grown in restricted spaces based in BBCH code were used to represent the life cycle of amaranth since germination until plant senescence (Fig. 5). The phenological characterization in this crop in restricted spaces is relevant for future studies which would be of great utility for agronomic and botanical research of amaranth.

5. Conclusions

In conclusion, these data allow us to envision amaranth as a model plant in which each phenological growth stage is easily managed under restricted spaces, which could be an advantage for better manipulation and can be considered for future studies, such as the selection and development of varieties in small areas. This could be an advantage for a better manipulation to generate new genetic variation and for laboratory studies. To our knowledge, this is the first study that determines the developmental stages using the BBCH scale, and proposes the life cycle of Amaranth growth under confined spaces conditions. We hope

the BBCH scale established and the life cycle of amaranth will be used to characterize development and facilitate comparison between studies.

Author contributions

MMN did the major experimental work. MRR contributed to the experimental analysis. RBM generated the variety "Gabriela." MMN and FFRC conceived the project. MMN, SLS, and FFRC designed the experiments. MMN, PFVH, and FFRC drafted the manuscript. All authors read and approved the final manuscript.

Conflicts of interest

The authors declare no conflict of interest.

Financial support

MMN, MRR, PFVH, were supported by the Mexican National Council of Science and Technology (CONACyT) fellowship (MMN: 270563, MRR: 251176, PFVH: 287820). This work was financed by the CONACyT grant CB-2013-221522, and SIP grants 20180545 and 20195904.

Acknowledgments

We thank Dr. Cesar Augusto Sandino Reyes López of the National School of Medicine and Homeopathy of the National Polytechnic Institute of Mexico for the donation of amaranth seeds. Thanks to CONACyT and SIP for financial support.

References

- Acosta-Quezada, P.G., Riofrio-Cuenca, T., Rojas, J., Vilanova, S., Plazas, M., Prohens, J., 2016. Phenological growth stages of tree tomato (*Solanum betaceum* Cav.), an emerging fruit crop, according to the basic and extended BBCH scales. *Sci. Hortic.* 199, 216–223. <https://doi.org/10.1016/j.scienta.2015.12.045>.
- Akin-Idowu, P., 2017. Nutritional evaluation of five species of grain amaranth – an underutilized crop. *Int. J. Sci.*, 18–27 <https://doi.org/10.18483/ijSci.1131>.
- Akin-Idowu, P., Gbadegehin, M., Orkpeh, U., Ibitoye, D., Oduola, O., 2016. Characterization of grain amaranth (*Amaranthus* spp.) germplasm in South West Nigeria using morphological, nutritional, and random amplified polymorphic DNA (RAPD) analysis. *Resources* 5, 6. <https://doi.org/10.3390/resources5010006>.
- Brenner, D., Baltensperger, D., Kulakow, P., Lehmann, J., Myers, R., Slabbert, M., Sleugh, B., 2010. Genetic resources and breeding of amaranthus. *Plant Breed. Rev.* 19, 227–285. <https://doi.org/10.1002/9780470650172.ch7>.
- Bussel, L., Stehfest, E., Siebert, S., Müller, C., Ewert, F., 2015. Simulation of the phenological development of wheat and maize at the global scale. *Glob. Ecol. Biogeogr.* 24, 1018–1029. <https://doi.org/10.1111/geb.12351>.
- Caselato-Sousa, V., Amaya-Farfan, J., 2012. State of knowledge on amaranth grain: a comprehensive review. *J. Food Sci.* 77, R93–104. <https://doi.org/10.1111/j.1750-3841.2012.02645.x>.
- Choi, D., Ban, H., Seo, B., Lee, K., Lee, B., 2016. Phenology and seed yield performance of determinate soybean cultivars grown at elevated temperatures in a temperate region. *PLoS One*. 11, e0165977. <https://doi.org/10.1371/journal.pone.0165977>.
- Das, S., 2016. Amaranthus: A Promising Crop of Future. Springer, Singapore <https://doi.org/10.1007/978-981-10-1469-7>.
- Delano-Frier, J., Aviles-Arnaut, H., Casarubias-Castillo, K., Casique-Arroyo, G., Castrillon-Arbelaez, P., Herrera-Estrella, L., Massange-Sanchez, J., Martinez-Gallardo, N., Parra-Cota, F., Vargas-Ortiz, E., 2011. Transcriptomic analysis of grain amaranth (*Amaranthus hypochondriacus*) using 454 pyrosequencing: comparison with *A. tuberculatus*, expression profiling in stems and in response to biotic and abiotic stress. *BMC Genomics* 12, 363. <https://doi.org/10.1186/1471-2164-12-363>.
- Erten, E., Rossi, C., Yuzugullu, O., Hajnsek, I., 2014. Phenological growth stages of paddy rice according to the BBCH scale and Sar images. *IEEE Int. Geosci. Remote Sens. Symp. (Igarss)*, 1017–1020 <https://doi.org/10.1109/Igarss.2014.6946600>.
- Fazlioglu, F., Bonser, S., 2016. Phenotypic plasticity and specialization in clonal versus non-clonal plants: a data synthesis. *Acta Oecol.* 77, 193–200. <https://doi.org/10.1016/j.actao.2016.10.012>.
- Gilmore, E.C., Rogers, J., 1958. Heat units as a method of measuring maturity in corn. *Agron. J.* 50, 611–615.
- Hack, H., Bleiholder, H., Buhr, L., Meier, U., Schnock-Fricke, U., Weber, E., Witzemberger, A., 1992. Einheitliche codierung der phänologischen entwicklungsstadien mono- und dikotylter pflanzen—erweiterte BBCH-Skala, *Allgemein. Nachrichtenbl. Deut. Pflanzenschutz.* 44, 265–270.
- Herraiz, F., Vilanova, J.S., Plazas, M., Gramazio, P., Andujar, I., Rodriguez-Burruezo, A., Fita, A., Anderson, G.J., Prohens, J., 2015. Phenological growth stages of pepino (*Solanum muricatum*) according to the BBCH scale. *Sci. Hortic.* 183, 1–7. <https://doi.org/10.1016/j.scienta.2014.12.008>.

- Hossain, A., da Silva, J., Lozovskaya, M., Zvolinsky, V., 2012. High temperature combined with drought affect rainfed spring wheat and barley in South-Eastern Russia: I. Phenology and growth. *Saudi J. Biol. Sci.* 19, 473–487. <https://doi.org/10.1016/j.sjbs.2012.07.005>.
- Huerta-Ocampo, J., Barrera-Pacheco, A., Mendoza-Hernandez, C., Espitia-Rangel, E., Mock, H., Barba de la Rosa, A.P., 2014. Salt stress-induced alterations in the root proteome of *Amaranthus cruentus* L. *J. Proteome Res.* 13, 3607–3627. <https://doi.org/10.1021/pr500153m>.
- Ihsan, M., El-Nakhlawy, F., Ismail, S., Fahad, S., Daur, I., 2016. Wheat phenological development and growth studies as affected by drought and late season high temperature stress under arid environment. *Front. Plant Sci.* 7, 795. <https://doi.org/10.3389/fpls.2016.00795>.
- Innovation NRCAC, 1984. *Amaranth: Modern Prospects for an Ancient Crop*. National Academy Press.
- Khanam, U., Oba, S., 2014. Phenotypic plasticity of vegetable amaranth, *Amaranthus tricolor* L. under a natural climate. *Plant Prod. Sci.* 17, 166–172. <https://doi.org/10.1626/pp.17.166>.
- Kirillova, L., Nazarova, G., Ivanova, E., 2016. Para-aminobenzoic acid stimulates seed germination plant growth, development, photosynthesis and nitrogen assimilation in the amaranth (*Amaranthus L.*). *Agric. Biol. Plant Biol. Sect.* 688.
- Kuluev, B., Mikhaylova, E., Taipova, R., Chemeris, A., 2017. Changes in phenotype of transgenic amaranth *Amaranthus retroflexus* L., overexpressing ARGOS-LIKE gene. *Russ. J. Genet.* 53, 67–75. <https://doi.org/10.1134/S1022795416120061>.
- Kumar, S., Hammer, G., Broad, L., Harland, P., McLean, G., 2009. Modeling environmental effects on phenology and canopy development of diverse sorghum genotypes. *Field Crop Res* 111, 157–165. <https://doi.org/10.1016/j.fcr.2008.11.010>.
- Lee, J., Hong, G., Dixit, A., Chung, J., Ma, K., Lee, J., Kang, H., Cho, Y., Gwag, J., Park, Y., 2008. Characterization of microsatellite loci developed for *Amaranthus hypochondriacus* and their cross-amplifications in wild species. *Conserv. Genet.* 9, 243–246. <https://doi.org/10.1007/s10592-007-9323-1>.
- Manikandan, S., Srimathi, P., 2015. Colour of spike as an index of harvestable maturity of grain amaranth (*Amaranthus hypochondriacus* L.) cv. Suvarna. *Curr. Biot.* 9, 173–177.
- Martinelli, T., Galasso, I., 2011. Phenological growth stages of *Camelina sativa* according to the extended BBCH scale. *Ann. Appl. Biol.* 158, 87–94. <https://doi.org/10.1111/j.1744-7348.2010.00444.x>.
- Massange-Sanchez, J., Palmeros-Suarez, P., Martinez-Gallardo, N., Castrillon-Arbelaiz, P., Aviles-Arnaut, H., Alatorre-Cobos, F., Tiessen, A., Delano-Frier, J., 2015. The novel and taxonomically restricted Ah24 gene from grain amaranth (*Amaranthus hypochondriacus*) has a dual role in development and defense. *Front. Plant Sci.* 6, 602. <https://doi.org/10.3389/fpls.2015.00602>.
- Meier, U., Bleiholder, H., Buhr, L., Feller, C., Hack, H., Heß, M., Lancashire, P., Schnock, U., Stauß, R., Van Den Boom, T., 2009. The BBCH system to coding the phenological growth stages of plants—history and publications. *J. für Kulturpflanzen.* 61, 41–52.
- Mlakar, S., Turinek, M., Jakop, M., Bavec, M., Bavec, F., 2009. Nutrition value and use of grain amaranth: potential future application in bread making. *Agricultura* 6.
- Munger, P., Bleiholder, H., Hack, H., Hess, M., Stauss, R., van den Boom, T., Weber, E., 1997. *J. Agron. Crop Sci.* 179, 209–217. <https://doi.org/10.1111/j.1439-037X.1997.tb00519.x>
- Phenological growth stages of the soybean plant (*Glycine max* L. MERR.): codification and description according to the BBCH scale.
- Palmeros-Suarez, P., Massange-Sanchez, J., Martinez-Gallardo, N., Montero-Vargas, J., Gomez-Leyva, J., Delano-Frier, J., 2015. The overexpression of an *Amaranthus hypochondriacus* NF-YC gene modifies growth and confers water deficit stress resistance in *Arabidopsis*. *Plant Sci.* 240, 25–40. <https://doi.org/10.1016/j.plantsci.2015.08.010>.
- Pandey, R., Singh, R., 2009. Genetic improvement of grain amaranths: a review. *Curr. Adv. Agric. Sci.* 1, 61–64.
- Price, T., Qvarnström, A., Irwin, D., 2003. The role of phenotypic plasticity in driving genetic evolution. *Proc. R. Soc. Lond. B: Biol. Sci.* 270, 1433–1440. <https://doi.org/10.1098/rspb.2003.2372>.
- Rastogi, A., Shukla, S., 2013. Amaranth: a new millennium crop of nutraceutical values. *Critic. Rev. Food Sci. Nutr.* 53, 109–125. <https://doi.org/10.1080/10408398.2010.517876>.
- Ray, T., Roy, S., 2009. Genetic diversity of *Amaranthus* species from the Indo-Gangetic plains revealed by RAPD analysis leading to the development of ecotype-specific SCAR marker. *J. Hered.* 100, 338–347. <https://doi.org/10.1093/jhered/esn102>.
- Salmeron, M., Purcell, L., 2016. Simplifying the prediction of phenology with the DSSAT-CROPGRO-soybean model based on relative maturity group and determinacy. *Agr. Syst.* 148, 178–187. <https://doi.org/10.1016/j.agry.2016.07.016>.
- Shukla, S., Bhargava, A., Chatterjee, A., Pandey, A., Mishra, B.K., 2010. Diversity in phenotypic and nutritional traits in vegetable amaranth (*Amaranthus tricolor*), a nutritionally underutilised crop. *J. Sci. Food Agric.* 90, 139–144. <https://doi.org/10.1002/jsfa.3797>.
- Sosa-Zuniga, V., Brito, V., Fuentes, F., Steinfurt, U., 2017. Phenological growth stages of quinoa (*Chenopodium quinoa*) based on the BBCH scale. *Ann. Appl. Biol.* 171, 117–124. <https://doi.org/10.1111/aab.12358>.
- Stetter, M., Zeitler, L., Steinhaus, A., Kroener, K., Biljecki, M., Schmid, K., 2016. Crossing methods and cultivation conditions for rapid production of segregating populations in three grain amaranth species. *Front. Plant Sci.* 7, 816. <https://doi.org/10.3389/fpls.2016.00816>.
- Vargas-Ortiz, E., Delano-Frier, J., Tiessen, A., 2015. The tolerance of grain amaranth (*Amaranthus cruentus* L.) to defoliation during vegetative growth is compromised during flowering. *Plant Physiol. Biochem.* 91, 36–40. <https://doi.org/10.1016/j.plaphy.2015.03.007>.
- Venkatesh, L., Murthy, N., Nehru, S., 2014. Analysis of genetic diversity in grain amaranth (*Amaranthus* spp.). *Ind. J. Genet. Plant Breed.* 74, 522–525. <https://doi.org/10.5958/0975-6906.2014.00882.7>.
- Zhang, D., Yuan, Z., An, G., Dreni, L., Hu, J., Kater, M., 2013. Panicle development. In: Zhang, Q., Wing, A.R. (Eds.), *Genetics and Genomics of Rice*. Springer New York, New York, NY, pp. 279–295.
- Zhang, T., Li, T., Yang, X., Simelton, E., 2016. Model biases in rice phenology under warmer climates. *Sci. Rep.* 6, 27355. <https://doi.org/10.1038/srep27355>.